DEVELOPMENT AND CHARACTERIZATION OF PQSD INHIBITORS TO INTERRUPT CELL-TO-CELL COMMUNICATION IN PSEUDOMONAS AERUGINOSA

DISSERTATION

zur Erlangung des Grades
des Doktors der Naturwissenschaften
der Naturwissenschaftlich-Technischen Fakultät III
Chemie, Pharmazie, Bio- und Werkstoffwissenschaften
der Universität des Saarlandes

von

Dipl. Chem. Michael Philipp Storz

Saarbrücken
2014

Tag des Kolloquiums:	07. November 2014
Dekan:	Prof. Dr.-Ing. Dirk Bähre
Vorsitz:	Prof. Dr. Claus-Michael Lehr
Berichterstatter:	Prof. Dr. Rolf W. Hartmann
	Prof. Dr. Uli Kazmaier
	Prof. Dr. Wulf Blankenfeldt
Akad. Mitarbeiter:	Dr. Silke Wenzel

Die vorliegende Arbeit wurde von November 2009 bis Juni 2014 unter Anleitung von Herrn Prof. Dr. Rolf W. Hartmann am Helmholtz-Institut für Pharmazeutische Forschung Saarland (HIPS) angefertigt.

INMITTEN DER SCHWIERIGKEIT
LIEGT DIE MÖGLICHKEIT

ALBERT EINSTEIN

SUMMARY

Due to the lack of new types of antibiotics and propagating resistance against all available classes, an increasing number of bacterial infections cannot be efficiently treated anymore. Anti-virulent compounds, which target bacterial pathogenesis without affecting cell viability and consequently exert less selection pressure, were recently suggested.

Most bacteria control pathogenesis via cell-density-dependent cell-to-cell communication (quorum sensing, QS), which makes QS an appropriate target to pursue an anti-virulence strategy. Besides the widespread acyl homoserine lactone signal molecules, the opportunistic pathogen *Pseudomonas aeruginosa* applies a rather unique quinolone-based QS system. Thus, inhibitors of PqsD, a key enzyme in the signal molecule biosynthesis, should be developed to specifically combat *P. aeruginosa* infections.

Using a ligand-based approach, the first class of PqsD inhibitors was identified. Simplification and rigidization led to a fragment with high ligand efficiency, which significantly inhibited signal molecule production and biofilm formation in *P. aeruginosa*.

Various methods to characterize the mode of action of PqsD inhibitors were developed, which allowed the proposal of their binding modes. Fine-tuning of the fragment provided PqsD inhibitors with high potential for further improvements. Furthermore, they constitute valuable tools to analyze QS regulation pathways, and to evaluate PqsD as drug target for the treatment of *P. aeruginosa*.

ZUSAMMENFASSUNG

Die Behandlung bakterieller Infektionen wird durch die stagnierende Entwicklung neuer Antibiotika und vermehrter Resistenzbildung zunehmend erschwert. Anti-virulente Verbindungen, welche die Pathogenität der Bakterien absenken ohne deren Lebensfähigkeit zu beeinflussen und damit keinen Selektivitätsdruck ausüben, stellen einen neuen Therapieansatz dar.

Die Pathogenität der meisten Bakterien wird durch ein zelldichteabhängiges interzelluläres Kommunikationssystem (Quorum Sensing, QS) gesteuert. Das opportunistische Pathogen *Pseudomonas aeruginosa* verwendet neben den üblichen Lactonen zusätzlich Chinolone als Signalmoleküle. Dabei ist das Enzym PqsD essentiell für deren Biosynthese und eignet sich daher als Wirkstoff-Target einer Anti-Virulenz Strategie für die spezifische Bekämpfung von *P. aeruginosa.*

In einem Ligand-basierten Ansatz wurde die erste PqsD Inhibitorenklasse identifiziert. Die Verkleinerung und Rigidisierung führten zu einem Fragment, das eine hohe Liganden-effizienz aufweist und die Signalmolekül- und Biofilmbildung in *P. aeruginosa* hemmt.

Mehrere Methoden zur Aufklärung der Wirkungsweisen von PqsD Inhibitoren wurden entwickelt, so dass konkrete Bindungsposen vorgeschlagen werden konnten. Die strukturelle Feinabstimmung des Fragments lieferte leicht weiteroptimierbare PqsD Inhibitoren, die als Tools zur Analyse der QS Regulationswege genutzt werden können und ferner der Beurteilung von PqsD als Drug-Target zur Behandlung von *P. aeruginosa* dienen.

PAPERS INCLUDED IN THIS THESIS

This thesis is divided into four publications, which are referred to in the text by their letter.

A **Validation of PqsD as an Anti-biofilm Target in *Pseudomonas aeruginosa* by Development of Small-Molecule Inhibitors**

Michael P. Storz, Christine K. Maurer, Christina Zimmer, Nathalie Wagner, Christian Brengel, Johannes C. de Jong, Simon Lucas, Mathias Müsken, Susanne Häussler, Anke Steinbach, and Rolf W. Hartmann

J. Am. Chem. Soc. **2012**, *134*, 16143-16146.

B **Biochemical and Biophysical Analysis of a Chiral PqsD Inhibitor Revealing Tight-Binding Behavior and Enantiomers with Contrary Thermodynamic Signatures**

Michael P. Storz, Christian Brengel, Elisabeth Weidel, Michael Hoffmann, Klaus Hollemeyer, Anke Steinbach, Rolf Müller, Martin Empting, and Rolf W. Hartmann

ACS Chem. Biol. **2013**, *8*, 2794-2801.

C **Combining in Silico and Biophysical Methods for the Development of *Pseudomonas aeruginosa* Quorum Sensing Inhibitors: An Alternative Approach for Structure-Based Drug Design**

J. Henning Sahner, Christian Brengel, Michael P. Storz, Matthias Groh, Alberto Plaza, Rolf Müller, and Rolf W. Hartmann

J. Med. Chem. **2013**, *56*, 8656-8664.

D **From *in vitro* to *in cellulo*: Structure-activity relationship of (2-nitrophenyl)-methanol derivatives as inhibitors of PqsD in *Pseudomonas aeruginosa***

Michael P. Storz, Giuseppe Allegretta, Benjamin Kirsch, Martin Empting, and Rolf W. Hartmann

Org. Biomol. Chem. **2014**, DOI: 10.1039/c4ob00707g.

FURTHER PAPER OF THE AUTHOR THAT IS NOT PART OF THIS DISSERTATION

E **Structure Optimization of 2-Benzamidobenzoic Acids as PqsD Inhibitors for *Pseudomonas aeruginosa* Infections and Elucidation of Binding Mode by SPR, STD NMR, and Molecular Docking**

Elisabeth Weidel, Johannes C. de Jong, Christian Brengel, Michael P. Storz, Matthias Negri, Alberto Plaza, Anke Steinbach, Rolf Müller, and Rolf W. Hartmann

J. Med Chem. **2013**, *56*, 6146-6155.

ABBREVIATIONS

2-AA	2-Aminoacetophenon
AA	Anthranilic acid
ACoA	Anthraniloyl coenzyme A
ADMET	Absorption, distribution, metabolism, excretion, and toxicity
AHL	*N*-Acyl homoserine lactone
BHL	*N*-Butanoyl-L-homoserine lactone (C_4-HSL)
Cmpd.	Compound
CNS	Central nervous system
CoA	Coenzyme A
DCM	Dichloromethane
DHQ	2,4-Dihydroxyquinoline
DMF	Dimethylformamide
DMSO	Dimethyl sulfoxide
eq	Äquivalente
Eq.	Equation
FDA	Food and drug administration
HAQs	4-Hydroxy-2-alkyl-4-quinolones
HPLC	High-performance liquid chromatography
HQNO	4-Hydroxy-2-heptylquinoline-*N*-oxide
IC_{50}	Concentration of a drug that is required for 50% inhibition *in vitro*
ITC	Isothermal titration calorimetry
K_d	Dissociation constant
LB	Lysogeny broth
LE	Ligand efficiency
logP	Octanol-water partition coefficient
MALDI	Matrix-assisted laser desorption/ionization
MS	Mass spectrometry
MW	Molecular weight
NMR	Nuclear magnetic resonance
OdDHL	*N*-(3-Oxododecanoyl)-L-homoserine lactone (3O-C_{12}-HSL)
nrotb	Number of rotatable bonds
OD_{600}	Optical density at 600 nm

PQS	*Pseudomonas* quinolone signal
QS	Quorum sensing
SPR	Surface plasmon resonance
STD	Saturation transfer difference
TOF	Time-of-flight

TABLE OF CONTENTS

1 Introduction

In 1967, the surgeon general of the United Stated, William Stewart, is supposed to have proclaimed, that "the time has come to close the book on infectious diseases. We have basically wiped out infection in the United States."[1] Whether Stewart was cited correctly or not, the exceeding optimism of many experts had its origin in the 1940s, when Penicillin was developed as the first commercial antibiotic. Besides the treatment of bacterial diseases, antibiotics allowed the advance of surgical methods and chemotherapy.[2] Between the 1950s and 1980s, several novel classes of antibiotics were developed.

However, since then the discovery of new antibiotic classes is extremely rare and the number of new antibacterial agents approved by the FDA rigorously decreased.[3,4] Furthermore, from 1940 to 2004 hundreds of new infections emerged. Additionally, some known infectious diseases rapidly increased in incidence or geographic range.[5,6] Combined with the fact, that for virtually every bacterial organism and every antibiotic the development of resistance mechanisms can be observed, the fear of non-treatable superbugs grows. Thus, the question arised if we have reached the beginning of the post-antibiotic era.[7,8] The lack of efficient antibiotics would have tremendous influence on modern life and society. Many surgeries including organ transplantations, birth of premature infants and cytotoxic therapies for cancer would be impossible. Slightest injuries would threaten life.[8] Beyond increased morbidity and mortality, higher costs for treatment represent a serious economical burden, with barely foreseeable consequences for the future.[9]

Thus, there is an urgent need for new treatments with diminished potential to promote resistance.[10] Therefore, it is important to understand the resistance mechanisms, which render previously successful drugs inefficient by mutations or acquisition of resistance genes.[11,12] Major biochemical mechanisms, which work synergistically, are:[13]

- Decrease of outer membrane permeability (e.g. downregulation of purin genes)
- Target mutations decrease drug affinity while functional activity is conserved
- Expression of efflux systems to decrease the drug concentration at the target
- Production of enzymes inactivating the antibiotic (e. g. β-lactamases)
- Development of by-passes turning the target non-essential

Several common strategies to overcome bacterial resistance address the underlying mechanisms itself[14] either by adaptation of the drugs according to the new requirements or by additional use of a second auxiliary drug blocking the acquired resistance mechanism. More

specifically, these strategies are the development of agents less susceptible to efflux systems, addition of efflux inhibitors[15] or inhibitors of modifying enzymes (e.g. β-lactamase inhibitors)[16] and development of permeabilizers[17] enhancing the susceptibility of resistant bacteria. However, the success of these strategies was limited, since many infections caused by *P. aeruginosa*, for example, are rarely eradicated by conventional treatment.[18] Furthermore, an inherent disadvantage of these strategies is that realization necessarily lags behind resistance development by several years.

A more innovative way to overcome this problem is to bypass the pathogen's reasons to develop resistances. Conventional antibiotics reduce the cell viability, thus exerting selection pressure on bacteria. Only those can survive, which adapt to the presence of the antibiotic by development of at least one of the resistance mechanisms described above. Since susceptible bacteria are killed by the antibiotic, the small fraction of resistant cells can grow to become the predominant species of the population.

However, if a drug decreases the pathogenicity of bacteria without bacteriostatic and bactericidal properties, there is less evolutionary pressure exerted on the bacteria. Ideally, inhibition of virulence factor production prevents host damage but allows non-resistant bacteria to survive. And even if single bacterial cells develop resistance mechanisms against the mode of action of the anti-virulent drug, they continue to be the minority within the population.[10,19]

1.1 *Pseudomonas aeruginosa*

P. aeruginosa is a ubiquitous Gram-negative bacterium, which is able to adapt to many natural environments.[20] This opportunistic pathogen shows an increasing clinical relevance and is a frequent cause for nosocomial infections. It is responsible for 10% of all hospital-acquired infections and the most common pathogen isolated from patients who have been hospitalized longer than one week.[21-23]

Several parts of the body can be affected by *P. aeruginosa* infections. Examples for typical diseases are given in brackets.[22,24]

- Respiratory tract (e.g., pneumonia)
- Bloodstream (e.g., bacteremia)
- Heart (e.g., endocarditis)
- CNS (e.g., meningitis)
- Ear (e.g., otitis externa)

- Eye (e.g., endophthalmitis, keratitis)
- Bones and Joints (e.g., osteomyelitis)
- GI tract (e.g., diarrhea, enteritis, enterocolitis)
- Urinary tract
- Skin (e.g. ecthyma gangraenosum)

In cystic fibrosis patients, *P. aeruginosa* is considered as the major cause of mortality.[25] Furthermore, it is especially prevalent among patients with burn wounds, acute leukemia, organ transplants, and intravenous drug addiction.[24]

Treatment of *P. aeruginosa* is particularly difficult, since this pathogen displays a high intrinsic resistance.[12] This is due to synergistically acting multi-drug efflux pumps, chromosomally encoded β-lactamases and highly restricted outer-membrane permeability.[8] Furthermore, *P. aeruginosa* forms biofilms,[26] which are defined as bacterial populations adherent to each other and/or surfaces or interfaces, embedded in a complex extracellular matrix.[27] Biofilms provide protection from the immune system and are refractory to antimicrobial treatment.[27] The actual mechanism behind this physiological resistance is still under discussion. One reason might be an additional diffusion barrier caused by the surrounding extracellular matrix consisting of polysaccharides, nucleic acids, and proteins.[28,29] Alternatively, a less susceptible mode of growth due to altered gene expression leading to slow growth, activation of stress responses and accumulation of modifying enzymes, was described as a resistance-mediating characteristic of biofilm populating bacteria.[30,31]

Additionally, the organism is able to acquire resistance to multiple classes of antimicrobial agents as β-lactams, fluoroquinolones, and aminoglycosides.[32,33] The analysis of multidrug-resistant *P. aeruginosa* isolates (as defined by resistance to three or more drug classes) from intensive care unit patients in the US showed an increasing prevalence from 4 to 14% in the period from 1993 to 2002.[34] Much higher values are observable in individual communities and hospitals. This is associated with significant increases in morbidity, mortality, need for surgical intervention, length of hospital stay and chronic care, as well as overall cost of infection treatment.[33] Furthermore, *P. aeruginosa* is able to develop resistances even during the course of attempted therapy, which doubles the length of hospitalization and overall costs for patient care.[35]

1.2 Inhibition of Quorum Sensing as Anti-virulence Strategy

The inhibition of bacterial pathogenicity was introduced above as novel approach to overcome bacterial resistance. But which targets are appropriate for this purpose? At this point it might be beneficial to start with a few definitions: Bacterial pathogenicity is the ability of a bacterium to cause a disease. The virulence of this bacterium is a quantitative measure of the pathogenicity or the likelihood of causing a disease. Therefore, bacteria produce virulence factors, which are gene products that can damage a susceptible host and that are specifically expressed during the disease process.[36] These products enable a bacterium to invade the host, to replicate and to disseminate within a host by subverting or eluding his defenses.[37]

Consequently, if it was possible to inhibit virulence factor production, e.g. by inhibition of a regulatory key factor, then a pathogenic bacterium would turn in a non-pathogenic microbe, which is by definition not able to cause a disease associated with symptoms.

Bacteria apply cell-to-cell communication to coordinate group behavior. “Quorum sensing” is the more specific term, which is used when regulation of gene expression responds to fluctuations in cell-population density.[38] Chemical signal molecules are produced by the bacteria and released into the environment. The extracellular concentrations reflect the cell density of the population, which can in turn be detected by single cells of the colony to simultaneously alter gene expression. This allows a population to behave coordinately and synergistically as pseudo-multicellular organism. In this way, single bacterial cells can limit their effort regarding group-beneficial activities to cell densities that guarantee an effective population-wide outcome.[39]

P. aeruginosa uses QS to regulate the coordinated production of a considerable arsenal of virulence factors determining the high pathogenicity. Initial colonization is mostly accomplished by cell-associated virulence factors as pili, lectins, alginate, and flagella. In chronic infections, low concentrations of extracellular virulence factors are produced. However, in acute infections high levels of exoproducts as proteases, exotoxin A, pyocyanin, siderophores, and hemolysins are required for tissue invasion and dissemination within the host. Thereby, the concentration-dependent coordination by QS is a perceptive strategy to overwhelm the host’s defense mechanisms.[40] Additionally, QS plays an important role in biofilm formation, which is a key factor for bacterial resistance.[41]

Taken together, QS plays an important role for *P. aeruginosa* pathogenicity. It is the key regulatory network for the production of virulence factors and, thus, seems to be an attractive target for pursuing an anti-virulence strategy.[42]

1.3 Quorum Sensing in *P. aeruginosa*

The nature of the signal molecules employed for QS strongly depends on the bacteria. Gram-positive bacteria primarily use modified oligopeptides, whereas *N*-acyl homoserine lactones (AHLs) are the major class of signal molecules in Gram-negative bacteria.[43] Dependent on the species, AHLs with different length and substitution of their acyl side chain are produced (Figure 1a).[44] Biosynthesis is accomplished by a LuxI-type synthase (named after the first discovered homolog, which regulated the luminescence gene *lux* in *V. fischeri*). Afterwards, the signal molecules diffuse between cells and can be detected by a LuxR-type transcriptional regulator, which changes expression of target genes after activation. Characteristically, activation of LuxR-type regulators increases the expression of the corresponding synthase, which is why the signal molecules are also called autoinducers. This positive feedback loop allows a rapid increase in signal molecule production after a certain threshold in cell density

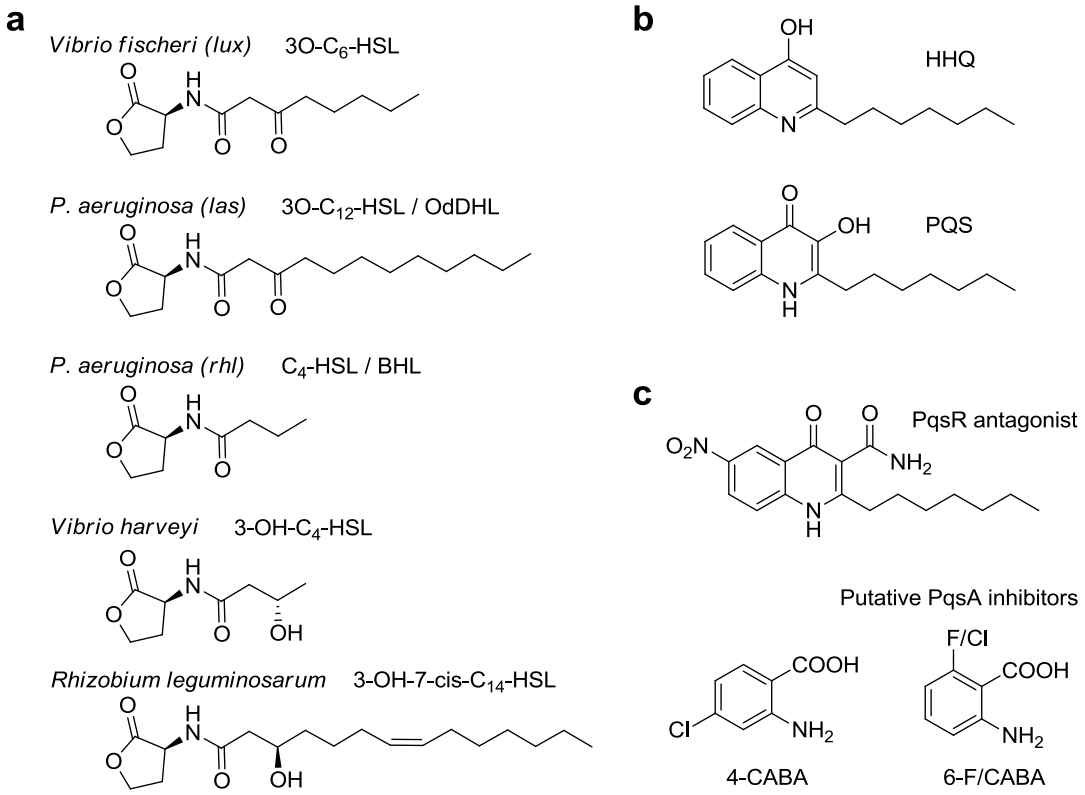

Figure 1. a) Selection of various AHLs applied as signal molecules by different bacteria. b) Structure of *pqs* signal molecules HHQ and PQS. c) Structures of known QS inhibitors.

has been reached. *P. aeruginosa* contains two AHL-based QS systems, the *las* and the *rhl* system. In the first one, LasI directs the synthesis of *N*-(3-oxododecanoyl)-L-homoserine lactone (3O-C_{12}-HSL or OdDHL), which is recognized by LasR.[45,46] The *rhl* system consists of the RhlI/R pair and uses *N*-butyryl-L-homoserine lactone (C_4-HSL or BHL, see Figure 1a) as autoinducer.[47,48] Furthermore, *P. aeruginosa* applies a third so-called *pqs* system, which is characteristic for particular *Pseudomonas* and *Burkholderia* species.[49] This system utilizes the *Pseudomonas* quinolone signal (PQS) and its precursor 2-heptyl-4-hydroxyquinoline (HHQ) as signal molecules (Figure 1b).[50,51] Both molecules are able to bind and activate the transcriptional regulator PqsR (formerly called MvfR for multiple virulence factor regulator), whereas PQS shows a ca. 100-fold higher affinity than HHQ.[52] Activation of PqsR positively regulates the expression of the *pqsABCDE* operon, which is responsible for HHQ and PQS production, establishing a feedback circuit similar to the *las* and *rhl* systems.[50] In addition to this PqsR autoinduction loop, PQS operates about at least two more distinct pathways (Figure 2). Firstly, *pqsE* is required for expression of many PQS controlled virulence factors and disruption leads to loss of several but not all PQS-dependent signal transductions. PqsE is not involved in PQS biosynthesis and its exact function remains unknown, hence it was designated as PQS response protein.[53,54] Secondly, PQS, but not HHQ, is able to chelate iron(III), which is an essential nutrient in *P. aeruginosa.*[53,55] Thereby, PQS does not act as an siderophore but it has been suggested that PQS acts as an iron trap at the cell surface, which might facilitate siderophore-mediated iron transport.[53] Furthermore, transcriptional analysis in response to PQS revealed altered gene expression, e.g. the upregulation of the siderophore pyoverdine.[55]

The QS systems present in *P. aeruginosa* are not strictly separated but rather closely linked and hierarchically organized (Figure 2). The *las* system is dominant over the *rhl* system, since the LasR/OdDHL complex positively regulates the expression of *rhlR*. Moreover, OdDHL is able to bind but not to activate RhlR, leading to a competition with RhlR's autoinducer BHL.[56] The expression of the PQS biosynthetic operon *pqsABCDE* is positively regulated by LasR/OdDHL and negatively regulated by RhlR/BHL.[57,58] The *pqs* system in turn causes a major induction of *rhlI* and a minor one on *lasR* and *rhlR*.[59]

However, the cross-linked network hampers the identification of direct regulation pathways. Only in a few cases, the specific interaction of a signal molecule/transcriptional regulator complex with a promoter region was demonstrated. Especially the regulation of virulence factor production is overly reliant on comparison of wild-type and mutant transcriptome. It

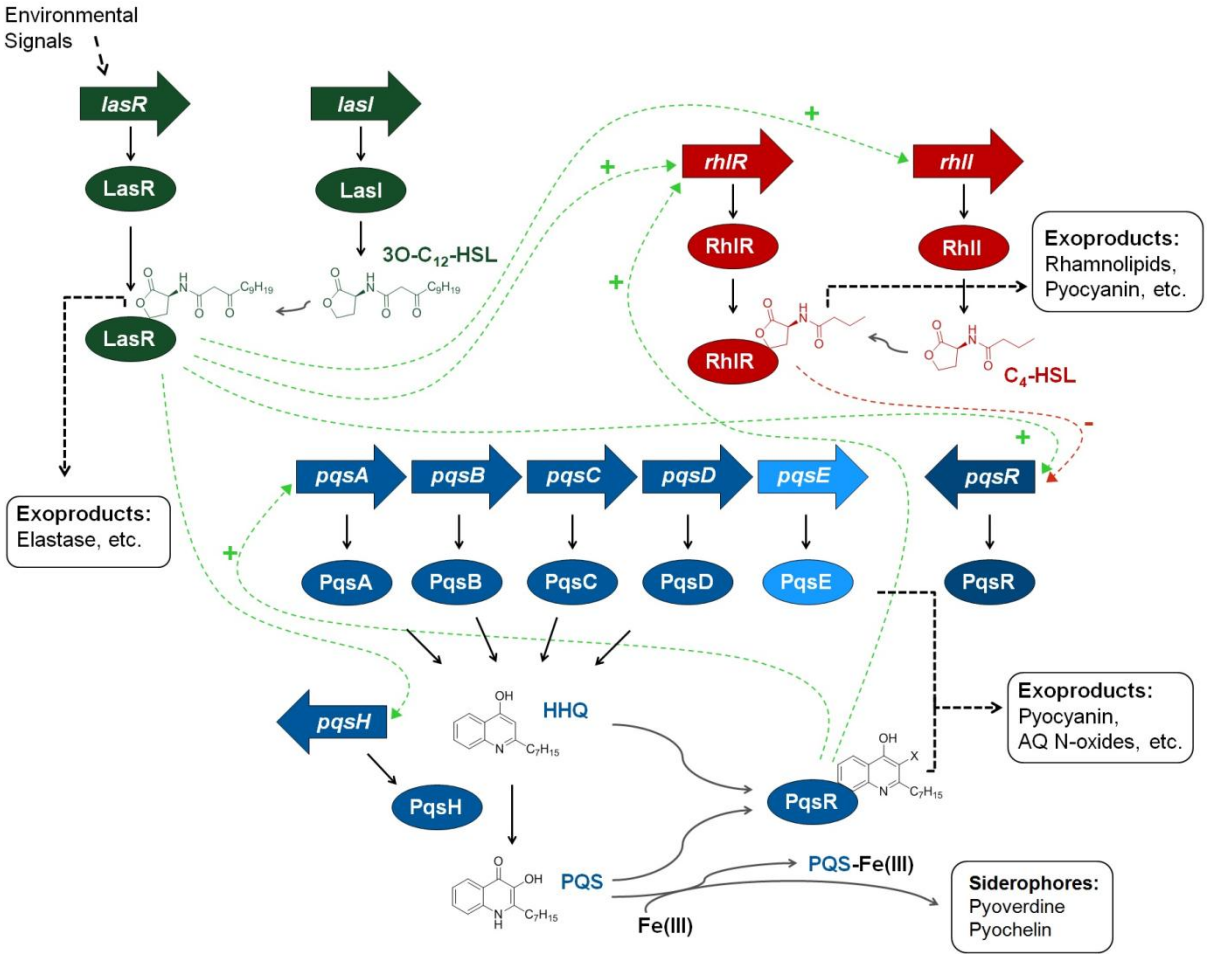

Figure 2. *P. aeruginosa* QS circuit. Genes and proteins of the *las*, *rhl*, and *pqs* systems are colored in green-grey, red, and blue, respectively. Bright green dashed arrows represent positive regulation; red dashed arrows represent negative regulation. Modified from Dubern and Diggle (2008).[60]

was claimed, for example, that pyocyanin production is directly controlled by the *rhl* system[61] even though it has never been proven and indirect effects may well be possible.

Indeed, several mutants of *P. aeruginosa* including *lasR*, *rhlR*, and *pqsR* (as well as the PQS biosynthetic genes *pqsC* and *pqsD*) are defective in the production of pyocyanin,[54] which is a crucial virulence factor causing serious tissue damage and necrosis during lung infections.[62] Thus, inhibition of one system might lead to decreased production of various virulence factors, even if these are only indirectly controlled by the affected system.

1.4 Inhibition of *pqs* QS in *P. aeruginosa*

Disruption of the *pqs* system seems to be an especially attractive anti-virulence strategy. As mentioned above, AHLs are widely spread among Gram-negative bacteria. And even if each species produces a unique AHL, which interacts with the species specific LuxR-type receptor,

there is a high risk that small molecule inhibitors interfere with cell-to-cell communication of multiple bacterial species. However, this is unintentional, since even non-pathogenic or beneficial bacteria would be affected. This is the key advantage of targeting the *pqs* system. Modulation of *pqs* QS would specifically discriminate quinolone-signaling competent *Pseudomonas* and *Burkholderia* species. Thus, populations of non-pathogenic bacteria may take advantage in the competition for limited nutrients and habitat leading to the repression of *P. aeruginosa*. Additionally, it has been shown that especially PQS is closely linked to biofilm formation and maturation, which is a key factor for bacterial resistance.[63,64]

There are several conceivable targets within the *pqs* system, which might be appropriate for interference by small molecules. PqsE participates in the regulation of several virulence factors, but is not required for 4-hydroxy-2-alkyl-4-quinolone (HAQ) biosynthesis.[54] The described function as cellular response on PQS might indicate, that PqsE is located downstream in the QS network having a minor impact on QS gene regulation in *P. aeruginosa*. Additionally, the fact, that the function of PqsE is still not understood, hampers a drug discovery process.

PqsR has been shown to drive the expression of nearly 200 genes, including genes encoding virulence factors as pyocyanin and hydrogen cyanide.[65-67] However, three pathways have been described for PQS mediated effects (PqsR, PqsE and iron chelation) and at least the regulation of pyoverdine production is independent of PqsR.[53] Furthermore, from a drug discovery point of view, the hydrophobic binding pocket optimized to bind HHQ and PQS might be challenging, since it has been proposed that (due to the outer membrane barrier) high hydrophilicity is beneficial or even required for activity in Gram-negative bacteria.[68] Nevertheless, several classes of PqsR antagonists were recently developed.[49,69-71] The most promising compound (Figure 1c) showed strong inhibition of pyocyanin and significantly reduced the mortality of *Caenorhabditis elegans* and *Galleria mellonella* infected with *P. aeruginosa* PA14, underlining the potential of the *pqs* system as target. This PQS-derived compound might use the HAQ transport system to overcome the cellular penetration barrier, but drug-likeness is limited due to the high lipophilicity.

Enzymes, which are essential for PQS biosynthesis, represent further promising targets for an anti-virulence strategy. Since PqsR has to be activated by PQS (or HHQ), similar effects as for PqsR inhibitors are expected. Furthermore, also the PqsE and Fe(III) mediated pathway should be inhibited. Taken together, there are several indications, that the biosynthetic enzymes play a central role within the *pqs* QS system.

Indeed, halogenated anthranilate analogs (Figure 1) were reported by Lesic *et al.* to inhibit PQS biosynthesis and PqsR regulated gene expression. Furthermore, these putative PqsA inhibitors (see Figure 3 for the role of PqsA) reduced the *P. aeruginosa* systemic dissemination and mortality in a burned mouse model. However, the compounds had to be used in unreasonably high concentrations and optimized derivatives were not reported until now.

1.5 HAQ Biosynthesis and the Role of PqsD

In contrast to the LuxI-type biosynthetic proteins, HHQ and PQS production is more complicated and accomplished by several enzymes (Figure 3). Anthranilate is one of the precursors from which PQS is synthesized.[72] It can be derived from tryptophan by the kynurenine (kyn) pathway or from chorismic acid via a unique anthranilate synthase operon *phnAB*, which is regulated by PqsR to ensure sufficient anthranilate supply when the *pqs* system is turned on.[52,73,74]

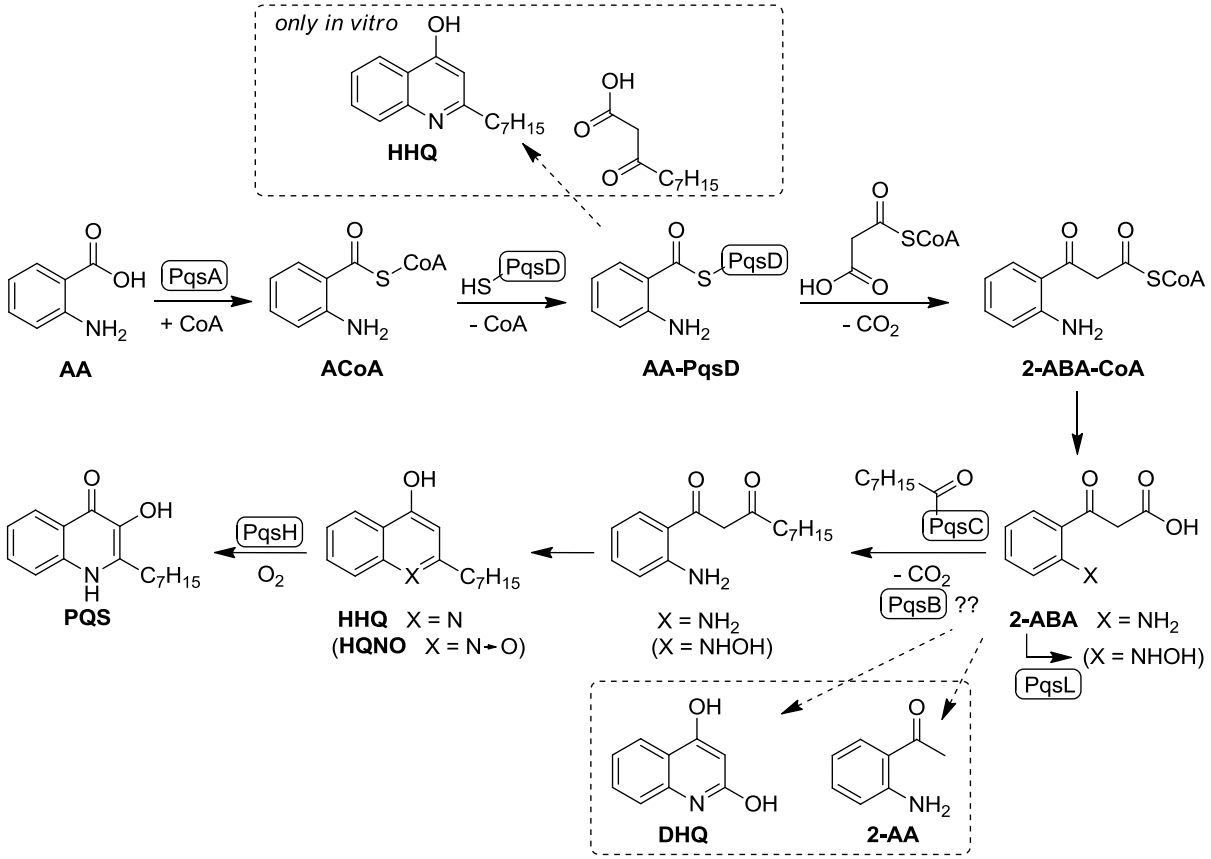

Figure 3. Proposed mechanism of HHQ and PQS biosynthesis. PqsD is an essential enzyme for all derivatives, since it is responsible for the production of the key intermediate 2-ABA. Furthermore, it is sufficient for the conversion of ACoA and malonyl-CoA into DHQ as well as HHQ production *in vitro*. Modified from Dulcey *et al.* (2013).[76]

The reaction cascade catalyzed by the gene products of the biosynthetic operon *pqsABCD* starts with the activation of anthranilate as thioester by the CoA ligase PqsA.[75] This enables the transfer of anthranilate to Cys112, forming a covalent AA-PqsD complex,[77] which has been proven unambiguously by an X-ray structure.[78] Recently, Dulcey *et al.* reported that reaction with malonyl-CoA leads in a two step reaction over the hypothetical CoA-activated 2-aminobenzoylacetate (2-ABA-CoA) to 2-ABA.[76] This reactive intermediate is then converted to HHQ by PqsC using octanoic acid as substrate. This conversion requires the presence of PqsB. However, the exact mechanism of the reaction remains unknown.

Interestingly, PqsD alone is able to synthesize HHQ *in vitro* directly from ACoA using β-ketodecanoic acid as secondary substrate,[79] which was recently ruled out to happen *in cellulo* by labeling experiments.[76]

The oxidation of HHQ to PQS is accomplished by the NADH-dependent flavin monooxygenase PqsH.[80] This enzyme is not encoded by the *pqsABCDE* operon, but positively regulated by OdDHL/LasR (but not PqsR/PQS). Since O_2 is essential for the oxidation and no PQS can be observed in an anaerobic environment, this reaction can be considered as trigger for aggressive group behavior when supplied with oxygen.[80]

P. aeruginosa produces at least 55 HAQ derivatives, but only HHQ and PQS have been shown to participate in cell-to-cell signaling.[81] This array of compounds was classified into 5 distinct series (Figure 4).[50] All series share the common 4-hydroxyquinoline structure of series A. Congeners of series B have a hydroxy group in 3-position, whereas derivatives of series C and D share an *N*-oxide group. Alkyl chains of series D and E are unsaturated. Many of these HAQs, especially HQNO, were described to be potent cytochrome inhibitors and antibiotics active against commensal and pathogenic bacteria, which give *P. aeruginosa* an ecological advantage in competitive environments.[50,82,83]

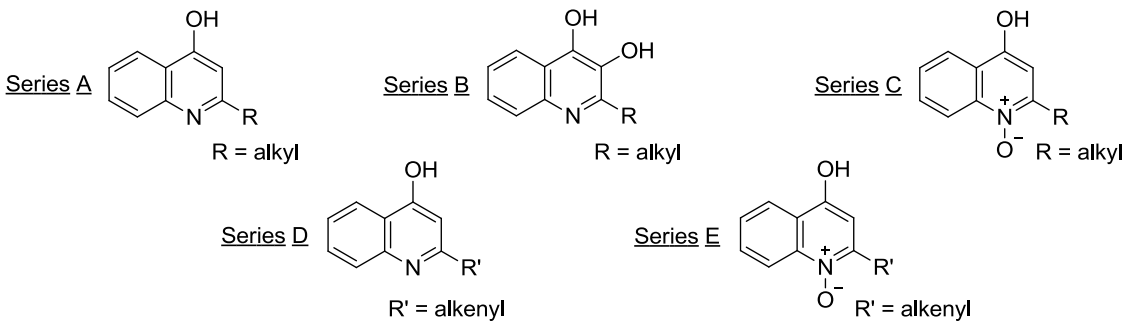

Figure 4. Structures of five distinct series of HAQs isolated from *P. aeruginosa* PA14 culture supernatant. Most prominent derivatives of Series A, B, and C are HHQ, PQS, and HQNO, respectively. This indicates the biosynthetic enzymes preference for R = C_7H_{15} side chains. Modified from Déziel *et al.* (2004).[50]

The monooxygenase PqsL has been shown to be required for synthesis of all *N*-oxide congeners (series C and E), including HQNO.[81] 2-ABA is likely the substrate of PqsL probably leading to a hydroxylamino derivative. Processing with PqsC and octanoic acid as described for HHQ and ring closure by nucleophilic attack on the carbonyl group should lead to HQNO production.[76]

When 2-ABA is purified it is unstable and degrades to DHQ (predominantly produced under acidic conditions) and 2-aminoacetophenone (2-AA), which might happen in absence of the required reactants and enzymes *in cellulo*.[76,77] Thus, PqsA and PqsD are sufficient for DHQ and 2-AA biosynthesis. The physiological role of DHQ is not fully understood, however, DHQ contributes to pathogenicity of *P. aeruginosa* by inhibition of the cell viability of mouse lung epithelial MLE-12 cells.[77] The recently identified 2-AA promotes the adaptation of *P. aeruginosa* to chronic infections, whereas the production of PqsR-regulated acute virulence factors is reduced. Accordingly, treatment with 2-AA has been shown to reduce mortality of PA14-infected flies and mice.[84]

Taken together, PqsA and PqsD are key players in the biosynthesis of all HAQs as well as DHQ and 2-AA. Thus, inhibition should have major influence on cell communication. Unfortunately, no structural information about PqsA exists in literature. In contrast, the X-ray structure of PqsD shows a deep and narrow substrate channel formed by several hydrophilic amino acids. Therefore, we consider PqsD as the most attractive target for an anti-virulence strategy to combat *P. aeruginosa* infections.

2 Aim of the Thesis

Antibiotic resistance is a serious risk for the major achievements of modern medicine in the last 60 years. Untreatable bacterial infections threaten life quality and expectancy, but are also an economic burden. Due to the rapid global spread of drug-resistant strains, the solution of this problem challenges politics and scientific communities world-wide. For example, the excessive and often irresponsible usage of antibiotics must be restricted. But, especially the development of new therapeutics is crucial. Otherwise we will lose the race against time, since the evolution of resistances might be slowed down but can hardly be prevented.

As a small part of the drug development community, we want to contribute to the finding of novel eligible treatment strategies against *P. aeruginosa*, one of today's most problematic pathogens. Anti-virulence strategies, which combat pathogenicity but do not restrict cell viability, could prevent pathogens from developing drug resistances, even though the proof of concept is pending. Thereby, we consider the biosynthetic enzyme PqsD as promising target, since it plays a key role in the regulatory *pqs* cell-to-cell communication system of *P. aeruginosa*.

This thesis is aimed at the development of the first PqsD inhibitors. Since no assay to evaluate the potency of molecules in a high-throughput fashion was available, experimental screening methods for the identification of hit compounds were excluded. Consequently, a ligand-based approach was pursued by mimicking the natural ligand ACoA and the corresponding transition state. The identified small molecules should ideally be capable of inhibiting signal molecule production in *P. aeruginosa* cells.

The detailed knowledge how an inhibitor binds and inhibits an enzyme enables the rational and efficient optimization. For this purpose, modern biophysical and biochemical methods were applied to propose plausible binding poses. These poses were additionally used to assess whether the inhibitors bind as expected for natural substrate or transition state mimics. Furthermore, beneficial binding characteristics for novel inhibitor classes could be derived. However, since inhibitors of intracellular targets in *P. aeruginosa* have to overcome multiple barriers to reach their targets, structure-activity relationships with respect to *in vitro* and *in cellulo* inhibitory activity provided information about crucial molecular properties.

The resulting optimized compounds are valuable tools to elucidate regulatory pathways of the QS system and virulence factor production in *P. aeruginosa*. No less important, they provide first distinct clues, whether PqsD is an appropriate target for the treatment of *P. aeruginosa* infections.

3 Results

3.1 Validation of PqsD as an Anti-biofilm Target in *Pseudomonas aeruginosa* by Development of Small-Molecule Inhibitors

Michael P. Storz, Christine K. Maurer, Christina Zimmer, Nathalie Wagner, Christian Brengel, Johannes C. de Jong, Simon Lucas, Mathias Müsken, Susanne Häussler, Anke Steinbach, and Rolf W. Hartmann

Publication A

Contribution Report

The author contributed significantly to the rational ligand design concept. He planned, synthesized and characterized all compounds. Furthermore, he conceived and wrote the manuscript.

JACS
JOURNAL OF THE AMERICAN CHEMICAL SOCIETY
Communication
pubs.acs.org/JACS

Validation of PqsD as an Anti-biofilm Target in *Pseudomonas aeruginosa* by Development of Small-Molecule Inhibitors

Michael P. Storz,[†] Christine K. Maurer,[†] Christina Zimmer,[†] Nathalie Wagner,[†] Christian Brengel,[†] Johannes C. de Jong,[†] Simon Lucas,[†,⊥] Mathias Müsken,[§,∥] Susanne Häussler,[§,∥] Anke Steinbach,*[,†] and Rolf W. Hartmann*[,†,‡]

[†]Helmholtz-Institute for Pharmaceutical Research Saarland (HIPS), Campus C2$_3$, 66123 Saarbrücken, Germany
[‡]Pharmaceutical and Medicinal Chemistry, Saarland University, Campus C2$_3$, 66123 Saarbrücken, Germany
[§]Institute for Molecular Bacteriology, TWINCORE, Feodor-Lynen-Str. 7, 30625 Hannover, Germany
[∥]Department of Molecular Bacteriology, Helmholtz Centre for Infection Research, Inhoffenstr. 7, 38124 Braunschweig, Germany

Supporting Information

ABSTRACT: 2-Heptyl-4-hydroxyquinoline (HHQ) and *Pseudomonas* quinolone signal (PQS) are involved in the regulation of virulence factor production and biofilm formation in *Pseudomonas aeruginosa*. PqsD is a key enzyme in the biosynthesis of these signal molecules. Using a ligand-based approach, we have identified the first class of PqsD inhibitors. Simplification and rigidization led to fragments with high ligand efficiencies. These small molecules repress HHQ and PQS production and biofilm formation in *P. aeruginosa*. This validates PqsD as a target for the development of anti-infectives.

Pseudomonas aeruginosa is the most common Gram-negative bacterium found in nosocomial infections. It primarily infects immunocompromised individuals, and cystic fibrosis patients are susceptible to chronic lung infections.[1] Its pathogenicity is strongly related to the expression of an unusually large number of virulence factors, which cause tissue damage, delay airway epithelium wound repair, and suppress innate immune response.[2] Drug therapy is hindered by biofilms. The sessile cell communities are embedded in a matrix of extracellular polymeric substances and show a reduced growth rate and altered gene transcription.[3] These factors prevent antimicrobial agents from penetrating and eradicating the bacteria. The regulation of virulence factor expression as well as biofilm formation is based on quorum sensing (QS), a cell-density-dependent intercellular communication system that uses small molecules.[2] Hence, selective inhibition of QS has been discussed as an alternative approach for addressing pathogenicity and biofilm formation without affecting cell viability, which selects for drug resistance.[4,5]

The *pqs* QS system is restricted to particular *Pseudomonas* and *Burkholderia* species and utilizes *Pseudomonas* quinolone signal (PQS) and its precursor, 2-heptyl-4-hydroxyquinoline (HHQ), for cell-to-cell communication (Scheme 1).[6] In *P. aeruginosa*, PQS and HHQ activate the transcriptional regulator PqsR, thereby enhancing the expression of their own biosynthetic operon *pqsABCDE*.[7] This autoinduction enables a rapid increase in the production of the signal molecules, and their dissemination in the environment allows coordinated behavior of the population. Furthermore, HHQ and PQS are involved in the expression of many genes encoding for virulence factors such as pyocyanine, elastase B, lectin A, rhamnolipids, and hydrogen cyanide.[1,8] In addition, PQS is capable of promoting biofilms, although the mechanism of action is unclear.[9,10]

PqsD is a key enzyme in the biosynthesis of HHQ and PQS (Scheme 1a). Anthraniloyl-CoA (ACoA), a "bioactivated" anthranilic acid formed by PqsA, is the first substrate used by PqsD. Nucleophilic attack by the sulfur atom of Cys112 leads to a tetrahedral transition state. Elimination of CoA results in a covalent anthranilate−PqsD complex, which has been characterized by an X-ray structure.[11] We have shown that PqsD is able to accomplish HHQ formation by catalyzing the condensation and cyclization reaction with multiple species of β-ketodecanoic acid in vitro, and we have elucidated its kinetic mechanism.[12,13] PqsH, which is not encoded by the *pqsABCDE* operon, is responsible for the conversion of HHQ to PQS.[14] Furthermore, PqsD has controversially been proposed to be responsible for the synthesis of 2,4-dihydroxyquinoline (DHQ) in *P. aeruginosa* (Scheme 1a).[15,16] Hence, we consider PqsD to be an attractive target for drug development.

Furthermore, it has been shown that anthranilic acid derivatives as potential PqsA inhibitors reduced HHQ and PQS production in *P. aeruginosa* and their systemic dissemination and mortality in mice.[17] We recently showed that two inhibitors of FabH, a structurally and functionally related enzyme, also inhibit PqsD[12] [the structures of these two inhibitors, denoted as **A** and **B**, are shown in the Supporting Information (SI)]. These were the first inhibitors described, but their inhibitory activity against PqsD is moderate, and their effects on *P. aeruginosa* cells have not been examined. For this reason, we applied a ligand-based approach for the development of a new class of nonbactericidal PqsD inhibitors. Two main strategies were pursued. First, ketones **1** and **2** (Scheme 1b) are substrate analogues mimicking ACoA. In these molecules, the scissile thioester is replaced by a methylene ketone moiety, thereby making the molecules potential covalent modifiers that can bind to the active-site residue Cys112 but cannot be hydrolyzed. In this case, electron-withdrawing groups such as

Received: July 24, 2012
Published: September 19, 2012

dx.doi.org/10.1021/ja3072397 | J. Am. Chem. Soc. 2012, 134, 16143−16146

Scheme 1. HHQ, PQS, and DHQ Biosynthesis in *P. aeruginosa* and Our Ligand-Based Design Concept[a]

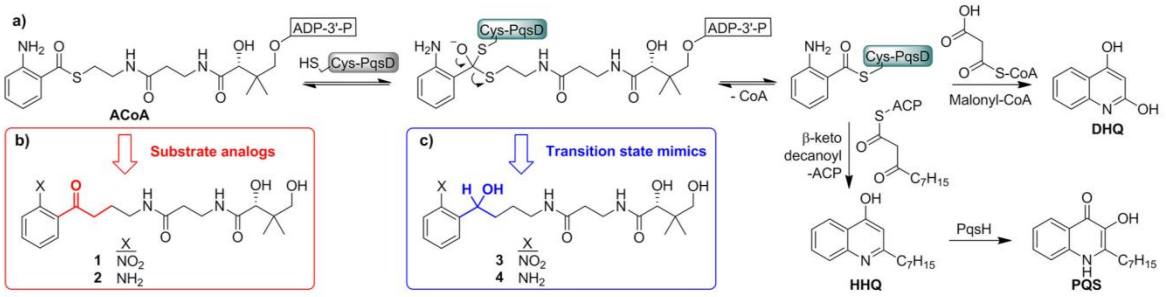

[a](a) PqsD-catalyzed HHQ, PQS, and DHQ formation. Attack by Cys112 on the carbonyl function of ACoA leads to a tetrahedral transition state. Elimination of CoA completes the transfer of anthranilate to PqsD and clears the way for the second substrate. (b) Analogues of the natural substrate ACoA. The sulfur atom of the scissile thioester is exchanged for methylene to prevent elimination of pantetheine. (c) Mimics of the transition state: sp^3 hybridization of the α-carbon atom results in a tetrahedral geometry similar to that in the transition state.

Scheme 2. Synthesis of Substrate Analogues 1 and 2 and Transition State Mimics 3 and 4[a]

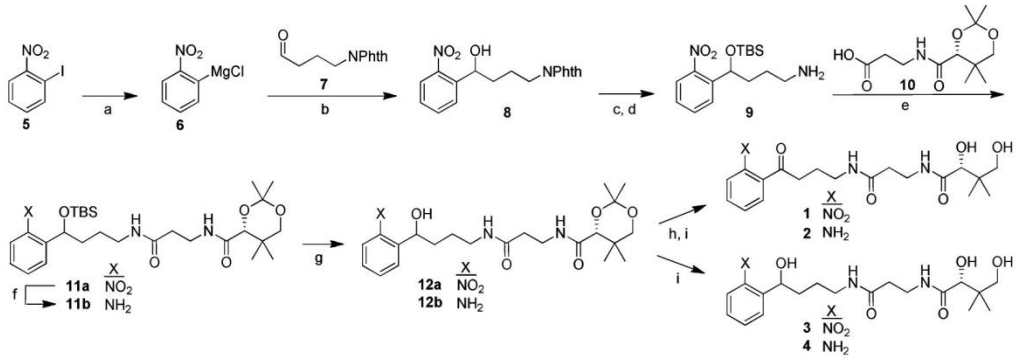

[a]Reagents and conditions: (a) PhMgCl, THF, −40 °C, 30 min; (b) THF, −40 °C, 30 min, 85% (two steps); (c) TBSCl, imidazole, DMF, rt, 18 h, 62%; (d) $N_2H_4 \cdot H_2O$, EtOH, reflux, 150 min, 98%; (e) DCC, 4-hydroxy-1*H*-benzotriazole, DMF, rt, 19 h, 67%; (f) H_2 (1 atm), Pd/C (10 wt %), ethyl acetate, rt, 20 h, 87%; (g) TBAF (1M), THF, rt, 80 min; (h) for **1**: DMP, DCM, rt, 90 min; for **2**: PCC, DCM, rt, 18 h; (i) HCl(aq) (1 N), ethyl acetate, rt, 3 h.

nitro groups should facilitate nucleophilic attack on the carbonyl moiety by Cys112, and the equilibrium should be shifted in favor of the hemiketal. In a second approach, analogues of the tetrahedral transition state (Scheme 1c) were examined. These molecules, **3** and **4**, bear a hydroxymethylene group that imitates the tetrahedral geometry of the transition state.

As shown in Scheme 2, the synthesis of compounds **1**−**4** started from 1-iodo-2-nitrobenzene (**5**). Iodine−magnesium exchange using a described method[18] provided the nitro-substituted Grignard reagent **6**. Subsequent reaction with aldehyde **7**, which was synthesized from 4-aminobutan-1-ol in a two-step procedure,[19] resulted in the formation of alcohol **8**. Protection as the *tert*-butyldimethylsilyl (TBS) ether and subsequent cleavage of the phthalimide moiety by hydrazine hydrate afforded primary amine **9**. *N*,*N*′-dicyclohexylcarbodiimide (DCC)-mediated coupling with the protected pantothenic acid **10**[20] completed the molecular scaffold in **11a**. Cleavage of the TBS ether using tetrabutylammonium fluoride (TBAF) afforded alcohol **12a**. The synthesis of ketone **1** was accomplished by oxidation of the benzylic alcohol using Dess−Martin periodinane (DMP) followed by acid-catalyzed hydrolysis of the ketal moiety, while direct ketal deprotection of **12a** gave compound **3**. For the synthesis of the amines **2** and **4**, the nitro group of **11a** was hydrogenated using Pd on carbon. A subsequent reaction cascade of TBS ether cleavage, oxidation of alcohol **12b** using pyridinium chlorochromate (PCC), and ketal hydrolysis afforded aminoketone **2**. Direct hydrolysis of **12b** yielded aminoalcohol **4**.

The synthesized compounds were tested for PqsD inhibition using ACoA and β-ketodecanoic acid as substrates and heterologously expressed and purified enyzme.[12] The HHQ product was quantified by HPLC−MS/MS. Ketones **1** and **2** showed little or no inhibition of PqsD (Table 1). However, the nitro-bearing transition state analogue **3** inhibited HHQ formation [half-maximal inhibitory concentration (IC_{50}) = 7.9 μM], while no activity was observed for the corresponding amino alcohol **4**.

Encouraged by the inhibitory activity of **3**, we shortened the side chain to reduce the molecular weight and restrict the flexibility (Table 1) while preserving the 1-(2-nitrophenyl)-alcohol moiety as the key pharmacophore. Truncated alcohol **14**, which was synthesized by treatment of intermediate **9** with acetic anhydride and subsequent removal of the TBS group (Scheme 3), showed a better IC_{50} (4.3 μM) and an improved ligand efficiency (LE). In contrast to the nitro-substituted ketone **1**, the truncated carbonyl compound **15** showed an activity (IC_{50} = 7.8 μM) similar to that of the corresponding alcohol **14**. The inhibitory potencies of the two truncated compounds indicate

dx.doi.org/10.1021/ja3072397 | *J. Am. Chem. Soc.* 2012, 134, 16143−16146

Journal of the American Chemical Society Communication

Table 1. PqsD Inhibition by Substrate Analogues 1 and 2, Transition State Mimics 3 and 4, and Compounds 14−25 and A

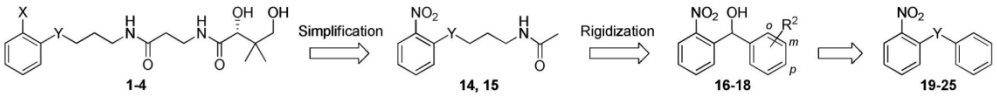

compound	X	Y	R^2	% inhibition[a,b]	IC_{50} (μM)[a,c]	K_d (μM)[d]	LE[e]
1	NO_2	CO		18			
2	NH_2	CO		n.i.			
3	NO_2	CH−OH		95	7.9		0.25
4	NH_2	CH−OH		n.i.			
14		CH−OH		99	4.3		0.42
15		CO		98	7.8		
16		CH−OH	*o*-NHAc	93	6.2		
17		CH−OH	*m*-NHAc	99	9.0		
18		CH−OH	*p*-NHAc	98	6.4		
19		CH−OH		99	3.2	13	0.45 (0.39)[f]
20		CO		n.i.			
21		CH_2		24 (25 μM)			
22		SO_2		87	14.8		
23		CH−OMe		97	4.3		0.42
24		C(CH_3)−OH		n.i.			
25		C(CF_3)−OH		n.i.			
A[g]					35		0.20

[a] *P. aeruginosa* PqsD (recombinantly expressed in *Escherichia coli*), anthraniloyl-CoA (5 μM), and β-ketodecanoic acid (70 μM). Under the conditions used, ~12% of the substrate (ACoA) was converted into HHQ. The inhibitor concentration was 50 μM. [b] Percent inhibition was calculated from the ratio of HHQ production with and without inhibitor; n.i. = no inhibition (i.e., <10% inhibition). [c] IC_{50} is the inhibitor concentration necessary to reduce product formation by 50%. [d] Isothermal titration calorimetry (ITC) was performed at 298 K. [e] For comparison, ligand efficiency (LE) values were calculated as LE = $-1.4 \log[IC_{50}/(\text{mol/L})]/N_{\text{non-H}}$, where $N_{\text{non-H}}$ is the heavy atom count (i.e., the number of non-hydrogen atoms). [f] The LE value in brackets was calculated as LE = $[\Delta G/(\text{kcal/mol})]/N_{\text{non-H}}$, where ΔG is the change in Gibbs energy as calculated using K_d. [g] **A** is a FabH-inhibitor-derived compound (for its structure, see the SI); data taken from ref 12.

Scheme 3. Synthesis of Compounds 14 and 15[a]

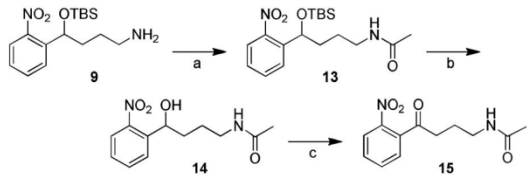

[a] Reagents and conditions: (a) Ac_2O, pyridine, rt, 17 h, 60%; (b) TBAF (1 M), THF, rt, 2 h, 60%; (c) DMP, DCM, rt, 4 h, 71%.

that the omitted moiety plays no significant role in protein binding.

Next, we rigidified alcohol **14** by substituting the flexible propyl chain with a phenyl moiety and then examined all of the regioisomers **16**−**18**. The inhibitory potency could not be improved, as the IC_{50} value remained between 6.2 and 9.0 μM. Since the position of the acetamido substituent had only a small impact on activity, the unsubstituted phenyl derivative **19** was synthesized. It showed enhanced activity (IC_{50} = 3.2 μM) and a high LE (0.39). Separation of **19** into its enantiomers revealed that the activity of **19** is not stereoselective (Table S1 in the SI). The corresponding ketone **20** was inactive, perhaps because of the planar conformation of the conjugated π system. Consequently, we examined **21**−**23**, each of which contains a tetrahedral linker between the two phenyl moieties. For compound **21** bearing a methylene linker, little activity was restored. Moreover, the sulfone linker in **22** resulted in moderate activity (IC_{50} = 14.8 μM). The only compound reaching activity similar to that of alcohol **19** was the corresponding methyl ether **23** (IC_{50} = 4.3 μM). To modify the electronic properties of the hydroxyl group, the methylene hydrogen was substituted with an electron-donating methyl group and an electron-withdrawing trifluoromethyl group to give **24** and **25**, respectively, both of which were inactive. The syntheses of the rigidified (2-nitrophenyl)methanol derivatives is described in Scheme 4.

Scheme 4. One-Pot Synthesis of Derivatives 16−19, 24, and 25 and Hydroxymethylene Linker Modification to Obtain 20 and 23[a]

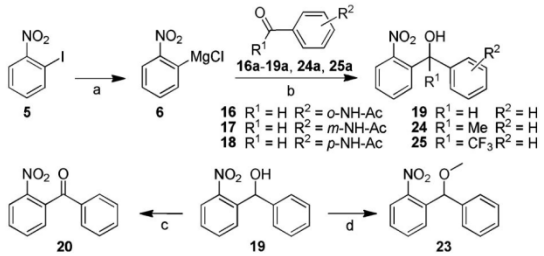

[a] Reagents and conditions: (a) PhMgCl, THF, −40 °C; (b) THF, $CeCl_3$ for R^1 = CH_3, −40 °C; (c) DMP, DCM, 40 °C, 16 h, 34%. (d) NaH, MeI, DMF, 0 °C, 1 h, 42%.

With compound **19** as a highly potent PqsD inhibitor in hand, experiments were performed to elucidate its physiological and pharmacological significance. First, the influence of **19** on HHQ, PQS, and DHQ production was determined in *P. aeruginosa* PA14 cultures at a concentration of 250 μM. As can be seen from Figure 1, both the HHQ and PQS levels were strongly reduced by 77 and 42%, respectively. Interestingly, the DHQ level increased in the presence of **19**, supporting the finding of Lépine

dx.doi.org/10.1021/ja3072397 | J. Am. Chem. Soc. 2012, 134, 16143−16146

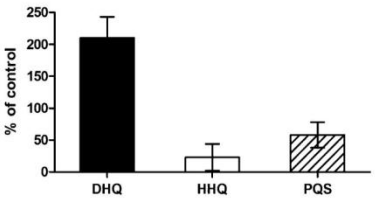

Figure 1. Determination of extracellular DHQ, HHQ, and PQS levels produced by *P. aeruginosa* PA14 in the presence of **19** (250 μM) using UHPLC–MS/MS. Experiments were performed twice independently.

and co-workers that *pqsA* is the only gene within the *pqsABCD* cluster that is necessary for DHQ production.[15] The physiological role of DHQ is not fully understood, but it should be mentioned that DHQ inhibits the cell viability of mouse lung epithelial MLE-12 cells, thereby contributing to the pathogenicity of *P. aeruginosa* PA14.[16]

In *P. aeruginosa* it was shown that a mutant having a transposon insertion within the *pqsA* gene (deficient in HHQ and PQS production[21]) forms less biofilm than the wild type.[22] Thus, we tested the influence of compound **19** for its potential to interfere with biofilm formation by *P. aeruginosa* PA14. Indeed, we found that addition of **19** to a 24 h old biofilm reduced the biovolume of the biofilm by 38% within a 24 h incubation period (Figure 2 and Figure S2 in the SI; representative single slices of **19**- and DMSO-treated biofilms are shown in Figures S3 and S4).

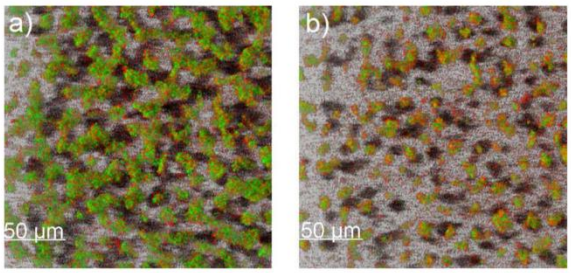

Figure 2. Representative Easy-3D biofilm projections of *P. aeruginosa* PA14: (a) control; (b) after treatment with **19** (500 μM). The 48 h old biofilms were stained with Syto9 (green) and propidium iodide (red), representing living and dead bacteria, respectively.

To exclude the possibility that the biological effects observed with **19** (inhibition of PQS, HHQ, and biofilm formation) were caused by reduction of bacterial viability, growth curves of PA14 were measured. At a concentration of 500 μM, compound **19** showed no antibacterial effects (Figure S5). Furthermore, no toxic effect of **19** against human THP-1 macrophages was observed at 250 μM. Cell proliferation was reduced by 45% at 500 μM (Figure S6).

In summary, we used a ligand-based approach to develop a new class of PqsD inhibitors with significantly improved inhibitory potency and LE. Using the most active compound, **19**, we showed for the first time that applying a PqsD inhibitor leads to a strong reduction of signal molecules HHQ and PQS and significant reduction of biofilm volume in *P. aeruginosa* PA14. This validates PqsD as a target for the development of anti-infectives.

■ ASSOCIATED CONTENT

Supporting Information

Experimental procedures, characterization data, additional results, and complete ref 4. This material is available free of charge via the Internet at http://pubs.acs.org.

■ AUTHOR INFORMATION

Corresponding Author

anke.steinbach@helmholtz-hzi.de; rolf.hartmann@helmholtz-hzi.de

Present Address

[⊥]Grünenthal Pharma GmbH, Global Drug Discovery, Ziegler-str. 6, 52099 Aachen, Germany.

Notes

The authors declare no competing financial interest.

■ ACKNOWLEDGMENTS

We thank Simone Amann for her help in performing the PqsD assay, Drs. Joseph Zapp and Stefan Boettcher for NMR and MS analyses, and Prof. Dr. Rolf Müller for kindly supplying pET28a(+)/*pqsD*.

■ REFERENCES

(1) Van Delden, C.; Iglewski, B. H. *Emerging. Infect. Dis.* **1998**, *4*, 551.
(2) For a recent review, see: Dubern, J.-F.; Diggle, S. P. *Mol. BioSyst.* **2008**, *4*, 882.
(3) Donlan, R. M.; Costerton, J. W. *Clin. Microbiol. Rev.* **2001**, *15*, 167.
(4) Hentzer, M.; et al. *EMBO J.* **2003**, *22*, 3803.
(5) Rasmussen, T. B.; Givskov, M. *Int. J. Med. Microbiol.* **2006**, *296*, 149.
(6) Diggle, S. P.; Lumjiaktase, P.; Dipilato, F.; Barrett, D. A.; Chhabra, S. R.; Cámara, M.; Williams, P. *Chem. Biol.* **2006**, *13*, 701.
(7) Wade, D. S.; Calfee, M. W.; Rocha, E. R.; Ling, E. A.; Engstrom, E.; Coleman, J. P.; Pesci, E. C. *J. Bacteriol.* **2005**, *187*, 4372.
(8) Déziel, E.; Gopalan, S.; Tampakaki, A. P.; Lépine, F.; Padfield, K. E.; Saucier, M.; Xiao, G.; Rahme, L. R. *Mol. Microbiol.* **2005**, *55*, 998.
(9) Diggle, S. P.; Winzer, K.; Chhabra, S. R.; Worrall, K. E.; Cámara, M.; Williams, P. *Mol. Microbiol.* **2003**, *50*, 29.
(10) Yang, L.; Nilsson, M.; Gjermansen, M.; Givskov, M.; Tolker-Nielsen, T. *Mol. Microbiol.* **2009**, *74*, 1380.
(11) Bera, A. K.; Atanasova, V.; Robinson, H.; Eisenstein, E.; Coleman, J. P.; Pesci, E. C.; Parsons, J. F. *Biochemistry* **2009**, *48*, 8644.
(12) Pistorius, D.; Ullrich, A.; Lucas, S.; Hartmann, R. W.; Kazmaier, U.; Müller, R. *ChemBioChem* **2011**, *12*, 850.
(13) Steinbach, A.; Maurer, C. K.; Henn, C.; Hartmann, R. W.; Negri, M. Submitted.
(14) Schertzer, J. W.; Brown, S. A.; Whiteley, M. *Mol. Microbiol.* **2010**, *77*, 1527.
(15) Lépine, F.; Dekimpe, V.; Lesic, B.; Milot, S.; Lesimple, A.; Mamer, O. A.; Rahme, L. G.; Déziel, E. *Biol. Chem.* **2007**, *388*, 839.
(16) Zhang, Y.-M.; Frank, M. W.; Zhu, K.; Mayasundari, A.; Rock, C. O. *J. Biol. Chem.* **2008**, *283*, 28788.
(17) Lesic, B.; Lépine, F.; Déziel, E.; Zhang, J.; Zhang, Q.; Padfield, K.; Castonguay, M.-H.; Milot, S.; Stachel, S.; Tzika, A. A.; Tompkins, R. G.; Rahme, L. G. *PLoS Pathog.* **2007**, *3*, No. e126.
(18) Sapountzis, I.; Knochel, P. *Angew. Chem., Int. Ed.* **2002**, *41*, 1610.
(19) Li, A.-H.; Moro, S.; Forsyth, N.; Melman, N.; Ji, X.-d.; Jacobson, K. A. *J. Med. Chem.* **1999**, *42*, 706.
(20) Osipov, V. N. Stimulant of Hair Growth Based on a Pantothenic Acid Derivative. WO/2007/021219, Feb 2, 2007.
(21) Gallagher, L. A.; McKnight, S. L.; Kuznetsowa, M. S.; Pesci, E. C.; Manoil, C. *J. Bacteriol.* **2002**, *184*, 6472.
(22) Müsken, M.; Di Fiore, S.; Dötsch, A.; Fischer, R.; Häussler, S. *Microbiology* **2010**, *156*, 431.

3.2 Biochemical and Biophysical Analysis of a Chiral PqsD Inhibitor Revealing Tight-Binding Behavior and Enantiomers with Contrary Thermodynamic Signatures

Michael P. Storz, Christian Brengel, Elisabeth Weidel, Michael Hoffmann, Klaus Hollemeyer, A. Steinbach, Rolf Müller, Martin Empting, and Rolf W. Hartmann

Reprinted with permission from *ACS Chem. Biol.* **2013**, *8*, 2794-2801.

Publication B

Contribution Report

The author planned and performed the experiments regarding time-dependency and reversibility. He was responsible for the design of the experiment. Furthermore, the author significantly contributed to the interpretation of the results. He conceived and wrote the manuscript.

ACS chemical biology

Articles

pubs.acs.org/acschemicalbiology

Biochemical and Biophysical Analysis of a Chiral PqsD Inhibitor Revealing Tight-binding Behavior and Enantiomers with Contrary Thermodynamic Signatures

Michael P. Storz,[⊥,†] Christian Brengel,[⊥,†] Elisabeth Weidel,[†,‡] Michael Hoffmann,[§] Klaus Hollemeyer,[∥] Anke Steinbach,[†] Rolf Müller,[§] Martin Empting,*[,†] and Rolf W. Hartmann*[,†,‡]

[†]Helmholtz-Institute for Pharmaceutical Research Saarland (HIPS), Department Drug Design and Optimization, Campus C2.3, 66123 Saarbrücken, Germany

[‡]Pharmaceutical and Medicinal Chemistry, Saarland University, Campus C2.3, 66123 Saarbrücken, Germany

[§]Helmholtz-Institute for Pharmaceutical Research Saarland (HIPS), Department Microbial Natural Products, Campus C2.3, 66123 Saarbrücken, Germany

[∥]Biochemical Engineering, Saarland University, Campus A1.5, 66123 Saarbrücken, Germany

Supporting Information

ABSTRACT: Antivirulence strategies addressing bacterial pathogenicity without exhibiting growth inhibition effects represent a novel approach to overcome today's crisis in antibiotic development. In recent studies, we examined various inhibitors of PqsD, an enzyme involved in formation of *Pseudomonas aeruginosa* cell-to-cell signaling molecules, and observed desired cellular effects for 2-nitrophenyl derivatives. Herein, we investigated the binding characteristics of this interesting compound class using several biochemical and biophysical methods. The inhibitors showed time-dependent activity, tight-binding behavior, and interactions with the catalytic center. Furthermore, isothermal titration calorimetry (ITC) experiments with separated enantiomers revealed contrary thermodynamic signatures showing either enthalpy- or entropy-driven affinity. A combination of site-directed mutagenesis and thermodynamic profiling was used to identify key residues involved in inhibitor binding. This information allowed the proposal of experimentally confirmed docking poses. Although originally designed as transition state analogs, our results suggest an altered position for both enantiomers. Interestingly, the main difference between stereoisomers was found in the orientation of the hydroxyl group at the stereogenic center. The predicted binding modes are in accordance with experimental data and, thus, allow future structure-guided optimization.

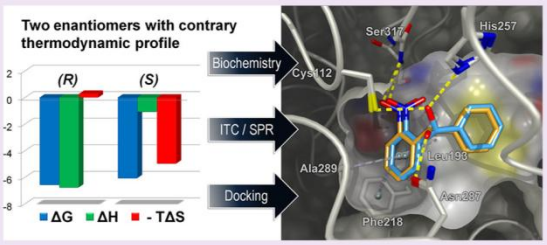

Antimicrobial resistance is a worldwide emerging problem since current treatment becomes more and more inefficient.[1] In *P. aeruginosa*, which is considered as the major cause of mortality in cystic fibrosis patients,[2] several resistance mechanisms against commonly used antibiotics are known. For example, the limited permeability of the outer membrane[3] in combination with broad spectrum multidrug efflux systems[4] can result in a dramatically lowered intracellular drug concentration. Thus, it is all the more important that the compound blocks its target efficiently providing sufficient drug residence time to achieve the desired effects. In the case of competitive inhibitors interacting with the same binding site as the substrate, effectiveness can be drastically diminished by mass-action competition with the substrate. Thus, it was proposed to avoid this unfavorable situation through (pseudo-) irreversible inhibition.[5]

Bacteria apply cell-to-cell communication to coordinate group behavior, a phenomenon that became known as quorum sensing (QS). Thereby, small diffusible signal molecules are produced by bacterial cells and released into the environment. The extracellular concentration reflects the cell density of the population, which can be in turn measured by single members of the colony. Once a special threshold is reached, the population collectively alters its gene expression pattern. Multiple QS systems based on various signal molecules are present in beneficial as well as pathogenic bacteria. *P. aeruginosa* utilizes the quinolone-based *pqs* system, which is characteristic for particular *Pseudomonas* and *Burkholderia* species.[6] The *pqs* system is reported to have crucial influence on biofilm formation and virulence factor production.[7,8] In this regard, inhibition of the *pqs* system is an attractive strategy to overcome biofilm-mediated resistance. Furthermore, QS inhibitors might ideally address pathogenicity without affecting bacterial cell viability. Hence, compared to the current treatment by bactericidal and bacteriostatic antibiotics, less

Received: July 15, 2013
Accepted: October 7, 2013
Published: October 7, 2013

   dx.doi.org/10.1021/cb400530d | ACS Chem. Biol. 2013, 8, 2794−2801

Scheme 1. PqsD-Mediated Formation of HHQ and PQS and Structures of Known PqsD Inhibitors[a]

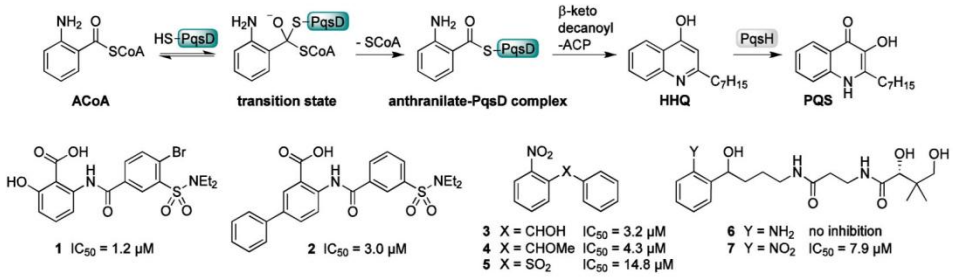

[a]IC_{50} values were taken from refs 11 and 12 and were measured using the screening procedure described in the methods section.

selection pressure to develop resistance against this novel mode of action is expected.[9] Another advantage of *pqs* inhibitors is the absence of quinolone signals in beneficial bacteria, and therefore, the natural microbial flora should not be affected.

PqsD is a key enzyme in the biosynthesis of the *pqs* signal molecules 2-heptyl-4-hydroxyquinoline (HHQ) and 2-heptyl-3-hydroxy-4-quinolone (*Pseudomonas* quinolone signal, PQS) (Scheme 1).[10] For this reason, we consider PqsD as an attractive target for the development of novel anti-infectives.[11] We have identified the first PqsD inhibitors by testing known inhibitors of FabH, a structurally and functionally related enzyme.[10] Structural optimization decreased IC_{50} values to 1.2 μM (Scheme 1, **1** and **2**).[12] However, these compounds were not capable of potently reducing the extracellular signal molecule levels in *P. aeruginosa* PA14 (unpublished data).

Recently, we have identified 2-nitrophenyl derivatives as potent PqsD inhibitors in a ligand-based approach (Scheme 1, **3**–**5**, **7**).[11] The most active compound of this series **3** was capable of reducing the HHQ and PQS levels as well as the biofilm volume in *P. aeruginosa* PA14 without affecting cell viability. In our original concept, (2-aminophenyl)methanol derivative **6** was designed as transition state analog of the reaction between PqsD and its primary substrate anthraniloyl-CoA (ACoA) (Scheme 1). Since transition states are the most tightly bound species of a catalytic reaction, transition state analogs are a reasonable strategy to achieve high potency.[13] However, we unexpectedly observed no activity for **6**, while the corresponding nitro compound **7** effectively inhibited PqsD. Thus, it is open to question how the optimized nitro compound **3** interacts with PqsD on a molecular level.

To address this question, we conducted a surface plasmon resonance (SPR) competition experiment to validate the binding site. Various modifications of the *in vitro* assay were used to elucidate time dependency of inhibition as well as functional reversibility. Mass spectrometry was applied to investigate the nature of interaction between the protein and the inhibitors. Site-directed mutagenesis in combination with ITC analysis revealed key interaction features responsible for affinity and astonishing differences in the thermodynamic profile of the separated enantiomers. This information was used to deduce plausible binding modes, which may explain the efficacy of the compound class.

RESULTS AND DISCUSSION

Binding Site Analysis by SPR. To investigate whether our compounds bind in the active site, we performed binding experiments using SPR. Compound **2**, which was described as a channel blocker interacting in the upper part of the tunnel[12] and **3** were separately added to PqsD immobilized on an SPR sensor chip. Figure 1A/B shows the resulting response curves, indicating affinity to the enzyme for both compounds.

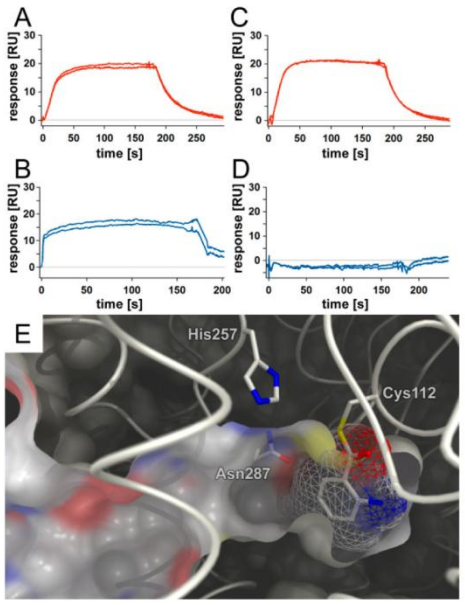

Figure 1. Elucidation of the binding site by SPR. Addition of inhibitor to native PqsD leads to response curves (A) and (B) for compounds **2** and **3**, respectively. In contrast to compound **2** (C), no response curve for **3** (D) is observed after addition to PqsD pretreated with ACoA. (E) Binding pocket of PqsD and space-filling model of covalent anthranilate adduct (wireframe). Picture was generated using the crystal structure [Protein Data Bank (PDB) entry 3H77].[14]

In a second experiment, the first substrate of PqsD, ACoA, was added until saturation of all active-site Cys112 by formation of an anthranilate thioester was reached (Figure 1E). Noteworthy, the X-ray structure of this key intermediate shows no significant conformational changes compared to untreated PqsD,[14] which eliminates the possibility of allosteric effects. Addition of inhibitors **2** or **3** was subsequently repeated. In the case of **2**, response curves were very similar to those obtained using unmodified enzyme (Figure 1C). Thus, affinity of **2** is not affected by covalently bound anthranilate, which is consistent with previous results.[12] In contrast, no response was observed for **3** (Figure 1D), indicating that the binding site of **3** is blocked by anthranilate. Moreover, this experiment shows

dx.doi.org/10.1021/cb400530d | ACS Chem. Biol. 2013, 8, 2794–2801

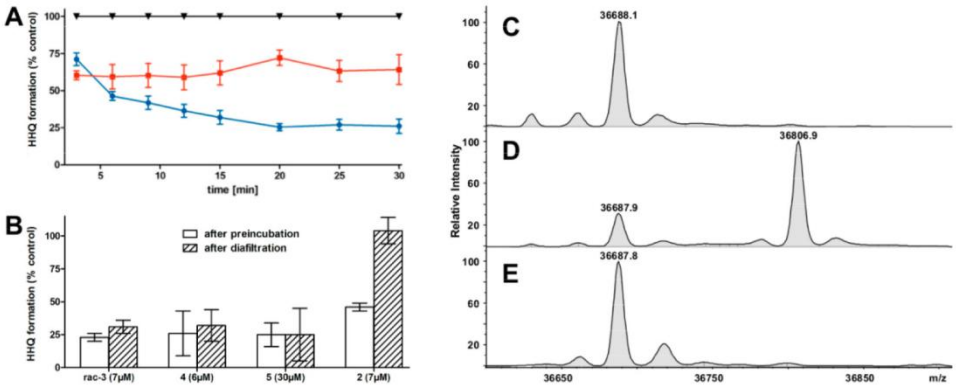

Figure 2. Mode of action analysis. (A) Time dependency of PqsD inhibition by 3 μM of FabH inhibitor-derived compound **2** (■) and 6 μM of 2-nitrophenyl derivative **3** (●) compared to untreated control (▼). Values are given in the Supporting Information. (B) Reversibility of PqsD inhibition by compounds **2**–**5**. Centrifugal filter devices with a molecular weight limit of 10k were used to remove at least 95% inhibitor by three diafiltration steps as controlled by HPLC analysis, while PqsD was retained. (C–E) HPLC-ESI mass spectra of untreated PqsD (C) and after preincubation with 5 mM ACoA (D) or 2.5 mM of compound **3** (E), respectively.

that the binding pocket around Cys112 is the only target site of **3**. This is supported by a 1:1 interaction stoichiometry determined in the ITC experiment.[11]

To gather further evidence for the proposed binding site, we preincubated PqsD with ACoA prior to continuation of the original assay procedure. In the case of the FabH inhibitor-derived compounds **1** and **2**, no significant differences in IC_{50} values determined by both procedures were observed ($IC_{50,mod}$ values in Supporting Information (SI) Table S2). In contrast to this, the IC_{50} values of **3**–**5** were increased at least 3-fold when PqsD was preincubated with the substrate. This provides further evidence that nitrophenyl derivatives and the anthraniloyl moiety share a common binding site.

Time-Dependent Inhibition and Reversibility. To investigate the time dependency of PqsD inhibition by **3**, the protein was added to a mixture of substrates and inhibitor before HHQ formation was measured at different time points. Figure 2A (blue) shows decreasing HHQ production over time compared to the untreated control, indicating slow binding kinetics for **3**. For reference compound **2** (red), a nearly constant HHQ formation rate is observed, which is due to a rapid establishment of binding equilibrium with the enzyme.

Inhibition by **3** has not reached the equilibrium after 10 min, which is the standard preincubation time in the *in vitro* assay. Consequently, IC_{50} data and structure–activity relationships derived in this compound class are dependent on the rate of complex formation. Furthermore, the potency is underestimated compared to the FabH inhibitor-derived compound class. This becomes apparent when the preincubation period was extended from 10 min (IC_{50}) to 30 min ($IC_{50,ext}$ values in SI Table S2). While the inhibitory potency of **1** and **2** did not increase, the $IC_{50,ext}$ of **3**–**5** showed significantly lowered values. This effect is most pronounced for the alcohol **3**, which is probably due to the slowest binding kinetics.

There are two general modes of interaction between enzyme and inhibitor resulting in time-dependent inhibition. First, the enzyme inactivation is practically irreversible, for example by covalent binding. As the reaction progresses, enzyme inhibition will be increased. In the second case, slow binding kinetics can lead to an equilibrium establishment of a reversible inhibition, which is slow compared to enzyme turnover. To address this issue, we examined the reversibility by modification of our *in vitro* functional assay. Therefore, PqsD was preincubated with inhibitor and the remaining HHQ formation was quantified with and without removal of unbound inhibitor by diafiltration. After preincubation with 7 μM of the FabH inhibitor-derived compound **2**, 46% of HHQ formation remained compared to the untreated control. After removal of unbound inhibitor, PqsD activity was fully restored, since binding of the inhibitor is nonpermanent (Figure 2B). In the case of the 2-nitrophenyl derivatives **3**–**5**, PqsD activity was not significantly increased. However, providing reversible inhibition, HHQ formation should be very sensitive to changes in inhibitor concentration, since the dose-inhibition curves are very steep at the concentrations used (SI Figure S1 for compound **3**). Hence, inhibition by this compound class is apparently irreversible. However, it should be mentioned that the time available for dissociation between the diafiltration steps is limited due to enzyme denaturation ($t_{1/2} \approx 100$ min at RT). Thus, the irreversible behavior of **3**–**5** may be restricted to the time period that is covered by the experiment.

To distinguish between irreversible inhibition by formation of a covalent bond or tight-binding characterized by slow off-rates, mass spectrometry (MS) techniques were applied. First, PqsD was incubated with or without ACoA as well as compound **3**, and the samples were subjected to HPLC-ESI analysis (Figure 2C). In absence of any additives, the main signal was observed at m/z = 36688.1, which corresponds to the calculated average mass of PqsD (36688.1 Da). Formation of the anthranilate–PqsD complex by addition of the substrate led to the expected mass shift of +119.2 toward 36806.9 (calculated: 36807.2). In presence of a 100 fold excess of inhibitor **3**, no covalent adduct or oxidation product was observed. This was also the case when any reductive reagents were avoided (SI Figure S2). Thus, we exclude a redox-based inhibition mechanism.

To exclude a possible dissociation during HPLC, we also analyzed PqsD with or without compound **3** by Maldi-TOF after tryptic digestion. In the case of unmodified PqsD, more than 99% of the sequence was covered by the peptides observed in the mass spectra. (Results are shown and discussed in detail in the Maldi-TOF section of the Supporting Information.) Thus, apart from 6 of 340 amino acids, which are unlikely to be involved in inhibitor binding, the

modification should be captured by this technique. However, no novel signal appeared after preincubation of PqsD with compound **3** (SI Table S4). The only difference compared to untreated PqsD is the disappearance of one fragment, which is not involved in substrate or inhibitor binding, since it is located far away from the active site. This fragment is also unresolved in the X-ray structure of PqsD, which is probably due to conformational flexibility. Thus, possible allosteric effects are unlikely. Considering both experiments, we exclude covalent binding, simultaneously denoting **3** as a tight-binding inhibitor.

Elucidation of the Binding Mode. The data presented so far were obtained using a racemic mixture of **3**, since we have already shown that both enantiomers possess very similar IC_{50} values.[11] The SPR experiment using the separated stereoisomers revealed that both enantiomers bind near the active site residues deep in the binding channel and in an exclusive manner with respect to one another (SI Figures S9). Furthermore, (*R*)-**3** and (*S*)-**3** showed the same behavior as the racemic mixture **3** in the diafiltration experiment (SI Figure S10). However, when we analyzed the thermodynamic profile of binding to PqsD by ITC, surprising differences between both enantiomers were observed, even though very similar values for ΔG were determined (Figure 3 and Table 1).

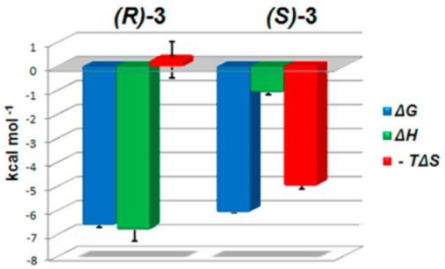

Figure 3. ITC analysis of thermodynamic profiles of enantiomers binding to PqsD wild-type.

Whereas the affinity of (*R*)-**3** is driven enthalpically, (*S*)-**3** shows a pronounced entropic binding profile. The combination of the values obtained for both enantiomers is in accordance with the balanced profile determined for their racemic mixture (ΔH = −3.47 kcal mol^{-1}, $-T\Delta S$ = −3.20 kcal mol^{-1}). The differences in the thermodynamic profiles are evident, even if uncertainties in ΔH, and thus also in $T\Delta S$, of ∼24% have to be expected for the technique (value determined by an interlaboratory comparison).[16]

With respect to the dissimilar thermodynamic profiles, we were interested whether differences in the interaction with the amino acid residues are detectable. Because of a lack in cocrystal structure, we decided to execute a combined approach of site-directed mutagenesis and ITC as a promising method to identify specific spots of interaction.[17] Due to the SPR results, the binding site of both enantiomers should be located near the catalytic triad characterized by Cys112, His257 and Asn287. Furthermore, the adjacent Ser317 represents another possible interaction partner. Thus, we mutated the aforementioned amino acids. Only S317A possessed catalytic activity comparable to the wild-type. C112S retained 8% activity, whereas all other mutations led to inactivity (SI Table S1). However, the aforementioned PqsD variants allowed to investigate the contribution of the respective residue side chains to inhibitor binding.

ITC analyses using (*R*)-**3** revealed Cys112 and His257 as mainly interacting residues, since mutation led to a loss of affinity by more than factor 2.3, as measured by deterioration in ΔG by more than 0.5 kcal mol^{-1} (Table 1). Binding affinity of (*S*)-**3** does not seem to be significantly changed by any of these mutations with the exception of a small loss in affinity for both Ser317 mutants. For C112A standard deviations in ΔG are too high for a reliable interpretation.

Based on these results, we docked both enantiomers to propose binding poses. Calculation of the protonation state revealed that the Cys112 and His257 residues exist in a neutral form at physiological pH. In all high-ranked docking poses, the scaffold of both enantiomers had the same position, whereas one phenyl ring was located directly adjacent to the bottom of the channel and the other oriented toward the tunnel entrance (Figure 4A). For (*R*)-**3**, the nitro group was observed at both phenyl rings. However, since both enantiomers retained comparable inhibitory activity even for elongated substituents instead of phenyl (data not shown), we concluded that the nitro-phenyl moiety is apparently located at the bottom of the channel. Thereby, the nitro group forms an asymmetrical bifurcated hydrogen bond (2.85 and 3.10 Å) to the backbone NH of Ser317 (Figure 4B).[18] The hydroxyl group is involved in a hydrogen bond network between the side chains of Cys112 (3.07 Å) and His257 (2.90 Å). The observed distances are typical for weak hydrogen bonds,[19,20] which explains the loss in affinity and enthalpy for the C112A and H257F mutants. The

Table 1. Effects of Mutated Amino Acids on Thermodynamic Profiles of the Enantiomers of 3[a]

	(*R*)-**3**[b]			(*S*)-**3**[b]		
	ΔG [kcal mol^{-1}]	ΔH [kcal mol^{-1}]	$-T\Delta S$ [kcal mol^{-1}]	ΔG [kcal mol^{-1}]	ΔH [kcal mol^{-1}]	$-T\Delta S$ [kcal mol^{-1}]
WT	−6.56 ± 0.14	−6.99 ± 1.02	0.43 ± 1.15	−6.13 ± 0.20	−1.11 ± 0.34	−5.02 ± 0.18
	$\Delta\Delta G$ [kcal mol^{-1}]	$\Delta\Delta H$ [kcal mol^{-1}]	$-T\Delta\Delta S$ [kcal mol^{-1}]	$\Delta\Delta G$ [kcal mol^{-1}]	$\Delta\Delta H$ [kcal mol^{-1}]	$-T\Delta\Delta S$ [kcal mol^{-1}]
C112A	−0.82 ± 0.11[c]	−5.36 ± 0.60[c]	4.54 ± 0.86[c]	0.10 ± 0.40	−0.30 ± 0.53	0.40 ± 0.22
C112S	−0.75 ± 0.14[c]	−5.87 ± 0.78[c]	5.12 ± 0.86[c]	−0.03 ± 0.10	−0.39 ± 0.36	0.36 ± 0.36
S317F	−0.58 ± 0.14[c]	−6.09 ± 0.72[c]	5.51 ± 0.86[c]	−0.30 ± 0.10[c]	−0.78 ± 0.22[c]	0.40 ± 0.20
S317A	0.10 ± 0.10	−1.10 ± 0.67	1.26 ± 0.76	−0.22 ± 0.10[c]	0.14 ± 0.36	−0.36 ± 0.36
N287A	−0.18 ± 0.10	−1.16 ± 0.61	0.98 ± 0.70	−0.02 ± 0.10	−0.02 ± 0.20	−0.01 ± 0.20
H257F	−0.61 ± 0.30[c]	−5.83 ± 0.67[c]	5.22 ± 0.76[c]	0.03 ± 0.30	−0.19 ± 0.36	0.22 ± 0.36

[a] $\Delta\Delta G$, $\Delta\Delta H$, and $-T\Delta\Delta S$ are $\Delta G_{WT} - \Delta G_{mutant}$, $\Delta H_{WT} - \Delta H_{mutant}$, and $-T(\Delta S_{WT} - \Delta S_{mutant})$, respectively. Negative values indicate a loss; positive values, a gain compared to wild-type. Significance: effect of the mutations on thermodynamic parameters of ligand binding compared to wild-type indicates a difference in interaction. [b] Absolute configurations were derived from measurement of the optical rotation and comparison to literature.[15] [c] $p < 0.05$.

dx.doi.org/10.1021/cb400530d | ACS Chem. Biol. 2013, 8, 2794−2801

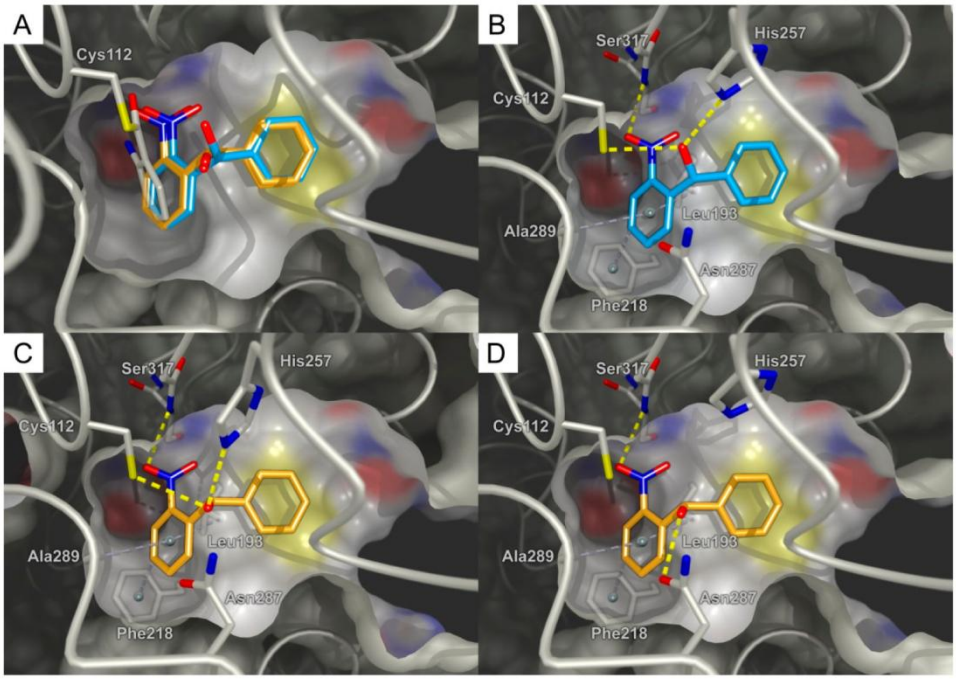

Figure 4. (A) Superimposition of the covalent anthranilate–PqsD complex (PDP entry 3H77) and docking poses for both enantiomers. Observed hydrogen bonds and CH-π interactions of *R*-enantiomer (B) and the *S*-enantiomer (C/D) of compound **3** in PqsD wild-type. Nitrogen, blue; oxygen, red; sulfur, yellow; carbons of PqsD, gray; carbons of *R*-enantiomer, light blue; carbons of *S*-enantiomer, orange; hydrogen left out for clarity.

C112S mutant showed strongly reduced affinity, which is probably due to the shorter van der Waals radius of oxygen compared to sulfur,[21] leading to an interruption of the hydrogen bond network. No interaction was observed with the side chains of Asn287 and Ser317, which is in accordance with the collected ITC data (Table 1). However, introduction of a bulky phenyl ring in S317F probably results in sterical hindrance.

In the case of (*S*)-**3**, docking results were unambiguous with respect to the positioning of the nitro group, since in all high-ranked poses a short hydrogen bond between NO_2 and NH of Ser317 was observed (Figure 4C/D). However, the hydroxyl group was involved in different interactions, either facing toward Asn287 or His256/Cys112. We speculate that no singular mutation of the aforementioned residues significantly reduced affinity, since the hydroxyl group is able to switch to an alternative interaction mode. Noteworthy, this is not possible for the *R*-enantiomer due to the different orientation of the OH functionality.

Recently, two enantiomers with similar binding affinity for acetylcholinesterase but different thermodynamic profiles were reported.[22] X-ray cocrystal structures revealed multiple conformations stabilized by weak interactions for one enantiomer, leading to a gain in $T\Delta S$ of 2.4 kcal mol^{-1} compared to its counterpart. A similar effect might be contributing to the significant change in $T\Delta S$ of 5.3 kcal mol^{-1} for our compounds. Furthermore, a gain in entropy is characteristic for the classical hydrophobic effect.[23] Thereby, the release of ordered water from well-solvated hydrophobic pockets upon ligand binding increases the water molecules degree of freedom.[24] However, we were not able to identify such a displacement of water when comparing our docking results with the published X-ray structures.

Since small changes in structure without significant effect on ΔG can lead to large changes in ΔH and $T\Delta S$, the phenomenon of entropy-enthalpy compensation may also help to explain the contrary thermodynamic profiles of the enantiomers.[25] The physical origin of the compensation is still not fully understood, and it has been repeatedly discussed whether a structural interpretation is even possible.[25,26] According to this, the altered position of OH may well be the source of the shift in thermodynamic contributions.

Nevertheless, besides the interpretation of the thermodynamic profile, the proposed models should enable us to perform structure-guided optimization. Thus, the docking poses have to be in accordance with previous structure–activity relationship observations.[11] First, as soon as the amino group of **6** was substituted by nitro, the compounds turned active. As has been described above, (2-nitrophenyl)(phenyl)-methanol **3** was originally designed as transition state analog. However, in the transition state, which has formed by attack of Cys112 on the thioester bond of ACoA, the generated oxyanion is stabilized by backbone nitrogen atoms of Cys112 and Ser317.[14] In our model, this position is in each case rather occupied by the nitro group (Figure 4A), which cannot be mimicked by the corresponding amine geometrically and spatially. As a consequence, this compound does not interact with PqsD as expected for a transition state analog. Furthermore, it is noteworthy that the nitrophenyl moiety aligns quite accurately with the benzoate moiety in an X-ray structure of anthranilate bound to a C112A mutant.[14] This indicates the preference for this kind of isoelectronic groups at this point of the channel. Second, a carbonyl linker between both phenyl rings, which conjugates the π-systems, leads to inactivity. This can now be explained, as the banana-shaped bottom of the channel is not able to accommodate the planar

molecule anymore. Furthermore, substitution of the methylene-H abolished inhibitory activity, either due to a steric clash with Asn287 (*R*), or because a substitution is followed by a twist of the molecule, which destabilizes the biological active conformation (*S*). Hence, the experimental results are in good accordance with our binding model.

Conclusions. 2-Nitrophenyl derivatives and FabH inhibitor-derived compounds show similar IC_{50} values, but only congeners of the former class are capable of significantly reducing signal molecule production and biofilm formation in *P. aeruginosa* PA14. We have shown that both inhibitor classes possess fundamentally different profiles regarding binding site, time-dependent inhibition and reversibility. Besides possible advantages in cell permeability of the (2-nitrophenyl)methanol derivatives due to their low molecular weight, the deeply buried binding site at the bottom of the substrate channel and the apparent irreversibility could be crucial factors for their intracellular efficacy.

Furthermore, the calorimetric characterization of two enantiomers revealed remarkable differences in their thermodynamic signatures. The detailed binding modes were examined by a combined approach using site-directed mutagenesis, ITC, and docking. This enabled us to propose binding poses for both enantiomers only differing in the position of the hydroxyl group. Notably, the nitro group occupies the oxyanion hole forming strong interactions with the enzyme backbone. However, this site was expected to accommodate the aforementioned hydroxyl group. Hence, the position of the scaffold is altered compared to the transition state (Figure 4A). The predicted enzyme−inhibitor complexes explain the reported structure−activity relationship and, therefore, enable the structure-guided design of PqsD inhibitors toward improved inhibitory activity.

METHODS

Preparation of PqsD Mutants. PqsD mutants were generated using the QuikChange Site-Directed Mutagenesis Kit (Stratagene) according to the manufacturer's instructions using the pET28b(+)/*pqsD* plasmid as a template. Briefly, *pqsD* gene was amplified through 16 cycles of PCR. After treatment with *Dpn*I, the PCR product was transformed into *E. coli* strain XL1-Blue. Plasmid DNA was purified using the GenElute HP Plasmid Miniprep Kit (Sigma-Aldrich) and sequenced to confirm the site-directed mutations. For the primer sequence of the mutations see Supporting Information.

Expression and Purification of Recombinant PqsD Wild-type and Mutants in *E. coli*. *E. coli* BL21 (λDE3) cells were transformed with plasmid harboring PqsD (pET28b(+)/*pqsD*).[10] Overexpression, purification, and storage of the His_6-tagged PqsD was performed as described recently.[11]

Screening Assay Procedures for *In Vitro* PqsD Inhibition. The standard assay for determination of IC_{50} values was performed monitoring the enzyme activity by measuring the HHQ concentration as described recently.[10] PqsD was preincubated with inhibitor for 10 min prior to addition of the substrates ACoA and β-ketodecanoic acid. The concentration of PqsD applied in the assay was 0.1 μM. Quantification of HHQ was performed analogously, but with some modifications: The flow rate was set to 750 μL min^{-1} and an Accucore RP-MS column, 150 × 2.1 mm, 2.6 μm, (Thermo Scientific) was used. All test compound reactions were performed in sextuplicate. Synthesis of ACoA and β-ketodecanoic acid was performed as described in the Supporting Information. In the modified protocol used for the determination of $IC_{50,mod}$, PqsD and the first substrate ACoA were preincubated for 30 min prior to adding them to the test compounds. Then, β-ketodecanoic acid was added and the further steps were performed identical to the standard protocol. $IC_{50,ext}$ values were determined analogously to the normal IC_{50} values, with the sole exception that PqsD was preincubated with inhibitor for 30 min.

Surface Plasmon Resonance (SPR) Spectrometry. SPR binding studies were performed using a Reichert SR7500DC instrument optical biosensor (Reichert Technologies) and CMD500 M sensor chips obtained from XanTec Bioanalytics. PqsD was immobilized on a CMD500 M (carboxymethyldextran-coated) sensor chip at 12 °C using standard amine coupling conditions according to the manufacturers' instructions. PqsD was diluted with sodium acetate buffer (10 mM, pH 4.5) to a final concentration of 100 μg mL^{-1}. PqsD was immobilized at densities of 2217 RU and 2918 RU.

SPR Competition Study. The binding studies were performed at a constant flow rate of 50 μL min^{-1} in instrument running buffer (50 mM MOPS, pH 8.0, 150 mM NaCl, 5% DMSO (*v*/*v*), 0.1% Triton X-100 (*v*/*v*)). 10 mM stock solutions of compounds **2** and **3** in DMSO were directly diluted to a concentration of 500 μM (50 mM MOPS, pH 8.0, 150 mM NaCl, 0.1% Triton X-100 (*v*/*v*)) and then diluted to a final concentration of 100 μM (**3**) and 20 μM (**2**) in running buffer. Before the compounds were injected, six warm-up blank injections were performed. Buffer blank injections and DMSO calibration were included for double referencing. The compounds were injected for 180 s association and 300 s dissociation times. Experiments were performed twice with two independently prepared PqsD coated CMD500 M sensor chips. Scrubber software was used for processing and analyzing the data.

Compounds **2** and **3** were first tested in the absence of ACoA. In the second experiment ACoA (100 μM) was injected for 40 min with a constant flow of 5 μL min^{-1} to reach saturation of the active-site Cys112. After this, the flow rate was increased to 50 μL min^{-1} for 30 min in order to remove residual reagents. Once the baseline signal was stable, additional ACoA (10 μM) was injected to ensure that the anthranilate binding site is completely saturated (no additional signal was observed). Afterward, compounds **2** (20 μM) and **3** (100 μM) were consecutively injected.

Elucidation of Time-Dependent PqsD Inhibition. The assay was performed analogously to the screening assay procedure for *in vitro* PqsD inhibition described above, except that inhibitor and substrate were mixed and the reaction was started by addition of enzyme. The reactions were stopped after 3, 6, 9, 12, 15, 20, 25, and 30 min by addition of methanol containing 1 μM amitriptyline as internal standard. The percentage of inhibition was determined as the mean value of duplicates and HHQ concentrations measured without inhibitor at each time point were set to 100%. The uncertainty was calculated assuming uncorrelated standard deviations of the HHQ levels with or without inhibitor using a first-order Taylor series expansion. Percentages of inhibition are given in the Supporting Information.

Examination of Reversibility by Diafiltration. The diafiltration experiment was performed using identical conditions as for the screening assay procedure, but with doubled enzyme concentration (0.2 μM). PqsD was preincubated with inhibitor for 10 min, and the solutions were divided into two fractions. While the first one was stored under 4 °C, the second was diafiltrated (3×) at 1200*g* for 6 min at 4 °C using Nanosep Centrifugal Devices equipped with a Omega membrane (MWCO = 10 K), which were obtained from Pall Corporation. Between diafiltration steps, the samples were diluted from 30 μL to 500 μL with buffer (identical chemical composition as used for preincubation). The enzyme inhibitor complex was allowed to dissociate for 1 min at RT. Afterward, the substrates ACoA and β-ketodecanoic acid were added to both fractions and the assay was continued as described in the screening assay procedure.

HPLC-ESI Experiment. PqsD (25 μM) was preincubated with compound **9** (2.5 mM) for 60 min at 37 °C in Tris-HCl buffer (50 mM, pH 8.0) with 0.5% DMSO (*v*/*v*). Dithiothreitol was added, and the samples were analyzed by HPLC-ESI. All ESI-MS-measurements were performed on a Dionex Ultimate 3000 RSLC system using an Aeris Widepore XB-C8, 150 × 2.1 mm, 3.6 μm dp column (Phenomenex). Separation of 2 μL samples were achieved by a linear gradient from (A) H_2O + 0.05% TFA (*v*/*v*) to (B) ACN + 0.05% TFA (*v*/*v*) at a flow rate of 250 μL min^{-1} and 45 °C. The gradient was

initiated by a 1.0 min isocratic step at 15% B, followed by an increase to 80% B within 4.5 min to end up with a 6 min step at 80% B before re-equilibration with initial conditions. UV spectra were recorded by a DAD in a range from 200 to 600 nm. The LC flow was split to 75 μL min^{-1} before entering the maXis 4G hr-ToF mass spectrometer (Bruker Daltonics) using the standard Bruker ESI source. In the source region, the temperature was set to 180 °C, the capillary voltage was 4000 V, the dry-gas flow was 6.0 l min^{-1}, and the nebulizer was set to 1.1 bar. Mass spectra were acquired in positive ionization mode ranging from 600 to 1800 m/z at 2.5 Hz scan rate. Protein masses were deconvoluted using the Maximum Entropy algorithm (Copyright 1991−2004 Spectrum Square Associates, Inc.).

Maldi-TOF Experiment. PqsD (10 μM) was preincubated with compound **3** (2.5 mM) for 60 min at 37 °C using identical buffer composition as in the screening assay procedure (50 mM MOPS, pH 7.0 with 0.005% (v/v) Triton X-100 and 0.5% DMSO (v/v)). The buffer was exchanged by an NH_4HCO_3 buffer (50 mM, pH 8.1) in three diafiltration steps. Diafiltration was performed at 1200 g for 6 min at 4 °C in Nanosep Centrifugal Devices (MWCO = 10 K) of Pall Corporation. The protein was digested with trypsin overnight and dithiothreitol was added. α-Cyano-4-hydroxycinnamic acid was used as matrix component. Analysis of the peptides were performed on a 4800 TOF/TOF Analyzer mass spectrometer (Applied Biosystems) in positive reflector mode using a pulsed 200 Hz solid state Nd:YAG laser with a wavelength of 355 nm. Laser energy was set to 2000−2300 units for standards and to 2700−3200 units for real samples. Source 1 voltage was set to 20 kV with a grid voltage of 16 kV. Reflector detector voltage was 2.19 kV. Spectra of standard peptides used for wide range calibration ranging from 0.8 to 4 kDa (des-arg1-bradykinin, angiotensin I, glu1-fibrinopeptide B, ACTH 1−17 clip, ACTH 18−39 clip and ACTH 7−38 clip) were measured with a delay time of 600 ns. One single mass spectrum was formed from 20 subspectra per spot using 25 accepted laser impulses each. From the standard peptides, exclusively monoisotopic ions were used with a minimum signal-to-noise (S/N) ratio of 20 and a resolution >10000. Mass tolerance was set to 0.3 Da with maximum outlier of 5 ppm. Accepted calibration settings were used to measure real sample spectra in the range 1−3.5 kDa with a minimum S/N range of 10 and a resolution >8000. An internal algorithm defined the isotope cluster area subsequently named intensity (I), based on the peptides' molecular weight and their general elemental composition. MALDI-TOF MS resulted in pmfs consisting of mass-intensity spectra (m/z−$I_{abs,\ ai}$).

Isothermal Titration Calorimetry (ITC). ITC experiments were carried out using an ITC200 instrument (Microcal Inc., GE Healthcare). Final ligand concentrations were obtained by dilution 1:20 (v/v) in the experimental buffer resulting in a final DMSO concentration of 5% (v/v). Protein concentration was determined by measuring the absorbance at 280 nm using a theoretical molarity extinction coefficient of 17 780 M^{-1} cm^{-1}. DMSO concentration in the protein solution was adjusted to 5% (v/v). ITC measurements were routinely performed at 25 °C in PBS-buffer, pH 7.4, 10% glycerol (v/v), 5% DMSO (v/v). The titrations were performed on 83−102 μM PqsD-His_6 and mutants-His_6 in the 200 μL sample cell using 2 μL injections of 3.5 mM ligand solution every 180 s. Raw data were collected, and the area under each peak was integrated. To correct for heats of dilution and mixing, the final baseline consisting of small peaks of the same size at the end of the experiment was subtracted. The experimental data were fitted to a theoretical titration curve (one site binding model) using MicroCal Origin 7 software, with ΔH (enthalpy change in kcal mol^{-1}), K_A (association constant in M^{-1}), and N (number of binding sites) as adjustable parameters. Thermodynamic parameters were calculated from equation

$$\Delta G = \Delta H - T\Delta S = RT \ln K_A = -RT \ln K_D$$

where ΔG, ΔH, and ΔS are the changes in Gibbs free energy, enthalpy, and entropy of binding, respectively. T is the absolute temperature, and R = 1.98 cal mol^{-1} K^{-1}. For every mutant, three independent experiments were performed.

***In Silico* Experiments.** Docking poses of PqsD inhibitors (*R*)-**3** and (*S*)-**3** were generated with YASARA structure (YASARA Biosciences) using the AMBER03 force field on an Intel Core i7-2600 workstation with eight virtual cores.[27,28] Receptor coordinates were prepared using a crystal structure of the PqsD-anthraniloyl complex (PDB entry 3H77).[14]

First, the covalent and noncovalent ligands were removed without altering the dihedral angle of the Cys112 side chain and protonation states were assigned automatically at pH 7.4. Then, a grid box of 27 × 20 × 20 $Å^3$ was set up around the residues forming the active site tunnel of PqsD. Finally, the binding mode of the ligandswas calculated using the flexible local docking procedure of the implemented AutoDock 4 algorithm with 999 docking runs.[29] In every case, at least the five highest-ranked poses were found to belong to one cluster. Predicted PqsD-inhibitor complexes were further refined by an additional energy minimization step with fixed receptor backbone atoms and then analyzed using MOE 2012 (Chemical Computing Group).[30]

■ ASSOCIATED CONTENT

Supporting Information

Primer sequence of mutations and catalytic activity; synthesis of the substrates used in the enzymatic inhibition assays; percentages of inhibition of the time dependency experiment; detailed analysis of the Maldi-TOF experiment; additional HPLC-ESI MS, diafiltration and SPR experiments; separation and purity of the enantiomers; representative ITC curves. This material is available free of charge *via* the Internet at http://pubs.acs.org.

■ AUTHOR INFORMATION

Corresponding Authors

*Phone: +49 681 302 70300. Fax: +49 681 302 70308. E-mail: rolf.hartmann@helmholtz-hzi.de.

*E-mail: martin.empting@helmholtz-hzi.de.

Author Contributions

⊥M.P.S. and C. B. contributed equally.

Notes

The authors declare no competing financial interest.

■ ACKNOWLEDGMENTS

We thank S. Amann and C. Scheid for their help in performing all HPLC-MS/MS-based assays.

■ REFERENCES

(1) Levy, S. B., and Marshall, B. (2004) Antibacterial resistance worldwide: Causes, challenges and responses. *Nat. Med. 10*, S122−S129.

(2) Govan, J. R., and Deretic, V. (1996) Microbial pathogenesis in cystic fibrosis: Mucoid *Pseudomonas aeruginosa* and *Burkholderia cepacia*. *Microbiol. Rev. 60*, 539−574.

(3) Nikaido, H. (1989) Outer membrane barrier as a mechanism of antimicrobial resistance. *Antimicrob. Agents Chemother. 33*, 1831−1836.

(4) Poole, K. (2001) Multidrug efflux pumps and antimicrobial resistance in *Pseudomonas aeruginosa* and related organisms. *J. Mol. Microbiol. Biotechnol. 3*, 255−264.

(5) Swinney, D. C. (2004) Biochemical mechanisms of drug action: What does it take for success? *Nat. Rev. Drug Discovery 3*, 801−808.

(6) Diggle, S. P., Lumjiaktase, P., Dipilato, F., Kunakorn, M., Barrett, D. A., Chhabra, S. R., Camara, M., and Williams, P. (2006) Functional genetic analysis reveals a 2-alkyl-4-quinolone signaling system in the human pathogen *Burkholderia pseudomallei* and related bacteria. *Chem. Biol. 13*, 701−710.

(7) Yang, L., Nilsson, M., Gjermansen, M., Givskov, M., and Tolker-Nielsen, T. (2009) Pyoverdine and PQS mediated subpopulation interactions involved in *Pseudomonas aeurginsoa* biofilm formation. *Mol. Microbiol. 74*, 1380−1392.

(8) Summarized in: Dubern, J.-F., and Diggle, S. P. (2008) Quorum sensing by 2-alkyl-4-quinolones in *Pseudomonas aeruginsoa* and other bacterial species. *Mol. BioSyst 4*, 882−888.
(9) Hentzer, M., Wu, H., Andersen, J. B., Riedel, K., Rasmussen, T. B., Bagge, N., Kumar, N., Schembri, M. A., Song, Z., Kristoffersen, P., Manefield, M., Costerton, J. W., Molin, S., Eberl, L., Steinberg, P., Kjelleberg, S., Hoiby, N., and Givskov, M. (2003) Attenuation of *Pseudomonas aeruginosa* virulence by quorum sensing inhibitors. *EMBO J. 22*, 3803−3815.
(10) Pistorius, D., Ullrich, A., Lucas, S., Hartmann, R. W., Kazmaier, U., and Müller, R. (2011) Biosynthesis of 2-alkyl-4(1*H*)-quinolones in *Pseudomonas aeruginosa*: Potential for therapeutic interference with pathogenicity. *ChemBioChem 12*, 850−853.
(11) Storz, M. P., Maurer, C. K., Zimmer, C., Wagner, N., Brengel, C., de Jong, J. C., Lucas, S., Müsken, M., Häussler, S., Steinbach, A., and Hartmann, R. W. (2012) Validation of PqsD as an anti-biofilm target in *Pseudomonas aeruginosa* by development of small-molecule inhibitors. *J. Am. Chem. Soc. 134*, 16143−16146.
(12) Weidel, E., de Jong, J. C., Brengel, C., Storz, M. P., Braunshausen, A., Negri, M., Plaza, A., Steinbach, A., Müller, R., and Hartmann, R. W. (2013) Structure optimization of 2-benzamidobenzoic acids as PqsD inhibitors for *Pseudomonas aeruginosa* infections and elucidation of binding mode by SPR, STD NMR, and molecular docking. *J. Med. Chem.*,.
(13) Schloss, J. V. (1988) Significance of slow-binding enzyme inhibition and its relationship to reaction-intermediate analogues. *Acc. Chem. Res. 21*, 348−353.
(14) Bera, A. K., Atanasova, V., Robinson, H., Eisenstein, E., Coleman, J. P., Pesci, E. C., and Parsons, J. F. (2009) Structure of PqsD, a *Pseudomonas* quinolone signal biosynthetic enzyme, in complex with anthranilate. *Biochemistry 48*, 8644−8655.
(15) Duan, H.-F., Xie, J.-H., Shi, W.-J., Zhang, Q., and Zhou, Q.-L. (2006) Enantioselective rhodium-catalyzed addition of arylboronic acids to aldehydes using chiral spiro monophosphite ligands. *Org. Lett. 8*, 1479−1481.
(16) Myszka, D. G., Abdiche, Y. N., Arisaka, F., Byron, O., Eisenstein, E., Hensley, P., Thomson, J. A., Lombardo, C. R., Schwarz, F., Stafford, W., and Doyle, M. L. (2003) The ABRF-MIRG'02 study: Assembly state, thermodynamic, and kinetic analysis of an enzyme/inhibitor interaction. *J. Biomol. Technol. 14*, 247−269.
(17) Ciulli, A., Williams, G., Smith, A. G., Blundell, T. L., and Abell, C. (2006) Probing hot spots at protein−ligand binding sites: A fragment-based approach using biophysical methods. *J. Med. Chem. 49*, 4992−5000.
(18) Allen, F. H., Baalham, C. A., Lommerse, J. P. M., Raithby, P. R., and Sparr, E. (1997) Hydrogen-bond acceptor properties of nitro-O atoms: A combined crystallographic database and *ab initio* molecular orbital study. *Acta Crystallogr. B53*, 1017−1024.
(19) Allen, F. H., Bird, C. M., Rowland, R. X., and Raithby, P. R. (1997) Hydrogen-bond acceptor and donor properties of divalent sulfur (Y-S-Z and R-S-H). *Acta Crystallogr. B53*, 696−701.
(20) Vianello, L., Kovačević, B., Ambrožič, G., Mavri, J., and Maksić, Z. B. (2004) Hydrogen bonding in complex of serine with histidine: Computational and spectroscopic study of model compounds. *Chem. Phys. Lett. 400*, 117−121.
(21) Bondi, A. (1964) Van der Waals volumes and radii. *J. Phys. Chem. 68*, 441−451.
(22) Berg, L., Niemiec, M. S., Qian, W., Andersson, C. D., Wittung-Stafshede, P., Ekström, F., and Linusson, A. (2012) Similar but different: Thermodynamic and structural characterization of a pair of enantiomers binding to acetylcholinesterase. *Angew. Chem., Int. Ed. 51*, 12716−12720.
(23) Tanford, C. (1978) The hydrophobic effect and the organization of living matter. *Science 200*, 1012−1018.
(24) Biela, A., Sielaff, F., Terwesten, F., Heine, A., Steinmetzer, T., and Klebe, F. (2012) Ligand binding stepwise disrupts water network in thrombin: Enthalpic and entropic changes reveal classical hydrophobic effect. *J. Med. Chem. 55*, 6094−6110.
(25) Bissantz, C., Kuhn, B., and Stahl, M. (2010) A medicinal chemist's guide to molecular interactions. *J. Med. Chem. 53*, 5061−5084.
(26) Chodera, J. D., and Mobley, D. L. (2013) Entropy−enthalpy compensation: Role and ramifications in biomolecular ligand recognition and design. *Annu. Rev. Biophys. 42*, 121−142.
(27) Krieger, E., Koraimann, G., and Virend, G. (2002) Increasing the precision of comparative models with YASARA NOVA—A self-parameterizing force field. *Proteins 47*, 393−402.
(28) Duan, Y., Wu, C., Chowdhury, S., Lee, M. C., Xiong, G., Zhang, W., Yang, R., Cieplak, P., Luo, R., and Lee, R. (2003) A point-charge force field for molecular mechanics simulations of proteins based on condensed-phase quantum mechanical calculations. *J. Comput. Chem. 24*, 1999−2012.
(29) Morris, G. M., Goodsell, D. S., Hallliday, R. S., Huey, R., Hart, W. E., Belew, R. K., and Olson, A. J. (1998) Automated docking using a Lamarckian genetic algorithm and empirical binding free energy function. *J. Comput. Chem. 19*, 1639−1662.
(30) *Molecular Operating Environment (MOE)*, 2012.10; (2012), H3A 2R7, Chemical Computing Group Inc., Montreal, QC, Canada.

3.3 Combining *in Silico* and Biophysical Methods for the Development of *Pseudomonas aeruginosa* Quorum Sensing Inhibitors: An Alternative Approach for Structure-Based Drug Design

J. Henning Sahner, Christian Brengel, Michael P. Storz, Matthias Groh, Alberto Plaza, Rolf Müller, and Rolf W. Hartmann

Reprint with permission from *J. Med. Chem.* **2013**, *56*, 8656-8664.

Publication C

Contribution Report

The author planned, performed, and interpreted the digestion/Maldi-TOF and the HPLC-MS-ESI experiment. He contributed to the interpretation of the results.

Journal of Medicinal Chemistry

Article

pubs.acs.org/jmc

Combining in Silico and Biophysical Methods for the Development of *Pseudomonas aeruginosa* Quorum Sensing Inhibitors: An Alternative Approach for Structure-Based Drug Design

J. Henning Sahner,[†] Christian Brengel,[†] Michael P. Storz,[†] Matthias Groh,[†] Alberto Plaza,[‡] Rolf Müller,[‡] and Rolf W. Hartmann*[,†]

[†]Helmholtz Institute for Pharmaceutical Research Saarland (HIPS), Department of Drug Design and Optimization & Pharmaceutical and Medicinal Chemistry, Saarland University, Campus C2 3, 66123 Saarbrücken, Germany

[‡]Helmholtz Institute for Pharmaceutical Research Saarland (HIPS), Department of Microbial Natural Products, Saarland University, Campus C2 3, 66123 Saarbrücken, Germany

Supporting Information

ABSTRACT: The present work deals with the optimization of an inhibitor of PqsD, an enzyme essential for *Pseudomonas aeruginosa* quorum sensing apparatus. Molecular docking studies, supported by biophysical methods (surface plasmon resonance, isothermal titration calorimetry, saturation transfer difference NMR), were used to illuminate the binding mode of the 5-aryl-ureidothiophene-2-carboxylic acids. Enabled to make profound predictions, structure-based optimization led to increased inhibitory potency. Finally a covalent inhibitor was obtained. Binding to the active site was confirmed by LC-ESI-MS and MALDI-TOF-MS experiments. Following this rational approach, potent PqsD inhibitors were efficiently developed within a short period of time. This example shows that a combination and careful application of in silico and biophysical methods represents a powerful complement to cocrystallography.

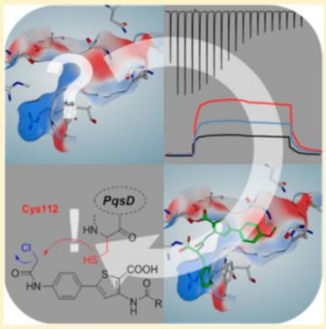

INTRODUCTION

Structure-based drug design is a rational strategy to develop bioactive molecules without the necessity of performing many rounds of modifications to derive structure−activity relationships (SAR). Frequently, data from X-ray cocrystallography are used to accelerate the lead optimization process. Although this method is undeniably efficient, there are some drawbacks: a cocrystal structure does not necessarily represent the biological state, as it results in a single "frozen" conformation that is affected by the crystallization conditions.[1,2] Furthermore, especially the ligand may not be well-defined even at high resolution.[3] In some cases, attempts of cocrystallizing ligands and their targets were not successful, forcing the research groups to make use of alternative strategies. The described problems can be overcome by the use of biophysical methods such as surface plasmon resonance (SPR), nuclear magnetic resonance (NMR), and isothermal titration calorimetry (ITC). An advantage of SPR, NMR, and ITC is that they can be performed in aqueous solution, which can be considered almost "physiological" conditions.

In the forefront of this work, compound **1** (Figure 1a) was identified as an inhibitor of PqsD. The target protein PqsD is a key player in the quorum sensing system of *Pseudomonas aeruginosa*. It mediates the formation of heptyl-4-hydroxyquinoline (HHQ), which is the precursor of *Pseudomonas* quinolone signal (PQS) (Scheme 1). Both molecules are potent virulence factors and function as signal molecules of *P. aeruginosa*, coordinating group behavior like the formation of biofilms.[4,5] The substrate channel of PqsD is about 15 Å long and rather narrow.[6] The channel can be divided into three parts, a positively charged entrance followed by a mainly hydrophobic middle segment, ending in a polar bottom part. The latter is delimited by the catalytic residues Cys112, His257, and Asp287. Suppression of PqsD activity has been shown recently by our group to inhibit biofilm formation.[7] This makes PqsD an attractive target for the therapy of chronic *P. aeruginosa* infections, especially in immunosuppressed individuals.[8−10]

Herein, we report on the optimization of **1** supported by biophysical methods and molecular docking. The approach described in the following represents a hit to lead optimization process that does not involve cocrystallographic structure determination.

RESULTS AND DISCUSSION

The IC_{50} value of compound **1** (Figure 1a) against PqsD was determined in a functional enzyme assay[11] to be 6 μM. The same compound has recently been reported as a weak inhibitor of bacterial RNA polymerase (IC_{50}: 241 μM),[12] a classical target for antibacterial therapy. Targeting quorum sensing an

Received: July 20, 2013
Published: October 1, 2013

   dx.doi.org/10.1021/jm401102e | J. Med. Chem. 2013, 56, 8656−8664

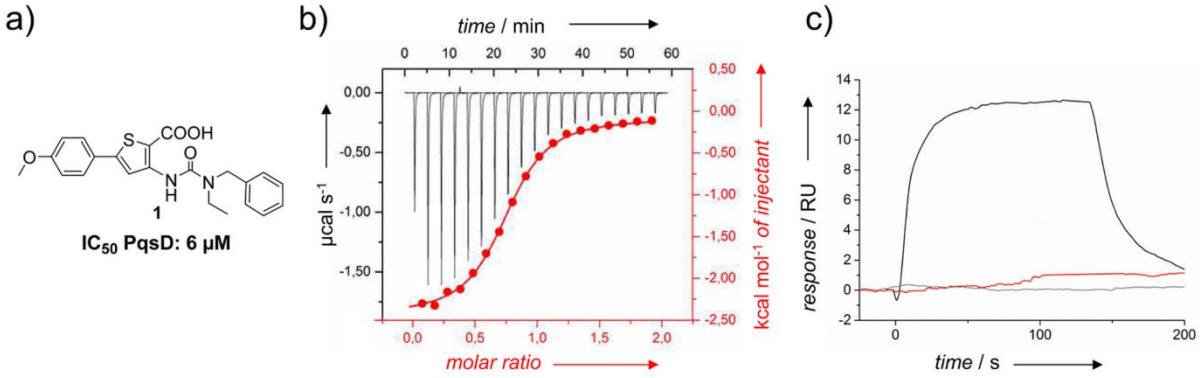

Figure 1. (a) Compound **1**. Biophysical characterization of **1**: (b) Thermogram (red) and titration curve (black) obtained from ITC of PqsD with **1**. (c) SPR experiment: ACoA binds to PqsD (black). ACoA binding is inhibited by preincubation with **1** (red). The reference signal is shown in gray.

Scheme 1. Biosynthesis of Signaling Molecules HHQ and PQS in *Pseudomonas aeruginosa*[a]

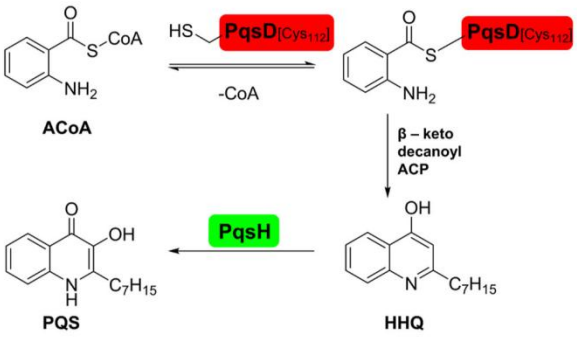

[a]Anthranilate is transferred to PqsD via thio-esterification of ACoA with Cys112. The next step is a condensation with acetyl carrier protein (ACP) bound β-ketodecanoic acid to form HHQ, which is finally transformed to PQS by PqsH.

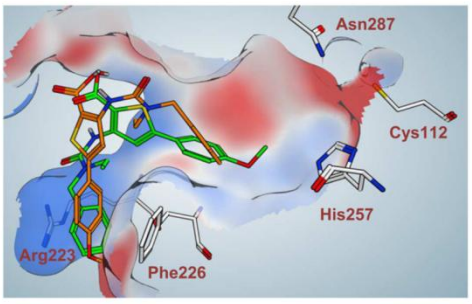

Figure 2. Docking poses of **1** within the ACoA channel of PqsD: (orange; Vina-Score, 8.3 kcal mol^{-1}) (green; Vina-Score, 8.2 kcal mol^{-1}).

antibacterial effect is not desired to avoid selection pressure inevitably, leading to the development of resistant strains.[13] Thus, other potential hit candidates from the 5-aryl-ureidothiophene-2-carboxylic acid class, displaying poor selectivity, were not considered for further optimization (see Table S1 in Supporting Information).

Attempts to obtain a cocrystal structure of **1** and PqsD, using soaking techniques, were not successful. Therefore, a combination of biophysical methods and molecular docking was used to elucidate the binding mode of **1**. To exclude a nonspecific binding behavior (e.g., via aggregation), **1** was examined in an isothermal titration calorimetry (ITC) experiment to ensure stoichiometric binding. Thereby an equimolar binding ratio (0.82 ± 0.05) with a K_D of 6.3 ± 2.6 μM was determined (Figure 1b), confirming that the discovered class of compounds represents a promising starting point for further optimization.

To clarify the binding site on PqsD, SPR experiments were conducted. It was shown that the natural substrate ACoA can no longer bind to the enzyme when PqsD was preincubated with **1** (Figure 1c). This result indicates that **1** binds inside the ACoA channel, thus blocking the first step of the catalytic reaction.

From docking simulations with **1**, two putative binding modes with similar scoring values but reverse orientations were obtained. In the first pose (Figure 2; orange), the ureido *N*-ethyl-benzyl moiety points to the bottom of the pocket (delimited by Cys112, His257, and Asn287), whereas in the second pose (Figure 2; green), the methoxy group is placed in this position.

To get a reliable starting point for a structure-based optimization, discrimination between the two poses was necessary. Therefore, we designed an SPR competition experiment with model compounds **1**–**3** from the 5-aryl-ureidothiophene-2-carboxylic acid class, differently substituted in the ureido and aryloxy parts (Figure 3b). As competitor compounds, the 2-nitrophenyl-methanols **A** and **B** were used (Figure 3a). They were recently reported as PqsD inhibitors[7] and were shown to interact with the catalytic residues, especially Cys112, at the bottom of the ACoA-channel.[14]

As illustrated in Figure 3a, the presence of **A** and **B** should influence the binding of the ureidothiophene model compounds depending on their substitution pattern. Compared with **2**, **1** bears a large substituent at the ureido part, whereas **3** is elongated in the aryloxy part at the opposite site. If the ureido part points to the bottom of the pocket, one would expect that **1** is more sterically hindered than **2** and **3** when the competitors are present. In contrast, the longer aryloxy part of **3** should lead to a reduced binding if the ureidothiophenes bind in the reversed orientation. In the absence of a competitor compound, **1**–**3** displayed comparable responses (Figure 3c). When the sterically less demanding 2-nitrophenyl-methanol derivative **A** was present, a reduction of affinity was observed exclusively for **3** bearing a bulky phenyl substituent in the

dx.doi.org/10.1021/jm401102e | J. Med. Chem. 2013, 56, 8656–8664

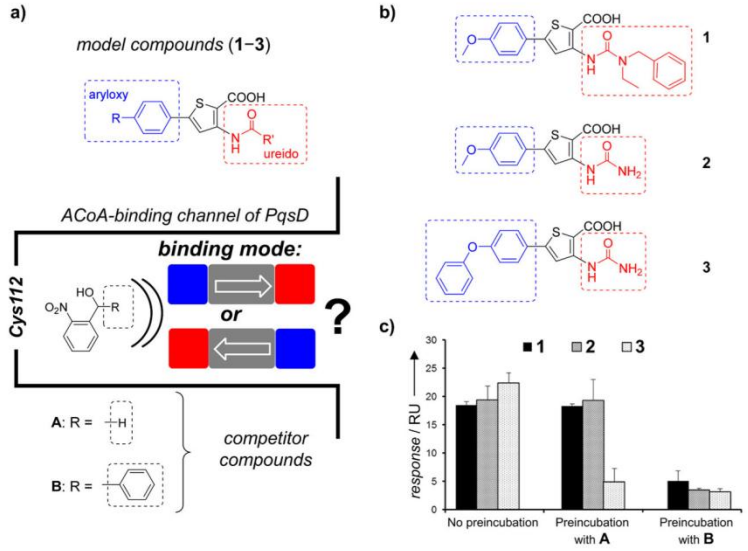

Figure 3. (a) Schematic illustration of the SPR competition experiments: PqsD was preincubated with competitor compounds **A** and **B** binding to the ACoA-channel, delimited by Cys112. The model compounds **1**–**3** were subsequently added, and the influence of **A** or **B** on their binding behaviors was investigated. The results shed light on the binding mode of the 5-aryl-ureidothiophene-2-carboxylic acids. (b) Structures of the model compounds **1**–**3**. (c) Results from SPR-competition experiments suggest the aryloxy-moiety to point into the pocket.

aryloxy part. In contrast, the ethyl-benzyl moiety at the ureido motif of **1** did not prevent a binding. These results fit to the docking prediction with the aryloxy part pointing into the pocket (Figure 2, green). In competition with **B**, the binding affinity of all three compounds was reduced as expected from the docking results (see Figure S1 and S2 in Supporting Information). Thus a deeper insight into the position of the new inhibitors in the binding channel was provided.

As the starting point for structure–activity exploration compound **2** was chosen, a truncated derivative of the initial hit **1**. It displays comparable ligand efficiency (LE, Table 1) while being more suitable for further modification at the ureido motif. The docking pose of **2** (Figure 4a) suggests an anchoring of the ureido moiety by interaction of the carbonyl oxygen with Arg223. To validate this assumption, binding of **2** to the R223A mutant, that should display weaker affinity, was investigated by SPR. The response of compound **2** was reduced to six response units (RU) in comparison to 25 RU for the wild-type enzyme (see Figure S4 in Supporting Information), confirming this hypothesis. Arg262, placed in the upper part of the binding pocket, should be a potential interaction partner for a negatively charged moiety. The introduction of a carboxylate resulting in compounds **4** and **5** (Table 1) indeed led to an increased activity, confirming this prediction. In the docking pose, the introduced carboxylic acid moiety of **4** is located closely to Arg262, enabling the formation of a new interaction (Figure 4b). On the basis of the finding that **4** is more active than **5**, we concluded that a methylene linker is more appropriate than a longer spacer unit. This allowed making use of α amino acids for simple variations in the next steps, taking advantage of their hydrophilicity to increase the polarity of the inhibitors, as low lipophilicity is an important requirement for drugs targeting Gram negative bacteria. A study of O'Shea et al. shows that almost all antibiotics, effective against *P. aeruginosa*, possess a clogD$_{7.4}$ value below 0.[15] While our hit compound **1** (log $D_{7.4}$: 2.58) did not meet this criterion, amino acid derivative **4** (log $D_{7.4}$: −1.62) did.

As illustrated in Figure 4b, docking simulations predict that the glycine derivative **4** is anchored by an interaction of the carboxylate group with Arg262. The narrow cleft, subjacent to the α-position of **4** and delimited by Arg223 and Phe226, is supposed to be addressable by expansion of **4**. A targeted approach should replace the *pro-S* hydrogen because the space adjacent to the *pro-R* hydrogen is blocked by Arg223, which could lead to a sterical clash (Figure 4d). Following this strategy, the introduction of *S*-amino acid residues improved the activity resulting in up to submicromolar IC$_{50}$ values in case of the *S*-alanine and *S*-phenylalanine derivatives **6** and **7** (Figure 4b–e). Compound **8**, the counterpart of **7** that lacks the COOH group next to the ureido moiety, displays a significantly weaker inhibition. This again highlights the importance of the carboxylic acid group, which is in accordance with our binding hypothesis.

To complete the picture, the *R*-enantiomers **9** and **10** were investigated. In both cases, the activity decreased dramatically. These data corroborate the highly selective three-dimensional interaction formed by the *S*-enantiomeric moieties with the target enzyme. To evaluate whether the decreased activity of the *R*-enantiomer **9** is due to a sterical clash, as expected, or associated with the absence of the *S*-methyl group of **6**, the dimethyl compound **11** was investigated. The fact that **11** was less active than **4** and **6** confirms the prediction of a sterical collision.

To test for selectivity toward bacterial RNA polymerase, the most potent derivatives **6** and **7** were tested for inhibition of this enzyme. Both displayed only slight inhibitory potency (~10–20%) at a concentration of 200 μM.

Saturation transfer difference (STD) NMR[16] was used to identify the binding epitopes of **7** (Figure S5 in Supporting Information). Strong STD enhancements were observed for all protons of **7**, with the methylene linker protons exhibiting the strongest enhancements. This is consistent with the docking simulations, which predict these methylene protons to be positioned at the entrance of the narrow subpocket delimited

Table 1. Inhibition of PqsD in Vitro, Ligand Efficiencies and clogD$_{7.4}$ Values of Compounds 1−11

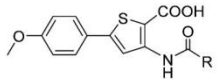

Cpd	R	IC_{50} PqsD	LE[a]	clogD$_{7.4}$[b]
1	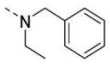	6 μM	0.25	2.58
2		170 μM	0.26	0.15
4		7 μM	0.30	−1.62
5	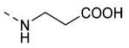	37 μM	0.25	−1.47
6		2 μM	0.32	−1.27
7	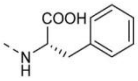	0.5 μM	0.28	0.59
8	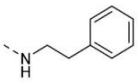	58 μM	0.21	2.61
9		54 μM	0.24	−1.27
10	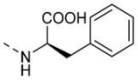	26 μM	0.19	0.59
11		56 μM	0.23	−0.93

[a]Ligand efficiency calculated as LE = 1.4(pIC$_{50}$/HAC) [b]clogD$_{7.4}$ calculated with ACDLabs Percepta 2012

by Arg223 and Phe226. Moreover, the fact that the other protons of **7** also displayed strong STD enhancements suggests that **7** is nearly completely surrounded by PqsD.

To confirm that the optimized inhibitors bind in a similar way as the model compounds **1**−**3**, the SPR-competition experiment with **A** and **B** was conducted for compound **7**. As expected, the binding response was only significantly reduced in the presence of **B** (Figure S3 in Supporting Information). In addition, we performed an STD-NMR competition experiment to validate the SPR results. Increasing amounts of compound **B** were added to a 100:1 complex of **7**/PqsD (Figure 5). Difference spectra were monitored for a change in intensity of signals belonging to either **7** or **B** during titration. As seen in the spectral expansions showing the aromatic region, stepwise addition of up to 3.0 equiv of **B** with respect to **7** resulted in a uniform decrease in intensity for signals corresponding to **7** while signals ascribable to **B** appeared and steadily increased. This confirms that **7** binds deep inside the ACoA-channel of PqsD.

Finally, we focused on the substituted 5-aryl ring that is predicted to be located near the active site within the ACoA

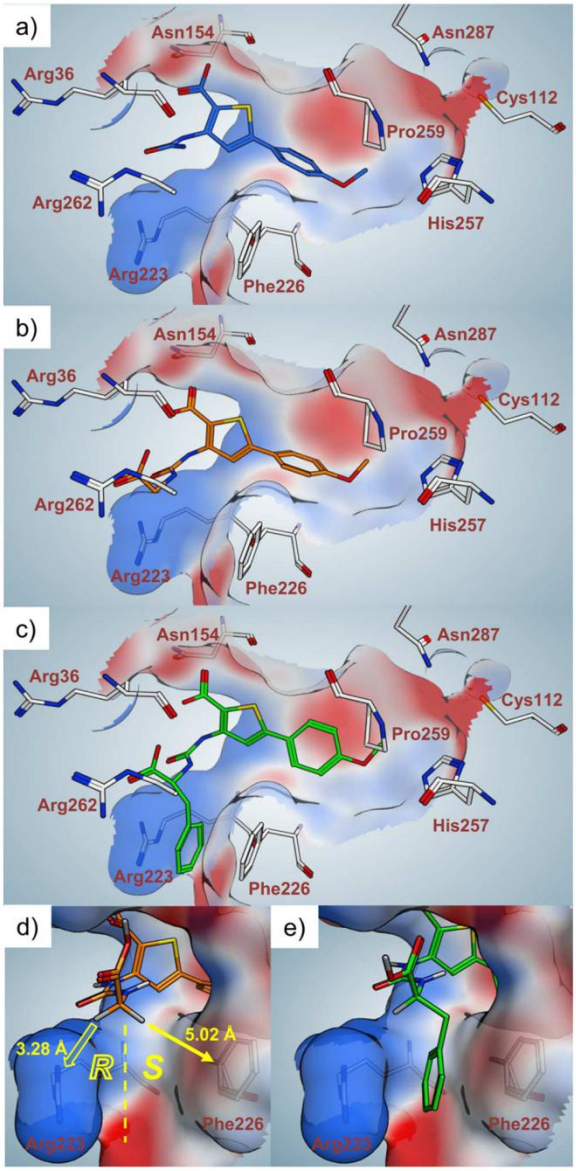

Figure 4. (a) Docking pose of **2**, the starting point for structure-based optimization. (b) Docking pose of glycine derivative **4**. (c) Docking pose of optimized compound **7**. (d) Illustration of the limited space in the narrow cleft formed by Arg223 and Phe226. (e) Close-up of the benzyl moiety of **7**, perfectly fitting into the narrow cleft.

channel (Figure 4). As already shown with phenoxy compound **3** (IC_{50} = 20 μM), larger substituents are tolerated in this part of the binding pocket. As Cys112 is pivotal for the catalytic activity of PqsD, a covalent trapping of this amino acid should lead to an effective blockade of the enzymatic machinery. For that purpose, a β-chloroacetyl moiety was introduced as an "electrophilic warhead",[17] at the appropriate position, linked to the 5-aryl ring via an amide function (Figure 6a).

The resulting compound **12** (clogD$_{7.4}$: −0.59) displays an IC_{50} value of 2 μM. The covalent binding of **12** to PqsD was demonstrated by LC-ESI-MS. The PqsD peak (m/z = 36687.5 $[M + H]^+$) shifted after preincubation with **12** to the calculated

dx.doi.org/10.1021/jm401102e | J. Med. Chem. 2013, 56, 8656−8664

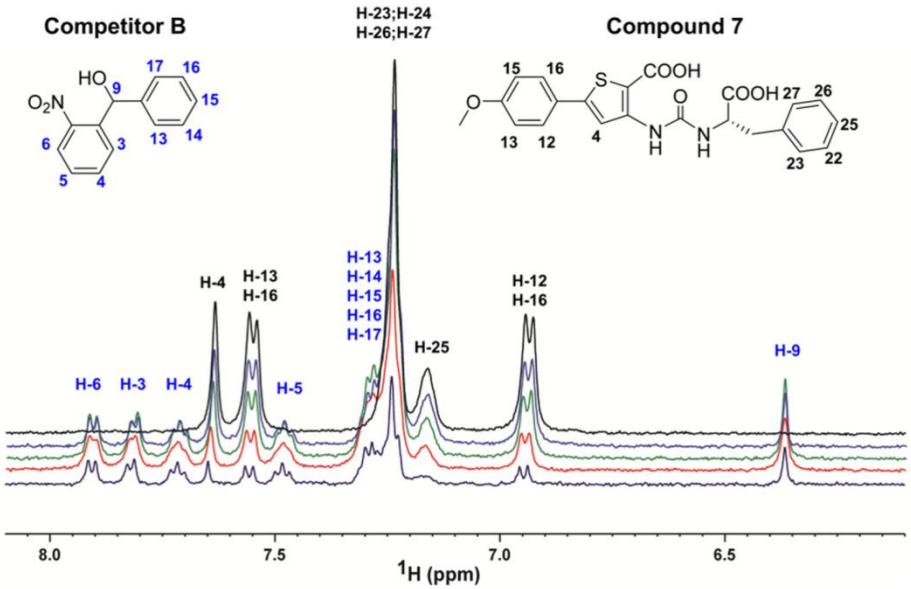

Figure 5. Competition of 7 and **B** binding to PqsD by STD NMR. Expanded ^{1}H STD NMR spectrum of 7 (1 mM) in the presence of PqsD (10 μM) (black curve). STD NMR spectra recorded on the same sample after addition of 0.5 (purple), 1.0 (green), 2.0 (red), and 3.0 (blue) equivalents of compound **B**. Signals of 7 are labeled in black, from **B** in blue.

adduct mass (m/z = 37153.1 $[M + H]^+$) (Figure S8 in Supporting Information). To evaluate whether indeed Cys112 is targeted by **12**, the tryptically digested protein was analyzed by MALDI-TOF-MS. The signal of the fragment containing Cys112, with a calculated m/z = 1510.8 $[M + H]^+$, was found in the reference sample without inhibitor. In the sample treated with **12**, this signal was absent while two new peaks at m/z = 1975.9 and 1931.9 $[M + H]^+$ appeared (Figure 6b,c). The former fits to the Cys112 fragment with covalently bound **12**. The latter refers to its fragmentation product missing a carboxylic acid moiety. Taking into account that a long residence time at the active site is considered important for in vivo potency of the inhibitor,[18] covalently binding compound **12** carries the potential of strong biological effects.

■ CONCLUSIONS

In conclusion, we optimized the PqsD inhibitor **1**, following a novel approach. First, an equimolar binding behavior to the target protein PqsD was determined by ITC. The binding mode was elucidated by examination of three model compounds (**1**–**3**) in SPR competition experiments. To the best of our knowledge, this is the first example of such an approach. These findings allowed profound docking calculations guiding our subsequent structure-based optimization process. This approach culminated in an irreversible inhibitor, which covalently binds to the active site of PqsD as predicted. The optimization of activity was accompanied by reduced lipophilicity (Table 1), caused by the introduction of amino acids at the ureido motif. According to the literature, this should facilitate permeation into Gram-negative cells.[15]

For several drug targets, inhibitors with known binding sites and the protein crystal structures are available. In such cases, the presented approach of determining the binding mode can be helpful to guide a structure-based design of new inhibitors, especially if cocrystallization fails.

While we mainly focused on the inhibitory potency at this early point of development, structural variations leading to more drug-like properties (e.g., bioisosteric exchange of the carboxylic groups) remains a challenging task and will be an element of future work. Additional efforts will also include studies on intracellular activity and inhibition of biofilm formation in *P. aeruginosa*. In the present study, shortcomings of in silico docking simulations (prediction of multiple binding modes) were compensated by the use of biophysical methods. This rational approach represents a powerful complement to X-ray cocrystallography and should be applicable to many drug targets with known ligands.

■ EXPERIMENTAL SECTION

Materials and Methods. Starting materials were purchased from commercial suppliers and used without further purification. Column flash chromatography was performed on silica gel (40–63 μM), and reaction progress was monitored by TLC on TLC Silica Gel 60 F_{254} (Merck). All moisture-sensitive reactions were performed under nitrogen atmosphere using oven-dried glassware and anhydrous solvents. ^{1}H and ^{13}C NMR spectra were recorded on Bruker Fourier spectrometers (500/300 or 176/126/75 MHz) at ambient temperature with the chemical shifts recorded as δ values in ppm units by reference to the hydrogenated residues of deuteriated solvent as internal standard. Coupling constants (J) are given in Hz, and signal patterns are indicated as follows: s, singlet; d, doublet; dd, doublet of doublets; t, triplet; m, multiplet, br, broad signal. The purity of the final compounds was >95% except for **12** (90%) measured by HPLC. The Surveyor LC system consisted of a pump, an autosampler, and a PDA detector. Mass spectrometry was performed on a MSQ electrospray mass spectrometer (ThermoFisher, Dreieich, Germany). The system was operated by the standard software Xcalibur. A RP C18 NUCLEODUR 100-5 (125 mm × 3 mm) column (Macherey-Nagel GmbH, Dühren, Germany) was used as the stationary phase. All solvents were HPLC grade. In a gradient run, the percentage of acetonitrile (containing 0.1% trifluoroacetic acid) was increased from an initial concentration of 0% at 0 min to 100% at 15 min and kept at 100% for 5 min. The injection volume was 10 μL, and flow rate was set

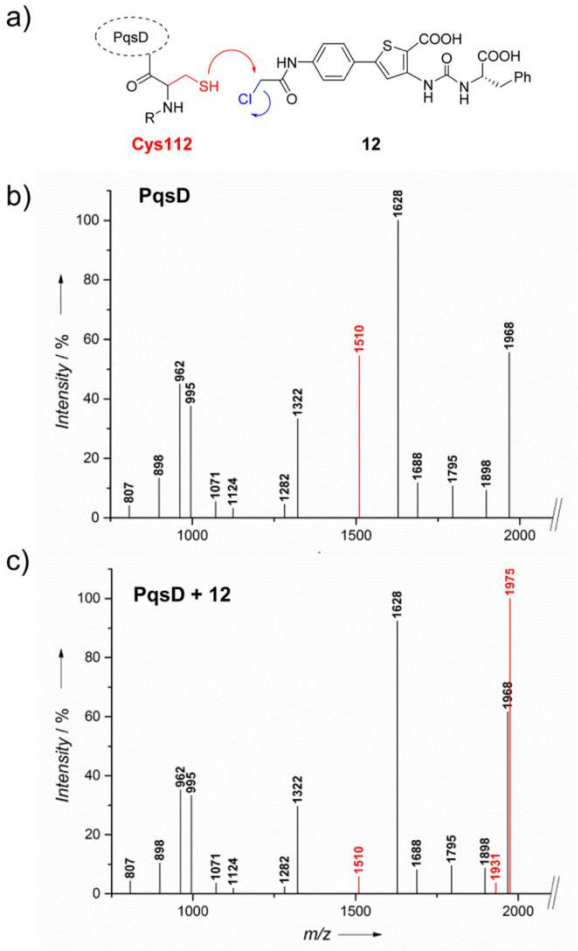

Figure 6. (a) Schematic illustration of the proposed trapping of Cys112 by the introduced electrophilic warhead of **12**. MALDI-TOF-MS after tryptic digestion. The mass of the fragment containing Cys112 is highlighted in red (b) PqsD, (c) PqsD after incubation with **12**. Signals below 3% intensity were removed for the sake of clarity (raw data is shown in Figure S6 and S7 in Supporting Information).

Scheme 2. Synthesis of 5-Aryl-3-ureidothiophene-2-carboxylic Acids

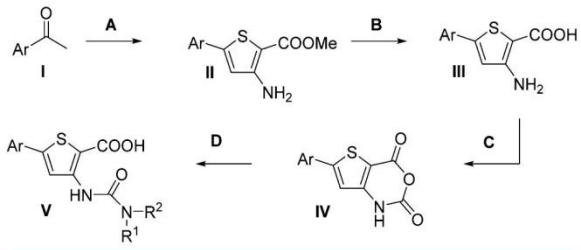

to 800 μL/min. MS analysis was carried out at a spray voltage of 3800 V and a capillary temperature of 350 °C and a source CID of 10 V. Spectra were acquired in positive mode from 100 to 1000 *m*/*z* at 254 nm for the UV trace.

Chemistry. *General Synthesis Procedures.* Experimental details on synthesis of **12** can be found in the Supporting Information.

Method A, General Procedure for the Synthesis of 5-Aryl-3-amino-2-carboxylic Acid Methylester (II) (Scheme 2).[19] $POCl_3$ (26.1 g, 0.17 mol) was added dropwise to DMF (24.9 g, 0.34 mol), maintaining the temperature below 25 °C (cooling in ice bath), and stirred for additional 15 min. The acetophenone **I** (85.0 mmol) was added slowly, and the temperature was kept between 40 and 60 °C. After complete addition, the mixture was stirred for 30 min at room temperature. Hydroxylamine hydrochloride (23.6 g, 0.34 mol) was carefully added portionwise (exothermic reaction!), and the reaction was stirred for additional 30 min without heating. After cooling to room temperature, the mixture was poured into ice water (300 mL). The precipitated β-chloro-cinnamonitrile was collected by filtration, washed with H_2O (2 × 50 mL), and dried under reduced pressure over $CaCl_2$. In the next step, sodium (1.93 g, 84.0 mmol) was dissolved in MeOH (85 mL) and methylthioglycolate (6.97 g, 65.6 mmol) was added to the stirred solution. The β-chloro-cinnamonitrile (61.1 mmol) was added, and the mixture was heated to reflux for 30 min. After cooling to room temperature, the mixture was poured in ice water (300 mL). The precipitated solid was collected by filtration, washed with H_2O (2 × 50 mL), and dried under reduced pressure over $CaCl_2$. If necessary, recrystallization was performed from EtOH.

Method B, General Procedure for the Synthesis of 5-Aryl-3-amino-2-carboxylic Acid (III) (Scheme 2). The 5-aryl-3-amino-2-carboxylic acid methyl ester **II** (16.6 mmol) was added to a solution of KOH (60 mL, 0.6 M in H_2O) and MeOH (60 mL). The mixture was heated to reflux for 3 h, concentrated, and washed with EtOAc (2 × 50 mL). The aqueous layer was cooled with ice and acidified with a saturated aqueous solution of $KHSO_4$. The precipitated solid was collected by filtration, washed with H_2O (2 × 30 mL), and dried under reduced pressure over $CaCl_2$.

Method C, General Procedure for the Synthesis of 5-Aryl-2-thiaisatoic-anhydride (IV) (Scheme 2).[20,21] To a solution of the 5-aryl-3-amino-2-carboxylic acid (**III**) (5.28 mmol) in THF (50 mL), a solution of phosgene (6.10 mL, 20 wt % in toluene, 11.6 mmol) was added dropwise over a period of 30 min. The reaction mixture was stirred for 2 h at room temperature, followed by the addition of saturated aqueous solution of $NaHCO_3$ (30 mL) and H_2O (50 mL). The resulting mixture was extracted with EtOAc/THF (1:1, 3 × 100 mL). The organic layer was washed with saturated aqueous NaCl (100 mL), dried ($MgSO_4$), and concentrated. The crude material was suspended in a mixture of *n*-hexane/EtOAc (2:1, 50 mL), heated to 50 °C, and after cooling to room temperature separated via filtration.

Method D, General Procedure for the Synthesis of 5-Aryl-3-ureidothiophene-2-carboxylic Acid (V) (Scheme 2).[22] The 5-aryl-2-thiaisatoic-anhydride (**IV**) (0.46 mmol) was suspended in water (7.5 mL), and the appropriate amine (4.60 mmol) was added. The reaction mixture was stirred, heated to 100 °C, and then cooled to room temperature. The reaction mixture was poured into a mixture of concentrated HCl and ice (1:1) and extracted with EtOAc/THF (1:1, 60 mL). The organic layer was washed with aqueous HCl (2M), followed by saturated aqueous NaCl (2 × 50 mL), dried ($MgSO_4$), and concentrated. The crude material was suspended in a mixture of *n*-hexane/EtOAc (2:1, 20 mL), heated to 50 °C, and after cooling to room temperature separated via filtration.

Spectroscopic data of final compounds and intermediates can be found in the Supporting Information. Compound **7** is presented as example.

(*S*)-3-(3″-(1-Carboxy-2-phenylethyl)ureido)-5-(4′-methoxyphenyl)thiophene-2-carboxylic acid (**7**).

^{1}H NMR (DMSO-d_6, 300 MHz): δ = 12.84 (br s, 2 H, COOH), 9.42 (s, 1 H), 8.15 (d, *J* = 7.9 Hz, 1 H), 8.09 (s, 1 H), 7.69−7.51 (m, *J* = 8.8 Hz, 2 H), 7.37−7.25 (m, 4 H), 7.25−7.17 (m, 1 H), 7.03−6.97 (m, *J* = 8.8 Hz, 2 H), 4.56−4.28 (m, 1 H), 3.79 (s, 3 H, OCH_3), 3.11 (dd, *J* = 13.9, 4.6 Hz, 1 H), 2.88 (dd, *J* = 13.9, 9.8 Hz, 1 H) ppm.

^{13}C NMR (DMSO-d_6, 75 MHz): δ = 173.6, 164.6, 160.1, 153.7, 147.1, 145.9, 137.7, 129.0, 128.2, 127.1, 126.4, 125.4, 116.7, 114.7, 105.8, 55.3, 54.4, 36.9 ppm.

Biology and Biophysics. *General Procedure for Expression and Purification of Recombinant PqsD WT and R223A Mutant in Escherichia coli.* His6-tagged PqsD (H6-PqsD) and mutants were

dx.doi.org/10.1021/jm401102e | *J. Med. Chem.* 2013, 56, 8656−8664

expressed in *E. coli* and purified using a single affinity chromatography step. Briefly, *E. coli* BL21 (λDE3) cells containing the pET28b(+)/pqsD (kindly provided by Prof. Rolf Müller) were grown in LB medium containing 50 μg/mL kanamycin at 37 °C to an OD_{600} of approximately 0.8 units and induced with 0.2 mM IPTG for 16 h at 16 °C. The cells were harvested by centrifugation (5000 rpm, 10 min, 4 °C), and the cell pellet was resuspended in 100 mL of binding buffer (10 mM Na_2HPO_4, 2 mM KH_2PO_4 pH 7.4, 3 mM KCl, 137 mM NaCl, 20 mM imidazole, 10% glycerol (v/v)) and lysed by sonication for a total process time of 2.5 min. Cell debris were removed by centrifugation (18500 rpm, 40 min, 4 °C), and the supernatant was filtered through a syringe filter (0.20 μm). The clarified lysate was immediately applied to a Ni-NTA column, washed with binding buffer, and eluted with 500 mM imidazole. The protein containing fractions were buffer-exchanged into 125 mM Na_2HPO_4, 50 mM KH_2PO_4 pH 7.6, 50 mM NaCl, and 10% glycerol (v/v), using a PD10 column and judged pure by SDS-PAGE analysis. Then protein was stored in aliquots at −80 °C.

Screening Assay Procedure for in Vitro PqsD Inhibition.[11] The assay was performed monitoring enzyme activity by measuring HHQ formed by condensation of anthraniloyl-CoA and β-ketodecanoic acid. The reaction mixture contained MOPS buffer (0.05 M, pH 7.0) with 0.005% (w/v) Triton X-100, 0.1 μM of the purified enzyme, and inhibitor. The test compounds were dissolved in DMSO and diluted with buffer. The final DMSO concentration was 0.5%. After 10 min preincubation at 37 °C, the reaction was started by the addition anthraniloyl-CoA to a final concentration of 5 μM and β-ketodecanoic acid to a final concentration of 70 μM. Reactions were stopped by addition of MeOH containing 1 μM amitriptyline as internal standard for LC/MS-MS analysis. HHQ was quantified using a HPLC-MS/MS mass spectrometer (ThermoFisher, Dreieich, Germany) in ESI mode. Ionization of HHQ and the internal standard amitriptyline was optimized in each case. The solvent system consisted of 10 mM ammonium acetate (A) and acetonitrile (B), both containing 0.1% trifluoroacetic acid. The initial concentration of B in A was 45%, increasing the percentage of B to 100% in 2.8 min and keeping it at 98% for 0.7 min with a flow of 500 μL/min. The column used was a NUCLEODUR-C18, 100-3/125-3 (Macherey & Nagel, Duehren, Germany). Control reactions without the inhibitor, but including identical amounts of DMSO, were performed in parallel, and the amount of HHQ produced was set to 100%. All reactions were performed in triplicate.

RNAP-Transcription Assay. *E. coli* RNA polymerase holo enzyme was purchased from Epicenter Biotechnologies (Madison, WI). Final concentrations in a total volume of 30 μL were one unit of RNA polymerase (0.5 μg), which were used along with 60 nCi of [5,6-^{3}H]-UTP, 400 μM of ATP, CTP, and GTP as well as 100 μM of UTP, 20 units of RNase inhibitor (RiboLock, Fermentas), 10 mM DTT, 40 mM Tris-HCl (pH 7.5), 150 mM KCl, 10 mM $MgCl_2$, and 0.1% CHAPS. As a DNA template 3500 ng of religated pcDNA3.1/V5-His-TOPO were used per reaction.[23] Prior to starting the experiment, the compounds were dissolved in DMSO (final concentration during experiments: 2%). Dilution series of compounds were prepared using a liquid handling system (Janus, Perkin-Elmer, Waltham, MA). The components described above (including the inhibitors) were preincubated in absence of NTPs and DNA for 10 min at 25 °C. Transcription reactions were started by the addition of a mixture containing DNA template and NTPs and incubated for 10 min at 37 °C. The reaction was stopped by the addition of 10% TCA, followed by a transfer of this mixture to a 96-well Multiscreen GFB plate (Millipore, Billerica, MA) and incubation for 45 min at 4 °C. The plate underwent several centrifugation and washing steps with 10% TCA and 95% ethanol to remove residual unincorporated ^{3}H-UTP. After that, the plate was dried (30 min, 50 °C) and 30 μL of scintillation fluid (Optiphase Supermix, Perkin-Elmer) was added to each well. After 10 min, the wells were assayed for presence of ^{3}H-RNA by counting using a Wallac MicroBeta TriLux system (Perkin-Elmer). To obtain inhibition values for each sample, their counts were related to DMSO controls.

Surface Plasmon Resonance. SPR binding studies were performed using a Reichert SR7500DC instrument optical biosensor (Reichert Technologies, Depew, NY, USA) and CMD500 M (carboxymethyl dextrane-coated) sensor chips obtained from XanTec (XanTec Bioanalytics, Düsseldorf, Germany).

Immobilization of Wild-Type PqsD and R223A Mutant. PqsD was immobilized on a CMD500 M sensor chip at 12 °C using standard amine coupling analogous to the manufacturers' instructions. PqsD was diluted into sodium acetate buffer (10 mM, pH 4.5) to a final concentration of 100 μg/mL. PqsD was immobilized at densities between 5000 and 6000 RU for binding studies and for mutagenesis studies. The PqsD mutant was immobilized analogously to the wild type.

Competition Studies. The competition studies were performed at a constant flow rate of 50 μL/min in instrument running buffer (50 mM MOPS, pH 8.0, 150 mM NaCl, 5% DMSO (v/v), 0.1% Triton X 100 (v/v)). Then 10 mM stock solutions of compounds **1**, **2**, and **3** in DMSO were directly diluted to a concentration of 500 μM (50 mM MOPS, pH 8.0, 150 mM NaCl, 0.1% Triton X-100 (v/v)) and then diluted to a final concentration of 100 μM in running buffer (50 mM MOPS, pH 8.0, 150 mM NaCl, 5% DMSO (v/v), 0.1% Triton X 100 (v/v)). Final concentration of DMSO was retained at 5% (v/v). Before the compounds were injected, six warm-up blank injections were performed. Buffer blank injections and DMSO calibration were included for double referencing.

ACoA Competition. PqsD was preincubated with compound **1**, therefore **1** was added to the running buffer (100 μM). The sensor chip surface was flushed for several hours at a constant flow rate of 50 μL/min until the baseline was stable. Afterward, the flow rate was decreased to 10 μL/min and ACoA was injected (100 μM) twice for 120 s association and 15 min dissociation times.

Competitor Competition. PqsD was preincubated with compounds **A** or **B**, therefore the competitor compound was added to the running buffer (100 μM). The sensor chip surface was flushed for several hours at a constant flow rate of 50 μL/min until the baseline was stable. Afterward, the flow rate was decreased to 10 μL/min and compounds **1**, **2**, or **3** were injected (100 μM) twice for 120 s association and 300 s dissociation times. Because of a slow k_{off} rate of the competitor compounds, k_D values referring to the concentrations do not play a decisive role during the competition experiment.

Studies with R223A Mutant. The experiments were performed at a constant flow rate of 50 μL/min in instrument running buffer (50 mM MOPS, pH 8.0, 150 mM NaCl, 5% DMSO (v/v), 0.1% Triton X 100 (v/v)) at 12 °C. Then 10 mM stock solutions of compounds **1** or **2** in DMSO were diluted to a concentration of 100 μM analogous to the binding studies. Before the compound was injected, 12 warm-up blank injections were performed. The obtained data were referenced against blank injections and DMSO calibration. The compounds were injected twice for 120 s association and 300 s dissociation time. Scrubber software was used for processing and analyzing data.

Isothermal Titration Calorimetry. ITC experiments were carried out using an ITC200 instrument (Microcal Inc., GE Healthcare). Concentration of the ligand in DMSO stock solutions was 20 mM. Final ligand concentrations were achieved by diluting 1:20 (v/v) in the experimental buffer, resulting in a final DMSO concentration of 5% (v/v). Protein concentration was determined by measuring the absorbance at 280 nm using a theoretical molarity extinction coefficient of 17780 M^{-1} cm^{-1}. DMSO concentration in the protein solution was adjusted to 5% (v/v). ITC measurements were routinely performed at 25 °C in PBS-buffer, pH 7.4, 10% glycerol (v/v), and 5% DMSO (v/v). The titrations were performed on 100 μM PqsD-His6 in the 200 μL sample cell using 2 μL injections of 1.0 mM ligand solution every 180 s. Raw data were collected, and the area under each peak was integrated. To correct for heats of dilution and mixing, the final baseline consisting of small peaks of the same size at the end of the experiment was subtracted. The experimental data were fitted to a theoretical titration curve (one site binding model) using MicroCal Origin 7 software, with ΔH (enthalpy change in kcal mol^{-1}), K_A (association constant in M^{-1}), and N (number of binding sites) as

adjustable parameters. Thermodynamic parameters were calculated from equation:

$$\Delta G = \Delta H - T\Delta S = \mathrm{RT} \ln K_A = -\mathrm{RT} \ln K_D$$

where ΔG, ΔH, and ΔS are the changes in free energy, enthalpy, and entropy of binding, respectively, T is the absolute temperature, and R = 1.98 cal mol^{-1} K^{-1}. For compound **1**, four independent experiments were performed.

Saturation Transfer Difference NMR. All NMR data were recorded at 298 K on a Bruker Avance 500 NMR instrument equipped with a cryogenically cooled *z*-shielded gradient probe. Experiments were recorded with the carrier set at −2 ppm for on-resonance irradiation and 40 ppm for off-resonance irradiation. Control spectra were recorded under identical conditions on samples containing free compound **7** to test for artifacts. Selective protein saturation (3 s) was accomplished using a train of 50 ms Gauss-shaped pulses, each separated by a 1 ms delay, at an experimental determined optimal power (50 dB on our probe); a T1ρ filter (15 ms) was incorporated to suppress protein resonances. Experiments were recorded using a minimum of 512 scans and 32K points. On- and off-resonance spectra were processed independently and subtracted to provide a difference spectrum. Samples containing **7** and PqsD at final concentrations of 1 mM and 10 μM, respectively, were prepared in 20 mM sodium phosphate, 50 mM NaCl, and 5 mM $MgCl_2$, pH 7.0.

LC-ESI-MS. PqsD (25 μM) was preincubated with compound **12** (25 μM) for 30 min at 37 °C in Tris-HCl buffer (0.05 M, pH 8.0) with 0.5% DMSO. Dithiothreitol was added, and the samples were analyzed by HPLC-ESI. All ESI-MS-measurements were performed on a Dionex Ultimate 3000 RSLC system using an Aeris Widepore XB-C8, 150 mm × 2.1 mm, 3.6 μm dp column (Phenomenex, USA). Separation of a 2 μL sample was achieved by a linear gradient from (A) H_2O + 0.05% TFA to (B) ACN + 0.05% TFA at a flow rate of 250 μL/min and 45 °C. The gradient was initiated by a 1.0 min isocratic step at 15% B, followed by an increase to 80% B in 4.5 min to end up with a 6 min step at 80% B before re-equilibration with initial conditions. UV spectra were recorded by a DAD in the range from 200 to 600 nm. The LC flow was split to 75 μL/min before entering the maXis 4G hr-ToF mass spectrometer (Bruker Daltonics, Bremen, Germany) using the standard Bruker ESI source. In the source region, the temperature was set to 180 °C, the capillary voltage was 4000 V, the dry-gas flow was 6.0 l/min, and the nebulizer was set to 1.1 bar. Mass spectra were acquired in positive ionization mode ranging from 600 to 1800 m/z at 2.5 Hz scan rate. Protein masses were deconvoluted by using the Maximum Entropy algorithm (Copyright 1991−2004 Spectrum Square Associates, Inc.).

MALDI-TOF-MS. PqsD (10 μM) was preincubated with compound **12** (10 μM) for 60 min at 37 °C using identical buffer composition as in the screening assay procedure (0.05 M MOPS, pH 7.0 with 0.005% (w/v) Triton X-100 and 0.5% DMSO). The buffer was exchanged by an NH_4HCO_3 buffer (0.05 M, pH 8.1) in three diafiltration steps. Diafiltration was performed at 1200*g* for 6 min at 4 °C in Nanosep centrifugal devices (MWCO = 10K) of Pall Corporation (Port Washington, NY, USA). The protein was digested with trypsin overnight, and dithiothreitol was added. α-Cyano-4-hydroxycinnamic acid was used as matrix component. Analyzes of the peptides were performed on a 4800 TOF/TOF Analyzer mass spectrometer (Applied Biosystems, Darmstadt, Germany) in positive reflector mode using a pulsed 200 Hz solid state Nd:YAG laser with a wavelength of 355 nm. Laser energy was set to 2000−2300 units for standards and to 2700−3200 units for real samples. Source 1 voltage was set to 20 kV with a grid voltage of 16 kV. Reflector detector voltage was 2.19 kV. Spectra of standard peptides used for wide range calibration ranging from 0.8 to 4 kDa (*des*-arg1-bradykinin, angiotensin I, glu1-fibrinopeptide B, ACTH 1−17 clip, ACTH 18−39 clip, and ACTH 7−38 clip) were measured with a delay time of 600 ns. One single mass spectrum was formed from 20 subspectra per spot using 25 accepted laser impulses each. From the standard peptides exclusively monoisotopic ions were used with a minimum signal-to-noise (S/N) ratio of 20 and a resolution >10000. Mass tolerance was set to 0.3 Da with maximum outlier of 5 ppm. Accepted calibration settings were used to measure real sample spectra in the range of 1−3.5 kDa with a minimum S/N range of 10 and a resolution >8000. An internal algorithm defined the isotope cluster area subsequently named intensity (I), based on the peptides' molecular weight and their general elemental composition. MALDI-TOF-MS resulted in pmfs consisting of mass-intensity spectra ($m/z - I_{abs,ai}$).

Molecular Modeling. *Docking.* Inhibitors were built in Molecular Operating Environment (MOE).[24] The receptor was derived from the cocrystal structure of anthraniloyl coenzyme A with PqsD (PDB code: 3H77)[6] ACoA, the covalently bound anthranilate and H_2O were removed and Cys112 was restored considering its conformation in 3H76.[6] AutoDockTools V.1.5.6 was used to add polar hydrogens and to save the protein in the appropriate file formate for docking with Vina. For docking AutoDockVina was used.[25] The docking parameters were kept at their default values. The docking grid was sized 18 Å × 24 Å × 24 Å, covering the entire ACoA channel.

■ ASSOCIATED CONTENT

Supporting Information

Further experimental procedures, analytical data and ^{13}C NMR spectra, selectivity data (PqsD vs RNAP), and more details concerning mutagenesis, SPR-competition, MALDI-TOF-MS, and LC-ESI-MS investigations. This material is available free of charge via the Internet at http://pubs.acs.org.

■ AUTHOR INFORMATION

Corresponding Author

*Phone: +(49) 681 302 70300. E-mail: rolf.hartmann@helmholtz-hzi.de.

Author Contributions

J.H.S. and C.B. contributed equally. The manuscript was written through contributions of all authors. All authors have given approval to the final version of the manuscript.

Notes

The authors declare no competing financial interest.

■ ACKNOWLEDGMENTS

We thank Carina Scheid for technical assistance, Patrick Fischer for his help performing the synthesis, Dr. K. Hollemeyer for MALDI-TOF investigations, and Michael Hoffmann for LC-ESI-MS measurements. J. H. Sahner gratefully acknowledges a scholarship from the Stiftung der Deutschen Wirtschaft (SDW).

■ ABBREVIATIONS USED

ACN, acetonitrile; ACoA, anthraniloyl coenzyme A; CHAPS, 3-[(3-cholamidopropyl)dimethylammonio]-1-propanesulfonate hydrate; CMD, carboxymethyl dextrane, cytidine triphosphate; EtOAc, ethylacetate; EtOH, ethanol; GTP, guanosine triphosphate; HAC, heavy atom count; HHQ, heptyl-4-hydroxyquinoline; ITC, isothermal titration calorimetry; MeOH, methanol; MOE, Molecular Operating Environment; MOPS, 4-morpholinepropanesulfonic acid; NTA, nitrilotriacetic acid; NTP, nucleotide triphosphate; PDA, photodiode array; PQS, *Pseudomonas* quinolone signal; RNAP, RNA polymerase; RP, reversed phase; RU, response unit; SPR, surface plasmon resonance; STD, saturation transfer difference; UTP, uridine triphosphate

■ REFERENCES

(1) Wagner, G.; Hyberts, S. G.; Havel, T. F. NMR structure determination in solution: a critique and comparison with X-ray crystallography. *Annu. Rev. Biophys. Biomol. Struct.* **1992**, *21*, 167−198.

(2) Davis, A. M.; Teague, S. J.; Kleywegt, G. J. Application and limitations of X-ray crystallographic Data in structure-based ligand and drug design. *Angew. Chem., Int. Ed.* **2003**, *42*, 2718−2736.
(3) Boström, J. Reproducing the conformations of protein-bound ligands: a critical evaluation of several popular conformational searching tools. *J. Comput.-Aided Mol. Des.* **2001**, *15*, 1137−1152.
(4) Xiao, G.; Déziel, E.; He, J.; Lépine, F.; Lesic, B.; Castonguay, M.-H.; Milot, S.; Tampakaki, A. P.; Stachel, S. E.; Rahme, L. G. MvfR, a key *Pseudomonas aeruginosa* pathogenicity LTTR-class regulatory protein, has dual ligands. *Mol. Microbiol.* **2006**, *62*, 1689−1699.
(5) For a recent review see Dubern, J.-F.; Diggle, S. P. Quorum sensing by 2-alkyl-4-quinolones in *Pseudomonas aeruginosa* and other bacterial species. *Mol. Biosyst.* **2008**, *4*, 882−888.
(6) Bera, A. K.; Atanasova, V.; Robinson, H.; Eisenstein, E.; Coleman, J. P.; Pesci, E. C.; Parsons, J. F. Structure of PqsD, a *Pseudomonas* quinolone signal biosynthetic enzyme, in complex with anthranilate. *Biochemistry* **2009**, *48*, 8644−8655.
(7) Storz, M. P.; Maurer, C. K.; Zimmer, C.; Wagner, N.; Brengel, C.; de Jong, J. C.; Lucas, S.; Müsken, M.; Häussler, S.; Steinbach, A.; Hartmann, R. W. Validation of PqsD as an anti-biofilm target in *Pseudomonas aeruginosa* by development of small-molecule inhibitors. *J. Am. Chem. Soc.* **2012**, *134*, 16143−16146.
(8) Gomez, M. I.; Prince, A. Opportunistic infections in lung disease: *Pseudomonas* infections in cystic fibrosis. *Curr. Opin. Pharmacol.* **2007**, *7*, 244−251.
(9) Hakki, M.; Limaye, A. P.; Kim, H. W.; Kirby, K. A.; Corey, L.; Boeckh, M. Invasive *Pseudomonas aeruginosa* infections: high rate of recurrence and mortality after hematopoietic cell transplantation. *Bone Marrow Transplant.* **2007**, *39*, 687−693.
(10) Asboe, D.; Gant, V.; Aucken, H. M.; Moore, D. A.; Umasankar, S.; Bingham, J. S.; Kaufmann, M. E.; Pitt, T. L. Persistence of *Pseudomonas aeruginosa* strains in respiratory infection in AIDS patients. *AIDS (Hagerstown, MD, U. S.)* **1998**, *12*, 1771−1775.
(11) Pistorius, D.; Ullrich, A.; Lucas, S.; Hartmann, R. W.; Kazmaier, U.; Müller, R. Biosynthesis of 2-alkyl-4(1*H*)-quinolones in *Pseudomonas aeruginosa*: potential for therapeutic interference with pathogenicity. *ChemBioChem* **2011**, *12*, 850−853.
(12) Sahner, J. H.; Groh, M.; Negri, M.; Haupenthal, J.; Hartmann, R. W. Novel small moleucle inhibitors targeting the "switch region" of bacterial RNAP: structure-based optimization of a virtual screening hit. *Eur. J. Med. Chem.* **2013**, *65*, 223−231.
(13) Hentzer, M.; Givskov, M. Pharmacological inhibition of quorum sensing for treatment of chronic bacterial infections. *J. Clin. Invest.* **2003**, *112*, 1300−1307.
(14) Storz, M. P.; Brengel, C.; Weidel, E.; Hoffmann, M.; Empting, M.; Steinbach, A.; Müller, R.; Hartmann, R. W. unpublished results.
(15) O'Shea, R.; Moser, H. E. Physicochemical properties of antibacterial compounds: implications for drug discovery. *J. Med. Chem.* **2008**, *51*, 2871−2878.
(16) Mayer, M.; Meyer, B. Characterization of ligand binding by saturation transfer difference NMR spectroscopy. *Angew. Chem., Int. Ed.* **1999**, *38*, 1784−1788.
(17) Henise, J. C.; Taunton, J. Irreversible Nek2 kinase inhibitors with cellular activity. *J. Med. Chem.* **2011**, *54*, 4133−4146.
(18) Copeland, R. A.; Pompliano, D. L.; Meek, T. D. Drug-target residence time and its implications for lead optimization. *Nature Rev. Drug Discovery* **2006**, *5*, 730−739.
(19) Hartmann, H.; Liebscher, J. A simple method for the synthesis of 5-aryl-3-amino-2-alkoxycarbonylthiophenes. *Synthesis* **1984**, 275−276.
(20) Fabis, F.; Jolivet-Fouchet, S.; Robba, M.; Landelle, H.; Rault, S. Thiaisatoic anhydrides: efficient synthesis under microwave heating conditions and study of their reactivity. *Tetrahedron* **1998**, *54*, 10789−10800.
(21) Foulon, L.; Braud, E.; Fabis, F.; Lancelot, J. C.; Rault, S. Synthesis and combinatorial approach of the reactivity of 6-and 7-arylthieno[3, 2-*d*][1, 3]oxazine-2, 4-diones. *Tetrahedron* **2003**, *59*, 10051−10057.
(22) Le Foulon, F. X.; Braud, E.; Fabis, F.; Lancelot, J. C.; Rault, S. Solution-phase parallel synthesis of a 1140-member ureidothiophene carboxylic acid library. *J. Comb. Chem.* **2005**, *7*, 253−257.
(23) Haupenthal, J.; Hüsecken, K.; Negri, M.; Maurer, C. K.; Hartmann, R. W. Influence of DNA template choice on transcription and inhibition of *E. coli* RNA polymerase. *Antimicrob. Agents Chemother.* **2012**, *56*, 4536−4539.
(24) *Molecular Operating Environment (MOE)*, 2010.10; Chemical Computing Group Inc.: 1010 Sherbooke Street West, Suite #910, Montreal, QC, Canada, H3A 2R7, 2010.
(25) Trott, O.; Olson, A. J. AutoDock Vina: improving the speed and accuracy of docking with a new scoring function, efficient optimization, and multithreading. *J. Comput. Chem.* **2009**, *31*, 455−461.

3.4 From *in vitro* to *in cellulo*: Structure-activity relationship of (2-nitrophenyl)-methanol derivatives as inhibitors of PqsD in *Pseudomonas aeruginosa*

Michael P. Storz, Giuseppe Allegretta, Benjamin Kirsch, Martin Empting, and Rolf W. Hartmann

Org. Biomol. Chem. **2014**, DOI: 10.1039/c4ob00707g – Reproduced by permission of The Royal Chemical Society

Publication D

Contribution Report

The author planned, synthesized and characterized all new compounds. He helped to perform the routine *in vitro* assay and contributed to data interpretation. Furthermore, he wrote the manuscript.

Organic & Biomolecular Chemistry

PAPER

View Article Online
View Journal

From *in vitro* to *in cellulo*: structure–activity relationship of (2-nitrophenyl)methanol derivatives as inhibitors of PqsD in *Pseudomonas aeruginosa*†

Cite this: DOI: 10.1039/c4ob00707g

Michael P. Storz,[a] Giuseppe Allegretta,[a] Benjamin Kirsch,[a] Martin Empting*[a] and Rolf W. Hartmann*[a,b]

Recent studies have shown that compounds based on a (2-nitrophenyl)methanol scaffold are promising inhibitors of PqsD, a key enzyme of signal molecule biosynthesis in the cell-to-cell communication of *Pseudomonas aeruginosa*. The most promising molecule displayed anti-biofilm activity and a tight-binding mode of action. Herein, we report on the convenient synthesis and biochemical evaluation of a comprehensive series of (2-nitrophenyl)methanol derivatives. The *in vitro* potency of these inhibitors against recombinant PqsD as well as the effect of selected compounds on the production of the signal molecules HHQ and PQS in *P. aeruginosa* were examined. The gathered data allowed the establishment of a structure–activity relationship, which was used to design fluorescent inhibitors, and finally, led to the discovery of (2-nitrophenyl)methanol derivatives with improved *in cellulo* efficacy providing new perspectives towards the application of PqsD inhibitors as anti-infectives.

Received 3rd April 2014,
Accepted 29th May 2014

DOI: 10.1039/c4ob00707g

www.rsc.org/obc

Introduction

Until recently, bacterial communities were seen as nothing more than an accumulation of autonomous single-celled organisms. But today, we are aware that bacteria use cell-to-cell communication systems like *quorum sensing* (QS) to behave collectively rather than as individuals.[1] Small diffusible molecules are produced by single bacterial cells that can be released into the environment and detected by surrounding bacteria. Upon proliferation, the extracellular signal molecule concentrations increase along with cell density. Once a certain threshold is reached, receptors are activated by these autoinducers resulting in population-wide changes in gene expression. This concerted switch from low- to high-cell-density mode allows single bacterial cells to limit their group-beneficial efforts to those cell densities which guarantee an effective group outcome. Even if QS may not be directly essential for the survival of a singular bacterial cell, it is very important for bacteria–host interactions and pathogenesis upon bacterial infections in general. In this regard, QS regulates a variety of virulence factors, which contribute to breaking the first line defences and damaging surrounding tissues leading to dissemination, systemic inflammatory-response syndrome, multiple organ failure, and, finally, death of the host.[2] Furthermore, QS contributes to the collective coordination of biofilm formation, a key reason for bacterial resistance against conventional antibiotics in clinical use.[3] Thus, the importance of these regulatory systems could be exploited for the design of novel anti-infectives.

Several groups have successfully targeted QS, which is discussed as an alternative to the traditional treatment using bactericidal or bacteriostatic agents (for reviews see ref. 4 and 5). Novel anti-virulence compounds ideally decrease pathogenicity without affecting bacterial survival or growth, whereas it is believed that no or less selection pressure is posed on the bacteria. Hence, a reduced rate of newly occurring resistances, which gradually render existing antibiotics ineffective, is expected.[6]

Among bacteria, very different communication systems based on distinct autoinducers are utilized. Gram-positive bacteria primarily use modified oligopeptides, whereas *N*-acyl homoserine lactones are a major class of signal molecules in Gram-negative bacteria.[1] The opportunistic pathogen *P. aeruginosa* additionally utilizes a characteristic *pqs* system, which is based on the quinolone PQS (*Pseudomonas* Quinolone Signal) and its biosynthetic precursor HHQ (2-heptyl-4-quinolone) (Fig. 1).[7]

[a]*Helmholtz-Institute for Pharmaceutical Research Saarland (HIPS), Campus C23, 66123 Saarbrücken, Germany. E-mail: rolf.hartmann@helmholtz-hzi.de; Fax: +49 681 302 70308; Tel: +49 681 302 70300*
[b]*Pharmaceutical and Medicinal Chemistry, Saarland University, Campus C23, 66123 Saarbrücken, Germany*

†Electronic supplementary information (ESI) available: Synthesis and analytics of all synthetic intermediates and all substrates used in the enzyme inhibition assay as well as procedure of the mutagenicity test; HHQ and PQS inhibition in the PA14 wild-type strain. See DOI: 10.1039/c4ob00707g

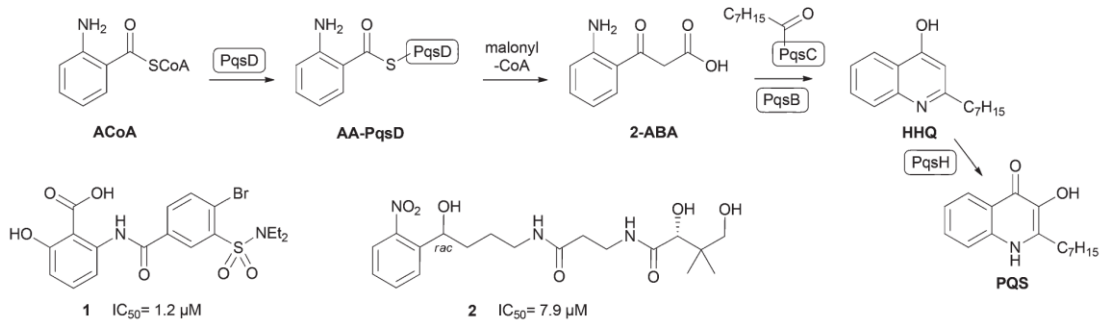

Fig. 1 Role of PqsD in HHQ and PQS biosynthesis (top). Structures of previously reported PqsD inhibitors **1** and **2**.

Both are able to activate the transcriptional regulator PqsR leading to the production of various virulence factors like pyocyanin and hydrogen cyanide (HCN).[8] We have shown, that PqsR antagonists efficiently decrease pyocyanin production and pathogenicity of *P. aeruginosa* PA14.[9,10] Furthermore, HHQ and PQS contribute to the formation of biofilms.[3]

Biosynthesis of HHQ and PQS is accomplished by proteins encoded by the *pqsABCD* operon. Thereby, experiments using transposon knockout mutants identified PqsD as key enzyme in the cellular signal molecule production route.[11,12] Recently, Dulcey *et al.* reported that cytoplasmic PqsD catalyses the condensation of anthraniloyl-CoA (ACoA) and malonyl-CoA to 2-aminobenzoylacetate (2-ABA, Fig. 1).[13] The resulting reactive intermediate is then processed to HHQ by PqsC using octanoic acid as substrate. This second reaction step is supported by PqsB by an unknown mechanism. Interestingly, PqsD alone is also capable of generating HHQ *in vitro* directly from ACoA using β-ketodecanoic acid as secondary substrate.[14] This enzymatic reaction has been routinely exploited by us to evaluate PqsD inhibitors.[14–18] Inhibition of PqsD is an attractive strategy to interfere with QS-controlled infection mechanisms, since it is essential for cellular HHQ/PQS formation. A *pqsD* transposon mutant strain of *P. aeruginosa* PAO1, which is deficient in PQS formation, shows decreased levels of pyocyanin and HCN as well as reduced lethality in nematodes.[11] Furthermore, putative inhibitors of PqsA, an enzyme involved in earlier stages of HHQ biosynthesis, block the cellular production of the corresponding signal molecules, prevent systemic dissemination, and attenuate mortality in infected mice.[19]

Derived from compounds active against FabH, a structurally and functionally related enzyme, we have identified and optimized the first PqsD inhibitors demonstrating IC_{50} values in the single-digit micromolar range (Fig. 1, **1**).[14,15] Unfortunately, these compounds had no pronounced effect on the extracellular signal molecule levels in cell-based assays using *P. aeruginosa* PA14 (unpublished data). Recently, in a ligand-based approach we have identified compound **2** as a novel inhibitor of PqsD (Fig. 1).[16] Ligand efficiency-guided optimisation led to compound **3** (Fig. 2), which was used for an initial examination of the effects on PA14 cells mediated by

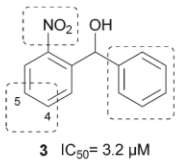

Fig. 2 Systematically varied structural features of inhibitor **3**.

PqsD inhibition.[16] Indeed, this compound was capable of reducing the HHQ and PQS levels. Furthermore, biofilm formation was significantly inhibited and no antibiotic effects were observed.

Binding studies of **3** revealed apparent irreversibility and that binding occurs near the active site residues.[17] Both enantiomers showed similar affinity but contrary thermodynamic profiles. Based on site-directed mutagenesis, isothermal titration calorimetry (ITC) analysis, and molecular docking, explicit binding modes were proposed. In these predicted enzyme–inhibitor complexes both enantiomers reside in nearly identical positions with the main difference being the orientation of the hydroxyl group at the stereogenic center.[17]

Herein, we present a target-oriented (*in vitro*) structure–activity relationship and optimization of this compound class based on the (2-nitrophenyl)methanol scaffold by systematic structure variation (Fig. 2) investigating also the time-dependent onset of inhibition. Previously, we reported, that a tetrahedral geometry including an acceptor function is favoured for the linker between both phenyl rings.[16] However, the intrinsic nitrophenyl moiety bears an increased risk of toxic, mutagenic and carcinogenic side effects.[20] Thus, we evaluated the mutagenicity in Ames *Salmonella* assays and investigated suitable chemical replacements. Additionally, the influences of substituents with opposed electronic and hydrophilic properties in 4- and 5-position of the nitrophenyl moiety were studied. Furthermore, a variety of aliphatic and aromatic residues instead of the second phenyl ring were examined.

The gathered information enabled us to design fluorescent inhibitors, which may be useful tools to investigate enzyme inhibitor interactions and to visualize the target in cells.[21,22]

Finally, selected compounds were examined regarding their potency to inhibit signal molecule production in *P. aeruginosa* PA14 cells. Thereby, we additionally applied a novel strategy to reduce costs and time by the usage of a *pqsH*-deficient mutant which has been selected from a transposon mutant library.[23] This procedure allows to evaluate the potency of a compound solely by quantification of HHQ instead of two signal molecules. In this way we identified compounds with increased *in cellulo* activity while a low molecular weight is retained (<250 Da). These optimized fragment-like molecules provide the potential for further improvements by a fragment growing approach. Additionally, an attempt to correlate *in vitro* data with the effects observed in the cellular assays is made.

Results and discussion

Chemistry

In order to find alternatives to the nitro group, a variety of molecules with different chemical functionalities were synthesized (Scheme 1). Assembly of (2-aminophenyl)(phenyl)-methanol **8** started with the formation of Boc-protected aniline **5**. Ortho-lithiation by *tert*-butyllithium and subsequent reaction with benzaldehyde yielded the alcohol **6**. The desired product **8** was obtained by a two-step deprotection using trifluoroacetic acid and basic hydrolysis. This route also provided access to the cyclic carbamate **7**.

The carboxylate **11** was prepared by iso-propylmagnesium chloride-mediated iodine–magnesium exchange on methyl 2-iodobenzoate **9** and subsequent addition to benzaldehyde. This reaction is followed by spontaneous cyclisation yielding lactone **10**, which was hydrolyzed under basic conditions to yield the desired carboxylate. An analogous method employing iodine–magnesium exchange was used for synthesis of the trifluoromethyl and nitril derivatives **14** and **15**. In the case of compounds **21–25** and **28–29**, corresponding aldehyde precursors were commercially available. Hence, the desired products were prepared by direct addition of phenylmagnesium chloride.

The synthesis of (2-nitrophenyl)methanol derivatives **3**, **33–35**, **39**, **40**, **43–44**, and **47–86** followed the general pathways outlined in Scheme 2. For all compounds, in which Z^1 or Z^2 were exclusively substituted by hydrogen or methyl, phenylmagnesium chloride was added to **36–38** to accomplish iodine–magnesium exchange in *ortho* position to NO_2 as described by Knochel and coworkers.[24] The generated Grignard reagents were reacted with the appropriate aldehydes to form the desired products.

For synthesis of the methoxy derivatives **43** (Z^1 = OMe) and **44** (Z^2 = OMe) from **41** and **42** we utilized 4-methoxyphenylmagnesium bromide as novel reagent to accomplish

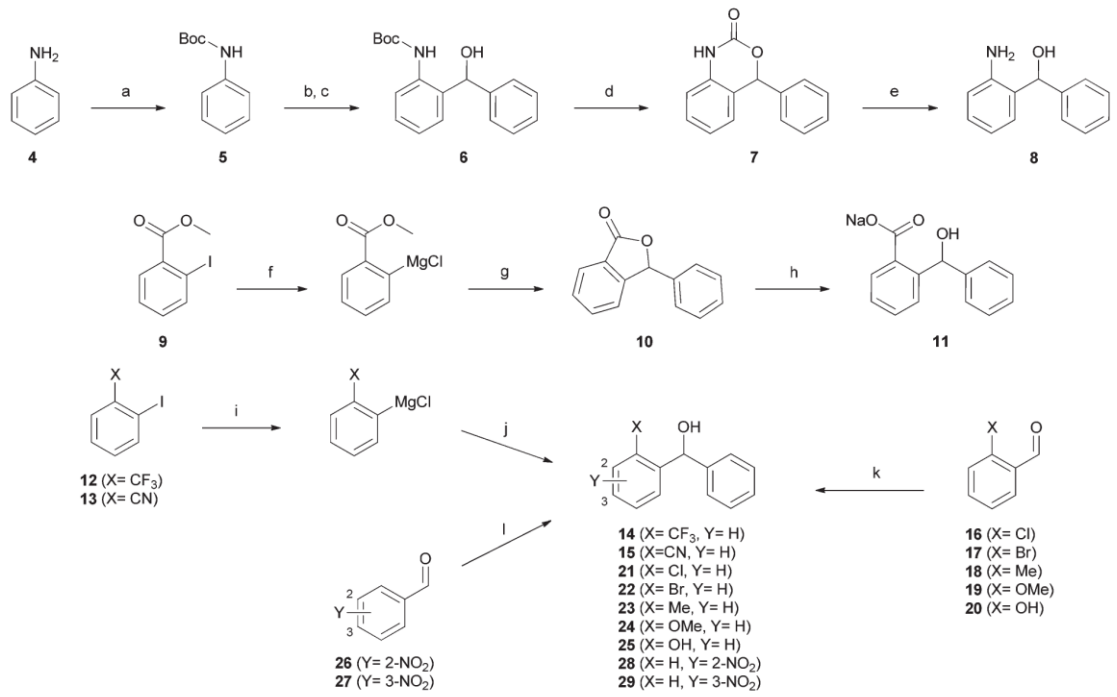

Scheme 1 Synthesis of compounds **8**, **11**, **14–15**, **21–25**, and **28–29**. Reagents and conditions: (a) Boc_2O, THF, reflux, 38%; (b) *t*BuLi, THF, −60 °C; (c) benzaldehyde, THF, −20 °C, 35% (2 steps); (d) TFA, DCM, 0 °C–room temp, 78%; (e) KOH, MeOH–H_2O, reflux, 17%; (f) iPrMgCl, THF, −40 °C; (g) benzaldehyde, THF, −40 °C, 63% (2 steps); (h) NaOH, MeOH–H_2O, 50 °C, 39%; (i) iPrMgCl, THF, −40 °C; (j) benzaldehyde, THF, −40 °C, 47–71% (2 steps); (k) PhMgCl, THF, 0–50 °C, 36–92%; (l) PhMgCl, THF, −40 °C, 7–12%.

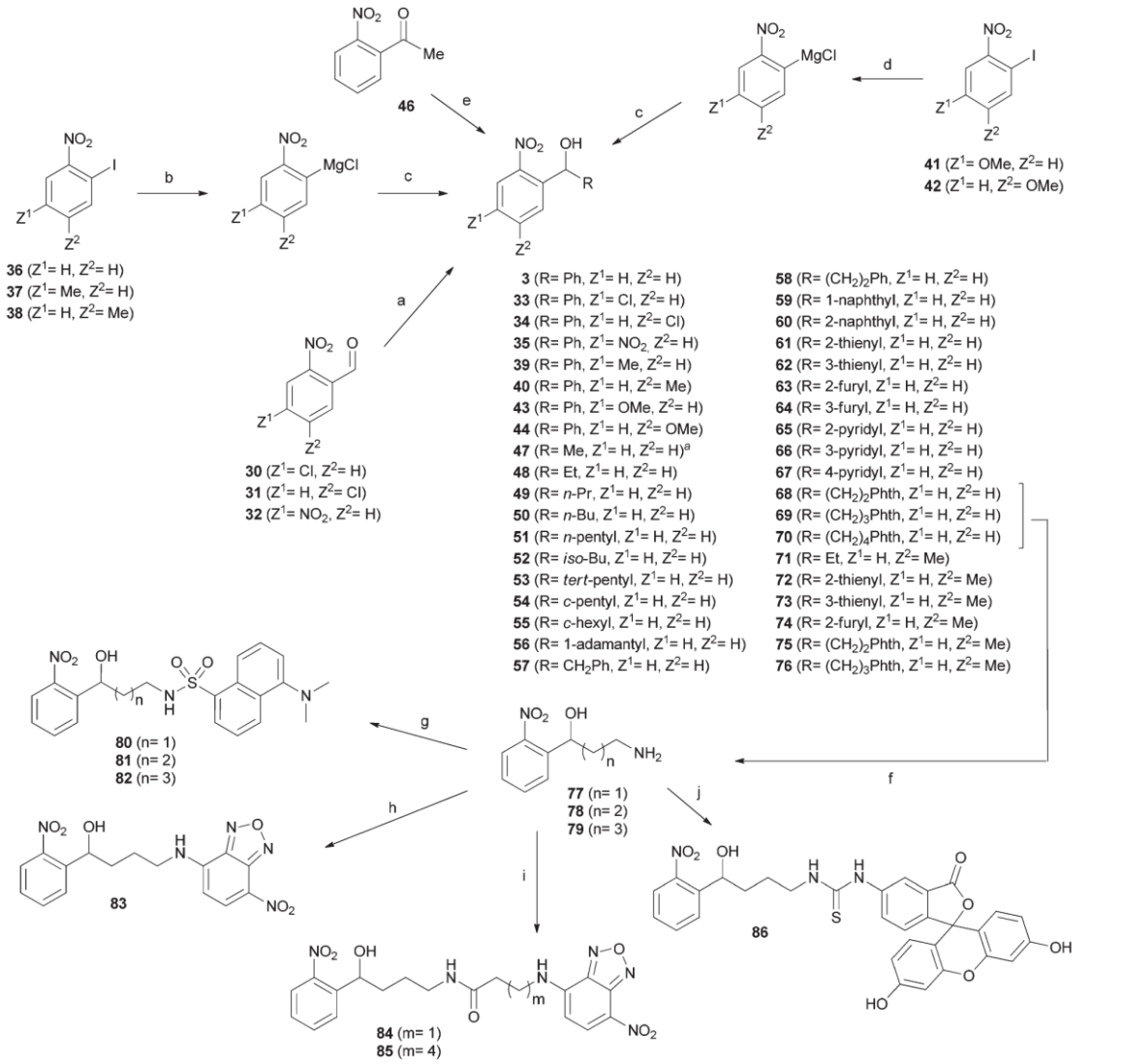

Scheme 2 Synthesis of compounds **3**, **33–35**, **39–40** and **43–44** and **47–86**. Reagents and conditions: (a) PhMgCl, THF, −40 °C; 20–58%; (b) PhMgCl, THF, −40 °C; (c) aldehyde, THF, −40 °C, 11–86% (2 steps); (d) 4-methoxyphenylmagnesium bromide, THF, −40 °C; (e) $NaBH_4$, MeOH, 0 °C–room temp, 62%; (f) hydrazine hydrate, EtOH, reflux, 62–89%; (g) NBD chloride, $NaHCO_3$, MeOH, room temp – 50 °C, 40%; (h) HOOC-$(CH_2)_m$NH-NBD (**84i**, **85i**), EDC·HCl, HOBt·H_2O, NMM, acetonitrile, room temp, 32–46%; (i) dansyl chloride, TEA, DCM, room temp, 29–45%; (j) fluorescein iso-thiocyanate, DIEA, DMF, room temp, 36%.

iodine–magnesium exchange in *ortho*-iodo-nitrobenzenes. Application of this method to a broader range of substrates will be discussed elsewhere.

Fluorescent derivatives were prepared by cleavage of the phthalimide moiety of **68–70** *via* the Ing-Manske procedure. The released amines **77–79** served as a starting point for the introduction of fluorophores. Coupling these amines with dansyl chloride yielded derivatives **80–82**. Direct attachment of NBD to the amine **78** using NBD-chloride afforded **83**, whereas **84** and **85** were synthesized by coupling with the NBD containing carboxylic acids. The fluorescein derivative **86** was formed upon reaction with fluorescein iso-thiocyanate.

Essentiality of the nitro-group and Ames test

After synthesis, compounds were evaluated regarding their inhibitory activity against heterologously expressed and purified PqsD using ACoA and β-ketodecanoic acid as substrates.[14] Until recently, β-ketodecanoic acid instead of malonyl-CoA has been considered as the second substrate in HHQ synthesis, since it has been shown, that addition of β-ketodecanoic acid

to the anthraniloyl-PqsD complex leads to HHQ formation *in vitro*.[14] We have clearly shown that (2-nitrophenyl)methanol derivatives interfere with the formation of the anthraniloyl-PqsD complex itself, which allows further usage of β-ketodecanoic acid independently of its function in the bacterial cells.[17]

First, a variety of substituents replacing the nitro group in *ortho* position were tested. An amino group (**8**) in analogy to ACoA, which served as template for the inhibitor design,[16] led to an inactive compound. This was also true for substituents with electron-withdrawing properties similar to the nitro group, as trifluoromethyl (**14**), nitril (**15**) and halogens (**21**, **22**). Furthermore, no activity was observed for molecules bearing potential hydrogen bond acceptors like **7**, **10**, the carboxylate **11**, **24** and **25**. Since the nitro group seems to be essential for activity, we shifted the position in *meta* or *para* position (**28**, **29**), but inhibitory potency was again completely abolished. An initial toxicity study provided promising results, since no toxic effect against human THP-1 macrophages was observed at 250 μM of compound **3**.[16] To assess the mutagenic risk of the compound class, Ames *Salmonella* assays were performed. Compound **3** was tested on *Salmonella typhimurium* derived strains TA100, TA1535 and TA102 with and without metabolic activation by liver homogenate (S9 mix). No biologically relevant increase in the number of revertant colonies was observed at dose levels up to 5000 μg per plate. Thus, the nitro group was retained and we focused our efforts on the improvement of inhibitory activity by introduction of additional substituents into the nitrophenyl moiety.

In vitro SAR

Recently, we have reported extensive studies on the mode of action of the (2-nitrophenyl)methanol scaffold.[17] In this regard, we demonstrated a time-dependent onset of inhibition based on a slow non-covalent (reversible) interaction. As we have observed that inhibition onset levels out after 20 min of preincubation for compound **3**,[17] we consider a period of 30 min appropriate for the rapid evaluation of the set of novel compounds ($n \sim 50$) described herein. Additionally, we measured the inhibitory activity using only 10 min of preincubation to gain qualitative insight into the effect of inhibitor modifications on binding behaviour.

This examination is relevant, as it has been reported that time-dependency of enzyme–inhibitor interactions can have significant impact in the efficacy of compounds in the cellular system.[25]

First, we re-evaluated our starting compound **3** applying an optimized protocol for the prolonged pre-treatment period of enzyme with inhibitor (Table 1). As described earlier,[17] an improvement of potency was observed rendering this compound now a sub-micromolar PqsD inhibitor.

In a subsequent step, we investigated the effect of different substituents within the nitrophenyl moiety. Compounds bearing electron-withdrawing substituents (EWG) as chlorine (**33**, **34**) or nitro (**35**) showed diminished inhibitory activity (Table 1). However, concerning target affinity (IC_{50} at 30 min of preincubation) the *para* substitution pattern (Z^2 in Table 1) seems to be more favourable. In contrast, introduction of the electron-donating (EDG) methyl (**39**, **40**) or methoxy (**43**, **44**) groups led to potent compounds with IC_{50} values in the range of the unsubstituted **3**. Again, a preference for the introduction of substituents at Z^2 was observed (**40**, **44**). These observations are in accordance with our proposed binding mode reported earlier,[17] as the *para* position to the nitro group provides more space to accommodate additional substituents. An explanation for the general detrimental effect of EWGs on affinity could be that the nitro group functions as hydrogen bond acceptor (as in our proposed binding model). This ability might possibly be diminished by electron-withdrawing substituents. Unfortunately, none of the modifications installed in this part of the scaffold led to an improvement of inhibitor potency. However, comparing the determined IC_{50} for 10 min and 30 min, it seems that the Z^2 position provides the opportunity to modulate the binding behaviour. Through the choice of either methyl (EDG) or chloro (EWG) substituents, the onset (see IC_{50} at 10 min) can be either slightly accelerated (**3** *vs.* **40**) or slowed down (**3** *vs.* **34**).

In light of the results gathered so far, we kept the unsubstituted nitrophenyl moiety constant and turned our attention to the second residue R of the methanol moiety. Hydrogen or linear alkyl chains of different length were introduced (**45**, **47–51**). Thereby, shorter residues up to ethyl (**45**, **47**, and **48**) were favoured over longer variants (**49–51**). A plausible explanation is the increasing entropic penalty caused by the limitation of rotational freedom upon formation of the inhibitor–enyzme complex.

Except iso-butyl-bearing compound **52**, branched and cyclic isomers **53–56** generally inhibited PqsD less efficiently than their linear congeners. This might be due to the narrow entrance channel, which hampers the binding of the bulky residues.

Short alkyl linkers were inserted between the tetrahedral carbon and the phenyl group, but neither compound **57** nor **58** showed improved IC_{50} values compared to **3**. Thus, we concluded that direct attachment to the methanol moiety brings the aromatic residue in an optimal position and fused a second benzene ring. But the resulting 1-naphthyl and 2-naphthyl isomers **59** and **60** were less potent PqsD inhibitors.

Hence, monocyclic heteroaromatic residues were introduced. For all the thiophene and pyridine derivatives **61**, **62**, and **65–67** moderate activity without further improvement was observed. The furane derivatives showed conspicuous behaviour, since the differences in activity between the oxygen in 2- or 3-position were tremendous. While the 3-furyl derivative **64** was almost inactive, the 2-furyl isomer **63** shows improved PqsD inhibition. The synthetic route towards fluorescent (2-nitrophenyl)methanol derivatives provided additional inhibitors of PqsD with non-fluorescent residues R as intermediates. The amines **77–79** may be considered as direct derivatives of the alkyl compounds **49–51**, whereas the terminal methyl was substituted by an amino group, which is expected to be protonated under assay conditions. In contrast

Table 1 PqsD inhibition by (2-nitrophenyl)methanol derivatives

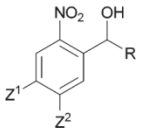

Compounds	Z^1	Z^2	R	IC_{50} [μM] (10 min)[a,b]	IC_{50} [μM] (30 min)[a,c]
3	H	H	Ph	3.2 ± 0.1	0.5 ± 0.1
33	Cl	H	Ph	13.4 ± 1.4	11.2 ± 0.9
34	H	Cl	Ph	15.0 ± 0.6	1.6 ± 0.1
35	NO_2	H	Ph	15.4 ± 2.0	5.8 ± 1.0
39	Me	H	Ph	3.7 ± 0.5	1.6 ± 0.1
40	H	Me	Ph	1.9 ± 0.4	0.6 ± 0.1
43	OMe	H	Ph	2.2 ± 0.5	1.6 ± 0.3
44	H	OMe	Ph	3.0 ± 0.4	0.5 ± 0.1
45	H	H	H	1.6 ± 0.5	0.7 ± 0.2
47	H	H	Me	1.3 ± 0.3	0.8 ± 0.1
48	H	H	Et	1.1 ± 0.2	0.8 ± 0.1
49	H	H	*n*-Pr	2.8 ± 0.4	1.0 ± 0.4
50	H	H	*n*-Bu	5.2 ± 0.8	2.9 ± 0.1
51	H	H	*n*-Pentyl	4.9 ± 0.9	1.0 ± 0.4
52	H	H	iso-Bu	7.9 ± 1.0	1.2 ± 0.3
53	H	H	*tert*-Pentyl	15.9 ± 1.1	6.7 ± 0.1
54	H	H	*c*-Pentyl	4.9 ± 1.0	1.4 ± 0.2
55	H	H	*c*-Hexyl	10.1 ± 1.4	4.5 ± 0.2
56	H	H	1-Adamantyl	11.6 ± 2.2	2.7 ± 0.1
57	H	H	CH_2Ph	5.4 ± 0.6	0.8 ± 0.1
58	H	H	CH_2CH_2Ph	4.6 ± 1.0	0.9 ± 0.1
59	H	H	1-Naphthyl	10.8 ± 2.5	5.8 ± 0.2
60	H	H	2-Naphthyl	13.1 ± 1.9	2.4 ± 0.5
61	H	H	2-Thienyl	14.3 ± 1.9	1.5 ± 0.2
62	H	H	3-Thienyl	5.9 ± 0.9	6.4 ± 1.9
63	H	H	2-Furyl	1.8 ± 0.4	0.9 ± 0.1
64	H	H	3-Furyl	28% @ 50 μM	13.1 ± 2.8
65	H	H	2-Pyridyl	6.7 ± 1.2	1.2 ± 0.1
66	H	H	3-Pyridyl	11.7 ± 2.1	1.7 ± 0.1
67	H	H	4-Pyridyl	6.8 ± 1.4	2.2 ± 0.1
68	H	H	$(CH_2)_2$Phth	1.2 ± 0.1	0.3 ± 0.1
69	H	H	$(CH_2)_3$Phth	1.9 ± 0.3	0.7 ± 0.2
70	H	H	$(CH_2)_4$Phth	1.7 ± 0.5	1.6 ± 0.4
71	H	Me	Et	0.7 ± 0.3	0.6 ± 0.1
72	H	Me	2-Thienyl	6.2 ± 1.8	2.7 ± 0.5
73	H	Me	3-Thienyl	3.3 ± 0.5	1.6 ± 0.3
74	H	Me	2-Furyl	0.9 ± 0.1	1.1 ± 0.1
75	H	Me	$(CH_2)_2$Phth	0.9 ± 0.1	0.7 ± 0.1
76	H	Me	$(CH_2)_3$Phth	0.7 ± 0.1	0.7 ± 0.2
77	H	H	$(CH_2)_2NH_2$	34.7 ± 4.6	40.0 ± 3.7
78	H	H	$(CH_2)_3NH_2$	44% @ 50 μM	27.8 ± 1.7
79	H	H	$(CH_2)_4NH_2$	8.2 ± 2.1	22.4 ± 4.3
80[d]				3.5 ± 0.1	5.8 ± 0.2
81[d]				3.0 ± 1.3	4.0 ± 0.7
82[d]				3.2 ± 0.4	1.4 ± 0.3
83[d]				4.3 ± 0.5	3.4 ± 0.2
84[d]				46.5 ± 2.1	12.5 ± 4.2
85[d]				13.1 ± 1.5	10.0 ± 0.7
86[d]				1.3 ± 0.7	1.5 ± 0.3

[a] *P. aeruginosa* PqsD (recombinantly expressed in *Escherichia coli*), anthraniloyl-CoA (5 μM), and β-ketodecanoic acid (70 μM). [b] IC_{50} values were determined using a 10 min preincubation period of inhibitor and enzyme followed by a 40 min reaction time. [c] IC_{50} values were determined using a 30 min preincubation period of inhibitor and enzyme followed by a 40 min reaction time. [d] For the structure of the fluorescent derivatives **80–86** see Scheme 2.

to the alkyl compounds, the amines **77–79** showed low activity. This result was expected, as the entrance of the substrate tunnel is decorated with arginine side chains providing a repulsive positive surface polarization.

The phthalimides **68–70**, on the other hand, also differing in the length of the alkyl linker, showed potent PqsD inhibition. Compound **68** even demonstrated the lowest IC_{50} value within the investigated set of compounds of around 300 nM.

So far, novel interesting derivatives with retained potency and reduced molecular weight (**45**, **47**, **48**, and **63**) or even improved target affinity (**68**) have been identified. Moreover, some compounds showed a pronounced difference between the IC_{50} values measured *via* the 10 min and 30 min protocol (**34**, **52**, **61**, and **66**) indicating a slow onset of inhibition. As described above, introduction of a methyl group in *para* position to the nitro group resulted in a reduction of time-dependency while retaining activity for compound **40**. These results encouraged us to synthesize additional selected derivatives possessing this methyl group (**71**, **72**). Indeed, all of these methyl-containing compounds showed a fast onset of inhibition (Table 1) while being potent inhibitors of PqsD in the single-digit micromolar to submicromolar range. However, no further improvement in target affinity has been gained compared to the most potent compound **68**. Nevertheless, together with the unmethylated congeners (**48**, **61–63**, **68**, and **69**) interesting pairs of PqsD inhibitors for further evaluation *in cellulo* have been yielded.

Apparently, various substituents of R are tolerated by PqsD, which encouraged us to introduce fluorescent groups in this position. Since promising inhibitory activity was observed for compound **2**, we substituted the pantothenate moiety by dansyl (5-(dimethylamino)-naphthalene-1-sulfonyl), NBD (7-nitrobenz-2-oxa-1,3-diazol-4-yl) and fluorescein fluorophores. The flexible linker of **2** was conserved to provide sufficient degrees of conformational freedom to adopt to the sterical requirements of the substrate tunnel. In the case of the dansyl derivatives **80–82**, the chain length of the alkyl linker was only slightly varied with the intention to position the hydrophobic fluorophore within the channel. For the more hydrophilic NBD derivatives **83–85** additional acyl linkers were introduced as well, thereby shifting the fluorophore towards the protein surface. Fortunately, an acceptable *in vitro* activity was observed for the dansyl derivatives **80–82**, and compounds with NBD (**83**) or fluorescein (**86**) directly attached to the amine **78**. However, the NBD fluorophores **84** and **85** containing an additional acyl-linker were less potent. Unfavourable interactions and/or entropic penalties might be possible reasons.

Inhibition of signal molecule production in a *P. aeruginosa pqsH* mutant

In an attempt to elucidate the physicochemical and/or functional requirements for high *in cellulo* efficacy, we tested selected compounds regarding their ability to reduce the signal molecule levels in *P. aeruginosa* PA14 (Table 2).

In the wild-type strain, HHQ is converted into PQS by PqsH and the expression of *pqsH* depends on the growth period.[26] Thus, we quantified HHQ in a *pqsH* mutant, which is not able to perform this oxidation, to increase simplicity and reproducibility of this cell-based assay. To ensure the validity of this novel methodology, we compared the results gathered using the *pqsH* mutant with additionally determined PA14 wild-type data for three selected compounds and observed a good correlation between both data sets (see ESI†).

Table 2 Comparison of inhibitory potency regarding HHQ production in a *P. aeruginosa pqsH* mutant with physicochemical properties

Cmpd	MW[a]	Log P[a,b]	LE[a,c]	IC_{50} (10 min)/IC_{50} (30 min)[a]	% HHQ inhibition[d]
3	229.23	2.47	0.52	6.4	43 ± 6
33	263.68	3.16	0.39	1.2	n.i.
34	263.68	3.12	0.45	9.4	n.i.
35	274.23	2.14	0.37	2.7	10 ± 4
39	243.26	2.93	0.45	2.3	20 ± 3
40	243.26	2.93	0.48	3.2	19 ± 7
43	259.26	2.69	0.43	1.4	n.i.
44	259.26	2.55	0.46	6.0	n.i.
45	153.14	0.76	0.78	2.3	13 ± 1
47	167.16	1.11	0.71	1.6	26 ± 6
48	181.19	1.64	0.66	1.4	61 ± 2
49	195.22	2.17	0.60	2.8	22 ± 7
50	209.24	2.71	0.52	1.7	n.i.
51	223.27	3.24	0.53	4.9	n.i.
61	235.26	2.15	0.51	8.7	64 ± 6
62	235.26	2.15	0.45	0.8	74 ± 6
63	219.19	1.63	0.53	2.0	51 ± 15
64	219.19	1.63	0.43	n.d.[e]	73 ± 2
68	326.30	2.61	0.38	4.0	n.i. @ 125 μM
69	340.33	2.84	0.34	2.7	n.i. @ 125 μM
70	354.36	2.98	0.31	1.1	n.i. @ 125 μM
71	195.22	2.10	0.62	1.2	n.i.
72	249.24	2.61	0.46	2.3	24 ± 0.2
73	249.24	2.61	0.48	2.1	23 ± 7
74	233.22	2.09	0.49	0.8	20 ± 2
75	340.33	3.07	0.34	1.3	n.i. @ 125 μM
76	354.36	3.30	0.33	1.0	n.i. @ 100 μM
80	429.49	3.71	0.24	0.6	n.i. @ 75 μM
81	443.52	3.94	0.24	0.8	n.i. @ 75 μM
82	457.54	4.08	0.26	2.3	n.i. @ 25 μM
83	373.32	1.10	0.28	1.3	n.i. @ 150 μM
84	444.40	2.15	0.21	3.7	17 ± 3
85	486.48	2.65	0.20	1.3	27 ± 1
86	599.61	2.94	0.19	0.9	n.i.

[a] Molecular weight (MW), calculated partition coefficient (log P), ligand efficiency index (LE), and the ratio of IC_{50} values measured using different preincubation periods. [b] Calculated by ACD/Labs 2012 using the ACD/Log P Classic algorithm. [c] Values calculated as LE = 1.4 (−log IC_{50})/N using the IC_{50} value for the prolonged incubation time (30 min) and N meaning number of non-hydrogen atoms. [d] Planctonic *P. aeruginosa* PA14 *pqsH* mutant. Inhibitor concentration 250 μM as not indicated otherwise. Percentage of inhibition was normalized regarding OD600. n.i. no significant inhibition (<10%). [e] n.d. means "not determined".

If soluble, all compounds were tested at 250 μM. The *in cellulo* results are summarized in Table 2 together with relevant parameters like molecular weight (MW), calculated partition coefficient (log P), ligand efficiency index (LE), and the ratio of IC_{50} values measured using different preincubation periods.

Inhibitor **3**, which served as a starting point, decreased HHQ production by 43%. Introduction of methyl groups into the nitro-phenyl moiety (**39** and **40**) reduced inhibitory potency, whereas methoxy substituents (**43** and **44**) led to inactivity. These results are disappointing, since two of the compounds showed submicromolar *in vitro* activity. A similar result was obtained for molecules bearing a substituent in the nitrophenyl moiety: the chloro compounds **33** and **34** as well as the dinitrophenyl-derivative **35** showed no or only low

activity in the cells. Furthermore, no effects on HHQ production despite of most promising IC_{50} values were observed for the phthalimides **68–70**, **75**, and **76**, which were tested at 100–125 μM due to limited solubility.

All congeners of the homologous series **45–51** containing unbranched alkyl residues showed good activity in the enzymatic assay, whereas the *in vitro* activity slightly decreased for the larger alkanes. In the cellular test system, the largest residues (**50** and **51**) led to inactivity, while a maximum HHQ inhibition was observed for ethyl (**48**). This compound showed an improved cellular activity compared to the starting point **3**. Interestingly, the variant with methyl in *para* position to the nitro group (**71**) was inactive, although it possesses a slightly improved IC_{50} value.

Surprisingly, all four compounds containing heteroaromatic pentacycles **61–64** potently reduced the HHQ formation. These compounds were not among the most potent PqsD inhibitors *in vitro*. Moreover, **64** showed only a moderate activity in the double-digit micromolar range against recombinant PqsD. We can only speculate whether additional alternative cellular targets are involved or whether the furanyl residue is converted into a more active compound inside the cell. Multiple examples for the instability of furan are reported in the literature. However, the thiophene **62** is the most potent inhibitor of cellular HHQ formation reported so far. Again, the methyl modification in Z^2 of the nitrophenyl moiety resulting in compounds **72–74** was detrimental to *in cellulo* efficacy.

Finally, we examined the effect of fluorophore-labelled derivatives **80–86** on *P. aeruginosa* to evaluate their potential for applications in cellular systems. Unfortunately, neither the dansyl- nor fluorescein-labelled inhibitors (**80–82** and **86**) were able to reduce HHQ formation at 250 μM. Consequently, their application is restricted to studies using lysed cells or isolated biomolecules. The best results were obtained for NBD derivatives **84** and **85**, which showed at least slight inhibition. This opens up avenues towards intracellular labelling experiments, which might be conducted in the future.

Interpretation of *in vitro* and *in cellulo* data

A first conclusion which can be drawn from the detailed experimental data reported herein is that in the case of (2-nitrophenyl)methanol derivatives *in vitro* potency expressed either as IC_{50} or ligand efficiency (LE, Table 2) does not directly translate into *in cellulo* activity. However, this observation is not utterly surprising as Gram-negative bacteria, in general, and *P. aeruginosa*, in particular, are known to provide challenging barriers for the effective inhibition of intracellular targets.[27–29] The orthogonal sieving ability of the two bacterial cell membranes blocking larger hydrophobic compounds (outer membrane) as well as smaller hydrophilic entities (inner membrane) from entering the cytoplasm is only one obstacle which an anti-infective agent has to overcome.[27,28] Additionally, an arsenal of efflux pumps and degrading/metabolizing enzymes may hinder a drug from reaching its target.[29] Hence, the physicochemical, structural, and functional features of compounds displaying intracellular activity are all the more worthwhile to investigate.

In this context, time-dependent inhibition was one characteristic of the presented compound class that has first drawn our attention. Reversible target interaction (inhibition) is characterized by inhibitor binding (k_{on}, "on-rate") and dissociation (k_{off}, "off-rate"). Thus, a slow binding behaviour in combination with promising (nanomolar) IC_{50} values would imply long drug-residence times as the "off-rate" should also be attenuated along with the inhibition onset ("on-rate"). Such an effective (long-lasting) enzyme blockade can be considered a favourable scenario in order to shut down cellular signal molecule synthesis. However, we were not able to establish a correlation between this phenomenon and improved HHQ reduction. Some compounds with either high or low ratios of IC_{50} values measured using 10 min or 30 min of preincubation were effective inhibitors of signal molecule production (compare for example **3** and **61** with **62** and **70**). Indeed, we showed that the methyl modification at the nitrophenyl core results in compounds with only low time-dependent onset of inhibition along with a decreased or even abolished *in cellulo* efficacy (**48** *vs.* **71** and **61** *vs.* **72**). Nevertheless, the most potent inhibitor in our cell assays was **62** showing almost no time-dependency of PqsD inhibition.

A parameter which seems to have direct influence on intracellular activity, though, was molecular weight. Most compounds with MW > 300 Da were inactive inside the cells. The only exceptions within the set of tested compounds were NBD-tagged fluorophores **84** and **85** showing only a moderate reduction of HHQ production. This observed mass cut-off is much lower than the general value of 600 Da reported for Gram-negative bacteria and should not be considered a strict criteria due exceptions mentioned above.[30] This finding might be explained by the described low permeability of outer membrane of *P. aeruginosa* compared to other Gram-negative bacteria.[31]

Another important physicochemical parameter for cellular availability is hydrophobicity usually expressed as the octanol–water partition coefficient log *P*. None of the fragment-like compounds reported herein can be considered as strongly lipophilic as none of them exceeds log $P \approx 4$ while the majority possesses a value below 3. However, it has been proposed by others that even lower log *P* values are beneficial or actually a prerequisite for activity against Gram-negative bacteria.[30] Indeed, our most active compound *in cellulo* possess a log *P* below 2.5.

Noteworthy, we have identified compounds within the set of tested (2-nitrophenyl)methanol derivatives that are interesting exceptions to the described MW/log *P* criteria. Compound **71**, for example, has low molecular weight (195.22 Da) and log *P* (0.62) combined with a substantial *in vitro* activity (IC_{50} = 0.6) but no relevant *in cellulo* activity. We account this finding to the general detrimental effect of the methyl group in *para* position to the nitro group which we have also found for the other compounds bearing this substitution pattern. On the other hand, developed NDB-tagged inhibitors possess

increased molecular weight and hydrophobicity, yet show moderate activity on signal molecule production. Hence, further optimization of our fragment-like molecules towards drug-like compounds *via* fragment growing approaches may be a rewarding endeavour.

Conclusions

More than fifty derivatives of (2-nitrophenyl)phenylmethanol **3** have been synthesized and tested for *in vitro* activity. In this regard, we demonstrated that 4-methoxyphenylmagnesium bromide is a suitable reagent to accomplish efficient I–Mg exchange for compound **42**. Whereas the nitro group in *ortho* position turned out to be essential for *in vitro* PqsD inhibition, no mutagenicity was observed for compound **3** in an Ames test. Improved potency was achieved by the replacement of the eastern phenyl residue. This position turned out to be very tolerant for various moieties, which allowed the design of fluorescence-labelled inhibitors.

For a straightforward evaluation of PqsD inhibitors in the cellular context, signal molecule production was investigated using a *pqsH*-deficient *P. aeruginosa* PA14 strain. Some of our compounds showed significantly improved inhibition of signal molecule production. An attempt to correlate *in vitro* data with *in cellulo* results has been made identifying low molecular weight and hydrophobicity as important, but not stringent, criteria for intracellular activity. Nevertheless, the presented work emphasizes the notion that optimization of intracellular activity is a challenging multi-parameter problem which requires further intense research.

Finally, novel PqsD inhibitors presented in this work possess a fragment-like size and improved efficiency *in cellulo*. Together with the structural insight provided by our studies regarding the mode of action, we have delivered the basis for a fragment-growing optimization process towards PqsD-targeting anti-infectives.

Experimental section

General

(2-Nitrophenyl)methanol **45** was purchased from Sigma-Aldrich and used for biological assays without further purification. Starting materials were purchased from ABCR, Acros, Sigma-Aldrich and Fluka and were used without further purification. All reactions were conducted under a nitrogen atmosphere. During workup drying was achieved by anhydrous sodium sulfate. Flash chromatography was performed using silica gel 60 (40–63 μm) and the reaction progress was determined by TLC analysis on ALUGRAM SIL G/UV254 (Macherey-Nagel). Visualization was accomplished through excitation using UV light. Purification by semi-preparative HPLC was carried out on an Agilent 1200 series HPLC system from Agilent Technologies, using an Agilent Prep-C18 column (30 × 100 mm/10 μm) as stationary phase with acetonitrile–water as eluent. The purity of compounds used in the biological assays was ≥95% as measured by LC/MS, monitored at 254 nm. The methods for LC/MS analysis and a table with analytical data (including melting points) for all tested compounds are provided in the purity section of the ESI.† All chiral alcohols were isolated as racemates. ^{1}H and ^{13}C NMR spectra were recorded on a Bruker DRX-500 instrument at 300 K. Chemical shifts are reported in δ values (ppm) and the hydrogenated residues of deuterated solvents were used as internal standard (acetone-d_6: 2.05, 29.84. $CDCl_3$: δ = 7.26, 77.16. MeOH-d_4: δ = 3.31, 49.00. DMSO-d_6: δ = 2.50, 39.52). Splitting patterns describe apparent multiplicities and are designated as s (singlet), d (doublet), dd (doublet of doublet), t (triplet), td (triplet of doublet), q (quartet), m (multiplet). All coupling constants (J) are given in hertz (Hz). Mass spectra (ESI) were measured on a Thermo Scientific Orbitrap. Mass spectra (EI) were measured on a DSQII instrument (ThermoFisher). Melting points of samples were determined in open capillaries using a SMP3 Melting Point Apparatus from Bibby Sterilin and are uncorrected. Infrared spectra were measured on a PerkinElmer Spectrum 100 FT-IR spectrometer.

General method A for synthesis of 3, 39, 40, 48–76

A solution of 2-iodo-nitrobenzene **36** or a close derivative (1.0 eq.) in THF (10 ml g^{-1} reagent) was cooled to −40 °C and a solution of phenylmagnesium chloride (2 M in THF, 1.1 eq.) was added dropwise. After stirring for 30 min at −40 °C, the aldehyde (1.0 eq.) was added. Then, the reaction mixture was continuously stirred at −40 °C until complete conversion (checked by TLC). The reaction was quenched with a saturated solution of NH_4Cl (5 ml) and diluted with water (5 ml). The aqueous phase was extracted with ethyl acetate (three times) and the combined organic layers were washed with brine, dried, and concentrated under reduced pressure. The residue was purified by column chromatography over silica gel to give the desired product.

General method B for synthesis of 10, 14, and 15

A solution of the iodobenzene **9**, **12** or **13** (1.00 g, 1.0 eq.) in 30 ml THF was cooled to −40 °C and a solution of iso-propylmagnesium chloride (2 M in THF, 1.1 eq.) was added dropwise. The solution was stirred for 60 min at −40 °C, benzaldehyde (1.0 eq.) was added and the reaction was completed at −40 °C (checked by TLC). The workup was carried out as described in method A.

General method C for synthesis of 21–25

To a solution of phenylmagnesium chloride (2 M in THF, 1.5 eq.) in 8 ml THF at 0 °C aldehydes **16–20** (1 eq.) were slowly added and the solution was stirred at 50 °C for 30 min. The mixture was cooled to 0 °C, quenched with a saturated solution of NH_4Cl (5 ml), and diluted with water (5 ml). The aqueous phase was extracted with diethyl ether (three times) and the combined organic layers were dried and concentrated under reduced pressure. The residue was purified by column chromatography over silica gel to give the desired product.

General method D for synthesis of 28 and 29

To a solution of phenylmagnesium chloride (3.31 ml, 2 M in THF, 6.62 mmol) in 20 ml THF at −40 °C nitrobenzaldehyde **26** or **27** (1.00 g, 6.62 mmol) was added slowly. The reaction mixture was stirred continuously at −40 °C until complete conversion (checked by TLC). The mixture was quenched with a saturated solution of NH_4Cl (5 ml) and diluted with water (5 ml). The workup was carried out as described in method A, followed by purification of the crude product by flash chromatography (petroleum ether–ethyl acetate 6 : 1).

General method E for synthesis of 77–79

To a solution of the phthalimides **68–70** (1.53 mmol, 1 eq.) in ethanol (40 ml) hydrazine hydrate (9.18 mmol, 6 eq.) was added and the mixture was refluxed for 3 h. Ethanol was removed *in vacuo* and ethyl acetate was added. The solution was washed with water and extracted twice with EtOAc. The organic phase was dried and the solvent was evaporated to yield the desired product in sufficient purity.

Expression and purification of recombinant PqsD

Expression and purification of recombinant PqsD was conducted as previously described.[16] Briefly, BL21 (λDE3) *E. coli* transformed with expression vector pT28b(+)/*pqsD* were induced with IPTG overnight. After harvesting and lysis through sonication, recombinant PqsD possessing a His_6-tag was isolated *via* immobilized metal ion affinity chromatography (IMAC) followed by gel filtration. The affinity tag was removed by thrombin cleavage and a second IMAC step.

Enzyme inhibition assay using recombinant PqsD

The standard assay for determination of IC_{50} values was performed monitoring the enzyme activity by measuring the HHQ concentration as described recently.[14] PqsD was preincubated with inhibitor for 10 min or 30 min prior to addition of the substrates ACoA and β-ketodecanoic acid. Quantification of HHQ was performed analogously, but with some modifications: The flow rate was set to 750 µl min^{-1} and an Accucore RP-MS column, 150 × 2.1 mm, 2.6 µm, (Thermo Scientific) was used. All test compound reactions were performed in sextuplicate. Synthesis of ACoA and β-ketodecanoic acid was performed as described in the ESI.†

Cultivation of *P. aeruginosa* PA14 *pqsH* mutant

For determination of extracellular HHQ levels, cultivation was performed in the following way: cultures of *P. aeruginosa* PA14 *pqsH* transposon mutant[23] (initial OD_{600} = 0.02) were incubated with or without inhibitor (final DMSO concentration 1%, v/v) at 37 °C, 200 rpm and a humidity of 75% for 16 h in 24-well Greiner Bio-One Cellstar plates (Frickenhausen, Germany) containing 1.5 ml medium per well. Cultures were generally grown in PPGAS medium (20 mM NH_4Cl, 20 mM KCl, 120 mM Tris-HCl, 1.6 mM $MgSO_4$, 0.5% (w/v) glucose, 1% (w/v) Bacto™ Tryptone). For each sample, cultivation and sample work-up were performed in triplicates.

Determination of extracellular HHQ levels

Extracellular levels of HHQ were determined according to the method of Lépine *et al.* with the following modifications.[32,33] An aliquot of 500 µl of bacterial cultures were supplemented with 50 µl of a 10 µM methanolic solution of the internal standard (IS) 5,6,7,8-tetradeutero-2-heptyl-4(1*H*)-quinolone (HHQ-d_4) and extracted with 1 ml of ethyl acetate by vigorous shaking. After centrifugation, 400 µl of the organic phase were evaporated to dryness in LC glass vials. The residue was re-dissolved in methanol. UHPLC-MS/MS analysis was performed as described in detail recently.[16] The following ions were monitored (mother ion [*m*/*z*], product ion [*m*/*z*], scan time [s], scan width [*m*/*z*], collision energy [V], tube lens offset [V]): HHQ: 244, 159, 0.5, 0.01, 30, 106; HHQ-d_4 (IS): 248, 163, 0.1, 0.01, 32, 113. Xcalibur software was used for data acquisition and quantification with the use of a calibration curve relative to the area of the IS.

Calculation of log *P* values

Experimental values of **67** and **79** were determined by Sirius T3 titrator from Sirius Analytical. Comparison with values calculated by ACD/Labs 2012 (Build 1996, 31. May 2012) revealed, that ACD/Log *P* Classic is the most appropriate algorithm. Consequently, the latter was used for the values given in Table 2.

Abbreviations

2-ABA	2-Aminobenzoylacetate
ACoA	Anthraniloyl-CoA
dansyl	5-(Dimethylamino)-naphthalene-1-sulfonyl
EDG/EWG	Electron-donating/withdrawing group
HHQ	2-Heptyl-4-quinolone
LE	Ligand efficiency
log *P*	Octanol–water partition coefficient
MW	Molecular weight
NBD	7-Nitrobenz-2-oxa-1,3-diazol-4-yl
PQS	2-Heptyl-3-hydroxy-4-quinolone
QS	*Quorum sensing*

Acknowledgements

We thank Carina Scheid, Simone Amann, and Christine Maurer for performing the PqsD and cellular assays. Furthermore, we thank Prof. Dr Susanne Häußler for kindly supplying the *P. aeruginosa* PA14 wild-type strain and PA14 *pqsH* mutant and Michael Hoffmann for performing HRMS measurements.

Notes and references

1 S. Swift, J. A. Downie, N. A. Whitehead, A. M. Barnard, G. P. Salmond and P. Williams, *Adv. Microb. Physiol.*, 2001, **45**, 199.

2 For a review see: L. C. M. Antunes, R. B. R. Ferreira, M. M. C. Buckner and B. B. Finlay, *Microbiology*, 2010, **156**, 2271.
3 L. Yang, M. Nilsson, M. Gjermansen, M. Givskov and T. Tolker-Nielsen, *Mol. Microbiol.*, 2009, **74**, 1380.
4 T. B. Rasmussen and M. Givskov, *Microbiology*, 2006, **152**, 895.
5 J. C. A. Janssens, S. C. J. De Keersmaecker, D. E. De Vos and J. Vanderleyden, *Curr. Med. Chem.*, 2008, **15**, 2144.
6 For a critical discussion see: T. Defoirdt, N. Boon and P. Bossier, *PLoS Pathog.*, 2010, **6**, e1000989.
7 E. C. Pesci, J. B. Milbank, J. P. Pearson, S. L. McKnight, A. Kende, E. P. Greenberg and B. Iglewski, *Proc. Natl. Acad. Sci. U. S. A.*, 1999, **96**, 11229.
8 J.-F. Dubern and S. P. Diggle, *Mol. BioSyst.*, 2008, **4**, 882.
9 C. Lu, B. Kirsch, C. Zimmer, J. C. de Jong, C. Henn, C. K. Maurer, M. Müsken, S. Häussler, A. Steinbach and R. W. Hartmann, *Chem. Biol.*, 2011, **19**, 381.
10 C. Lu, C. K. Maurer, B. Kirsch, A. Steinbach and R. W. Hartmann, *Angew. Chem., Int. Ed.*, 2014, **53**, 1109.
11 L. A. Gallagher, S. L. McKnight, M. S. Kuznetsowa, E. C. Pesci and C. Manoil, *J. Bacteriol.*, 2002, **184**, 6472.
12 Y.-M. Zhang, M. W. Frank, K. Zhu, A. Mayasundari and C. O. Rock, *J. Biol. Chem.*, 2008, **283**, 28788.
13 C. E. Dulcey, V. Dekimpe, D.-A. Fauvelle, S. Milot, M.-C. Groleau, N. Doucet, L. G. Rahme, F. Lépine and E. Déziel, *Chem. Biol.*, 2013, **20**, 1481.
14 D. Pistorius, A. Ullrich, S. Lucas, R. W. Hartmann, U. Kazmaier and R. Müller, *ChemBioChem*, 2011, **12**, 850.
15 E. Weidel, J. C. de Jong, C. Brengel, M. P. Storz, A. Braunshausen, M. Negri, A. Plaza, A. Steinbach, R. Müller and R. W. Hartmann, *J. Med. Chem.*, 2013, **56**, 6146.
16 M. P. Storz, C. K. Maurer, C. Zimmer, N. Wagner, C. Brengel, J. C. de Jong, S. Lucas, M. Müsken, S. Häussler, A. Steinbach and R. W. Hartmann, *J. Am. Chem. Soc.*, 2012, **134**, 16143.
17 M. P. Storz, C. Brengel, E. Weidel, M. Hoffmann, K. Hollemeyer, A. Steinbach, R. Müller, M. Empting and R. W. Hartmann, *ACS Chem. Biol.*, 2013, **8**, 2794.
18 J. H. Sahner, C. Brengel, M. P. Storz, M. Groh, A. Plaza, R. Müller and R. W. Hartmann, *J. Med. Chem.*, 2013, **56**, 8656.
19 B. Lesic, F. Lépine, E. Déziel, J. Zhang, Q. Zhang, K. Padfield, M.-H. Castonguay, S. Milot, S. Stachel, A. A. Tzika, R. G. Tompkins and L. G. Rahme, *PLoS Pathog.*, 2007, **3**, e126.
20 R. Padda, C. Wang, J. Hughes, R. Kutty and G. Bennett, *Environ. Toxicol. Chem.*, 2003, **22**, 2293.
21 S. Xu, A. N. Butkevich, R. Yamada, Y. Zhou, B. Debnath, R. Duncan, E. Zandi, N. A. Petasis and N. Neamati, *Proc. Natl. Acad. Sci. U. S. A.*, 2012, **109**, 16348.
22 K. A. Kozlowski, F. H. Wezeman and R. M. Schultz, *Proc. Natl. Acad. Sci. U. S. A.*, 1984, **81**, 1135.
23 N. T. Liberati, J. M. Urbach, S. Miyata, D. G. Lee, E. Drenkard, G. Wu, J. Villanueva, T. Wei and F. M. Ausubel, *Proc. Natl. Acad. Sci. U. S. A.*, 2006, **103**, 2833.
24 I. Sapountzis and P. Knochel, *Angew. Chem., Int. Ed.*, 2002, **41**, 1610.
25 R. A. Copeland, D. L. Pompliano and T. D. Meek, *Nat. Rev. Drug Discovery*, 2006, **5**, 730.
26 E. Déziel, F. Lépine, S. Milot, J. He, M. N. Mindrinos, R. Tompkins and L. G. Rahme, *Proc. Natl. Acad. Sci. U. S. A.*, 2004, **101**, 1345.
27 L. L. Silver, *Clin. Microbiol. Rev.*, 2011, **24**, 71.
28 H. Nikaido, *Antimicrob. Agents Chemother.*, 1989, **33**, 1831.
29 K. Poole, *J. Mol. Microbiol. Biotechnol.*, 2001, **3**, 255.
30 R. O'Shea and H. E. Moser, *J. Med. Chem.*, 2008, **51**, 2871.
31 B. L. Angus, A. M. Carey, D. A. Caron, A. M. Kropinski and R. E. Hancock, *Antimicrob. Agents Chemother.*, 1982, **21**, 299.
32 C. K. Maurer, A. Steinbach and R. W. Hartmann, *J. Pharm. Biomed. Anal.*, 2013, **86**, 127.
33 F. Lépine, F. E. Déziel, S. Milot and L. G. Rahme, *Biochim. Biophys. Acta*, 2003, **1622**, 36.

4 Final Discussion

4.1 Hit Identification and Efficiency Guided Optimization

The superior goal of this thesis was the development of efficient small molecule inhibitors of PqsD. As reported in publication **A**, a ligand-based design strategy was pursued (Figure 4). Firstly, two substrate analogues bearing a methylene ketone instead of the scissile thioester, which is naturally cleaved by Cys^{112} of PqsD in a transthioesterification reaction, were examined (Figure 4b). Besides the natural amino group, electron withdrawing groups (EWG), which might facilitate the nucleophilic attack on the carbonyl moiety, are promising. Since NO_2 served as stable precursor of the nucleophilic amino function during synthesis, NO_2 was retained as EWG. Unfortunately, none of the compounds **I** or **II** showed inhibitory activity in the enzymatic PqsD assay.

In a second approach, we mimicked the transition state by introduction of a tetrahedral hydroxymethylene moiety instead of the carbonyl function (Figure 4c). Since we applied the

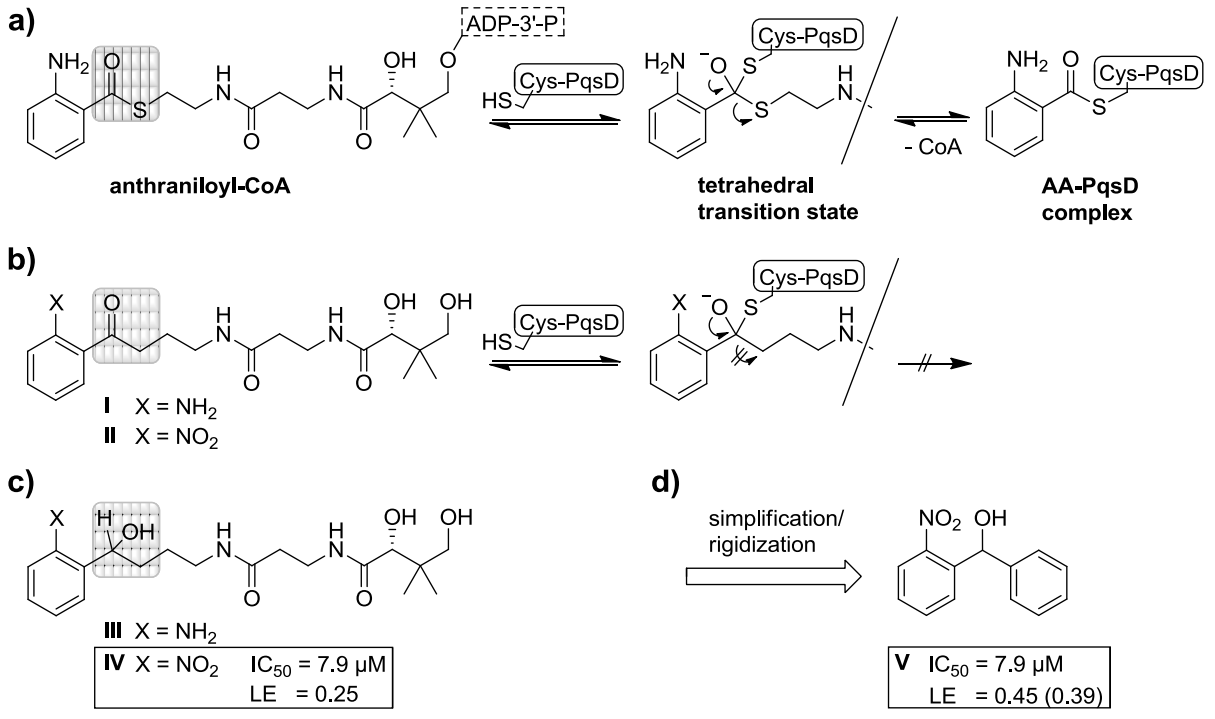

Figure 4. Ligand-based design strategy to identify PqsD inhibitors. a) Transthioesterification reaction of PqsD and ACoA proceeds via a tetrahedral transition state and results in a covalent anthraniloyl-PqsD complex. b) Substrate analogues **I** and **II** could analogously be attacked by Cys^{112}-PqsD. However, elimination of a CoA-type leaving group cannot occur due to the high stability of carbon-carbon bonds. c) Transition state mimics **III** and **IV** bearing a tetrahedral geometry. d) Structure of simplified and ridigized compound **V**. The LE value in brackets was calculated according to Eq.1 using an ITC derived K_d. LE values for comparison were calculated according to Eq. 2.

same synthetic route as for the substrate analogs, the corresponding nitro derivative was easily accessible. No activity was observed for the amino compound **III**, whereas unexpectedly, the nitro compound **IV** was identified as the first inhibitor of PqsD.

Compared to the median affinity for current small-molecule drugs of around 20 nM,[85] an IC_{50} value of 7.9 µM reflects moderate activity. Since IC_{50} is not a thermodynamically derived metric, it strongly depends on assay conditions (especially substrate concentration for competitive inhibitors). In our assay, an enzyme concentration of 0.1 µM was necessary to obtain reasonable HHQ formation. This relativizes the IC_{50} value of **IV**, since the theoretical minimum IC_{50} is 50 nM. However, there is plenty of room for improvements.

Furthermore, this first hit showed inadequate drug-likeness due to the potential toxicity of the nitrobenzene moiety[86] (as discussed in detail in publication **D**) and the high flexibility of the alkyl side chain. A high number of rotatable bonds (nrotb ≥ 10) are reported to restrict oral bioavailability (here: nrotb=12)[87] and causes a penalty in binding affinity due to a loss of configurational entropy.[88] Furthermore, the complicated and time-consuming synthesis impedes efficient optimization.

Thus, we reduced MW, flexibility, and complexity by simplification of the side chain as described in detail in publication **A**. The resulting compound **V** bears a lower MW (229 g/mol), only one chiral center, low flexibility (nrotb = 3) and is easily accessible by a one pot synthesis. Surprisingly, *in vitro* activity was increased from IC_{50} = 7.9 µM for compound **IV** to IC_{50} = 3.2 µM (**V**), which was the lowest value observed so far. This indicates that the side chain has a minor contribution to the overall affinity. Significant reduction of the molecular size while slightly enhancing the activity led to a tremendous increase in ligand efficiency (LE), which is an important metric in drug discovery.[89]

Hit optimization process usually aims at increasing the affinity (ΔG, K_d) and selectivity regarding a target and typically involves an increase in molecular size.[90] However, various values for upper limits of molecular weight have been reported in literature. Most prominent, MW ≤ 500 has been suggested to gain a high probability of adequate oral bioavailability,[91] while analysis of key ADMET assays even suggest a cut off of MW = 400.[92] It is all the more important to start the optimization process with the molecule bearing the highest potential to reach sufficient affinity without crossing the MW limit. Ligand efficiency is an appropriate metric for this potential as it reflects the affinity of a compound normalized by molecular size:[89]

$$LE = \Delta G / N_{non-H} = -RT \ln K_d / N_{non-H} \quad \text{(Eq. 1)}$$

where ΔG is the change in Gibbs energy in kcal/mol and $N_{non\text{-}H}$ the number of non-hydrogen atoms. At 300 K and consistent assay parameters, this formula can be simplified to give an estimate of LE based on measured IC_{50}:

$$LE = -1.4 [\log IC_{50}] / N_{non-H} \quad \text{(Eq. 2)}$$

From this point of view, the optimization of **IV** to **V** was highly successful, as LE significantly increased (Figure 4). Thereby, the thermodynamically derived LE of 0.39 reached a range, which is generally considered to be suitable for further optimization.[93]

4.2 Effects on *P. aeruginosa*

Before spending much more effort on the optimization of compound **V**, the ability to inhibit signal molecule production in *P. aeruginosa* cells was examined. This cannot be taken for granted, since especially in *P. aeruginosa* access to the intracellular targets is hindered by an unusually restricted outer-membrane permeability and multidrug efflux systems.[8] Thus, higher concentrations are necessary to achieve a comparable degree of inhibition. Fortunately, 250 µM of compound **V** significantly reduced both HHQ and PQS levels produced by *P. aeruginosa* PA14.

Since inhibition of QS is considered an anti-virulence strategy, no bactericidal or bacteriostatic effect was expected. To proof that compound **V** does not affect cell viability of the bacterial population, we measured a growth curve of *P. aeruginosa* PA14 in LB medium in the presence of 500 µM compound **V**, which is the highest concentration used in the assays. No differences in the OD_{600} of the treated and untreated culture could be observed (see section 6.1.7). This indicates that signal molecule production results from QS inhibition, even if the modulation of a superior regulator cannot be excluded.

The influence of compound **V** on the secondary metabolite DHQ was also examined and in contrast to HHQ and PQS, increased levels of DHQ were observed. At the time of these experiments, it was not yet clarified how *P. aeruginosa* accomplishes DHQ biosynthesis. Contrary results about the enzymes involved were reported in literature. Lépine and

coworkers found *pqsA* as the only gene within the *pqsABCDE* operon, which is required for DHQ production,[94] whereas Zhang *et al.* reported, that PqsA and PqsD account for DHQ synthesis in *P. aeruginosa* PAO1.[77] In this context, our results seemed to be in accordance to those of Lépine and coworkers. However, according to the mechanism recently elucidated by Dulcey *et al.* in 2013 (Figure 3),[76] PqsD is essential for biosynthesis of all quinolones including DHQ. On the contrary, inhibition of PqsB or PqsC would lead to an accumulation of 2-ABA, which has been shown to degrade to DHQ under acidic conditions. Since PqsB (48%) and PqsC (42%) share some sequence homology to PqsD, this seems to be a possible explanation for the increased DHQ level. However, preliminary SPR measurements suggest much lower affinity of compound **V** to a PqsB/PqsC complex than for PqsD (E. Weidel, unpublished data).

PQS has often been associated with biofilm formation. For example, increasing PQS concentrations strongly promoted the coverage of *P. aeruginosa* PAO1 on stainless steel coupons.[63] Furthermore, a *pqsA* mutant, which is deficient in HHQ and PQS biosynthesis, was assigned as poor biofilm producer.[95] Thus, we added 500 µM of compound **V** to a 24h old biofilm of *P. aeruginosa* PA14 and analyzed the biovolume after further 24h incubation period. Indeed, the biovolume was decreased by 38% (see publication **A**, Figure 2). Unfortunately, there are no quantitative data for *pqsA* or *pqsD* mutants making an assessment of this value difficult. However, biofilm assays are sensitive and reproducibility is often poor. Results generated by different groups can hardly be compared due to various incalculable variables:

1) Even two *P. aeruginosa* PA14 strains can show tremendous differences in biofilm formation.
2) It is not clear, which readout (as biovolume, surface coverage etc.) is appropriate for data analysis. This bears further problems: Maturation of biofilms commonly involves development of a mushroom-shaped structure, which does not occur in *pqsA* mutants.[96] This structure was suggested to contribute to antibiotic resistance.[97] However, when only biovolume is measured, the PqsD inhibitor's influence might remain unknown.
3) Bacteria living in a biofilm secrete a surrounding biofilm matrix, consisting of alginate (an exopolysaccaride), lipids, proteins, and extracellular DNA. Biovolume is usually measured after staining of various biofilm components. Depending on the dye used, only the modulation of a specific component can be observed.

Extracellular DNA is generated via an AHL- and PQS-dependent mechanism.[64,96] Consequently, the DNA binding stains Syto9 and propidium iodide were used in our assay.

4) Different assay procedures might have major impact on results (e.g., if the biofilm is washed before analysis).

Taken together, results of biofilm assays should be considered in a differentiated manner under a multitude of aspects. Unfortunately, we were only able to determine the biovolume, which provides only an incomplete picture.

4.3 Binding Mode Analysis and Eligibility of the *In Vitro* Assay

(2-Nitrophenyl)methanol derivatives as **V** were identified by a ligand-based approach (Figure 4). Surprisingly, the transition state mimic **III** bearing the aminophenyl moiety in analogy to the natural substrate was not able to inhibit PqsD *in vitro*, even though the amino group was reported to form hydrogen bonds to the γ-oxygen of Ser317 and two active site water molecules.[78] A totally different interaction profile is expected for NO_2. However, in contrast to **III**, the corresponding nitrophenyl derivative **IV** efficiently inhibited PqsD. Therefore, doubts arised whether compound **V**, which was considered as starting point for further optimization, binds as expected for a transition state analog. This doubt was reinforced by the fact, that omission of a large part of the side chain increased potency, indicating that only a minor part of the molecule is responsible for affinity. To find answers to this question, we studied the binding mode by application of several biochemical and biophysical methods, as described in detail in publication **B**. Thereby, various experiments confirmed that compound **V** binds PqsD in the active site deep in the ACoA channel:

1) Preincubation of PqsD with ACoA (before the usual preincubation step of PqsD and inhibitor) results in an 8-fold increased IC_{50} value for **V**, indicating that the inhibitor's access to the binding site was hindered by covalently bound anthraniloyl or ACoA itself (for exact values see section 6.2.4).
2) Both enantiomers of compound **V** bind to PqsD but not to the AA-PqsD complex as shown by SPR spectroscopy. The binding site of **V** is blocked by the anthraniloyl moiety.
3) Mutation of amino acids located near the active site resulted in a drop of affinity as measured by ITC.

Notably, the binding site of a given compound has an influence on the biological relevance of the *in vitro* inhibition data gathered by the applied enzyme assay, as it is based on the PqsD-

catalyzed HHQ production from ACoA and β-ketodecanoic acid. This reaction was considered to be responsible for HHQ production in *P. aeruginosa* until recently.[79] However, Dulcey *et al*. showed, that after transfer of anthraniloyl from ACoA to PqsD, malonyl-CoA and octanoyl-PqsC are used as further substrates for HHQ synthesis.[76] This is not problematic, since our compounds clearly interfere with the reaction of PqsD and ACoA, which is independent of the second substrate used.

A further fundamental question in mode of action analysis is the nature of the molecular interaction. Since we observed time-dependent inhibition and apparent irreversibility (on the time scale of the experiment), MS techniques were applied to proof or to exclude covalent binding. As initial test, PqsD was incubated in presence of an excess of inhibitor **V**. Subsequent analysis by HPLC-ESI did not provide indications of a covalent adduct (see section 6.2.7). However, a possible covalent bond might be cleaved during ESI-MS or HPLC due to the non-physiological conditions (water/acetonitrile + 0.05% TFA eluent) present on the reversed phase column. Thus, PqsD incubated with an excess of inhibitor **V** was digested by trypsin to generate peptides suitable for MALDI-TOF MS, which is characterized by soft ionization and, in our case, enabled us to avoid HPLC conditions. In the mass spectra analysis, all relevant amino acids of PqsD were represented by at least one peptide (as discussed in detail in section 6.2.8), but again, no shift or disappearance of a specific peptide could be observed. This strongly suggests a non-covalent interaction between **V** and PqsD.

The methods developed to disproof covalent binding of (2-nitrophenyl)methanol derivatives are also applicable to other classes of PqsD inhibitors. 5-Arylureidothiophene-2-carboxylic acids were developed recently and have been shown to bind farther outside in the substrate

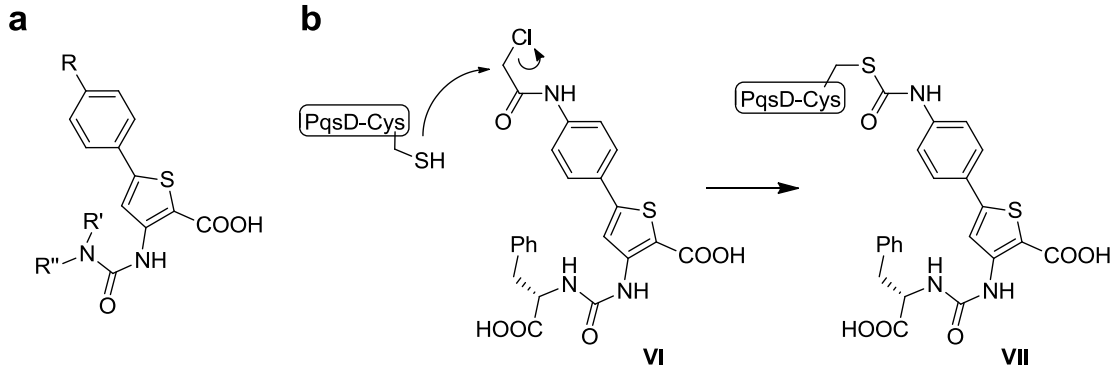

Figure 5. a) General structure 5-arylureidothiphene-2-carboxylic acid derivatives. b) Nucleophilic attack of Cys112 on the reactive β-chloroacetyl moiety leads to the covalent **VI**-PqsD complex **VII**.

channel (publication **C**). Competition experiments with (2-nitrophenyl)methanol derivatives of different size were applied to specify the precise position and binding poses were proposed by STD NMR and molecular docking. Additionally, a reactive β-chloroacetyl moiety was added in compound **VII**. If the binding pose was correct, this "electrophilic warhead"[98] would be in immediate vicinity to the active site Cys112, which allows covalent bond formation (Figure 5b). **VII** was still able to inhibit PqsD, and indeed, incubation with **VII** resulted in the expected mass shift as measured by HPLC-ESI MS (spectra shown in 6.3.8). To show that Cys112 is responsible for binding, the covalent PqsD-**VII** complex was digested by Trypsin and analyzed by MALDI-TOF MS. Thereby, we observed the expected mass shift (and a corresponding decarboxylation product) for the peptide bearing the Cys112 residue. Since none of the nucleophilic amino acids on this peptide have access to the substrate channel, this confirms the proposed binding site. Furthermore, this compound **VII** served as some kind of positive control and demonstrates the reliability of our strategy to proof a non-covalent binding mode for (2-nitrophenyl)methanol derivatives.

4.4 Structure-activity Relationships

Compound **V** has high ligand efficiency and low molecular weight, which enables a fragment-growing strategy. To this end, we fine-tuned the fragment by systematic variation of several structural features: substitution of the nitro group, introduction of substituents in the nitrophenyl moiety, and substitution of the phenyl ring by various aliphatic and (hetero-)aromatic groups. Over 60 derivatives were synthesized and evaluated *in vitro* (including a 10 min as well as 30 min preincubation step, since compound **V** showed time-dependent behavior). The most conspicuous characteristics were the essentiality of the nitro group, improved inhibition by electron donating substituents in the nitrophenyl moiety, and high tolerance for modifications of the phenyl residue. Selected compounds were tested for their ability to inhibit signal molecule production in *P. aeruginosa* PA14 cells. Detailed structure-activity relationship for each assay is discussed in detail in publication **D**.

Unfortunately, we observed tremendous differences when we compared *in vitro* and *in cellulo* data. For example, introduction of a phthalimide moiety in compound **68** resulted in at least equal *in vitro* activity, but abolished activity in *P. aeruginosa*. Considering the challenging barriers of *P. aeruginosa*, which an inhibitor has to overcome, this observation is not surprising. Differences in permeability, efflux, and metabolism depend on the molecular structure and possibly cause the discrepancy between enzymatic and cellular activity.

These observations led to the recognition that optimization only on the basis of enzymatic activity is unreasonable. To minimize the effort of compound evaluation *in cellulo*, we measured HHQ formation in a *pqsH* mutant, which is unable to convert HHQ to PQS. This method provided consistent results when compared to the wild-type and enables to examine the effect on signal molecule production efficiently by quantification of only one metabolite.

Table 1. Structure and % inhibition of the most potent (2-nitrophenyl)methanol derivatives.[a]

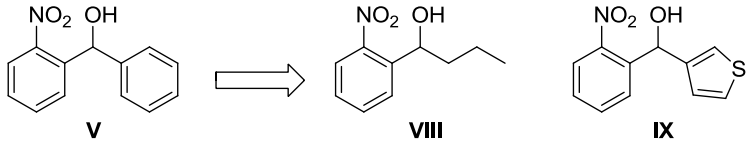

V VIII IX

Cmpd.	HHQ (*pqsH*⁻)	HHQ (*PA14*)	PQS (*PA14*)
V (250 µM)	43 ± 6	38 ± 6	37 ± 6
VIII (250 µM)	61 ± 2	33 ± 6	60 ± 11
IX (250 µM)	74 ± 6	49 ± 1	68 ± 1

[a]Values were derived from section 3.4 and 6.4.6 and differ from section 3.1 due to improvements of the assay procedure.

Based on this assessment tool, systematic variation led to the structural diverse and efficient fragments **VIII** and **IX** (Table 1). The most potent compound **IX** achieved HHQ and PQS inhibition in *P. aeruginosa* wild-type of 49 and 68 %, respectively.

4.5 Outlook

Compound **VIII** and **IX** are the PqsD inhibitors with the highest potency in *P. aeruginosa* cells, which were reported until now. Due to their low molecular weight and calculated logP values of less than 240 g/mol or 2.2, respectively, they bear a high potential in a fragment growing optimization process.

We have shown *in vitro*, that the binding pocket is very tolerant to modifications of the right part of the molecule. In *P. aeruginosa*, introduction of substituents in the nitrophenyl moiety led to poor activity, even if they were favorable in the enzymatic assay. Thus, we consider the right part of the molecule as promising site for new substituents. Improvement of **VIII** might be complicated due to the high flexibility of the propyl chain. Furthermore, substitution of a hydrogen atom would mostly create a new chiral center, which increases complexicity and slows down compound preparation/isolation. Consequently, introduction of substituents in the thiophene ring of **IX** is a promising optimization strategy by fine-tuning electronic properties of the thiophene ring or the establishment of additional interactions. This should be supported by the binding poses proposed in publication **B**.

By the development of PqsD inhibitors, we wanted to pursue an anti-virulence strategy. However, the inhibition of HHQ and PQS *per se* is not sufficient to reduce the pathogenicity of *P. aeruginosa*. Rather, the production of relevant virulence factors should be inhibited. In this regard, the optimized compounds serve as valuable tools to examine the impact on virulence factor production. For example, pyoverdine production is directly linked to the presence of PQS.[53,55] Furthermore, PqsD mutants are defective in pyocyanin production,[54] and PqsR antagonists showed significant inhibition.[99] Similar effects on pyocyanin were expected for PqsD inhibitors, since PQS is needed for full activation of PqsR.[100] However, preliminary data suggest no cellular effect by **VIII** or **IX** at 250 µM (unpublished data). It is unclear, whether PqsD is (contrary to previous reports) not crucial for pyocyanin production, or whether partly inhibition of HHQ and PQS is not sufficient to obtain the desired effects.

Further metabolites, which should be affected, are DHQ (inhibits the cell viability of mouse lung epithelial cells[77]) and *N*-oxides as HQNO (series C and E in Figure 4), for which only antimicrobial activity has been reported until now.[50]

Due to the influence of the *pqs* system on the *las*, and especially on the *rhl* system (Figure 2), various virulence factors, which are directly controlled by the latter systems, might be affected. This includes the exoproducts as elastase, the galactophilic lectin LecA, exotoxin A, HCN, alkaline proteases, and rhamnolipids as well as phenotypes as swarming and biofilm

formation. The examination of the effects exerted by PqsD inhibitors on these virulence factors and connected phenotypes should provide information, if PqsD is an appropriate drug-target.

5 References

(1) Upshur, R. (2008): Ethics and infectious disease. *Bull. World Health Organ. 86*, 654.

(2) Weese, J. S. (2011): Antimicrobial resistance: Time for action. *Vet. Rec. 169*, 122.

(3) Aminov, R. I. (2010): A brief history of the antibiotic era: Lessons learned and challenges for the future. *Front. Microbiol. 1*, 134.

(4) Infectious Diseases Society of America. (2004): Bad bugs, no drugs. As antibiotic discovery stagnates… A public health crisis brews.

(5) Jones, K. E.; Patel, N. G.; Levy, M. A.; Storeygard, A.; Balk, D.; Gittleman, J. L.; Daszak, P. (2008): Global trends in emerging infectious diseases. *Nature 451*, 990.

(6) Morens, D. M.; Folkers, G. K.; Fauci, A. S. (2004): The challenge of emerging and re-emerging infectious diseases. *Nature 430*, 242.

(7) Alanis, A. J. (2005): Resistance to antibiotics: Are we in the post-antibiotic era? *Arch. Med. Res. 36*, 697.

(8) Hancock, R. E.; Speert, D. P. (2000): Antibiotic resistance in *Pseudomonas aeruginosa*: Mechanisms and impact on treatment. *Drug Resist. Updat. 3*, 247.

(9) Maragakis, L. L.; Perencevich, E. N.; Cosgrove, S. E. (2008): Clinical and economic burden of antimicrobial resistance. *Expert Rev. Anti Infect. Ther. 6*, 751.

(10) Spellberg, B.; Bartlett, J. G.; Gilbert, D. N. (2013): The future of antibiotics and resistance. *N. Engl. J. Med. 368*, 299.

(11) Hogan, D.; Kolter, R. (2002): Why are bacteria refractory to antimicrobials? *Curr. Opin. Microbiol. 5*, 472.

(12) Normark, B. H.; Normark, S. (2002): Evolution and spread of antibiotic resistance. *J. Intern. Med. 252*, 91.

(13) Hawkey, P. M. (1998): The origins and molecular basis of antibiotic resistance. *BMJ 317*, 657.

(14) Poole, K. (2001): Multidrug efflux pumps and antimicrobial resistance in *Pseudomonas aeruginosa* and related organisms. *J. Mol. Microbiol. Biotechnol. 3*, 255.

(15) Lomovskaya, O.; Watkins, W. (2001): Inhibition of efflux pumps as a novel approach to combat drug resistance in bacteria. *J. Mol. Microbiol. Biotechnol. 3*, 225.

(16) Miller, L. A.; Ratnam, K.; Payne, D. J. (2001): β-Lactamase-inhibitor combinations in the 21st century: Current agents and new developments. *Curr. Opin. Pharmacol. 1*, 451.

(17) Helander, I. M.; Nurmiaho-Lassila, E. L.; Ahvenainen, R.; Rhoades, J.; Roller, S. (2001): Chitosan disrupts the barrier properties of the outer membrane of gram-negative bacteria. *Int. J. Food Microbiol. 71*, 235.

(18) Pedersen, S. S. (1992): Lung infection with alginate-producing, mucoid *Pseudomonas aeruginosa* in cystic fibrosis. *APMIS. Suppl. 28*, 1.

(19) Rasko, D. A.; Sperandio, V. (2010): Anti-virulence strategies to combat bacteria-mediated disease. *Nat. Rev. Drug Discov. 9*, 117.

(20) Khan, N. H.; Ahsan, M.; Taylor, W. D.; Kogure, K. (2010): Culturability and survival of marine, freshwater and clinical *Pseudomonas aeruginosa*. *Microbes Environ. 25*, 266.

(21) Morrison, A. J., Jr.; Wenzel, R. P. (1984): Epidemiology of infections due to *Pseudomonas aeruginosa*. *Rev. Infect. Dis. 3*, 627.

(22) Lessnau, K.-D. (2014): *Pseudomonas aeruginosa* infections. *Medscape*, http://emedicine.medscape.com/article/226748-overview.

(23) National Nosocomial Infections Surveillance (NNIS) System Report (2004): Data summary from January 1992 through June 2004, issued October 2004. *Am. J. Infect. Control 32*, 470.

(24) Bodey, G. P.; Bolivar, R.; Fainstein, V.; Jadeja, L. (1983): Infections caused by *Pseudomonas aeruginosa*. *Rev. Infect. Dis. 5*, 279.

(25) Govan, J. R.; Deretic, V. (1996): Microbial pathogenesis in cystic fibrosis: Mucoid *Pseudomonas aeruginosa* and *Burkholderia cepacia*. *Microbiol. Rev. 60*, 539.

(26) Singh, P. K.; Schaefer, A. L.; Parsek, M. R.; Moninger, T. O.; Welsh, M. J.; Greenberg, E. P. (2000): Quorum-sensing signals indicate that cystic fibrosis lungs are infected with bacterial biofilms. *Nature 407*, 762.

(27) Sauer, K.; Camper, A. K.; Ehrlich, G. D.; Costerton, J. W.; Davies, D. G. (2002): *Pseudomonas aeruginosa* displays multiple phenotypes during development as a biofilm. *J. Bacteriol. 184*, 1140.

(28) Gilbert, P.; Allison, D. G.; McBain, A. J. (2002): Biofilms *in vitro* and *in vivo*: Do singular mechanisms imply cross-resistance? *J. Appl. Microbiol. 92*, 98.

(29) Mann, E. E.; Wozniak, D. J. (2012): *Pseudomonas* biofilm matrix composition and niche biology. *FEMS Microbiol. Rev. 36*, 893.

(30) Stone, G.; Wood, P.; Dixon, L.; Keyhan, M.; Matin, A. (2002): Tetracycline rapidly reaches all the constituent cells of uropathogenic *Escherichia coli* biofilms. *Antimicrob. Agents Chemother. 46*, 2458.

(31) Whiteley, M.; Bangera, M. G.; Bumgarner, R. E.; Parsek, M. R.; Teitzel, G. M.; Lory, S.; Greenberg, E. P. (2001): Gene expression in *Pseudomonas aeruginosa* biofilms. *Nature 413*, 860.

(32) Gad, G. F.; El-Domany, R. A.; Zaki, S.; Ashour, H. M. (2007): Characterization of *Pseudomonas aeruginosa* isolated from clinical and environmental samples in Minia, Egypt: prevalence, antibiogram and resistance mechanisms. *J. Antimicrob. Chemother. 60*, 1010.

(33) Lister, P. D.; Wolter, D. J.; Hanson, N. D. (2009): Antibacterial-resistant *Pseudomonas aeruginosa*: clinical impact and complex regulation of chromosomally encoded resistance mechanisms. *Clin. Microb. Rev. 22*, 582.

(34) Obritsch, M. D.; Fish, D. N.; MacLaren, R.; Jung, R. (2004): National surveillance of antimicrobial resistance in *Pseudomonas aeruginosa* isolates obtained from intensive care unit patients from 1993 to 2002. *Antimicrob. Agents Chemother. 48*, 4606.

(35) Dimatatac, E. L., Alejandria, M. M., Montalban, C., Pineda, C., Ang, C., Delino, R., (2003): Clinical outcomes and costs of care of antibiotic resistant *Pseudomonas*. *Philipp. J. Microbiol. Infect. Dis. 32*, 159.

(36) Casadevall, A.; Pirofski, L. A. (2009): Virulence factors and their mechanisms of action: The view from a damage-response framework. *J. Water Health 7*, S2.

(37) Cross, A. S. (2008): What is a virulence factor? *Crit. Care, 12,* 196.

(38) Miller, M. B.; Bassler, B. L. (2001): Quorum sensing in bacteria. *Annu. Rev. Microbiol. 55*, 165.

(39) Brown, S. P.; Johnstone, R. A. (2001): Cooperation in the dark: Signalling and collective action in quorum-sensing bacteria. *Proc. R. Soc. Lond. B. 268*, 961.

(40) Strateva, T.; Mitov, I. (2011): Contribution of an arsenal of virulence factors to pathogenesis of *Pseudomonas aeruginosa* infections. *Ann. Microbiol. 61*, 717.

(41) de Kievit, T. R.; Iglewski, B. H. (2000): Bacterial quorum sensing in pathogenic relationships. *Infect. Immun. 68*, 4839.

(42) Köhler, T.; Perron, G. G.; Buckling, A.; van Delden, C. (2010): Quorum sensing inhibition selects for virulence and cooperation in *Pseudomonas aeruginosa*. *PloS Pathog. 6*, e1000883.

(43) Swift, S.; Downie, J. A.; Whitehead, N. A.; Barnard, A. M. L.; Salmond, G. P. C.; Williams, P. (2001): Quorum sensing as a population-density-dependent determinant of bacterial physiology. *Adv. Microb. Physiol. 45*, 199.

(44) Eberhard, A.; Widrig, C. A.; Mcbath, P.; Schineller, J. B. (1986): Analogs of the autoinducer of bioluminescence in *Vibrio fischeri*. *Arch. Microbiol. 146*, 35.

(45) Gambello, M. J.; Iglewski, B. H. (1991): Cloning and characterization of the *Pseudomonas aeruginosa lasR* gene, a transcriptional activator of elastase expression. *J. Bacteriol. 173*, 3000.

(46) Pearson, J. P.; Gray, K. M.; Passador, L.; Tucker, K. D.; Eberhard, A.; Iglewski, B. H.; Greenberg, E. P. (1994): Structure of the autoinducer required for expression of *Pseudomonas aeruginosa* virulence genes. *Proc. Natl. Acad. Sci. U.S.A. 91*, 197.

(47) Ochsner, U. A.; Koch, A. K.; Fiechter, A.; Reiser, J. (1994): Isolation and characterization of a regulatory gene affecting rhamnolipid biosurfactant synthesis in *Pseudomonas aeruginosa*. *J. Bacteriol. 176*, 2044.

(48) Ochsner, U. A.; Reiser, J. (1995): Autoinducer-mediated regulation of rhamnolipid biosurfactant synthesis in *Pseudomonas aeruginosa*. *Proc. Natl. Acad. Sci. U.S.A. 92*, 6424.

(49) Diggle, S. P.; Lumjiaktase, P.; Dipilato, F.; Winzer, K.; Kunakorn, M.; Barrett, D. A.; Chhabra, S. R.; Camara, M.; Williams, P. (2006): Functional genetic analysis reveals a 2-alkyl-4-quinolone signaling system in the human pathogen *Burkholderia pseudomallei* and related bacteria. *Chem. Biol. 13*, 701.

(50) Deziel, E.; Lepine, F.; Milot, S.; He, J.; Mindrinos, M. N.; Tompkins, R. G.; Rahme, L. G. (2004): Analysis of *Pseudomonas aeruginosa* 4-hydroxy-2-alkylquinolines (HAQs) reveals a role for 4-hydroxy-2-heptylquinoline in cell-to-cell communication. *Proc. Natl. Acad. Sci. U.S.A. 101*, 1339.

(51) Pesci, E. C.; Milbank, J. B.; Pearson, J. P.; McKnight, S.; Kende, A. S.; Greenberg, E. P.; Iglewski, B. H. (1999): Quinolone signaling in the cell-to-cell communication system of *Pseudomonas aeruginosa*. *Proc. Natl. Acad. Sci. U.S.A. 96*, 11229.

(52) Xiao, G.; Deziel, E.; He, J.; Lepine, F.; Lesic, B.; Castonguay, M. H.; Milot, S.; Tampakaki, A. P.; Stachel, S. E.; Rahme, L. G. (2006): MvfR, a key *Pseudomonas aeruginosa* pathogenicity LTTR-class regulatory protein, has dual ligands. *Mol. Microbiol. 62*, 1689.

(53) Diggle, S. P.; Matthijs, S.; Wright, V. J.; Fletcher, M. P.; Chhabra, S. R.; Lamont, I. L.; Kong, X.; Hider, R. C.; Cornelis, P.; Camara, M.; Williams, P. (2007): The *Pseudomonas aeruginosa* 4-quinolone signal molecules HHQ and PQS play multifunctional roles in quorum sensing and iron entrapment. *Chem. Biol. 14*, 87.

(54) Gallagher, L. A.; McKnight, S. L.; Kuznetsova, M. S.; Pesci, E. C.; Manoil, C. (2002): Functions required for extracellular quinolone signaling by *Pseudomonas aeruginosa*. *J. Bacteriol. 184*, 6472.

(55) Bredenbruch, F.; Geffers, R.; Nimtz, M.; Buer, J.; Häussler, S. (2006): The *Pseudomonas aeruginosa* quinolone signal (PQS) has an iron-chelating activity. *Environ. Microbiol. 8*, 1318.

(56) Pesci, E. C.; Pearson, J. P.; Seed, P. C.; Iglewski, B. H. (1997): Regulation of *las* and *rhl* quorum sensing in *Pseudomonas aeruginosa*. *J. Bacteriol. 179*, 3127.

(57) McGrath, S.; Wade, D. S.; Pesci, E. C. (2004): Dueling quorum sensing systems in *Pseudomonas aeruginosa* control the production of the *Pseudomonas* quinolone signal (PQS). *FEMS Microbiol. Lett. 230*, 27.

(58) Latifi, A.; Foglino, M.; Tanaka, K.; Williams, P.; Lazdunski, A. (1996): A hierarchical quorum-sensing cascade in *Pseudomonas aeruginosa* links the transcriptional activators LasR and RhIR (VsmR) to expression of the stationary-phase sigma factor RpoS. *Mol. Microbiol. 21*, 1137.

(59) McKnight, S. L.; Iglewski, B. H.; Pesci, E. C. (2000): The *Pseudomonas* quinolone signal regulates *rhl* quorum sensing in *Pseudomonas aeruginosa*. *J. Bacteriol. 182*, 2702.

(60) Dubern, J. F.; Diggle, S. P. (2008): Quorum sensing by 2-alkyl-4-quinolones in *Pseudomonas aeruginosa* and other bacterial species. *Mol. BioSyst. 4*, 882.

(61) O'Loughlin, C. T.; Miller, L. C.; Siryaporn, A.; Drescher, K.; Semmelhack, M. F.; Bassler, B. L. (2013): A quorum-sensing inhibitor blocks *Pseudomonas aeruginosa* virulence and biofilm formation. *Proc. Natl. Acad. Sci. U.S.A. 110*, 17981.

(62) Lau, G. W.; Ran, H.; Kong, F.; Hassett, D. J.; Mavrodi, D. (2004): *Pseudomonas aeruginosa* pyocyanin is critical for lung infection in mice. *Infect. Immun. 72*, 4275.

(63) Diggle, S. P.; Winzer, K.; Chhabra, S. R.; Worrall, K. E.; Camara, M.; Williams, P. (2003): The *Pseudomonas aeruginosa* quinolone signal molecule overcomes the cell density-dependency of the quorum sensing hierarchy, regulates *rhl*-dependent genes at the onset of stationary phase and can be produced in the absence of LasR. *Mol. Microbiol. 50*, 29.

(64) Yang, L.; Nilsson, M.; Gjermansen, M.; Givskov, M.; Tolker-Nielsen, T. (2009): Pyoverdine and PQS mediated subpopulation interactions involved in *Pseudomonas aeruginosa* biofilm formation. *Mol. Microbiol. 74*, 1380.

(65) Cao, H.; Krishnan, G.; Goumnerov, B.; Tsongalis, J.; Tompkins, R.; Rahme, L. G. (2001): A quorum sensing-associated virulence gene of *Pseudomonas aeruginosa* encodes a LysR-like transcription regulator with a unique self-regulatory mechanism. *Proc. Natl. Acad. Sci. U.S.A. 98*, 14613.

(66) Deziel, E.; Gopalan, S.; Tampakaki, A. P.; Lepine, F.; Padfield, K. E.; Saucier, M.; Xiao, G.; Rahme, L. G. (2005): The contribution of MvfR to *Pseudomonas aeruginosa* pathogenesis and quorum sensing circuitry regulation: Multiple quorum sensing-regulated genes are modulated without affecting *lasRI*, *rhlRI* or the production of N-acyl-L-homoserine lactones. *Mol. Microbiol. 55*, 998.

(67) Gallagher, L. A.; Manoil, C. (2001): *Pseudomonas aeruginosa* PAO1 kills *Caenorhabditis elegans* by cyanide poisoning. *J. Bacteriol. 183*, 6207.

(68) O'Shea, R.; Moser, H. E. (2008): Physicochemical properties of antibacterial compounds: Implications for drug discovery. *J. Med. Chem. 51*, 2871.

(69) Klein, T.; Henn, C.; de Jong, J. C.; Zimmer, C.; Kirsch, B.; Maurer, C. K.; Pistorius, D.; Müller, R.; Steinbach, A.; Hartmann, R. W. (2012): Identification of small-molecule antagonists of the *Pseudomonas aeruginosa* transcriptional regulator PqsR: Biophysically guided hit discovery and optimization. *ACS Chem. Biol. 7*, 1496.

(70) Zender, M.; Klein, T.; Henn, C.; Kirsch, B.; Maurer, C. K.; Kail, D.; Ritter, C.; Dolezal, O.; Steinbach, A.; Hartmann, R. W. (2013): Discovery and biophysical characterization of 2-amino-oxadiazoles as novel antagonists of PqsR, an important regulator of *Pseudomonas aeruginosa* virulence. *J. Med. Chem. 56*, 6761.

(71) Ilangovan, A.; Fletcher, M.; Rampioni, G.; Pustelny, C.; Rumbaugh, K.; Heeb, S.; Camara, M.; Truman, A.; Chhabra, S. R.; Emsley, J.; Williams, P. (2013): Structural basis for native agonist and synthetic inhibitor recognition by the *Pseudomonas aeruginosa* quorum sensing regulator PqsR (MvfR). *PloS Pathog. 9*, e1003508.

(72) Bredenbruch, F.; Nimtz, M.; Wray, V.; Morr, M.; Müller, R.; Häussler, S. (2005): Biosynthetic pathway of *Pseudomonas aeruginosa* 4-hydroxy-2-alkylquinofines. *J. Bacteriol. 187*, 3630.

(73) Essar, D. W.; Eberly, L.; Hadero, A.; Crawford, I. P. (1990): Identification and characterization of genes for a second anthranilate synthase in *Pseudomonas aeruginosa*: Interchangeability of the two anthranilate synthases and evolutionary implications. *J. Bacteriol. 172*, 884.

(74) Essar, D. W.; Eberly, L.; Han, C. Y.; Crawford, I. P. (1990): DNA sequences and characterization of four early genes of the tryptophan pathway in *Pseudomonas aeruginosa*. *J. Bacteriol. 172*, 853.

(75) Coleman, J. P.; Hudson, L. L.; McKnight, S. L.; Farrow, J. M.; Calfee, M. W.; Lindsey, C. A.; Pesci, E. C. (2008): *Pseudomonas aeruginosa* PqsA is an anthranilate-coenzyme a ligase. *J. Bacteriol. 190*, 1247.

(76) Dulcey, C. E.; Dekimpe, V.; Fauvelle, D. A.; Milot, S.; Groleau, M. C.; Doucet, N.; Rahme, L. G.; Lepine, F.; Deziel, E. (2013): The end of an old hypothesis: The *Pseudomonas* signaling molecules 4-hydroxy-2-alkylquinolines derive from fatty acids, not 3-ketofatty acids. *Chem. Biol. 20*, 1481.

(77) Zhang, Y. M.; Frank, M. W.; Zhu, K.; Mayasundari, A.; Rock, C. O. (2008): PqsD is responsible for the synthesis of 2,4-dihydroxyquinoline, an extracellular metabolite produced by *Pseudomonas aeruginosa*. *J. Biol. Chem. 283*, 28788.

(78) Bera, A. K.; Atanasova, V.; Robinson, H.; Eisenstein, E.; Coleman, J. P.; Pesci, E. C.; Parsons, J. F. (2009): Structure of PqsD, a *Pseudomonas* quinolone signal biosynthetic enzyme, in complex with anthranilate. *Biochemistry 48*, 8644.

(79) Pistorius, D.; Ullrich, A.; Lucas, S.; Hartmann, R. W.; Kazmaier, U.; Müller, R. (2011): Biosynthesis of 2-alkyl-4(1H)-quinolones in *Pseudomonas aeruginosa*: Potential for therapeutic interference with pathogenicity. *ChemBioChem 12*, 850.

(80) Schertzer, J. W.; Brown, S. A.; Whiteley, M. (2010): Oxygen levels rapidly modulate *Pseudomonas aeruginosa* social behaviours via substrate limitation of PqsH. *Mol. Microbiol. 77*, 1527.

(81) Lepine, F.; Milot, S.; Deziel, E.; He, J. X.; Rahme, L. G. (2004): Electrospray/mass spectrometric identification and analysis of 4-hydroxy-2-alkylquinolines (HAQs) produced by *Pseudomonas aeruginosa*. *J. Am. Soc. Mass Spectr. 15*, 862.

(82) Lightbown, J. W.; Jackson, F. L. (1956): Inhibition of cytochrome systems of heart muscle and certain bacteria by the antagonists of dihydrostreptomycin: 2-Alkyl-4-hydroxyquinoline N-oxides. *Biochem. J. 63*, 130.

(83) Machan, Z. A.; Taylor, G. W.; Pitt, T. L.; Cole, P. J.; Wilson, R. (1992): 2-Heptyl-4-hydroxyquinoline N-oxide, an antistaphylococcal agent produced by *Pseudomonas aeruginosa*. *J. Antimicrob. Chemother. 30*, 615.

(84) Kesarwani, M.; Hazan, R.; He, J. X.; Que, Y. A.; Apidianakis, Y.; Lesic, B.; Xiao, G. P.; Dekimpe, V.; Milot, S.; Deziel, E.; Lepine, F.; Rahme, L. G. (2011): A quorum sensing regulated small volatile molecule reduces acute virulence and promotes chronic infection phenotypes. *PloS Pathog. 7*, e1002192.

(85) Overington, J. P.; Al-Lazikani, B.; Hopkins, A. L. (2006): Opinion - How many drug targets are there? *Nat. Rev. Drug Discov. 5*, 993.

(86) Boelsterli, U. A.; Ho, H. K.; Zhou, S. F.; Leow, K. Y. (2006): Bioactivation and hepatotoxicity of nitroaromatic drugs. *Curr. Drug Metab. 7*, 715.

(87) Veber, D. F.; Johnson, S. R.; Cheng, H. Y.; Smith, B. R.; Ward, K. W.; Kopple, K. D. (2002): Molecular properties that influence the oral bioavailability of drug candidates. *J. Med. Chem. 45*, 2615.

(88) Chang, C. E. A.; Chen, W.; Gilson, M. K. (2007): Ligand configurational entropy and protein binding. *Proc. Natl. Acad. Sci. U.S.A. 104*, 1534.

(89) Hopkins, A. L.; Groom, C. R.; Alex, A. (2004): Ligand efficiency: A useful metric for lead selection. *Drug Discov. Today 9*, 430.

(90) Hughes, J. P.; Rees, S.; Kalindjian, S. B.; Philpott, K. L. (2011): Principles of early drug discovery. *Brit. J. Pharmacol. 162*, 1239.

(91) Lipinski, C. A.; Lombardo, F.; Dominy, B. W.; Feeney, P. J. (2001): Experimental and computational approaches to estimate solubility and permeability in drug discovery and development settings. *Adv. Drug Deliver. Rev. 46*, 3.

(92) Gleeson, M. P. (2008): Generation of a set of simple, interpretable ADMET rules of thumb. *J. Med. Chem. 51*, 817.

(93) Hopkins, A. L.; Keseru, G. M.; Leeson, P. D.; Rees, D. C.; Reynolds, C. H. (2014): The role of ligand efficiency metrics in drug discovery. *Nat. Rev. Drug Discov. 13*, 105.

(94) Lepine, F.; Dekimpe, V.; Lesic, B.; Milot, S.; Lesimple, A.; Mamer, O. A.; Rahme, L. G.; Deziel, E. (2007): PqsA is required for the biosynthesis of 2,4-dihydroxyquinoline (DHQ), a newly identified metabolite produced by *Pseudomonas aeruginosa* and *Burkholderia thailandensis*. *Biol. Chem. 388*, 839.

(95) Müsken, M.; Di Fiore, S.; Dötsch, A.; Fischer, R.; Häussler, S. (2010): Genetic determinants of *Pseudomonas aeruginosa* biofilm establishment. *Microbiology 156*, 431.

(96) Allesen-Holm, M.; Barken, K. B.; Yang, L.; Klausen, M.; Webb, J. S.; Kjelleberg, S.; Molin, S.; Givskov, M.; Tolker-Nielsen, T. (2006): A characterization of DNA release in *Pseudomonas aeruginosa* cultures and biofilms. *Mol. Microbiol. 59*, 1114.

(97) Hentzer, M.; Teitzel, G. M.; Balzer, G. J.; Heydorn, A.; Molin, S.; Givskov, M.; Parsek, M. R. (2001): Alginate overproduction affects *Pseudomonas aeruginosa* biofilm structure and function. *J. Bacteriol. 183*, 5395.

(98) Henise, J. C.; Taunton, J. (2011): Irreversible Nek2 kinase inhibitors with cellular activity. *J. Med. Chem. 54*, 4133.

(99) Lu, C.; Kirsch, B.; Zimmer, C.; de Jong, J. C.; Henn, C.; Maurer, C. K.; Müsken, M.; Häussler, S.; Steinbach, A.; Hartmann, R. W. (2012): Discovery of antagonists of PqsR, a key player in 2-alkyl-4-quinolone-dependent quorum sensing in *Pseudomonas aeruginosa*. *Chem. Biol. 19*, 381.

(100) Wade, D. S.; Calfee, M. W.; Rocha, E. R.; Ling, E. A.; Engstrom, E.; Coleman, J. P.; Pesci, E. C. (2005): Regulation of *Pseudomonas* quinolone signal synthesis in *Pseudomonas aeruginosa*. *J. Bacteriol. 187*, 4372.

6 Supporting Information

This section contains the relevant supporting information of the studies presented in section 3. It includes additional details on experimental procedures, as well as further figures and results.

6.1 Supporting Information for Publication A

Full supporting information is available online:
http://pubs.acs.org/doi/suppl/10.1021/ja3072397/suppl_file/ja3072397_si_001.pdf

6.1.1 Chemistry

a) General Chemistry Methods

1-Benzyl-2-nitrobenzene **21** and 1-nitro-2-(phenylsulfonyl)-benzene **22** were purchased from Sigma-Aldrich and used for biological assays without further purification. Starting materials were purchased from Aldrich, Acros, Fluka and ABCR and were used without further purification. All reactions were conducted under a nitrogen atmosphere unless otherwise indicated. Experimental procedures were not optimized. During workup drying was achieved by anhydrous sodium sulfate. Flash chromatography was performed using silica gel 60 (40-63 μm) and the reaction progress was determined by TLC analysis on ALUGRAM SIL G/UV254 (Macherey-Nagel). Visualization was accomplished with UV light. Purification by preparative HPLC was carried out on an Agilent 1200 series HPLC system from Agilent Technologies, using an Agilent Prep-C18 column (30x100 mm/10 μm) as stationary phase with acetonitrile/water as eluent. The purity of compounds used in the biological assays was ≥ 95 % as measured by LC/MS, monitored at 254 nm. The methods for LC/MS analysis and a table with data (including melting points) for all tested compounds are provided in the purity section. All chiral alcohols were isolated as racemates. ^{1}H and ^{13}C NMR spectra were recorded on a Bruker DRX-500 instrument at 300 K. Chemical shifts are reported in δ values (ppm) and the hydrogenated residues of deuterated solvents were used as internal standard ($CDCl_3$: δ = 7.26, 77.16. CD_3OD: δ = 3.31, 49.00. DMSO-d_6: δ = 2.50, 39.52). Splitting patterns describe apparent multiplicities and are designated as s (singlet), d (doublet), dd (doublet of doublet), t (triplet), td (triplet of doublet), q (quartet), and m (multiplet). All coupling constants (*J*) are given in hertz (Hz). Mass spectra (ESI) were measured on a Finnigan Surveyor MSQ Plus instrument (ThermoFisher). Mass spectra (EI) were measured on a DSQII instrument (ThermoFisher). Melting points of samples were determined in open capillaries using a SMP3 Melting Point Apparatus of Bibby Sterilin and are uncorrected.

*b) Synthesis and Spectroscopic Data of Intermediate **7***[S1]

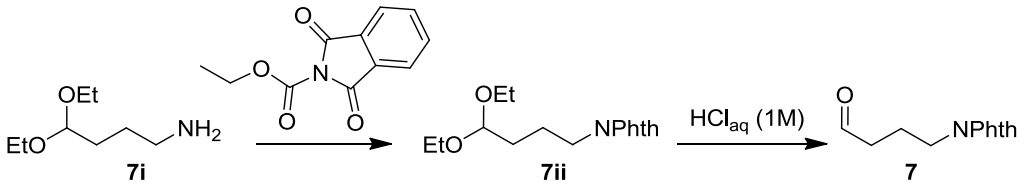

2-(4,4-Diethoxybutyl)isoindoline-1,3-dione (**7ii**). *N*-Carbethoxy-phthalimide (13.04 g, 59.50 mmol) and 4-aminobutyraldehyde diethyl acetal **7i** (10.28 g, 59.50 mmol) were dissolved in THF (90 ml) and triethylamine (8.36 ml, 59.50 mmol) was added. After stirring for 20 h at room temperature the solvent was evaporated under reduced pressure and the remaining oil was purified by flash chromatography (*n*-hexane/ethyl acetate 8:1) to yield the title compound **7ii** (15.40 g, 88 %) as a colorless oil. ^{1}H NMR (500 MHz, $CDCl_3$) δ 1.17 (t, J = 7.0, 6H), 1.62-1.67 (m, 2H), 1.72-1.78 (m, 2H), 3.44-3.50 (m, 2H), 3.58-3.64 (m, 2H), 3.70 (t, J = 7.3, 2H), 4.49 (t, J = 5.5, 1H), 7.69 (dd, J = 5.5, J = 3.0, 2H), 7.82 (dd, J = 5.5, J = 3.0, 2H). ^{13}C NMR (125 MHz, $CDCl_3$) δ 15.4, 24.1, 31.1, 37.9, 61.4, 102.5, 123.3, 132.3, 134.0, 168.5. MS (ESI) *m/z*: 246 $(M\text{-}OEt)^+$.

4-(1,3-Dioxoindolin-2-yl)butanal (**7**). A mixture of 2-(4,4-diethoxybutyl)-isoindoline-1,3-dione **7ii** (15.40 g, 52.86 mmol) and 1M aqueous HCl (101 ml) in acetone (108 ml) was heated under reflux for 2 h. The acetone was removed in vacuo and the residue was extracted with ether (three times). The combined organic extracts were washed with water, dried, filtered, and concentrated in vacuo to yield the product **7** (11.12 mmol, 97 %) as a white solid. This was used for the next step without further purification. ^{1}H NMR (500 MHz, $CDCl_3$) δ 2.02 (quintet, J = 7.0, 2H), 2.53 (td, J = 7.3, J = 0.9, 2H), 3.74 (t, J = 6.7, 2H), 7.72 (dd, J = 5.5, J = 3.0, 2H), 7.84 (dd, J = 5.5, J = 3.0, 2H), 9.77 (s, 1H). ^{13}C NMR (125 MHz, $CDCl_3$) δ 21.3, 37.3, 41.2, 123.4, 132.2, 134.2, 168.5, 200.9. MS (ESI) *m/z*: 218 $(M+H)^+$.

*c) General Method for the Synthesis of Compounds **8**, **16**-**19** and **25***

A solution of 2-iodo-nitrobenzene **5** (1.0 eq) in THF (10 ml/g reagent) was cooled to -40°C and a solution of phenylmagnesium chloride (2M in THF, 1.1 eq) was added dropwise. The solution was stirred for 30 min at -40°C, the aldehyde (1.0 eq for **7**, **19a** and **25a**; 0.5 eq for **16a**-**18a**) was added and reaction was completed at -40°C (checked by TLC). The mixture was quenched with a saturated solution of NH_4Cl (5 ml) and diluted with water (5 ml). The aqueous phase was extracted with ethyl acetate (three times) and the combined organic layers were washed with brine, dried, and concentrated under reduced pressure. The residue was purified by column chromatography over silica gel to give the desired product (**8**, **16**-**19** or **25**).

*d) General Procedure for Syntheses of the Starting Materials **16a** and **17a***[S2]

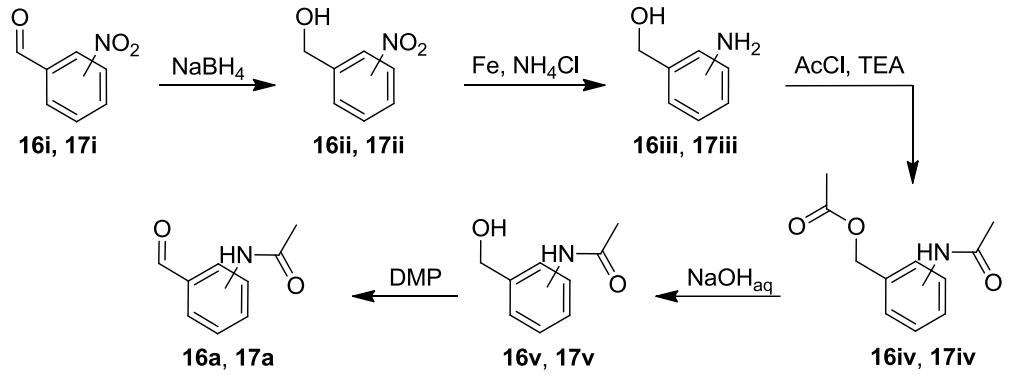

(Nitrophenyl)methanol (**16ii** and **17ii**). Sodium borohydride (1.5 eq) was added to a solution of nitrobenzaldehyde **16i** or **17i** (1.0 eq) in ethanol (130 ml) at 0°C and stirred for 2 h at room temperature. Ethanol was removed in vacuo and a saturated solution of NH_4Cl was carefully added. The mixture was extracted with DCM (three times) and the combined organic layers were washed with brine, dried and concentrated to dryness. The crude product was sufficiently pure for the next step. 2-(Nitrophenyl)methanol **16ii** (91 % yield): ^{1}H NMR (500 MHz, CD_3OD) δ 4.94 (s, 2H), 7.48 (t, J = 7.6, 1H), 7.71 (t, J = 7.6, 1H), 7.85 (d, J = 7.9, 1H), 8.44 (d, J = 8.2, 1H). ^{13}C NMR (125 MHz, CD_3OD) δ 61.9, 125.5, 129.0, 129.6, 134.7, 139.0, 148.7. 3-(Nitrophenyl)methanol **17ii** (95 % yield): ^{1}H NMR (500 MHz, CD_3OD) δ 4.72 (s, 2H), 7.57 (t, J = 7.9, 1H), 7.73 (d, J = 8.2, 1H), 8.11 (dd, J = 8.2, J = 1.9, 1H), 8.44 (s, 1H). ^{13}C NMR (125 MHz, CD_3OD) δ 63.9, 122.2, 122.9, 130.5, 133.8, 145.5, 149.7.

(Aminophenyl)methanol (**16iii** and **17iii**). Iron powder (5.5 eq) and NH_4Cl (0.7 eq) were suspended in ethanol/water 10:1 (100 ml) and refluxed with (nitrophenyl)methanol **16ii** or **17ii** (1.0 eq) for 2 h. The solvent was evaporated and DCM was added. The mixture was washed with a saturated solution of sodium carbonate, dried, filtered and concentrated in vacuo. The crude product was sufficiently pure for the next step. 2-(Aminophenyl)methanol **16iii** (88 % yield): ^{1}H NMR (500 MHz, CD_3OD) δ 4.57 (s, 2H), 6.67 (td, J = 7.4, J = 1.3, 1H), 6.73 (dd, J = 7.9, J = 1.0, 1H), 7.04-7.09 (m, 2H). ^{13}C NMR (125 MHz, CD_3OD) δ 63.6, 117.2, 119.1, 127.0, 129.7, 129.8, 147.2. 3-(Aminophenyl)methanol **17iii** (68 % yield): ^{1}H NMR (500 MHz, CD_3OD) δ 4.85 (s, 2H), 6.63 (dd, J = 7.9, J = 2.2, 1H), 6.68 (d, J = 7.6, 1H), 6.72-6.74 (m, 1H), 7.06 (t, J = 7.7, 1H). ^{13}C NMR (125 MHz, CD_3OD) δ 65.4, 115.2, 115.6, 117.9, 130.0, 143.5, 148.7.

Acetamidobenzyl acetate (**16iv** and **17iv**). At 0°C acetyl chloride (6.0 eq) was added dropwise to a stirred solution of (aminophenyl)methanol **16iii** or **17iii** (1.0 eq) and triethylamine (3.0 eq) in DCM. After stirring for 16 h at room temperature, a saturated solution of sodium bicarbonate was added and extracted with DCM (three times). The combined organic layers were washed with 1M HCl, dried, filtered and evaporated in vacuo. The crude product was used for the next step without further purification.

***N*-(Hydroxymethylphenyl)acetamide** (**16v** and **17v**). To a solution of acetamidobenzyl acetate **16iv** or **17iv** (1.0 eq) in methanol was added NaOH (3.0 eq) and stirred for 2.5 h at room temperature. After evaporation of the solvent under reduced pressure, water was added and extracted with ethyl acetate (four times). The combined organic layers were washed with brine, dried and concentrated in vacuo. The crude product was sufficiently pure for the next step. *N*-(2-(Hydroxymethyl)phenyl)acetamide **16v** (87 % yield, 2 steps): ^{1}H NMR (500 MHz, CD_3OD) δ 2.16 (s,

3H), 4.61 (s, 2H), 7.20 (td, *J* = 7.6, *J* = 1.3, 1H), 7.28 (td, *J* = 7.6, *J* = 1.6, 1H), 7.41 (dd, *J* = 7.6, *J* = 1.3, 1H), 7.51 (dd, *J* = 7.9, *J* = 1.3, 1H). ^{13}C NMR (125 MHz, CD_3OD) δ 23.4, 62.4, 125.9, 126.9, 128.9, 129.2, 135.8, 136.6, 172.1. *N*-(3-(Hydroxymethyl)phenyl)acetamide **17v** (86 % yield, 2 steps): ^{1}H NMR (500 MHz, CD_3OD) δ 2.12 (s, 3H), 4.58 (s, 2H), 7.08-7.10 (m, 1H), 7.27 (t, *J* = 7.9, 1H), 7.43-7.45 (m, 1H), 7.54-7.56 (m, 1H). ^{13}C NMR (125 MHz, CD_3OD) δ 23.8, 65.1, 119.7, 120.1, 123.6, 129.8, 139.9, 143.6, 171.6.

***N*-(Formylphenyl)acetamide** (**16a** and **17a**). To a solution of *N*-(hydroxymethyl-phenyl)acetamide **16v** or **17v** (1.0 eq) in DCM was added Dess-Martin periodinane (1.5 eq) and stirred for 20 min at room temperature. The mixture was washed with $Na_2S_2O_3$ (4.5 eq) in a saturated solution of sodium carbonate and extracted with DCM (two times). The combined organic layers were dried, filtered and concentrated in vacuo. *N*-(2-Formylphenyl)acetamide **16a** (56 % yield) was purified by flash chromatography (petroleum ether/ethyl acetate 3:1). ^{1}H NMR (500 MHz, CD_3OD) δ 2.22 (s, 3H), 7.29 (t, *J* = 7.6, 1H), 7.62 (t, *J* = 8.2, 1H), 7.82 (d, *J* = 7.6, 1H), 8.46 (d, *J* = 8.5, 1H), 9.94 (s, 1H). ^{13}C NMR (125 MHz, CD_3OD) δ 24.8, 121.3, 124.7, 136.6, 136.7, 141.3, 171.9, 196.7. *N*-(3-Formylphenyl)acetamide **17a** (74 % yield) was purified by flash chromatography (petroleum ether/ethyl acetate 1:1). ^{1}H NMR (500 MHz, CD_3OD) δ 2.15 (s, 3H), 7.51 (t, *J* = 7.9, 1H), 7.63 (d, *J* = 7.6, 1H), 7.82 (d, *J* = 7.9, 1H), 8.14 (s, 1H), 9.95 (s, 1H). ^{13}C NMR (125 MHz, CD_3OD) δ 23.8, 121.3, 126.4, 126.7, 130.6, 171.9, 193.8.

***N*-(4-Formylphenyl)acetamide** (**18e**). The title compound was purchased from Sigma-Aldrich with a purity of 97 % as specified by the producer and was used for synthesis without further purification.

*e) Synthesis and Spectroscopic Data of Compounds **1-4**, **8-20** and **23-25***

(*R*)-2,4-Dihydroxy-3,3-dimethyl-*N*-(3-((4-(2-nitrophenyl)-4-oxobutyl)amino)-3-oxopropyl)-butanamide (**1**). To a solution of **12a** (250 mg, 0.55 mmol) in DCM (4 ml) was added Dess-Martin periodinane (376 mg, 0.68 mmol) and the mixture was stirred for 90 min at room temperature. The suspension was filtered and the filtrate was concentrated to dryness. The residue was purified on silica gel (6 % MeOH/DCM) to give the ketal (*R*)-2,2,5,5-tetramethyl-*N*-(3-((4-(2-nitrophenyl)-4-oxobutyl)amino)-3-oxopropyl)-1,3-dioxane-4-carbox-amide (186 mg, 75 %) as a brown oil. ^{1}H NMR (500 MHz, CD_3OD) δ 0.95 (s, 3H), 0.98 (s, 3H), 1.42 (s, 3H), 1.43 (s, 3H), 1.91-1.96 (m, 2H), 2.42 (t, *J* = 6.6, 2H), 2.91 (t, *J* = 7.3, 2H), 3.24 (d, *J* = 11.7, 1H), 3.28 (t, *J* = 6.9, 2H), 3.41-3.52 (m, 2H), 3.72 (d, *J* = 11.7, 1H), 4.11 (s, 1H), 7.59 (dd, *J* = 7.6, *J* = 1.3, 1H), 7.67-7.71 (m, 1H), 7.80 (td, *J* = 7.6, *J* = 1.3, 1H), 8.12 (dd, *J* = 8.2, *J* = 0.7, 1H). ^{13}C NMR (125 MHz, CD_3OD) δ 19.1, 19.4, 22.5, 24.8, 34.0, 36.2, 36.4, 39.6, 40.8, 72.3, 78.4, 100.4, 125.5, 128.8, 132.1, 135.4, 138.8, 172.2, 173.8, 203.6. MS (ESI) *m/z*: 410 $(M+H)^+$. To a solution of the intermediate described above (168 mg, 0.37 mmol) in ethyl acetate (20 ml) was added 1M aqueous HCl (3 ml) and the mixture was stirred for 16 h at room temperature. The water phase was extracted with ethyl acetate (two times) and the combined organic phases were dried, filtered and concentrated in vacuo. The residue was purified by flash chromatography (6 % MeOH/DCM) to give compound **1** (67 mg, 44 %) as a brown oil. ^{1}H NMR (500 MHz, CD_3OD) δ 0.92 (s, 6H), 1.93 (quintet, *J* = 6.9, 2H), 2.45 (t, *J* = 6.3, 2H), 2.92 (t, *J* = 7.3, 2H), 3.28 (t, *J* = 6.9, 2H), 3.38 (d, *J* = 11.3, 1H), 3.44 (d, *J* = 11.3, 1H), 3.52 (t, *J* = 6.6, 1H), 3.92 (s, 1H), 7.60 (dd, *J* = 7.6, *J* = 1.3, 1H), 7.70 (m, 1H), 7.81 (td, *J* = 7.6, *J* = 0.9, 1H), 8.12 (dd, *J* = 8.2, *J* = 1.3, 1H). ^{13}C NMR (125 MHz, CD_3OD) δ 21.2, 21.5, 24.6, 36.4, 36.5, 39.7, 40.3, 40.8, 70.2, 77.6, 125.4, 128.8, 132.1, 135.4, 138.7, 142.5, 173.8, 176.2, 203.7. MS (ESI) *m/z*: 410 $(M+H)^+$.

(4*R*)-*N*-(3-((4-(2-Aminophenyl)-4-oxobutyl)amino)-3-oxopropyl)-2,4-dihydroxy-3,3-dimethylbutanamide (**2**). Crude **12b** (1.70 g) was dissolved in DCM (30 ml) and added to a solution of pyridinium chlorochromate (0.58 g, 2.69 mmol) in DCM and molecular sieves 4Å. The mixture was stirred for 18 h at room temperature. The molecular sieves were filtered off and the DCM was evaporated in vacuo. Ethyl acetate was added to the residue and washed with saturated Na_2CO_3, extracted with ethyl acetate (three times), washed with brine, filtered and concentrated in vacuo. The crude product was purified by flash chromatography (3 % MeOH/DCM + 1 ‰ TEA). The identity of the oxidation product (0.39 g) was proven by LC/MS, indicating a contamination by tetrabutylammonium. LC/MS (ESI) 96 % purity (UV), *m/z*: 420 $(M+H)^+$, 242 $(n\text{-}Bu_4N)^+$. Ethyl acetate (20 ml) and 1M aqueous HCl were added and the mixture was stirred for 3 h at room temperature. The pH value was adjusted to 9-10 by addition of concentrated Na_2CO_3 solution and the solvent was removed in vacuo. Methanol was added, the mixture was filtered and the filtrate was concentrated to dryness. The residue obtained after flash column chromatography (8 % MeOH/DCM) was further purified by preparative HPLC to afford **2** (20 mg, 2 %, 3 steps) as a brown oil. ^{1}H NMR (500 MHz, CD_3OD) δ 0.91 (s, 6H), 1.85-1.91 (quintet, J = 7.0, 2H), 2.42 (t, J = 6.4, 2H), 2.99 (t, J = 7.3, 2H), 3.26 (t, J = 7.0, 2H), 3.38 (d, J = 10.7, 1H), 3.42-3.53 (m, 3H), 3.88 (s, 1H), 6.56-6.61 (m, 1H), 6.73 (dd, J = 8.2, J = 0.9, 1H), 7.21-7.24 (m, 1H), 7.77 (dd, J = 8.2, J = 1.2, 1H). ^{13}C NMR (125 MHz, CD_3OD) δ 20.9, 21.3, 25.6, 36.4, 36.5, 37.3, 40.1, 40.3, 70.4, 77.3, 106.2, 118.4, 118.5, 132.3, 135.3, 152.6, 173.7, 176.0, 203.0. MS (ESI) *m/z*: 380 $(M+H)^+$.

(2*R*)-2,4-Dihydroxy-*N*-(3-((4-hydroxy-4-(2-nitrophenyl)butyl)amino)-3-oxopropyl)-3,3-dimethylbutanamide (**3**). The title compound was prepared by reaction of **12a** (175 mg, 0.39 mmol) with aqueous HCl (3 ml, 1M) in ethyl acetate (20 ml) according to the procedure described for compound **1**. Compound **3** (73 mg, 43 %) was obtained after purification by flash chromatography (10 % MeOH/DCM) as a red-brown solid. ^{1}H NMR (500 MHz, CD_3OD) δ 0.91 (s, 6H), 1.63-1.81 (m, 4H), 2.43 (t, J = 6.6, 2H), 3.20-3.24 (m, 2H), 3.37 (d, J = 11.0, 1H), 3.45 (d, J = 11.0, 1H), 3.46-3.53 (m, 2H), 3.90 (s, 1H), 5.16 (dd, J = 7.8, J = 3.2, 1H), 7.44-7.47 (m, 1H), 7.68 (td, J = 7.6, J = 1.3, 1H), 7.84 (dd, J = 7.9, J = 1.3, 1H), 7.87 (dd, J = 8.2, J = 1.3, 1H). ^{13}C NMR (125 MHz, CD_3OD) δ 21.2, 27.1, 36.4, 36.5, 37.2, 40.2, 40.3, 69.4, 70.3, 77.4, 125.0, 129.0, 129.1, 134.3, 142.0, 149.3, 173.7, 176.1. MS (ESI) *m/z*: 412 $(M+H)^+$.

(2*R*)-*N*-(3-((4-(2-Aminophenyl)-4-hydroxybutyl)amino)-3-oxopropyl)-2,4-dihydroxy-3,3-dimethylbutanamide (**4**). The title compound was prepared according to the procedure described for compound **1** by reaction of the crude product **12b** (0.32 mg) with 1M aqueous HCl (2.5 ml) in ethyl acetate (25 ml). The crude product was purified by flash chromatography (8 % MeOH/DCM) and preparative HPLC to afford **4** (24 mg, 5 %, 2 steps) as a yellow oil. ^{1}H NMR (500 MHz, CD_3OD) δ 0.90 (s, 6H), 1.44-1.53 (m, 1H), 1-58-1.69 (m, 1H), 1.77-1.88 (m, 2H), 2.40 (t, J = 6.7, 2H), 3.14-3.25 (m, 2H), 3.38 (d, J = 11.0, 1H), 3.41-3.52 (m, 2H), 3.88 (s, 1H), 4.70 (t, J = 6.7, 1H), 6.67 (td, J = 7.5, J = 1.2, 1H), 6.71 (dd, J = 7.9, J = 0.9, 1H), 7.00 (td, J = 7.6, J = 1.5, 1H), 7.08 (d, J = 7.6, 1H). ^{13}C NMR (125 MHz, CD_3OD) δ 20.9, 21.3, 27.1, 34.1, 36.4, 36.5, 70.4, 73.2, 73.3, 77.3, 117.9, 119.1, 128.2, 128.9, 129.8, 146.2, 173.6, 176.0. MS (ESI) *m/z*: 364 $(M\text{-}OH)^+$, 382 $(M+H)^+$.

2-(4-Hydroxy-4-(2-nitrophenyl)butyl)isoindoline-1,3-dione (**8**). Following the general method described in c) using 2-iodonitrobenzene **5** (2.49 g, 10.0 mmol) and aldehyde **7** (2.61 g, 12.0 mmol), the crude product was purified by flash chromatography (petroleum ether/ethyl acetate 5:2) to give **8** (2.89 g, 85 %) as a yellowish solid. ^{1}H NMR (500 MHz, DMSO-d_6) δ 1.56-1.61 (m, 1H), 1.63-1.72 (m, 2H), 1.78-1.86 (m, 1H), 3.58-3.61 (m, 2H), 4.93-4.96 (m, 1H), 5.54 (d, J = 4.7, 1H), 7.46-7.49 (m, 1H), 7.70 (td, J = 7.3, J = 1.3, 1H), 7.76 (dd, J = 7.9, J = 1.3, 1H), 7.82-7.87 (m, 5H). ^{13}C NMR (125

MHz, DMSO-d_6) δ 24.0, 35.7, 37.4, 67.3, 123.0, 123.6, 128.0, 131.6, 133.2, 134.3, 140.6, 147.5, 167.9. MS (ESI) *m/z*: 341 $(M+H)^+$.

2-(4-((*tert*-Butyldimethylsilyl)oxy)-4-(2-nitrophenyl)butyl)-isoindoline-1,3-dione. To a solution of **8** (4.48 g, 13.16 mmol) in DMF (120 ml) were added *tert*-butyldimethylsilyl chloride (7.93 g, 52.61 mmol) and imidazole (7.16 g, 105.17 mmol). The reaction mixture was stirred for 18 h at room temperature, washed with saturated $NaHCO_3$ and the aqueous layer was extracted with DCM (three times). The combined organic layers were washed with brine, dried, and concentrated under reduced pressure. The residue was purified on silica gel (petroleum ether/ethyl acetate 3:1) to give the title compound (3.67 g, 62 %) as a yellowish solid. ^{1}H NMR (500 MHz, $CDCl_3$) δ -0.21 (s, 3H), 0.04 (s, 3H), 0.85 (s, 9H), 1.67-1.90 (m, 4H), 3.62-3.76 (m, 2H), 5.30 (dd, *J* = 7.6, *J* = 2.5, 1H), 7.35-7.40 (m, 1H), 7.57-7.61 (m, 1H), 7.66-7.72 (m, 2H), 7.79-7.85 (m, 3H), 7.86 (dd, *J* = 8.2, *J* = 1.3, 1H). ^{13}C NMR (125 MHz, $CDCl_3$) δ -5.0, -4.8, 18.2, 25.1, 25.9, 37.4, 38.1, 69.5, 123.3, 124.2, 127.9, 129.0, 132.3, 133.3, 134.0, 141.1, 147.2, 168.5, 190.0. MS (ESI) *m/z*: 455 $(M+H)^+$.

4-((*tert*-Butyldimethylsilyl)oxy)-(2-nitrophenyl)butan-2-amine (**9**). A mixture of 2-(4-((*tert*-butyldimethylsilyl)oxy)-4-(2-nitrophenyl)butyl)-isoindoline-1,3-dione (3.55 g, 7.80 mmol) and hydrazinium hydroxide (0.97 ml, 19.94 mmol) in ethanol (190 ml) was refluxed for 2.5 h. The reaction mixture was diluted with ethyl acetate and washed with saturated $NaHCO_3$. The aqueous phase was extracted with ethyl acetate (three times) and the combined organic layers were washed with brine, dried and evaporated to afford the title compound **9** (2.49 g, 98 %) as a yellow oil. ^{1}H NMR (500 MHz, CD_3OD) δ -0.19 (s, 3H), 0.05 (s, 3H), 0.89 (s, 9H), 1.54-1.63 (m, 1H), 1.66-1.83 (m, 3H), 2.63-2.70 (m, 2H), 5.26 (dd, *J* = 7.9, *J* = 3.5, 1H), 7.45-7.49 (m, 1H), 7.68 (td, *J* = 7.6, *J* = 1.3, 1H), 7.83 (dd, *J* = 7.9, *J* = 1.3, 1H), 7.86 (dd, *J* = 8.2, *J* = 1.3, 1H), ^{13}C NMR (125 MHz, CD_3OD) δ -4.9, -4.8, 19.0, 26.3, 29.9, 38.6, 42.3, 70.9, 124.9, 129.3, 129.8, 134.2, 141.7, 149.0. MS (ESI) *m/z*: 366 $(M+H+CH_3CN)^+$.

(*R*)-3-(2,2,5,5-Tetramethyl-1,3-dioxane-4-carboxamido)propanoic acid (**10**).[S3] Calcium pantothenate (22.00 g, 46.20 mmol) and anhydrous oxalic acid (4.16 g, 46.20 mmol) were suspended in acetone (200 ml). 2,2-Dimethoxypropane (31.2 ml, 255 mmol) and molecular sieves (4Å) were added and the mixture was refluxed for 20 h. The solid was removed by filtration, the filtrate was concentrated in vacuo, the residue was dissolved in ethyl acetate and washed with water. After drying and evaporation of the solvent, product **10** was obtained as a white solid (12.46 g, 52 %). ^{1}H NMR (500 MHz, $CDCl_3$) δ 0.97 (s, 3H), 1.03 (s, 3H), 1.42 (s, 3H), 1.45 (s, 3H), 2.61 (t, *J* = 6.1, 2H), 3.28 (d, *J* = 11.6, 1H), 3.45-3.52 (m, 1H), 3.56-3.63 (m, 1H), 3.68 (d, *J* = 11.6, 1H), 4.11 (s, 1H), 7.04 (s, 1H). ^{13}C NMR (125 MHz, $CDCl_3$) δ 18.9, 19.0, 22.2, 29.5, 33.1, 34.0, 34.2, 71.6, 99.2, 170.3, 176.6. MS (ESI) *m/z*: 260 $(M+H)^+$.

(4*R*)-*N*-(3-((4-((*tert*-Butyldimethylsilyl)oxy)-4-(2-nitrophenyl)butyl)amine)-3-oxo-propyl)-2,2,5,5-tetramethyl-1,3-dioxane-4-carboxamide (**11a**). To a solution of amine **9** (2.45 g, 7.56 mmol) and acid **10** (2.15 g, 8.29 mmol) in DMF (50 ml) were added *N*,*N*'-dicyclohexylcarbodiimide (1.71 g, 8.29 mmol) and 4-hydroxy-1*H*-benzotriazole (1.12 g, 8.29 mmol) at 5°C. The reaction mixture was allowed to warm slowly to room temperature by stirring for 19 h. The solution was washed with saturated Na_2CO_3, extracted with DCM (three times) and the combined organic layers were washed with water and brine. After drying and evaporation the crude product was purified on silica gel (petroleum ether/ethyl acetate 1:2) to give product **11a** (2.87 g, 67 %). ^{1}H NMR (500 MHz, $CDCl_3$) δ -0.21 (s, 3H), 0.02 (s, 3H), 0.87 (s, 9H), 0.94 (d, *J* = 11.0, 3H), 1.02 (d, *J* = 3.8, 3H), 1.40 (s, 3H), 1.44 (s, 3H), 1.57-1.71 (m, 3H), 1.77-1.81 (m, 1H), 2.41 (t, *J* = 6.3, 2H), 3.20-3.26 (m, 3H), 3.45-3.52 (m, 1H), 3.54-3.61 (m, 1H), 3.66 (dd, *J* = 11.7, *J* = 1.9, 1H), 4.05 (s, 1H), 5.28 (dd, *J* = 7.3, *J* = 3.2, 1H),

5.81 (s, 1H), 7.02 (s, 1H), 7.37-7.40 (m, 1H), 7.60-7.63 (m, 1H), 7.81 (d, *J* = 7.9, 1H), 7.88 (dd, *J* = 8.2, *J* = 1.3, 1H). ^{13}C NMR (125 MHz, CD_3OD) δ -4.9, -4.7, 18.2, 18.8, 22.3, 25.1, 25.8, 25.9, 30.0, 34.1, 35.0, 35.0, 36.3, 36.6, 37.7, 37.4, 39.3, 39.4, 69.4, 71.6, 99.2, 124.2, 128.0, 128.8, 133.3, 141.3, 170.3, 171.0. MS (ESI) *m/z*: 566 $(M+H)^+$.

(4*R*)-*N*-(3-((4-(2-Aminophenyl)-4-((tert-butyldimethylsilyl)oxy)-butyl)amino)-3-oxopropyl)-2,2,5,5-tetramethyl-1,3-dioxane-4-carboxamide (**11b**). Nitro compound **11a** (1.00 g, 1.77 mmol) was dissolved in ethyl acetate (40 ml) and palladium on activated charcoal (200 mg, 10 wt. %) was added. The reaction mixture was stirred at room temperature under hydrogen (1 atm) for 20 h. Silica gel was added and the suspension was evaporated to dryness. Amine **11b** (0.83 g, 87 %) was isolated by flash chromatography (petroleum ether/ethyl acetate 1:4). ^{1}H NMR (500 MHz, CD_3OD) δ -0.11 (s, 3H), 0.08 (s, 3H), 0.89 (s, 9H), 0.94 (s, 3H), 0.98 (s, 3H), 1.41-1.42 (m, 6H), 1.56-1.65 (m, 1H), 1.69-1.90 (m, 3H), 2.39 (t, *J* = 6.6, 2H), 3.10-3.25 (m, 2H), 3.25 (d, *J* = 11.7, 1H), 3.39-3.50 (m, 2H), 3.72 (d, *J* = 11.7, 1H), 4.08 (s, 0.5H), 4.10 (s, 0.5H), 4.73 (dd, *J* = 7.9, *J* = 5.9, 1H), 6.60-6.64 (m, 1H), 6.68 (dd, *J* = 8.2, *J* = 1.2, 1H), 6.97-7.01 (m, 2H). ^{13}C NMR (125 MHz, CD_3OD) δ -4.96, -4.94, 19.0, 19.1, 19.4, 22.4, 26.4, 27.2, 29.7, 33.9, 34.7, 34.9, 36.2, 36.3, 40.1, 72.2, 76.7, 76.8, 78.3, 100.4, 117.9, 118.7, 128.9, 129.4, 146.2, 172.1, 173.6. MS (ESI) *m/z*: 536 $(M+H)^+$.

(4*R*)-*N*-(3-((4-Hydroxy-4-(2-nitrophenyl)butyl)amino)-3-oxopropyl)-2,2,5,5-tetra-methyl-1,3-dioxane-4-carboxamide (**12a**). A solution of **11a** (0.82 g, 1.45 mmol) in THF (14.5 ml) and 1M TBAF in THF (14.5 ml, 14.5 mmol) was stirred for 4 h at 50°C. The solution was washed with water and the aqueous phase was extracted with ethyl acetate (two times). The organic phase was washed with brine, dried and concentrated to dryness. The residue was purified on silica gel to yield **12a** (0.45 g, 69 %). ^{1}H NMR (500 MHz, CD_3OD) δ 0.95 (d, *J* = 4.6, 3H), 0.98 (s, 3H), 1.42 (s, 3H), 1.43 (s, 3H), 1.58-1.87 (m, 4H), 2.41 (t, *J* = 6.7, 2H), 3.19-3.26 (m, 3H), 3.40-3.52 (m, 2H), 3.73 (d, *J* = 11.6, 1H), 4.10 (s, 1H), 5.16 (dd, *J* = 8.2, *J* = 3.0, 1H), 7.44-7.47 (m, 1H), 7.68 (td, *J* = 7.8, *J* = 0.9, 1H), 7.84 (d, *J* = 7.9, 1H), 7.87 (d, *J* = 8.0, 1H). ^{13}C NMR (125 MHz, CD_3OD) δ 13.9, 13.9, 19.0, 19.4, 22.4, 27.2, 29.7, 34.0, 36.2, 36,3, 37.2, 40.2, 69.4, 72.3, 78.4, 100.4, 125.0, 129.0, 129.1, 134.3, 142.1, 149.3, 172.1, 173.6. MS (ESI) *m/z*: 452 $(M+H)^+$.

(4*R*)-*N*-(3-((4-(2-Aminophenyl)-4-hydroxybutyl)amino)-3-oxopropyl)-2,2,5,5-tetramethyl-1,3-dioxane-4-carboxamide (**12b**). To a solution of **11b** (1.67 g, 3.12 mmol) in THF (31.2 ml) was added 1M TBAF in THF (31.2 ml, 31.20 mmol) and the mixture was stirred for 80 min at room temperature. The solvent was evaporated under reduced pressure, the residue was redissolved in ethyl acetate and washed with water. The aqueous phase was extracted with ethyl acetate (three times) and the organic phase was washed with brine, dried and concentrated in vacuo. The crude product (2.19 g) was used for synthesis of compound **2** and **4** without further purification. LC/MS (ESI) 54 % purity (UV), *m/z*: 404 $(M-OH)^+$, 422 $(M+H)^+$, 242 $(n\text{-}Bu_4N)^+$.

***N*-(4-((*tert*-Butyldimethylsilyl)oxy)-4-(2-nitrophenyl)acetamide** (**13**). A mixture of **9** (1.93 g, 5.95 mol), pyridine (14 ml) and acetic anhydride (14 ml) was stirred for 17 h at room temperature. Pyridine was removed in vacuo, ethyl acetate was added and washed with 1M HCl. The aqueous phase was extracted with ethyl acetate (three times) and the organic phase was washed with brine and dried. After evaporation under reduced pressure, the residue was purified on silica gel (petroleum ether/ethyl acetate 2:1) to yield **13** (1.31 g, 60 %) as a yellowish oil. ^{1}H NMR (500 MHz, CD_3OD) δ -0.19 (s, 3H), 0.05 (s, 3H), 0.88 (s, 9H), 1.53-1.62 (m, 1H), 1.65-1.73 (m, 2H), 1.75-1.83 (m, 1H), 1.91 (s, 3H), 3.17 (td, 2H), 5.25 (dd, 1H), 7.47 (m, 1H), 7.68 (td, 1H), 7.82 (dd, 1H), 7.86 (dd, 1H). ^{13}C NMR (125 MHz, CD_3OD) δ -5.0, -4.8, 19.0, 22.5, 26.3, 27.0, 38.5, 40.3, 70.9, 124.9, 129.3, 129.8, 134.1, 141.5, 149.0, 173.2. MS (ESI) *m/z*: 367 $(M+H)^+$, 408 $(M+H+CH_3CN)^+$.

***N*-(4-Hydroxy-4-(2-nitrophenyl)butyl)acetamide** (**14**). A solution of 1M TBAF in THF (13.6 ml, 13.6 mmol) was added to **13** (0.50 g, 1.36 mmol) and the solution was stirred for 2 h at room temperature. Ethyl acetate was added and the solution was washed with water. After extraction of the aqueous phase with ethyl acetate (three times) the combined organic phases were washed with brine, dried and concentrated in vacuo. The residue was purified by flash chromatography to give **14** (207 mg, 60 %) as a brown oil. ^{1}H NMR (500 MHz, CD_3OD) δ 1.61-1.71 (m, 2H), 1.72-1.84 (m, 2H), 1.92 (s, 3H), 3.16-3.25 (m, 2H), 5.16 (dd, J = 7.9, J = 3.5, 1H), 7.44-7.47 (m, 1H), 7.68 (td, J = 7.3, J = 0.9, 1H), 7.84 (dd, J = 7.9, J = 0.9), 1H), 7.87 (dd, J = 8.2, J = 1.2, 1H). ^{13}C NMR (125 MHz, CD_3OD) δ 22.5, 27.1, 37.2, 40.2, 69.4, 125.0, 129.0, 129.1, 134.2, 142.0, 149.3, 173.3. MS (ESI) *m/z*: 253 $(M+H)^+$.

***N*-(4-(2-Nitrophenyl)-4-oxobutyl)acetamide** (**15**). To a solution of **14** (120 mg, 0.48 mmol) in DCM (4 ml) was added Dess-Martin periodinane (81 mg, 0.19 mmol) and the mixture was stirred for 4 h at room temperature. The solid was filtered off and the filtrate was washed with water. The aqueous phase was extracted with DCM (three times) and the organic phase was washed with brine, dried and concentrated under reduced pressure. The residue was purified by flash chromatography (5 % MeOH/DCM) and preparative HPLC to afford **15** (85 mg, 71 %) as a brown powder. ^{1}H NMR (500 MHz, CD_3OD) δ 1.92 (quintet, J = 7.3, 2H), 1.94 (s, 3H), 2.90 (t, J = 7.3, 2H), 3.26 (t, J = 7.3, 2H), 7.58 (d, J = 7.6, 1H), 7.69 (t, J = 7.9, 1H), 7.80 (t, J = 7.6, 1H), 8.12 (d, J = 7.9, 1H). ^{13}C NMR (125 MHz, CD_3OD) δ 22.6, 24.7, 39.6, 40.8, 125.4, 128.8, 132.0, 135.4, 138.7, 173.4, 203.7. MS (ESI) *m/z*: 251 $(M+H)^+$, 292 $(M+H+CH_3CN)^+$.

***N*-(2-(Hydroxy(2-nitrophenyl)methyl)phenyl)acetamide** (**16**). Following the general method described in c) using 2-iodonitrobenzene **5** (1.00 g, 4.01 mmol) and *N*-(2-formylphenyl)acetamide **16a** (180 mg, 2.01 mmol), the crude product was purified by flash chromatography (petroleum ether/ethyl acetate 3:2) to give **16** (210 mg, 18 %) as a yellow-brown powder. ^{1}H NMR (500 MHz, CD_3OD) δ 2.03 (s, 3H), 6.53 (s, 1H), 7.18-7.25 (m, 2H), 7.31 (td, J = 7.3, J = 1.6, 1H), 7.43 (dd, J = 7.9, J = 0.9, 1H), 7.44 (m, 1H), 7.60-7.65 (m, 2H), 7.88 (dd, J = 8.2, J = 0.9, 1H). ^{13}C NMR (125 MHz, CD_3OD) δ 23.2, 69.0, 125.4, 127.2, 128.9, 129.4, 129.6, 130.2, 133.9, 136.7, 137.7, 138.6, 150.2, 172.3. MS (ESI) *m/z*: 310 $(M+Na)^+$.

***N*-(3-(Hydroxy(2-nitrophenyl)methyl)phenyl)acetamide** (**17**). Following the general method described in c) using 2-iodonitrobenzene **5** (1.00 g, 4.01 mmol) and *N*-(3-formylphenyl)acetamide **17a** (180 mg, 2.01 mmol), the crude product was purified by flash chromatography (petroleum ether/ ethyl acetate 2:3) and recrystallized from water to give **17** (287 mg, 25 %) as a yellow-brown solid. ^{1}H NMR (500 MHz, CD_3OD) δ 2.08 (s, 3H), 6.37 (s, 1H), 7.02-7.04 (m, 1H), 7.24 (t, J = 7.9, 1H), 7.46-7.47 (m, 1H), 7.48-7.51 (m, 2H), 7.67-7.70 (m, 1H), 7.85-7.87 (m, 1H), 7.87 (dd, J = 7.9, J = 1.3, 1H). ^{13}C NMR (125 MHz, CD_3OD) δ 23.8, 73.5, 120.1, 120.4, 124.1, 125.2, 129.3, 129.7, 130.0, 134.1, 140.0, 140.0, 144.8, 149.8, 171.7. MS (ESI) *m/z*: 269 $(M-OH)^+$.

***N*-(4-(Hydroxy(2-nitrophenyl)methyl)phenyl)acetamide** (**18**). Following the general method described in c) using 2-iodonitrobenzene **5** (1.00 g, 4.01 mmol) and *N*-(4-formylphenyl)acetamide **18a** (180 mg, 2.01 mmol), the crude product was purified by flash chromatography (petroleum ether/ethyl acetate 1:1) to give **18** (416 mg, 66 %) as a yellow-brown solid. ^{1}H NMR (500 MHz, CD_3OD) δ 2.10 (s, 3H), 6.35 (s, 1H), 7.20-7.23 (m, 2H), 7.46-7.50 (m, 3H), 7.69 (t, J = 7.6, 1H), 7.88 (t, J = 8.5, 2H). ^{13}C NMR (125 MHz, CD_3OD) δ 23.8, 71.3, 121.0, 125.2, 128.8, 129.3, 129.7, 134.1, 139.2, 139.7, 140.2, 149.8, 171.7. MS (ESI) *m/z*: 227 $(M-OH-Ac)^+$, 269 $(M-OH)^+$.

(2-Nitrophenyl)(phenyl)-methanol (**19**). Following the general method described in c) using 2-iodonitrobenzene **5** (1.00 g, 4.01 mmol) and benzaldehyde **19a** (0.41 ml, 4.02 mmol), the crude product was purified by flash chromatography (petroleum ether/ethyl acetate 6:1) to give **19** (681 mg, 70 %) as a brown solid (mp. 55°C). ^{1}H NMR (500 MHz, $CDCl_3$): δ 6.44 (s, 1H), 7.27-7.32 (m, 1H), 7.33-7.34 (m, 4H), 7.44-7.47 (m, 1H), 7.62-7.65 (m, 1H), 7.73-7.75 (m, 1H), 7.93 (dd, J = 8.2, J = 1.3, 1H). ^{13}C NMR (125 MHz, $CDCl_3$): δ 71.7, 124.9, 127.1, 128.2, 128.7, 128.7, 129.6, 133.6, 138.6, 141.7. MS (ESI) *m/z*: 221.1 $(M\text{-}OH)^+$.

(2-Nitrophenyl)(phenyl)methanone (**20**). Alcohol **19** (107 mg, 0.47 mmol) was dissolved in DCM (3 ml), Dess-Martin periodinane (317 mg, 0.75 mmol) was added and the mixture was stirred for 5 h at room temperature and filtered. The filtrate was washed with water and the aqueous layer was extracted with DCM (three times). The combined organic layers were washed with brine, dried and purified by flash chromatography (petroleum ether/ethyl acetate 10:1) to yield ketone **20** (38 mg, 36 %) as a brownish solid. ^{1}H NMR (500 MHz, $CDCl_3$) δ 7.43-7.47 (m, 2H), 7.49 (dd, J = 7.6, J = 1.6, 1H), 7.57-7.61 (m, 1H), 7.66-7.70 (m, 1H), 7.74-7.76 (m, 2H), 7.78 (td, J = 7.3, J = 1.3, 1H), 8.24 (dd, J = 8.2, J = 1.3, 1H). ^{13}C NMR (125 MHz, $CDCl_3$) δ 124.6, 128.9, 129.1, 129.4, 130.6, 133.9, 134.3, 136.1, 136.4, 146.9, 193.6.

1-(Methoxy(phenyl)methyl)-2-nitrobenzene (**23**). A 60 % dispersion of sodium hydride (21 mg, 0.87 mmol) in mineral oil was washed with petroleum ether and DMF (2 ml) was added. The mixture was cooled to 0°C and alcohol **19** (200 mg, 0.87 mmol) dissolved in DMF (2 ml) was added. After 10 min iodomethane (0.05 ml) was added and the mixture was stirred for 1 h at 0°C and quenched with water. After extraction with diethyl ether (four times), the combined organic layers were washed with brine, dried, filtered and concentrated in vacuo. The residue was purified by flash chromatography to give **23** (88 mg, 42 %) as a brown oil. ^{1}H NMR (500 MHz, CD_3OD) δ 3.32 (s, 3H), 5.90 (s, 1H), 7.26-7.35 (m, 5H), 7.47-7.50 (m, 1H), 7.60-7.66 (m, 1H), 7.86 (dd, J = 8.2, J = 1.3, 1H). ^{13}C NMR (125 MHz, $CDCl_3$) δ 57.6, 81.4, 125.2, 128.8, 129.1, 129.5, 129.7, 133.9, 137.6, 141.1.

1-(2-Nitrophenyl)-1-phenylethanol (**24**). Mixture 1: $CeCl_3$ (989 mg, 4.02 mmol) was added to THF (4 ml) at 0°C and stirred for 1 h at room temperature. Acetophenone (0.47 ml, 4.02 mmol) was added at 0°C and the mixture was stirred at room temperature for 1 h. Mixture 2: 2-Iodo-nitrobenzene **5** (1.00 g, 4.02 mmol) was dissolved in THF (10 ml), a solution of phenylmagnsium chloride (2.21 ml, 2 M in THF, 4.02 mmol) was added dropwise at -40°C and the mixture was stirred for 90 min. Mixture 1 was added slowly to mixture 2 and stirred for 4 h at -40°C. The reaction was quenched with saturated NH_4Cl solution and the aqueous layer was extracted with ethyl acetate (three times). The combined organic layers were dried, filtered and concentrated in vacuo. The residue was purified by flash chromatography (petroleum ether/ethyl acetate 15:1) to yield **24** (269 mg, 27 %) as a brown solid. ^{1}H NMR (500 MHz, CD_3OD) δ 1.97 (s, 3H), 7.21-7.23 (m, 1H), 7.25-7.29 (m, 1H), 7.32-7.35 (m, 1H), 7.40-7.44 (m, 2H), 7.52-7.55 (m, 1H), 7.65-7.67 (m, 1H). ^{13}C NMR (125 MHz, CD_3OD) δ 31.2, 76.6, 125.0, 127.0, 128.0, 128.9, 129.2, 130.1, 131.7, 141.8, 148.2.

2,2,2-Trifluoro-1-(2-nitrophenyl)-1-phenylethanol (**25**). Following the general method described in c) using 2-iodonitrobenzene **5** (1.00 g, 4.01 mmol) and 2,2,2-trifluoro-acetophenone **25a** (180 mg, 2.01 mmol), the crude product was purified by flash chromatography (petroleum ether/ethyl acetate 9:1) to give **25** (596 mg, 50 %) as a brownish solid. ^{1}H NMR (500 MHz, CD_3OD) δ 7.32-7.35 (m, 3H), 7.39-7.42 (m, 2H), 7.50 (dd, J = 7.9, J = 1.6, 1H), 7.55 (td, J = 7.9, J = 1.6, 1H), 7.60 (td, J = 7.6, J = 1.6, 1H), 7.70-7.73 (m, 1H). ^{13}C NMR (125 MHz, CD_3OD) δ 80.4 (q, J_{CF} = 28.4), 125.3, 126.5 (q, J_{CF} = 287.2), 127.6, 128.2, 128.3, 129.0, 129.5, 130.0 (q, J_{CF} = 3.7), 130.9, 131.2, 132.5, 139.9, 152.1. MS (EI) *m/z*: 228 $(M\text{-}CF_3^{\bullet})^+$, 251 $(M\text{-}NO_2^{\bullet})^+$.

6.1.2 Purity (LC/MS Determination)

The purity of all compounds tested in the biological assays was determined using LC/MS as follows and are indicated in Table 1:

Table 1. Purity

Cmpd	R_t (min)	HPLC purity (≥ %)	MS (ESI) m/z	mp (°C)
1	7.23	97	410.1 $(M+H)^+$	66-72
2	6.97	97	380.2 $(M+H)^+$	-
3	7.39	98	412.2 $(M+H)^+$	88-95
4	4.81	98	382.2 $(M+H)^+$	-
14	7.42	98	253.2 $(M+H)^+$	-
15	7.20	99	251.2 $(M+H)^+$	81-85
16	7.93	99	309.7 $(M+Na)^+$	162-164
17	8.14	96	268.8 $(M-OH)^+$	166-167
18	7.96	95	268.9 $(M-OH)^+$	92-96
19	10.52	99	212.1 $(M-OH)^+$	54-55
20	10.66	97	-	92-93
21	11.22	99	* 228.3 $(M-CF_3^{\bullet})^+$	97-98
22	10.89	98	-	92-94
23	13.32	99	-	-
24	13.21	93	-	-
25	10.85	99	-	146

*** MS (EI) m/z**

A SpectraSystems® LC system consisting of a pump, an autosampler, and a PDA detector was employed. Mass spectrometry was performed on an MSQ® electro spray mass spectrometer (ThermoFisher, Dreieich, Germany) unless indicated otherwise. m/z values determined by DSQII electron ionization analyzer (ThermoFisher, Dreieich, Germany) are marked by an asterisk (*). The system was operated by the standard software Xcalibur®. An RP-C18 NUCLEODUR® 100-5 (125x3 mm) column (Macherey-Nagel GmbH, Düren, Germany) was used as stationary phase. All solvents were HPLC grade.

In a gradient run the percentage of acetonitrile (containing 0.1 % trifluoroacetic acid) in 0.1 % trifluoroacetic acid was increased from an initial concentration of 0 % at 0 min to 100 % at 15 min and kept at 100 % for 5 min. The injection volume was 15 µL and flow rate was set to 800 µL/min. MS analysis was carried out at a spray voltage of 3800 V, a capillary temperature of 350°C, and a source CID of 10 V. Spectra were acquired in positive mode from 100 to 1000 m/z at 254 nm for the UV trace.

6.1.3 ITC Characterization of (2-Nitrophenyl)(phenyl)methanol (**19**)

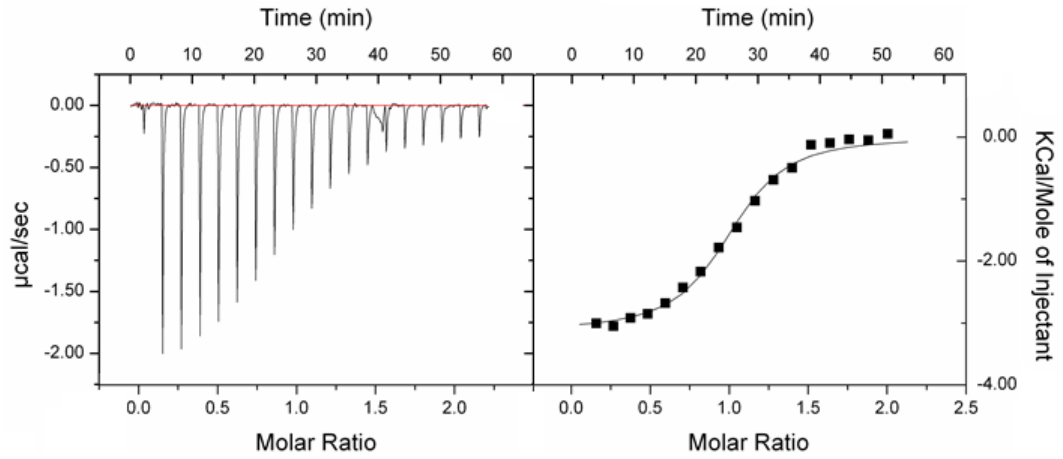

Figure S1. ITC titration of **19** (3500 µM) against PqsD (328 µM). The recorded change in heat is shown in units of µcal/sec as a function of time for successive injections of the ligand (upper panel). Integrated heats (black squares) plotted against the molar ratio of the binding reaction. The continuous line represents the results of the non-linear least squares fitting of the data to a binding model (lower panel). K_d (**19**) = 13 µM is a mean value of three experiments and standard deviation is less than 25 %.

6.1.4 Biological Methods

Expression and purification of recombinant PqsD in *E. coli*. His_6-tagged PqsD (H_6-PqsD) was expressed in *E. coli* and purified using a single affinity chromatography step. Briefly, *E. coli* BL21 (λDE3) cells containing the pET28b(+)/*pqsD* (kindly provided by Prof. Rolf Müller) were grown in LB medium containing 50 µg ml^{-1} kanamycin at 37°C to an OD_{600} of approximately 0.8 units and induced with 0.2 mM IPTG for 16 h at 16°C. The cells were harvested by centrifugation (5000 rpm, 10 min, 4°C) and the cell pellet was resuspended in 100 ml binding buffer (25 mM Tris pH 7.8, 150 mM NaCl, 20 mM imidazole, 1 mM β-mercaptoethanol) and lysed by sonication for a total process time of 2.5 min. Cell debris were removed by centrifugation (18500 rpm, 40 min, 4°C) and the supernatant was filtered through a syringe filter (0.20 µm). The clarified lysate was immediately applied to a Ni-NTA column, washed with binding buffer and eluted with 500 mM imidazole. The protein containing fractions were buffer-exchanged into 50 mM Tris pH 8.0, 150 mM NaCl, 10 % glycerol (*v/v*), 1 mM β-mercaptoethanol using a PD10 column and judged pure by SDS-PAGE analysis. Subsequently, the His_6-tag was removed by thrombin cleavage using 1 unit thrombin per mg protein in presence of 2.5 mM $CaCl_2$ for 16 h at 16°C. The protein was separated from any uncleaved or His_6-tag containing protein by running the mixture through a second Ni-NTA column under the same conditions. The cleaved protein was buffer-exchanged into 50 mM Tris pH 8.0, 150 mM NaCl, 10 % glycerol (*v/v*), 1 mM β-mercaptoethanol using a PD10 column and stored in aliquots at -80°C.

Synthesis of anthraniloyl-S-CoA thioester.[S4] Anthraniloyl-CoA (ACoA) was synthesized from isatoic anhydride and coenzyme A (CoA) using a previously described method. ACoA was purified by HPLC (Agilent 1200 series consisting of a quaternary pump, a fraction collector and an MWD; Agilent Technologies, USA) after freeze drying of the aqueous reaction mixture (25 ml) and resuspending of the dried residue in 3 ml of a mixture of 50 % methanol and water. A 10 µm RP C18 150-30 column (30 x 100 mm, Agilent) was used along with a mobile phase consisting of water

containing 1‰ TFA (A) and acetonitrile containing 1‰ TFA (B) with a flow rate of 5 ml/min. The following gradient was used: 0-35 min, linear gradient 10 % - 100 % B; 35-42 min, 100 % B; 42-43 min, 10 % B (initial conditions). ACoA containing fractions were pooled and freeze dried.

Synthesis of β-ketodecanoic acid.[S5] Ethyl 3-oxodecanoate (300 mg, 1.4 mmol, 1.0 eq) was stirred with NaOH (56 mg, 1.4 mmol, 1.0 eq) in water (2 ml) overnight. Any remaining ester was removed by washing with Et_2O (10 ml). The aqueous layer was cooled and acidified with 32 % HC1 to pH = 6. After filtration the 3-oxodecanoic acid was dried *in vacuo* and obtained as white solid (100 mg, 0.54 mmol, 38 %). ^{1}H-NMR (500 MHz, $CDCl_3$) δ 0.86 (t, J = 7.0 Hz, 3H), 1.25-1.29 (m, 8H), 1.58 (quintet, J = 7.0 Hz, 2H), 2.54 (t, J = 7.5 Hz, 2H), 3.49 (s, 2H). LC/MS (ESI) no ionization, 99 % (UV).

Synthesis of ethyl 3-oxodecanoate.[S6] To a THF solution of 2M LDA (20 ml, 40 mmol 2.4 eq) was added ethyl acetoacetate (2.16 g, 16.6 mmol, 1.0 eq) at 0°C. The deep yellow clear solution was stirred at 0°C for 1 h. To this solution the 1-iodohexane was added (4.20 g, 19.81 mmol, 1.2 eq) at -78°C. The temperature was allowed to reach an ambient temperature over 14 h and the solution was stirred at room temperature for 2 h. To the solution was added 10 % HCl (200 ml) and the mixture was extracted with Et_2O (4 × 250 ml). The combined organic layers were dried over Na_2SO_4, filtered, and the filtrate was concentrated in vacuo. The residue was purified by column chromatography (*n*-hexane/ethyl acetate, 30/1) to give ethyl 3-oxodecanoate as a yellow oil (1.98 g, 9.24 mmol, 55 %). ^{1}H-NMR (500 MHz, $CDCl_3$) δ 0.84 (t, J = 7.0 Hz, 3H), 1.23-1.28 (m, 11H), 1.54 (quintet, J = 7.0 Hz, 2H), 2.49 (t, J = 7.0 Hz, 2H), 3.39 (s, 2H), 4.16 (m, 2H).

Screening assay procedure for *in vitro* PqsD inhibition. The assay was performed monitoring enzyme activity by measuring HHQ formed by condensation of anthraniloyl-CoA and β-ketodecanoic acid. The reaction mixture contained MOPS buffer (0.05 M, pH 7.0) with 0.005 % (w/v) Triton X-100, 0.1 µM of the purified enzyme and inhibitor. The test compounds were dissolved in DMSO and diluted with buffer. The final DMSO concentration was 0.5 %. Control reactions without inhibitor containing identical amounts of DMSO were performed in parallel. After 10 min preincubation at 37°C, the reaction was started by the addition of 5 µM anthraniloyl-CoA and 70 µM β-ketodecanoic acid. Reactions were stopped by addition of methanol containing 1 µM amitriptyline as internal standard for LC/MS-MS analysis. All reactions were performed in triplicates.

HHQ was quantified using a HPLC-MS/MS mass spectrometer (ThermoFisher, Dreieich, Germany) in ESI mode. Ionization of HHQ and the internal standard amitriptyline was optimized in each case. The solvent system consisted of 10 mM ammonium acetate (A) and acetonitrile (B), both containing 0.1 % trifluoroacetic acid. The initial concentration of B in A was 45 %, increasing the percentage of B to 100 % in 2.8 min and keeping it at 98 % for 0.7 min with a flow of 500 µl/min. The column used was a NUCLEODUR-C18, 100-3/125-3 (Macherey&Nagel, Duehren, Germany).

Absolute concentration values for HHQ were calculated by comparison of peak area ratios (HHQ versus internal standard) to a calibration curve in which the peak area ratios of the calibrators had been plotted against their nominal concentration. Without inhibitor approximately 12 % of ACoA were converted into HHQ and these HHQ concentrations were set to 100 %. Percentage of inhibition is a mean value of at least two independent experiments and standard deviations were less than 25 %. IC_{50} values were calculated from at least three experiments with standard deviations less than 25 %.

Cultivation and Determination of Extracellular PQS, HHQ and DHQ Levels. Extra-cellular levels of PQS, HHQ and DHQ produced by *P. aeruginosa* PA14 were determined using the method of Lépine *et al.*[S7] with some modifications: Cultures were inoculated with a starting OD_{600} = 0.02 in 24 well plates (Greiner, Cellstar) containing 1.5 ml LB medium per well. DMSO as a control or DMSO solutions of inhibitors were added to the cultures to a final DMSO concentration of 1 %. Plates were

incubated at 37°C, 200 rpm and a humidity of 75 % for 14 h. For PQS, HHQ and DHQ analysis, 1 ml of methanol containing 750 nM of the internal standard was mixed with 500 µl of each culture by vigorously pipetting. After centrifugation (4500 rpm, 20 min), 200 µL of the supernatant were transferred to glass vials for UHPLC-MS/MS analysis. For each sample, cultivation and extraction were performed in triplicates.

UHPLC-MS/MS analysis of extracellular PQS, HHQ and DHQ levels. The analyses were performed using a TSQ Quantum Access Max mass spectrometer equipped with an HESI-II source and a triple quadrupole mass detector (Thermo Scientific, Dreieich, Germany). For MS detection, the spray voltage, the nitrogen sheath gas pressure, the auxiliary gas pressure and the capillary temperature were optimized. Observed ions were (mother ion [m/z], product ion [m/z], scan time [s], scan width [m/z], collision energy [V], tube lens offset [V]): PQS: 260.098, 175.028, 0.1, 0.010, 28, 107; HHQ: 244.130, 159.050, 0.5, 0.010, 33, 88; DHQ: 162.130, 89.138, 0.3, 0.010, 33, 52; internal standard (amitriptyline): 278.100, 233.100, 0.1, 0.010, 15, 58. Xcalibur software was used for data acquisition and quantification with the use of a calibration curve relative to the area of the internal standard. All samples were injected by autosampler (Accela®, Thermo Scientific, Dreieich, Germany) with a volume of 10 µl. An Accucore RP-MS® 2.6 µm (150 × 2.1 mm) column (Thermo Scientific, Dreieich, Germany) was used as stationary phase along with a mobile phase consisting of 10 mM ammonium acetate buffer containing 1 ‰ TFA (v/v; A) and acetonitrile containing 1 ‰ TFA (v/v; B) and a flow rate of 0.8 ml/min (PQS, HHQ) or 0.7 ml/min (DHQ).
For PQS and HHQ analysis, the following chromatographic conditions were used: 0.00-1.70 min, isocratic 40 % A, 1.71-3.00 min, 95 % A, 3.01-4.50, initial conditions 40 % A. The column oven temperature was 45°C. The chromatographic conditions used for DHQ determination were: 0.00-2.00 min, linear gradient 20 % - 98 % A, 2.00-3.30 min, 98 % A, 3.32-4.50 min, initial conditions 20 % A.

Biofilm growth assay. Static biofilms at the bottom of 96 well microtiter plates were grown with small modifications as previously described.[S8] In brief, overnight *P. aeruginosa* LB cultures of PA14 were adjusted to an OD_{600} of 0.002 with fresh medium and transferred into a half-area 96 well µClear plate (Greiner Bio-One, 100 µl/well). The plate was covered with an air-permeable foil and incubated at 37°C in a chamber with humid atmosphere. After 24 h, a staining solution including Syto9 and propidium iodide (LIVE/DEAD BacLight Bacterial Viability kit, Molecular Probes/Invitrogen) and the test compound solved in DMSO was added to the biofilms (final concentration 500 µM, 1 % DMSO (v/v)) and biofilms were further incubated for 24 h at 37°C. After in total 48 h, biofilm stacks were acquired in the center of each well (step size: 2 µm) using a confocal microscope (Fluoview 1000, Olympus) equipped with an x60/1.20 water objective. The acquired image stacks were processed and analyzed as previously described[S9] to determine the parameter total biovolume estimating the μm^3 covered by biofilm.[S10] 3D-projections of the biofilms are visualized with the software IMARIS (version 5.7.2, Bitplane).

Determination of the Growth Curves of *P. aeruginosa* PA14. Cultures of *P. aeruginosa* PA14 were inoculated with an overnight culture to obtain a starting OD_{600} = 0.05 and grown in three replicates in 100 ml Erlenmeyer flasks containing 10 ml LB medium at 37°C, 200 rpm and a humidity of 75 %. DMSO solutions of compound **19** were added to the cultures to a final concentration of 500 µM inhibitor and 1 % DMSO. Bacterial growth was measured as a function of OD_{600} using FLUOstar Omega (BMG LABTECH, Ortenberg, Germany). *P. aeruginosa* PA14 cultures containing 1 % DMSO were used as a control.

***In vitro* cytotoxicity test**. THP-1 cells (DSMZ, Braunschweig) were routinely cultured in RPMI 1640 (Pan Biotech, Aidenbach) supplemented with 10 % FCS (CCPro, Oberdola) and 1 % Pen/Strep (Pan Biotech). Prior to seeding, viability of cells was determined by trypan blue staining. Cells in

exponential growth phase were plated in 96-well flat bottom plates at 2.5x10E4 cells / mL, 100 µL / well. Cells were differentiated into macrophages for 24 h with 100 nM Phorbol-12-myristate-13-acetate (Sigma Aldrich). Dilutions of **19** were added at 100 µL / well. Plates were incubated for 48 hrs at 37^0C and 5% CO_2 in a humidified atmosphere. For proliferation measurement, resazurin (Sigma Aldrich) was added at 45µM (final) and plates were incubated for an additional 3.5 hrs. Plates were measured in a Victor3 (Perkin Elmar) fluorescent plate reader at 544/590nM (Ex/Em). Relative proliferation was calculated as % of untreated control.

6.1.5 Separation into the Enantiomers of 19 and their PqsD Inhibitory Activity

The separation was performed using an Agilent 1200 HPLC system equipped with an MWD triggering an automated fraction collector (Agilent Technologies, Inc. Headquarters, Santa Clara, CA, USA**)** in "time based" mode. ChemStation® software was used for control and report. The sample was manually injected. A Nucleocel Delta S® 5µm (250 / 8 mm) column (Macherey-Nagel GmbH, Duehren, Germany) was used as stationary phase. The solvent system consisted of *n*-hexane (A) and *iso*-propanol (B). HPLC-Method: Flow rate 2 mL/min. Isocratic run of 2 % of B in A.
Determination of enantiomeric excess was performed using a Nucleocel Alpha S® 5µm (250 / 4,6 mm) column (Macherey-Nagel GmbH, Duehren, Germany) as stationary phase. HPLC-Method: Flow rate 0.5 mL/min. Isocratic run of 2 % of B in A, using the above mentioned solvents. The % ee of **(*R*)-19** was determined using the relative peak areas in the MWD trace.

Table S1. Comparison of the PqsD Inhibition by *rac*-**19** and the (*R*)-**19**.

Compd.[a]	**direction of rotation**	**% ee**	**% inhibition**	**IC_{50} [µM]**
rac-19		0	99	3.2
(*R*)-19	(+)	65.8	99	3.5

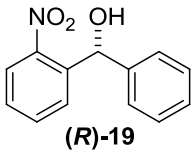

(*R*)-19

[a]Absolute configuration was derived from measurement of the optical rotation and comparison to literature.[S11]

6.1.6 Biovolume and Representative Biofilm Slices of PA14 Biofilms

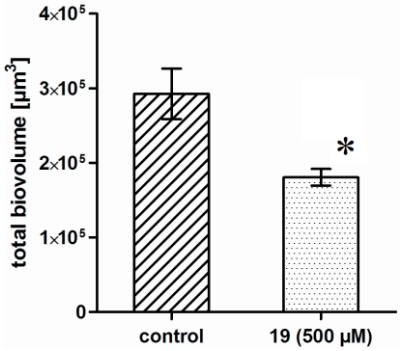

Figure S2. Biovolume of PA14 biofilms. The total biovolume was decreased by compound **19**. Bars represent mean values of n = 4, ±SD. * $P < 0.003$.

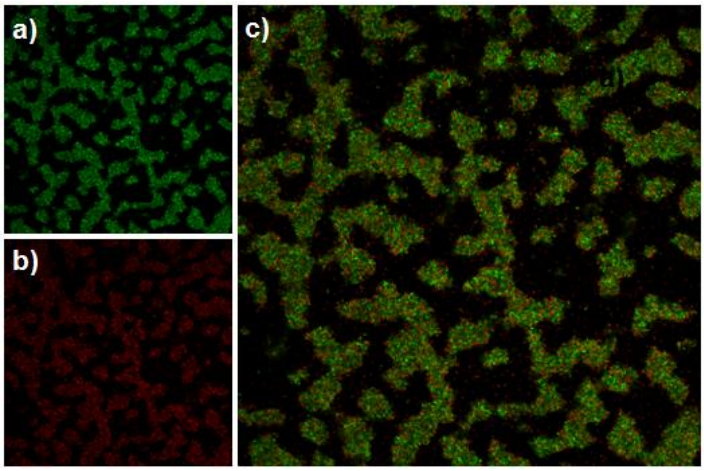

Figure S3. Representative slices of the (a) green and (b) red stained biofilm proportion as well as the (c) overlay of the DMSO control at the approx. height of 20 µm. 48 h old biofilms were stained with Syto9 (green) and propidium iodide (red) representing live and dead bacteria, respectively.

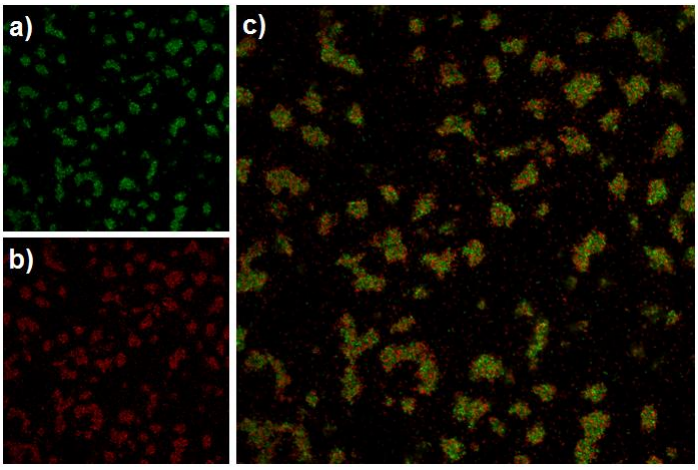

Figure S4. Representative slices of the (a) green and (b) red stained biofilm proportion as well as the (c) overlay of the **19** treated biofilm at the approx. height of 20 µm. 48 h old biofilms were stained with Syto9 (green) and propidium iodide (red) representing live and dead bacteria, respectively.

6.1.7 Growth Curves of *P. aeruginosa* PA14

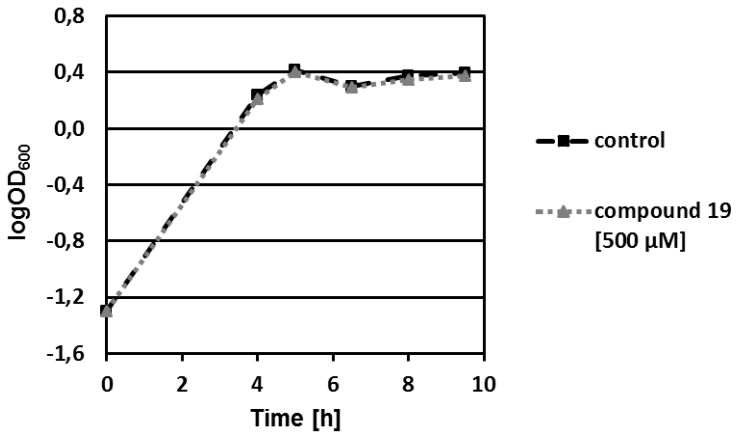

Figure S5. Growth Curves of *P. aeruginosa* PA14. Strains were grown in the absence (■) / presence of 500 µM of compound **9** (▲) in LB. Samples were taken at 0h, 4h, 5 h, 6.5h, 8 h and 9.5 h to measure OD_{600}. Mean value of one experiment with n = 3, standard deviation less than 7 %.

6.1.8 Results of the *in vitro* Cytotoxicity against Human THP-1 Macrophages

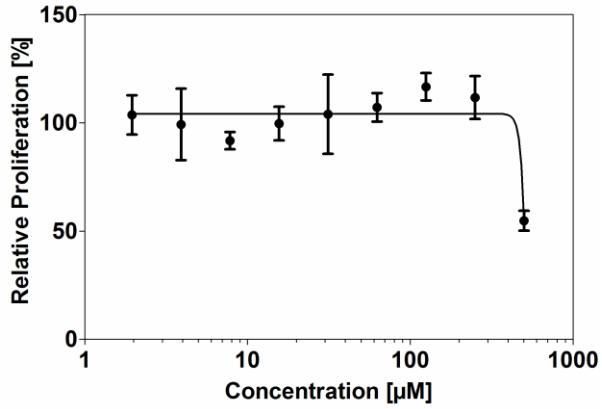

Figure S6. Proliferation of human THP-1 macrophages in presence of compound **19** compared to untreated control. Points represent mean values of n = 6, ±SD. IC_{50} > 500 µM; 45 % inhibition at 500 µM.

6.1.9 Structures of PqsD Inhibitors A and B, Derived from Known FabH Inhibitors.[S12]

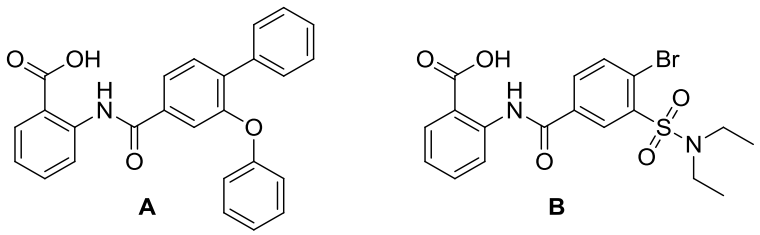

6.1.10 References

(S1) A.-H. Li, S. Moro, N. Forsyth, N. Melman, X.-D. Ji, K. A. Jacobson; Synthesis, CoMFA analysis, and receptor docking of 3,5-diacyl-2,4-dialkylpyridine derivatives as selective A_3 adenosine receptor antagonists. *J. Med. Chem.* **1999**, *42*, 706.

(S2) N. Vicker, H. V. Bailey, W. Heaton, J. M. Day, A. Purohit, B. V. L. Potter; Compound capable of inhibiting 17-beta hydroxysteriod dehydrogenase. US 2010/0286204 A1.

(S3) V. N. Osipov; Stimulant of hair growth based on a pantothenic acid derivative. WO/2007/021219, February 2, 2007.

(S4) E. J. Simon, D. Shemin; The preparation of *S*-succinyl coenzyme A. *J. Am. Chem. Soc.* **1953**, *75*, 2520.

(S5) L. Cook, B. Ternai, P. Ghosh; Inhibition of human sputum elastase by substituted 2-pyrones. *J. Med. Chem.* **1987**, *30*, 1017.

(S6) Synthesized according to: V. T. H. Nguyen, E. Bellur, B. Appel, P. Langer; Synthesis of 4-alkyl- and 4-(ω-chloroalkyl)-3-hydroxy-5-alkylidenebutenolides based on cyclizations of 4-alkyl- and 4-(ω-chloroalkyl)-1,3-bis(trimethylsilyloxy)buta-1,3-dienes with oxalyl chloride. *Synthesis* **2006**, *17*, 2865.

(S7) F. Lépine, E. Déziel, S. Milot, L G. Rahme; A stable isotope dilution assay for the quantification of the *Pseudomonas* quinolone signal in *Pseudomonas aeruginosa* cultures. *Biochim Biophys. Acta.* **2003**, *1622*, 36.

(S8) M. Müsken, S. Di Fiore, A. Dötsch, R. Fischer, S. Häussler; Genetic determinants of *Pseudomonas aeruginosa* biofilm establishment. *Microbiology* **2010**, *156*, 431.

(S9) M. Müsken, S. Di Fiore, U. Römling, S. Häussler; A 96-well-plate-based optical method for the quantitative and qualitative evaluation of *Pseudomonas aeruginosa* biofilm formation and its application to susceptibility testing. *Nat. Protoc.* **2010**, *5*, 1460.

(S10) L. N. Mueller, J. F. de Brouwer, J. S. Almeida, L. J. Stal, J. B. Xavier; Analysis of a marine phototrophic biofilm by confocal laser scanning microscopy using the new image quantification software PHLIP. *BMC. Ecol.* **2006**, *6*, 1.

(S11) H.-F. Duan, J.-H. Xie, W.-J. Shi, Q. Zhang, Q.-L. Zhou; Enantioselective rhodium-catalyzed addition of arylboronic acids to aldehydes using chiral spiro monophosphite ligands. *Organic Letters* **2006**, *8*, 1479.

(S12) D. Pistorius, A. Ullrich, S. Lucas, R. W. Hartmann, U. Kazmaier, R. Müller; Biosynthesis of 2-alkyl-4(1*H*)-quinolones in *Pseudomonas aeruginosa*: Potential for therapeutic interference with pathogenicity. *ChemBioChem* **2011**, *12*, 850.

6.2 Supporting Information for Publication B

Full supporting information is available online:

http://pubs.acs.org/doi/suppl/10.1021/cb400530d/suppl_file/cb400530d_si_001.pdf

6.2.1 Primer Sequence of Mutations

Mutant	Primer	
	forward 5' → 3'	**reverse 3' →5'**
S317F	GCTGGTCCTGACCTACGGTTTTGGC GCGACCTGGGGCG	CGCCCCAGGTCGCGCCAAAACCGTA GGTCAGGACCAGC
C112A	GCTGGATATCCGGGCACAGGCGAG CGGGTTGCTGTACG	CGTACAGCAACCCGCTCGCCTGTGC CCGGATATCCAGC
H257F	CGACCATGTGATCTGCTTTCAACC GAACCTGC	GCAGGTTCGGTTGAAAGCAGATCAC ATGGTCG
C112S	GCTGGATATCCGGGCACAGAGCAG CGGGTTGCTGTACG'	CGTACAGCAACCCGCTGCTCTGTGC CCGGATATCCAGC
S317A	GCTGGTCCTGACCTACGGTGCGGG CGCGACCTGGGGCG	CGCCCCAGGTCGCGCCCGCACCGTA GGTCAGGACCAGC
N287A	CGTCTGGGCGCGATGGCTTCGGCC	GGCCGAAGCCATCGCGCCCAGACG

6.2.2 Table S1: Catalytic Activity of PqsD Wild-type and Mutants[a]

	wild-type	**S317F**	**C112A**	**H257F**	**C112S**	**S317A**	**N287A**
Formed HHQ [nM]	2154	15	1	18	171	2182	7

[a]Reactions were performed according to the screening assay procedure described in the Methods Section using 1.0 µM of *P. aeruginosa* PqsD.

6.2.3 Synthesis of Substrates Used in the Enzymatic Inhibition Assays

Synthesis of anthraniloyl-S-CoA thioester.[S1] Anthraniloyl-CoA (ACoA) was synthesized from isatoic anhydride and coenzyme A (CoA) using a previously described method. ACoA was purified by HPLC (Agilent 1200 series consisting of a quaternary pump, a fraction collector and an MWD; Agilent Technologies) after freeze drying of the aqueous reaction mixture (25 ml) and resuspending of the dried residue in 3 ml of a mixture of 50% methanol and water (*v*/*v*). A 10 µm RP C18 150-30 column (30 x 100 mm, Agilent) was used along with a mobile phase consisting of water containing 1‰ TFA (A) and acetonitrile containing 1‰ TFA (B) with a flow rate of 5 ml min^{-1}. The following gradient was used: 0–35 min, linear gradient 10% – 100% B (*v*/*v*); 35–42 min, 100% B; 42–43 min, 10% B (*v*/*v*) (initial conditions). ACoA containing fractions were pooled and freeze dried.

Synthesis of β-ketodecanoic acid.[S2] Ethyl 3-oxodecanoate (300 mg, 1.4 mmol) was stirred with NaOH (56 mg, 1.4 mmol) in 2 ml of water overnight. Any remaining ester was removed by washing with Et_2O (10 ml). The aqueous layer was cooled and acidified with 32% HCl (*w*/*v*) to pH = 6. After filtration the 3-oxodecanoic acid was dried *in vacuo* and obtained as white solid (100 mg, 38%). ^{1}H-NMR (500 MHz, $CDCl_3$) δ 0.86 (t, J = 7.0, 3H), 1.25–1.29 (m, 8H), 1.58 (m, 2H), 2.54 (t, J = 7.5, 2H), 3.49 (s, 2H). LC/MS (ESI) *m/z* 242.0, 99% (UV).

Synthesis of ethyl 3-oxodecanoate.[S3] To a THF solution of 2 M LDA (20 ml, 40 mmol) was added ethyl acetoacetate (2.16 g, 16.6 mmol) at 0°C. The deep yellow clear solution was stirred at 0°C for 1 h. To this solution the 1-iodohexane was added (4.20 g, 19.81 mmol) at -78°C. The temperature was allowed to reach an ambient temperature over 14 h and the solution was stirred at room temperature for 2 h. To the solution was added 200 ml of 10% HCl (v/v) and the mixture was extracted with Et_2O (4 × 250 ml). The combined organic layers were dried over Na_2SO_4, filtered, and the filtrate was concentrated *in vacuo*. The residue was purified by column chromatography (*n*-hexane/ethyl acetate, 30/1) to give ethyl 3-oxodecanoate as a yellow oil (1.98 g, 55%). ^{1}H-NMR (500 MHz, $CDCl_3$) δ 0.84 (t, J = 7.0, 3H), 1.23–1.28 (m, 11H), 1.54 (m, 2H), 2.49 (t, J = 7.0, 2H), 3.39 (s, 2H), 4.16 (m, 2H). LC/MS (ESI) *m/z* 458.0, 87% (UV).

6.2.4 Table S2: Comparison of IC_{50} Values Determined by Different Assay Procedures

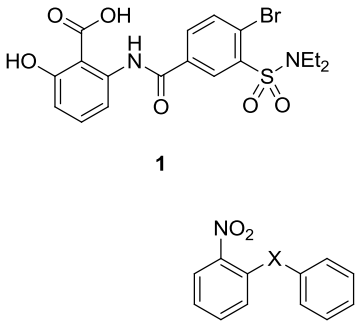

1

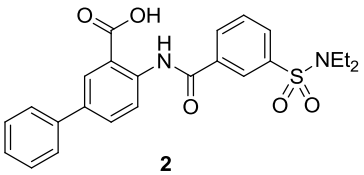

2

3 X = CHOH
4 X = CHOMe
5 X = SO_2

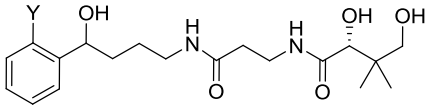

6 Y = NH_2
7 Y = NO_2

Cmpd.	IC_{50} [µM][ab]	$IC_{50,mod}$ [µM][ac]	$IC_{50,ext}$ [µM][ad]
1	1.2 ± 0.1	1.1 ± 0.2	1.8 ± 0.4
2	3.0 ± 0.7	4.2 ± 0.3	7.6 ± 1.5
3	3.2 ± 0.1	24.6 ± 6.2	1.0 ± 0.4
4	4.3 ± 1.0	19.7 ± 8.9	2.6 ± 0.5
5	14.8 ± 2.9	>50	9.7 ± 1.4
6	n.i.	n.d.	n.d.
7	7.9 ± 0.7	n.d.	n.d.

[a]n.i. no inhibition (<10% at 50 µM); n.d. not determined. [b]PqsD and inhibitor were preincubated for 10 min prior to addition of the substrates. [c]Modified procedure including additional 30 min preincubation of enzyme and ACoA. [d]Preincubation time of PqsD/inhibitors was extended to 30 min.

6.2.5 Percentages of Inhibition and Uncertainty of the Time Dependency Experiment

Table S3. HHQ formation in presence of compounds **2** and **3** relative to untreated control.

time	control [%]	Cmpd. 2, 3 µM [%]	uncertainty [%]
3 min	100	60.37	2.95
6 min	100	59.36	8.27
9 min	100	60.21	8.09
12 min	100	58.95	8.34
15 min	100	61.99	8.16
20 min	100	72.15	5.19
25 min	100	63.28	7.17
30 min	100	64.18	10.05

time	control [%]	Cmpd. 3, 6 µM [%]	uncertainty [%]
3 min	100	71.17	4.33
6 min	100	46.38	2.91
9 min	100	41.85	4.49
12 min	100	36.40	4.36
15 min	100	31.98	4.58
20 min	100	25.39	2.41
25 min	100	27.01	3.60
30 min	100	26.07	4.82

6.2.6 Figure S1: Dose-response Curve of PqsD Inhibition by Compound 3

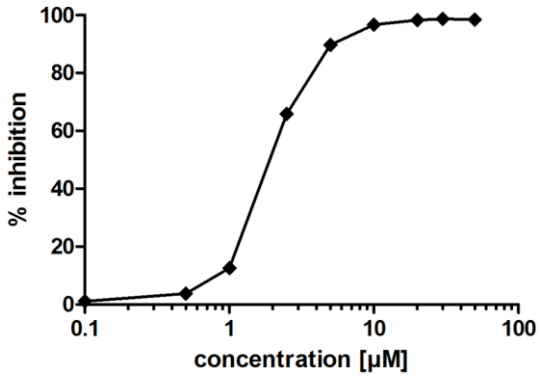

Figure S1. Inhibition of PqsD by compound **3** is plotted against the concentration (log scale). Data were generated using the screening assay procedure for *in vitro* PqsD inhibition as described above. Compounds **4** and **5** show similar curve shapes (data not shown).

6.2.7 Further HPLC-ESI MS Experiments

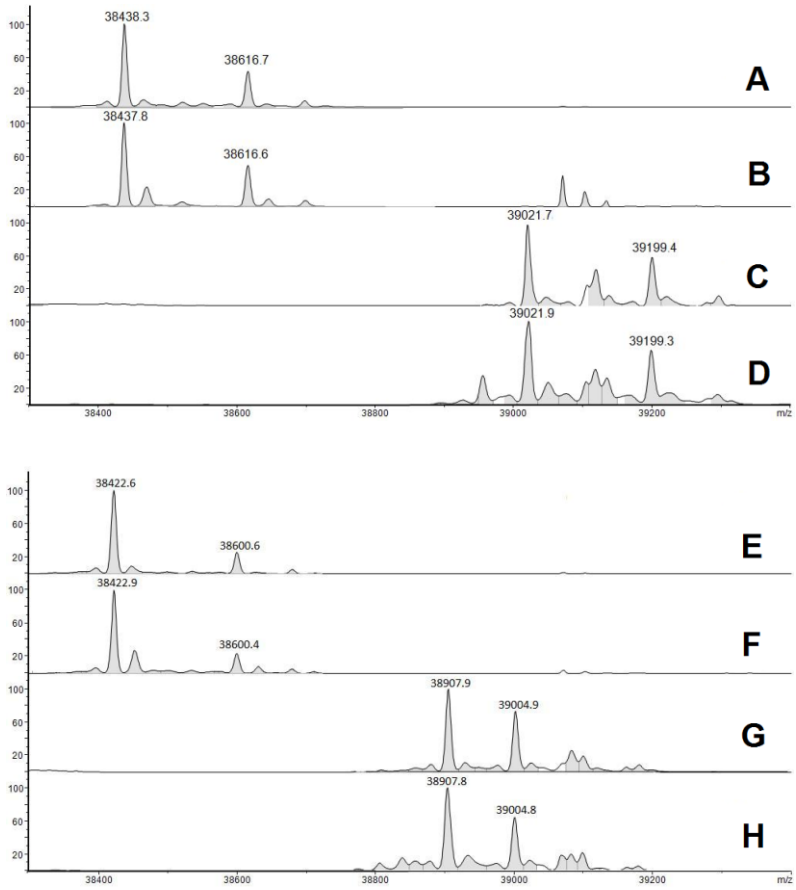

Figure S2. (A-D) PqsD containing a His_6-tag was incubated in absence (A) or in presence (B) of compound **3**. Thereby, no anti-oxidative reagent was present. Samples were subjected to HPLC-ESI MS analysis, whereas no relevant amounts of oxidation products were observed. Subsequent addition of an excess of maleimid resulted in a shift of +582 (corresponding to a 6-fold addition of the labeling agent regardless of the presence of compound **3** (C: PqsD; D: PqsD pretreated with compound **3**). Maleimid labels all available cystein residues present in PqsD, indicating that no cystein was oxidized previously. (E-H) C112S mutant containing a His_6-tag was treated in absence (E) or in presence (F) of compound **3** using the same procedure as described above. Subsequent addition of an excess of maleimid resulted in a shift of +485 (corresponding to a 5-fold addition of the labeling agent regardless of the presence of compound **3** (G: PqsD; H: PqsD pretreated with compound **3**). In all spectra, signals with a shift of +178 Da were observed. This is probably due to spontaneous *α-N*-6-Phosphogluconoylation of the His_6-tag in *E. coli* (S4).

6.2.8 Maldi-TOF Analysis

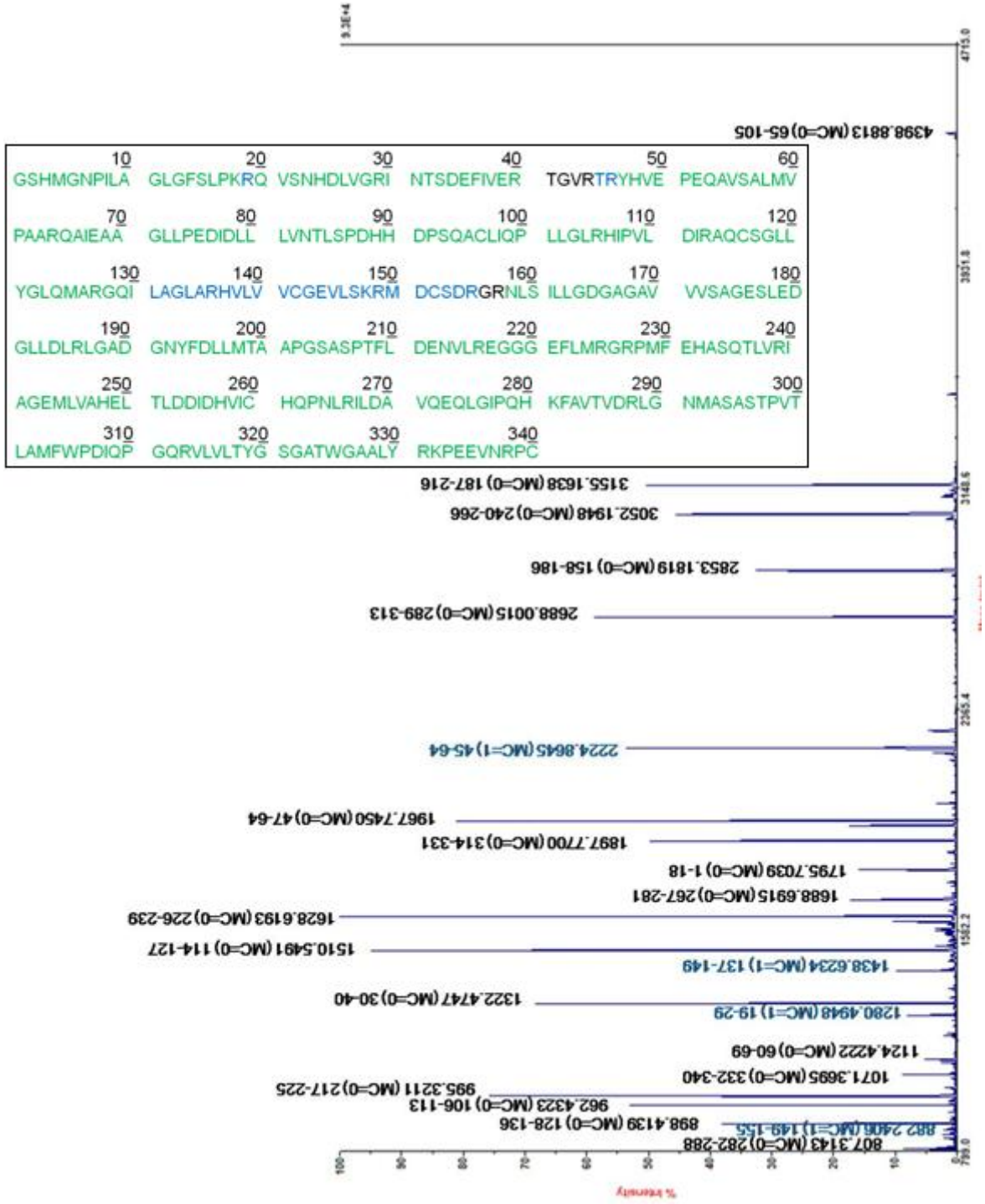

Figure S3. Maldi-TOF spectra of native PqsD after tryptic digestion. Blue labeled fragments bear one missed cleavage (MC). Fragments generated by complete digestion (MC=0) were labeled in black.

Figure S4. Sequence of the PqsD. 334 of 340 amino acids are visible in at least one peptide observed by Maldi-TOF, when native PqsD has been digested. Amino acids not observed in the experiment are Thr41, Gly42, Val43, Arg44, Gly156 and Arg157. (Numbering refers to the sequence of PqsD used in the experiment; in the X-ray structure denoted as Thr37, Gly38, Val39, Arg40, Gly152, Arg153 (A. K. Bera et al. *Biochemistry* **2009**, *48*, 8644).

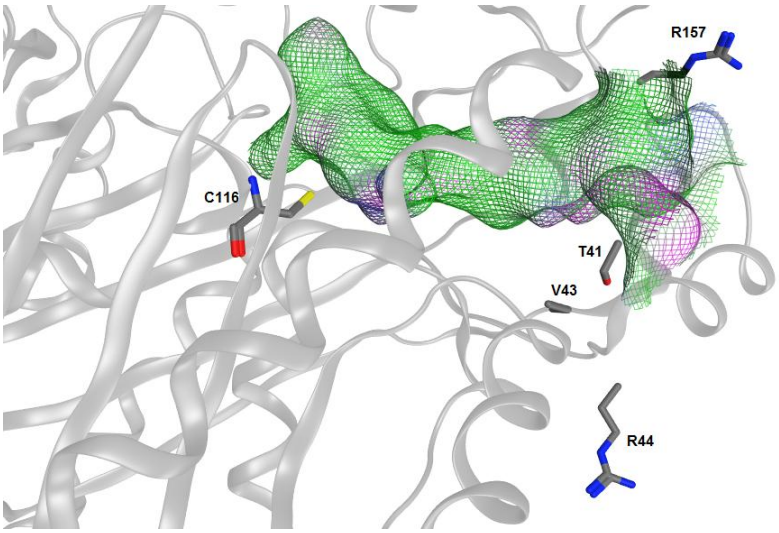

Figure S5. Molecular surface of the PqsD binding channel and side chains of the uncaptured amino acids Thr41, Gly42, Val43, Arg44, Gly156 and Arg157. The alkyl residues of Gly42, Val43 and Gly156 are unable to form covalent bonds. Thr41, Arg44 and Arg157 are located at the tunnel entrance, too far away from the binding site of compound **3**, which is located deep in the active site near the catalytically active Cys116 (in the construct used for X-ray analysis denoted as Cys112).

Table S4. Comparison of peptide masses (calculated and observed by Maldi-TOF analysis) formed by tryptic digestion of untreated PqsD and PqsD treated with compound **3**.

m/z (PqsD) calculated	*m/z* (PqsD) measured	*m/z* (PqsD+ cmpd. 3) measured	Position (Number of missed cleaves)	peptide sequence
4399.3329	4398.8813	4398.8477	65–105 (*MC*=0)	QAIEAAGLLPEDIDLLLVNTLSPDH HDPSQACLIQPLLGLR
3155.5353	3155.1638	3155.1670	187–216 (*MC*=0)	LGADGNYFDLLMTAAPGSASPTF LDENVLR
3052.5342	3052.1948	3052.1858	240–216 (MC=0)	IAGEMLVAHELTLDDIDHVI**CH**QP NLR
2853.5203	2853.1819	2853.1846	158–186 (*MC*=0)	NLSILLGDGAGAVVVSAGESLED GLLDLR
2688.3272	2688.0015	2687.9995	289–313 (*MC*=0)	LGNMASASTPVTLAMFWPDIQPG QR
2225.1495	2224.8645	2224.8713	45–64 (*MC*=1)	TRYHVEPEQAVSALMVPAAR
1968.0007	1967.7450	1967.7517	47–64 (*MC*=0)	YHVEPEQAVSALMVPAAR
1898.0170	1897.7700	1897.7756	314–331 (*MC*=0)	VLVLTYGSGATWGAALYR
1795.9523	1795.7039	1795.7120	1–18 (*MC*=0)	GSHMGNPILAGLGFSLPK
1688.9329	1688.6915	1688.6960	267–281 (*MC*=0)	ILDAVQEQLGIPQHK
1628.8325	1628.6193	1628.6277	226–239 (*MC*=0)	GRPMFEHASQTLVR
1510.7505	1510.5491	1510.5503	114–127 (*MC*=0)	AQCSGLLYGLQMAR

1438.8198	1438.6234	1438.6323	137–149 (*MC*=1)	HVLVVCGEVLSK
1322.6586	1322.4747	1322.4774	30–40 (*MC*=0)	INTSDEFIVER
1282.7187	-	-	137–148 (*MC*=0)	HVLVVCGEVLSK
1280.6818	1280.4948	1280.5020	19–29 (*MC*=1)	RQVSNHDLVGR
1124.5807	1124.4222	1124.4231	60–69 (*MC*=0)	QVSNHDLVGR
1071.5251	1071.3695	-	332–340 (*MC*=0)	KPEEVNRPC
995.4615	995.3211	995.3254	217–225 (*MC*=0)	EGGGEFLMR
962.5781	962.4323	962.4278	106–113 (*MC*=0)	HIPVLDIR
898.5468	898.4139	898.4203	128–136 (*MC*=0)	GQILAGLAR
882.3556	882.2406	882.2174	149–155 (*MC*=1)	RMDCSDR
807.4359	807.3143	807.3203	282–288 (*MC*=0)	FAVTVDR

All fragments without missed cleavages (*MC*=0) with *m*/*z* >800 are listed. Fragments with *MC*=1 contributing to coverage of the amino acid sequence were added.

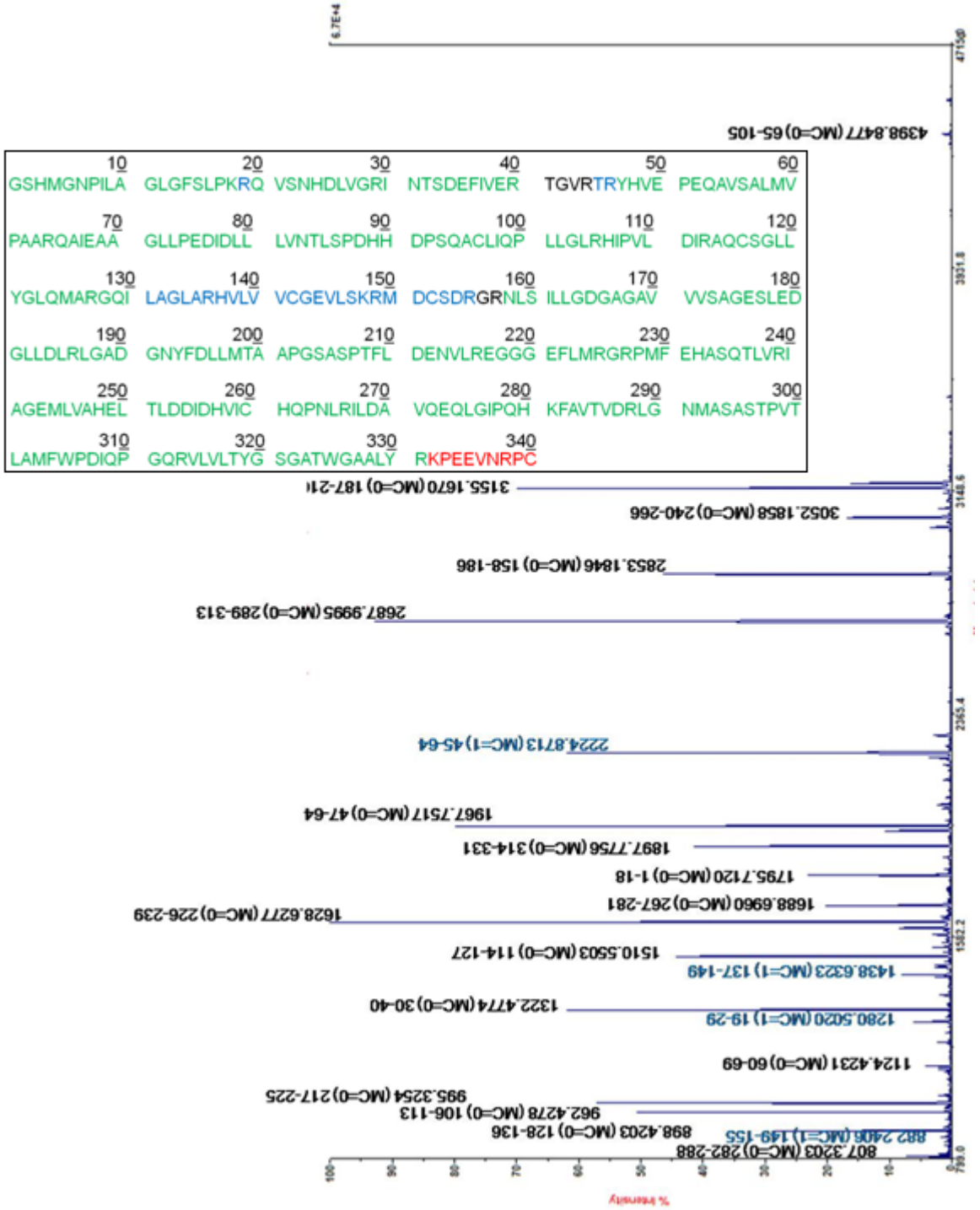

Figure S6. Maldi-TOF spectra of PqsD/compound **3** after tryptic digestion. Blue labeled fragments bear one missed cleavage (MC). Fragments generated by complete digestion (MC=0) were labeled in black. Compared to untreated PqsD the only difference is the disappearance of the peptide *m*/*z* of 1071.

Figure S7. Amino acids observed after preincubation of PqsD with compound **3**. Compared to untreated PqsD the red labeled peptide at the *C*-terminus disappeared, maybe because of an oxidation of the terminal Cys340.

6.2.9 Separation of 3 into the Enantiomers (*R*)-3 and (*S*)-3 by Chiral-HPLC

The separation was performed using an Agilent 1200 HPLC system equipped with an MWD triggering an automated fraction collector (Agilent Technologies) in "time based" mode. ChemStation® software was used for control and report. The sample was manually injected. A Chiralpak IE® 5µm (250 / 10 mm) column (DAICEL Corporation) was used as stationary phase. The solvent system consisted of *n*-hexane (A) and *iso*-propanol (B). HPLC-Method: Flow rate 2.4 ml min^{-1}. Isocratic run of 7% of B in A (*v*/*v*).

Determination of enantiomeric excess was performed using a Chiralpak IE® 5µm (250 / 4.6 mm) column (DAICEL Corporation) as stationary phase. The solvent system consisted of *n*-heptane (A) and *iso*-propanol (B). HPLC-Method: Flow rate 1 ml min^{-1}. Isocratic run of 7% of B in A (*v*/*v*). The % ee of (*R*)-**9** and (*S*)-**9** was determined using the relative peak areas in the MWD trace.

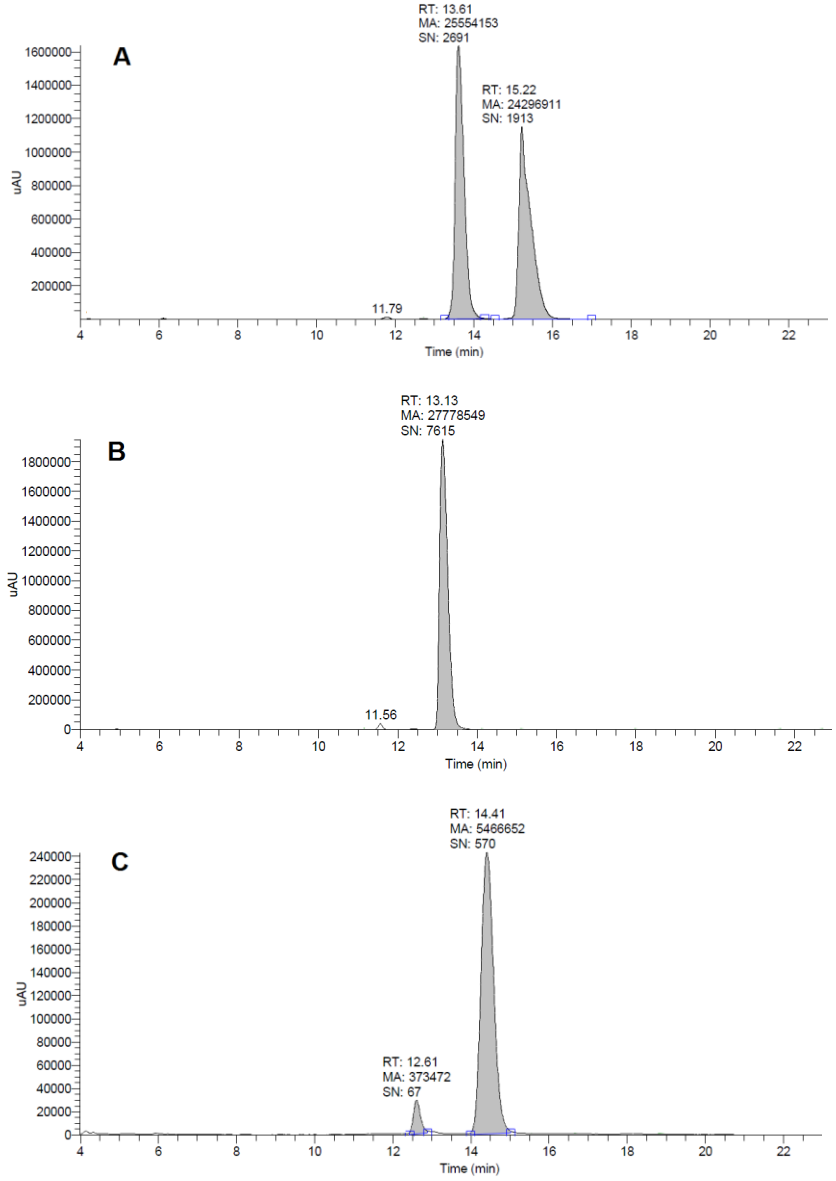

Figure S8. HPLC analysis of enantiomeric purity. (A) Racemic mixture **9**, (B) *S*-enantiomer (–) of **9** (>99.9% ee) and (C) *R*-enantiomer (+) of **9** (87.2% ee). Absolute configurations were derived from measurement of the optical rotation and comparison to literature.[S6]

6.2.10 Figure S9: Binding Site analysis of (*R*)-3 and (*S*)-3 by SPR

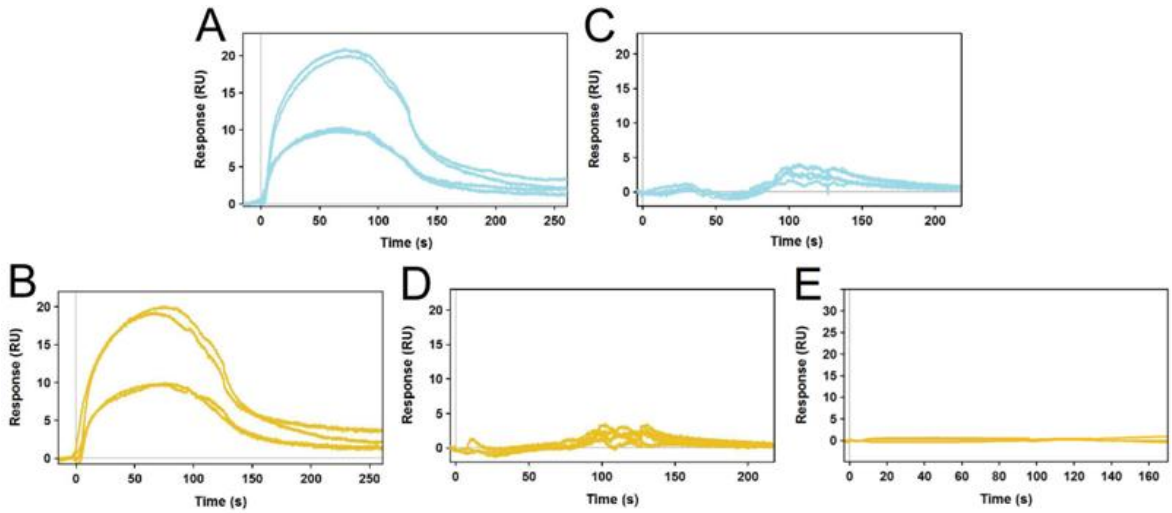

Figure S9. Binding site analysis of (*R*)-**3** and (*S*)-**3** by SPR. Addition of 250 and 125 µM (*R*)-**3** (blue) or (*S*)-**3** (orange), respectively, to native PqsD resulted in response curves (A) and (B). When added to PqsD pretreated with ACoA, no response was observed in (C) and (D). When (*R*)-**3** was added until saturation, subsequent addition of (*S*)-**3** did not affect the observed response (E). The results indicate that the binding sites of both enantiomers are blocked by anthranilate.

6.2.11 Figure S10: Reversibility of PqsD Inhibition by the Enantiomers (*R*)-3 and (*S*)-3

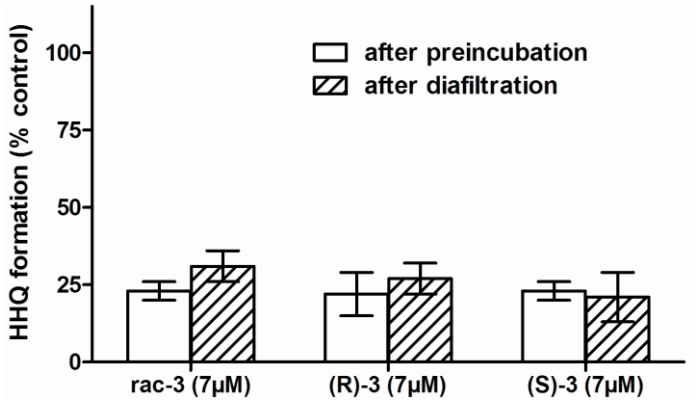

Figure S10. PqsD was preincubated with enantiomers (*R*)-**3** and (*S*)-**3** and the remaining HHQ formation was quantified with and without removal of unbound inhibitor by diafiltration. Centrifugal filter devices with a molecular weight limit of 10k were used to remove at least 95% inhibitor by three diafiltration steps as controlled by HPLC analysis, while PqsD was retained.

6.2.12 Representative ITC Curves

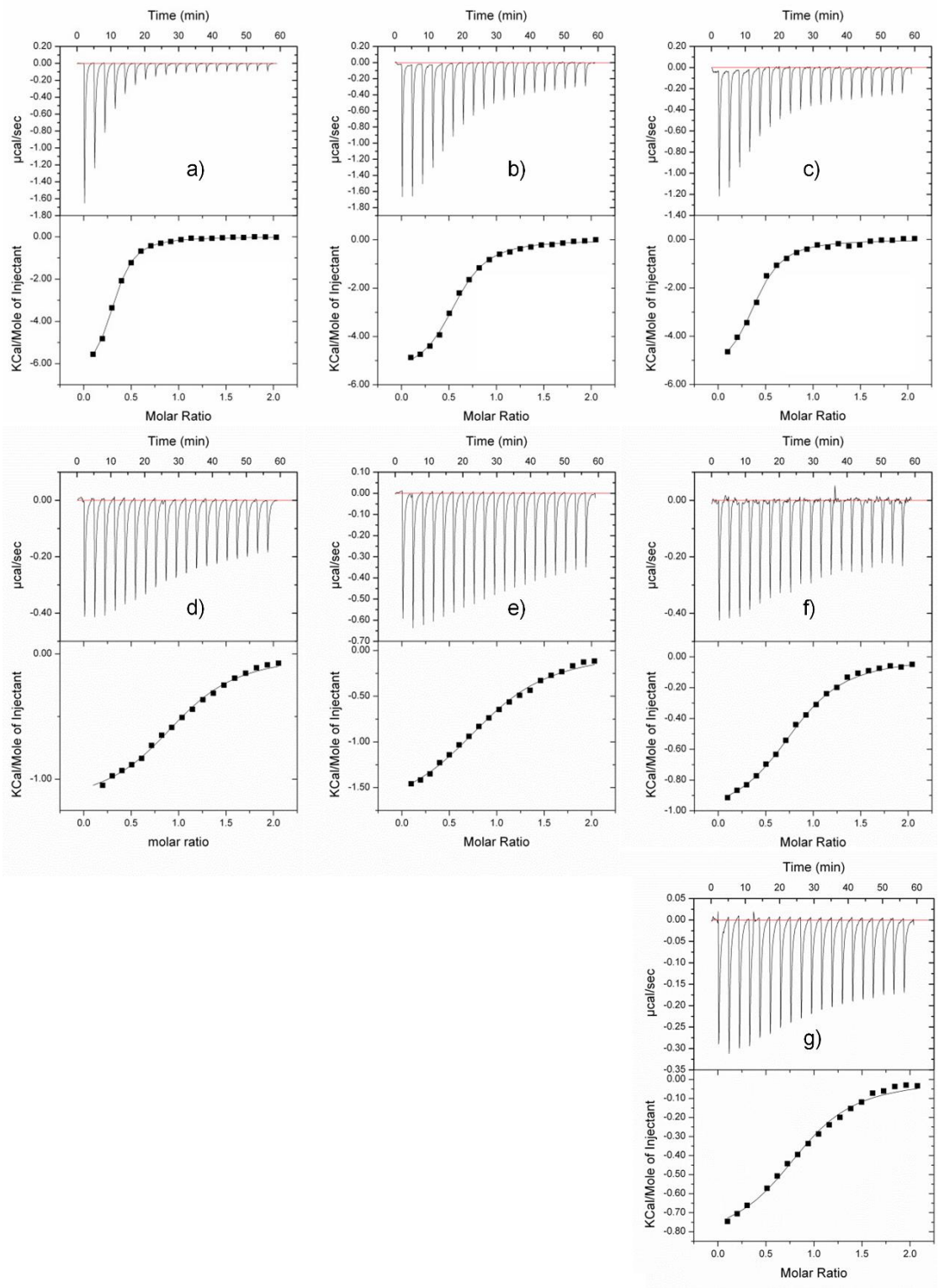

Figure S11. Representative ITC titrations of *R*-enantiomer against PqsD wild-type and mutants. 3500 µM of compound against: a) PqsD wild-type (347µM), b) S317A (351µM), c) N287A (347µM), d) C112A (350µM), e) C112S (354µM), f) H257F (352µM), g) S317F (345µM). The recorded change in heat is shown in units of µcal sec^{-1} as a function of time for successive injections of the ligand (upper panel). Integrated heats (black squares) plotted against the molar ratio of the binding reaction. The continuous line represents the results of the non-linear least squares fitting of the data to a binding model (lower panel).

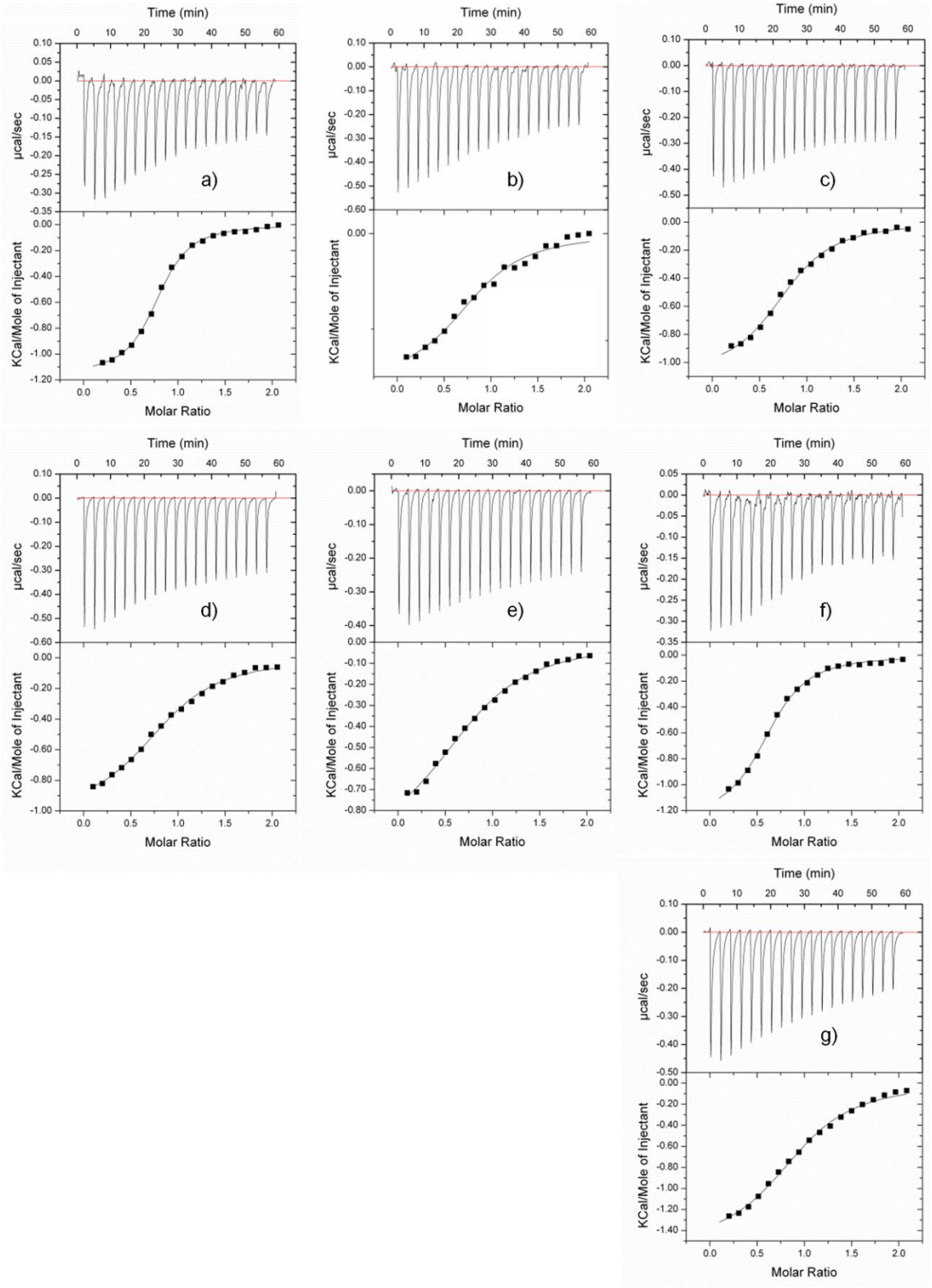

Figure S12. Representative ITC titrations of *S*-enantiomer against PqsD wild-type and mutants. 3500 µM of compound against: a) PqsD wild-type (347µM), b) S317A (351µM), c) N287A (347µM), d) C112A (350µM), e) C112S (354µM), f) H257F (352µM), g) S317F (345µM). The recorded change in heat is shown in units of µcal sec^{-1} as a function of time for successive injections of the ligand (upper panel). Integrated heats (black squares) plotted against the molar ratio of the binding reaction. The continuous line represents the results of the non-linear least squares fitting of the data to a binding model (lower panel).

6.2.13 References

(S1) E. J. Simon, D. Shemin; The preparation of *S*-succinyl coenzyme A. *J. Am. Chem. Soc.* **1953**, *75*, 2520.

(S2) L. Cook, B. Ternai, P. Ghosh; Inhibition of human sputum elastase by substituted 2-pyrone. *J. Med. Chem.* **1987**, *30*, 1017.

(S3) V. T. H. Nguyen, E. Bellur, B. Appel, P. Langer; Synthesis of 4-alkyl- and 4-(ω-chloroalkyl)-3-hydroxy-5-alkylidenebutenolides based on cyclizations of 4-alkyl- and 4-(ω-chloroalkyl)-1,3-bis(trimethylsilyloxy)buta-1,3-dienes with oxalyl chloride. *Synthesis* **2006**, *17*, 2865.

(S4) K. F. Geoghegan, H. B. F. Dixon, P. J. Rosner, L. R: Hoth, A. J. Lanzetti, K. A. Borzilleri, E. S. Marr, L. H. Pezzullo, L. B. Martin, P. K. LeMotte, A. S. McColl, A. V. Kamath, J. G. Stroh; Spontaneous *α-N*-6-phosphogluconoylation of a "His tag in *Escherichia coli*: The cause of extra mass of 258 or 178 Da in fusion proteins. *Analytical Biochemistry* **1999**, *267*, 169.

(S5) A. K. Bera, V. Atanasova, H. Robinson, E. Eisenstein, J. P. Coleman, E. C. Pesci; Structure of PqsD, a *Pseudomonas* quinolone signal biosynthetic enzyme, in complex with anthranilate. *Biochemistry* **2009**, *48*, 8644.

(S6) H.-F. Duan, J.-H. Xie, W.-H. Shi, Q. Zhang, Q.-L. Zhou; Enantioselective rhodium-catalyzed addition of arylboronic acids to aldehydes using chiral spiro monophosphite ligands. *Organic Letters* **2006**, *8*, 1479.

6.3 Supporting Information for Publication C

Full supporting information is available online:

http://pubs.acs.org/doi/suppl/10.1021/jm401102e/suppl_file/jm401102e_si_001.pdf

6.3.1 Chemistry

Methyl 3-amino-5-(4'-methoxyphenyl)thiophene-2-carboxylate (**IIa**). The title compound was prepared from 4'-methoxyacetophenone according to general procedure **A** and used directly in the next step without further purification. ^{1}H NMR (500 MHz, DMSO-d_6) δ 7.56 (d, J = 8.8 Hz, 2H), 7.00 (d, J = 8.8 Hz, 2H), 6.86 (s, 1H), 6.56 (s, 2H), 3.79 (s, 3H), 3.72 (s, 3H). ^{13}C NMR (125 MHz, DMSO-d_6) δ 163.9, 160.0, 155.7, 147.7, 127.0, 125.3, 114.9, 114.6, 95.7, 55.3, 50.8.

Methyl 3-amino-5-(4'-phenoxyphenyl)thiophene-2-carboxylate (**IIb**). The title compound was prepared from 4'-phenoxyacetophenone according to general procedure **A** and used directly in the next step without further purification. ^{1}H NMR (500 MHz, DMSO-d_6) δ 7.64 (d, J = 8.8 Hz, 2H), 7.46−7.40 (m, 2H), 7.22−7.17 (m, 1H), 7.11−7.06 (m, 2H), 7.04 (d, J = 8.8 Hz, 2H), 6.91 (s, 1H), 6.59 (s, 2H), 3.72 (s, 3H). ^{13}C NMR (125 MHz, DMSO-d_6) δ 163.9, 157.7, 155.9, 147.0, 130.2, 127.8, 127.4, 124.1, 119.3, 118.7, 115.7, 96.2, 50.9.

Methyl 3-amino-5-(4'-bromophenyl)thiophene-2-carboxylate (**IIc**). The title compound was prepared from 4'-bromoacetophenone according to general procedure **A**. ^{1}H NMR (300 MHz, $CDCl_3$) δ 7.51 (d, J = 8.0 Hz, 2H), 7.43 (d, J = 8.0 Hz, 2H), 6.75 (s, 1H), 5.49 (s, 2H), 3.85 (s, 3H). ^{13}C NMR (75 MHz, $CDCl_3$) δ 164.8, 154.2, 147.6, 132.3, 132.1, 127.3, 123.0, 115.8, 100.7, 51.3.

3-Amino-5-(4'-methoxyphenyl)thiophene-2-carboxylic acid (**IIIa**). The title compound was prepared from **IIa** according to general procedure **B**. ^{1}H NMR (300 MHz, DMSO-d_6) δ 7.55 (d, J = 8.8 Hz, 2H), 6.99 (d, J = 8.8 Hz, 2H), 6.84 (s, 1H), 3.79 (s, 3H). ^{13}C NMR (75 MHz, DMSO-d_6) δ 165.3, 159.9, 155.3, 147.0, 127.0, 125.6, 115.0, 114.6, 97.1, 55.3.

3-Amino-5-(4'-phenoxyphenyl)thiophene-2-carboxylate (**IIIb**). The title compound was prepared from **IIb** according to general procedure **B**. ^{1}H NMR (500 MHz, DMSO-d_6) δ 7.63 (d, J = 8.8 Hz, 2H), 7.47−7.38 (m, 2H), 7.23−7.16 (m, 1H), 7.08 (d, J = 8.8 Hz, 2H), 7.06−6.99 (m, 2H), 6.90 (s, 1H). ^{13}C NMR (125 MHz, DMSO-d_6) δ 165.2, 157.5, 155.9, 146.3, 130.2, 128.1, 127.3, 124.0, 119.2, 118.7, 115.8, 97.7.

3-Amino-5-(4'-bromophenyl)thiophene-2-carboxylic acid (**IIIc**). The title compound was prepared from **IIc** according to general procedure **B**. ^{1}H NMR (500 MHz, DMSO-d_6) δ 7.63 (d, J = 8.8 Hz, 2H), 7.57 (d, J = 8.8 Hz, 2H), 6.98 (s, 1H). ^{13}C NMR (125 MHz, DMSO-d_6) δ 165.2, 155.1, 145.3, 132.2, 132.1, 127.5, 122.0, 116.8, 98.5.

6-(4'-Methoxyphenyl)-2,4-dihydro-1*H*-thieno[3,2-d][1,3]oxazine-2,4-dione (**IVa**). The title compound was prepared from **IIIa** according to general procedure **C**. ^{1}H NMR (300 MHz, DMSO-d_6) δ 12.28 (s, 1H), 7.74 (d, J = 8.9 Hz, 2H), 7.12 (s, 1H), 7.04 (d, J = 8.9 Hz, 2H), 3.82 (s, 3H). ^{13}C NMR (75 MHz, DMSO-d_6) δ 161.1, 155.5, 155.0, 149.6, 148.6, 127.9, 124.1, 114.8, 111.2, 103.1, 55.4.

6-(4'-Phenoxyphenyl)-2,4-dihydro-1*H*-thieno[3,2-d][1,3]oxazine-2,4-dione (**IVb**). The title compound was prepared from **IIIb** according to general procedure **C**. ^{1}H NMR (500 MHz, DMSO-d_6) δ 12.33 (s, 1H), 7.83 (d, J = 8.8 Hz, 2H), 7.48−7.43 (m, 2H), 7.23 (t, J = 7.4 Hz, 1H), 7.18 (s, 1H), 7.13−7.10 (m, 2H), 7.08 (d, J = 8.8 Hz, 2H). ^{13}C NMR (125 MHz, DMSO-d_6) δ 158.9, 155.4, 155.0, 154.8, 149.6, 148.5, 130.3, 128.4, 126.4, 124.4, 119.6, 118.6, 112.1, 103.8.

6-(4'-Bromophenyl)-2,4-dihydro-1*H*-thieno[3,2-d][1,3]oxazine-2,4-dione (**IVc**). The title compound was prepared from **IIIc** according to general procedure **C**. ^{1}H NMR (500 MHz, DMSO-d_6) δ 12.39 (s, 1H), 7.77 (d, J = 8.8 Hz, 2H), 7.70 (d, J = 8.8 Hz, 2H), 7.29 (s, 1H). ^{13}C NMR (125 MHz, DMSO-d_6) δ 155.1, 153.5, 149.7, 148.6, 132.4, 130.8, 128.3, 123.8, 113.4, 104.7.

3-(3''-Benzyl-3''-ethylureido)-5-(4'-methoxyphenyl)thiophene-2-carboxylic acid (**1**). The title compound was prepared from **IVa** according to general procedure **D**. ^{1}H NMR (300 MHz, DMSO-d_6) δ 13.21 (s, 1H), 10.10 (s, 1H), 8.17 (s, 1H), 7.63 (d, J = 8.9 Hz, 2H), 7.38–7.29 (m, 5H), 7.02 (d, J = 8.9 Hz, 2H), 3.80 (s, 3 H), 3.39 (q, J = 7.1 Hz, 2H), 1.16 (t, J = 7.1 Hz, 3H). ^{13}C NMR (75 MHz, DMSO-d_6) δ 165.8, 160.2, 153.1, 147.9, 147.0, 138.1, 128.5, 127.2, 127.1, 127.1, 125.3, 116.1, 114.7, 105.6, 55.3, 49.3, 41.8, 13.1.

5-(4'-Methoxyphenyl)-3-ureidothiophene-2-carboxylic acid (**2**). The title compound was prepared from **IVa** according to general procedure **D**. ^{1}H NMR (300 MHz, DMSO-d_6) δ 12.92 (s, 1H), 9.30 (s, 1H), 8.15 (s, 1H), 7.60 (d, J = 8.8 Hz, 2H), 7.01 (d, J = 8.8 Hz, 2H), 6.81 (s, 2H), 3.76 (s, 3H). ^{13}C NMR (75 MHz, DMSO-d_6) δ 164.8, 160.0, 154.7, 147.1, 146.6, 127.1, 125.4, 116.7, 114.7, 105.4, 55.3.

5-(4'-Phenoxyphenyl)-3-ureidothiophene-2-carboxylic acid (**3**). The title compound was prepared from **IVb** according to general procedure **D**. ^{1}H NMR (300 MHz, DMSO-d_6) δ 12.99 (s, 1H), 9.30 (s, 1H), 8.21 (s, 1H), 7.68 (d, J = 8.8 Hz, 2H), 7.49−7.38 (m, 2H), 7.25−7.14 (m, 1H), 7.13−7.02 (m, 4H), 6.90−6.60 (m, 2H). ^{13}C NMR (75 MHz, DMSO-d_6) δ 164.7, 157.7, 155.9, 154.6, 146.5, 146.4, 130.2, 127.9, 127.5, 124.1, 119.3, 118.8, 117.5, 106.1.

3-(3''-(Carboxymethyl)ureido)-5-(4'-methoxyphenyl)thiophene-2-carboxylic acid (**4**). The title compound was prepared from **IVa** according to general procedure **D**. ^{1}H NMR (300 MHz, DMSO-d_6) δ 12.79 (s, 2H, COOH), 9.47 (s, 1H), 8.13 (s, 1H), 8.08 (t, J = 5.6 Hz, 1H), 7.61 (d, J = 8.8 Hz, 2H), 7.01 (d, J = 8.8 Hz, 2H), 3.83−3.77 (m, 2H) 3.80 (s, 3H, OCH_3). ^{13}C NMR (75 MHz, DMSO-d_6) δ 171.9, 164.7, 160.1, 154.1, 147.2, 146.1, 127.1, 125.4, 116.7, 114.7, 105.7, 55.3, 41.3.

3-(3''-(2-Carboxyethyl)ureido)-5-(4'-methoxyphenyl)thiophene-2-carboxylic acid (**5**). The title compound was prepared from **IVa** according to general procedure **D**. ^{1}H NMR (300 MHz, DMSO-d_6) δ 12.58 (s, 2H, COOH), 9.34 (s, 1H), 8.16 (s, 1H), 7.90− 7.72 (m, 1H), 7.60 (d, J = 8.4 Hz, 2H), 7.01 (d, J = 8.4 Hz, 2H), 3.80 (s, 3H, OCH_3), 3.33−3.24 (m, 2H), 2.44 (t, J = 6.2 Hz, 2H). ^{13}C NMR (75 MHz, DMSO-d_6) δ 173.0, 164.7, 160.1, 153.8, 147.1, 146.3, 127.1, 125.4, 116.7, 114.7, 105.4, 55.3, 35.6, 34.3.

(*S*)-3-(3''-(1-Carboxyethyl)ureido)-5-(4'-methoxyphenyl)thiophene-2-carboxylic acid (**6**). The title compound was prepared from **IVa** according to general procedure **D**. ^{1}H NMR (300 MHz, DMSO-d_6) δ 12.76 (s, 2H, COOH), 9.43 (s, 1H), 8.14 (s, 1H), 8.09 (d, J = 7.1 Hz, 1H), 7.61 (d, J = 8.8 Hz, 2H), 7.03 (d, J = 8.8 Hz, 2H), 4.22−4.08 (m, 1H), 3.81 (s, 3H, OCH_3), 1.32 (d, J = 7.30 Hz, 3H, CH_3). ^{13}C NMR (75 MHz, DMSO-d_6) δ 174.7, 164.7, 160.1, 153.5, 147.2, 146.1, 127.1, 125.4, 116.6, 114.7, 105.6, 55.3, 48.3, 17.4.

(*S*)-3-(3”-(1-Carboxy-2-phenylethyl)ureido)-5-(4’-methoxyphenyl)thiophene-2-carboxylic acid (**7**). The title compound was prepared from **IVa** according to general procedure **D**. ^{1}H NMR (300 MHz, DMSO-d_6) δ 12.84 (s, 2H, COOH), 9.42 (s, 1H), 8.15 (d, J = 7.9 Hz, 1H), 8.09 (s, 1H), 7.69−7.51 (m, J = 8.8 Hz, 2H), 7.37−7.25 (m, 4H), 7.25−7.17 (m, 1H), 7.03−6.97 (m, J = 8.8 Hz, 2H), 4.56−4.28 (m, 1H), 3.79 (s, 3H, OCH_3), 3.11 (dd, J = 13.9, 4.6 Hz, 1H), 2.88 (dd, J = 13.9, 9.8 Hz, 1H). ^{13}C NMR (75 MHz, DMSO-d_6) δ 173.6, 164.6, 160.1, 153.7, 147.1, 145.9, 137.7, 129.0, 128.2, 127.1, 126.4, 125.4, 116.7, 114.7, 105.8, 55.3, 54.4, 36.9.

5-(4’-Methoxyphenyl)-3-(3”-phenethylureido)thiophene-2-carboxylic acid (**8**). The title compound was prepared from **IVa** according to general procedure **D**. ^{1}H NMR (300 MHz, DMSO-d_6) δ 12.96 (s, 1H, CCOH), 9.33 (s, 1H), 8.18 (s, 1H), 7.84−7.70 (m, 1H), 7.61 (d, J = 8.3 Hz, 2H), 7.39−7.13 (m, 5H), 7.02 (d, J = 8.3 Hz, 2H), 3.80 (s, 3H, OCH_3), 3.42−3.26 (m, 2H), 2.90−2.67 (m, 2H). ^{13}C NMR (75 MHz, DMSO-d_6) δ 164.8, 160.0, 153.8, 147.2, 146.5, 139.5, 128.6, 128.3, 127.1, 126.1, 125.4, 116.7, 114.7, 105.2, 55.3, 41.0, 35.5.

(*R*)-3-(3”-(1-Carboxyethyl)ureido)-5-(4’-methoxyphenyl)thiophene-2-carboxylic acid (**9**). The title compound was prepared from **IVa** according to general procedure **D**. ^{1}H NMR (300 MHz, DMSO-d_6) δ 12.76 (s, 2H, CCO), 9.43 (s, 1H), 8.14 (s, 1H), 8.09 (d, J = 7.1 Hz, 1H), 7.61 (d, J = 8.9 Hz, 2H), 7.01 (d, J = 8.9 Hz, 2H), 4.22−4.08 (m, 1H), 3.80 (s, 3H, OCH_3), 1.31 (d, J = 7.4 Hz, 3H, CH_3). ^{13}C NMR (75 MHz, DMSO-d_6) δ 174.7, 164.7, 160.1, 153.5, 147.2, 146.1, 127.1, 125.4, 116.6, 114.7, 105.6, 55.3, 48.3, 17.4.

(*R*)-3-(3”-(1-Carboxy-2-phenylethyl)ureido)-5-(4’-methoxyphenyl)thiophene-2-carboxylic acid (**10**). The title compound was prepared from **IVa** according to general procedure **D**. ^{1}H NMR (300 MHz, DMSO-d_6) δ 12.84 (s, 2H, CCOH), 9.42 (s, 1H), 8.15 (d, J = 7.9 Hz, 1H), 8.09 (s, 1H), 7.59 (d, J = 8.8 Hz, 2H), 7.37−7.25 (m, 4H), 7.25−7.17 (m, 1H), 7.00 (d, J = 8.8 Hz, 2H), 4.56−4.28 (m, 1H), 3.79 (s, 3H, OCH_3), 3.11 (dd, J = 13.9, 4.6 Hz, 1H), 2.88 (dd, J = 13.9, 9.8 Hz, 1H). ^{13}C NMR (75 MHz, DMSO-d_6) δ 173.6, 164.6, 160.1, 153.7, 147.1, 145.9, 137.7, 129.0, 128.2, 127.1, 126.4, 125.4, 116.7, 114.7, 105.8, 55.3, 54.4, 36.9.

3-(3”-(2-Carboxypropan-2-yl)ureido)-5-(4’-methoxyphenyl)thiophene-2-carboxylic acid (**11**). The title compound was prepared from **IVa** according to general procedure **D**. ^{1}H NMR (300 MHz, DMSO-d_6) δ 12.59 (s, 2H, CCOH), 9.37 (s, 1H), 8.13 (s, 1H), 8.01 (s, 1H), 7.61 (d, J = 8.8 Hz, 2H), 7.00 (d, J = 8.8 Hz, 2H), 3.80 (s, 3H, OCH_3), 1.40 (s, 6H, $(CH_3)_2$). ^{13}C NMR (75 MHz, DMSO-d_6) δ 176.0, 164.7, 160.0, 153.0, 147.2, 146.1, 127.1, 125.4, 116.5, 114.7, 105.4, 55.3, 54.9, 25.3.

Scheme S2: Synthesis of compound 12.

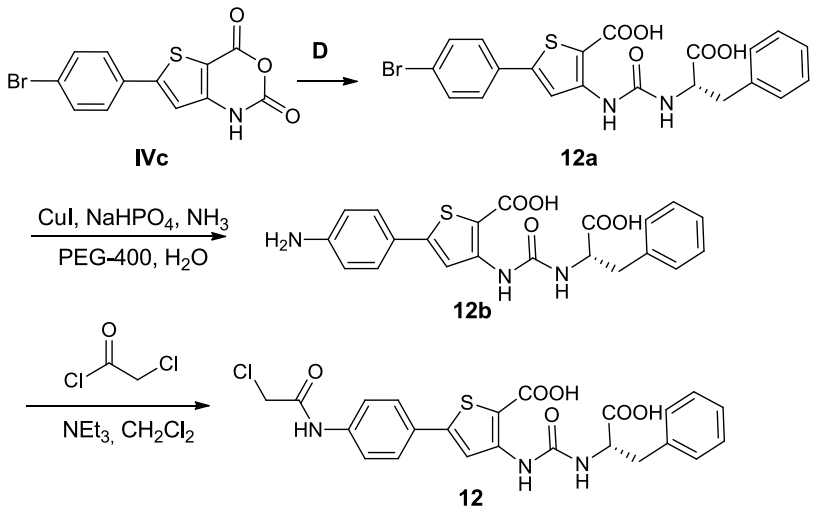

(*S*)-3-(3”-(1-Carboxy-2-phenylethyl)ureido)-5-(4’-bromophenyl)thiophene-2-carboxylic acid (**12a**) was prepared from **IVc** according to general procedure **D**. ^{1}H NMR (300 MHz, DMSO-d_6) δ 12.93 (s, 2H, CCOH), 9.42 (s, 1H), 8.23 (s, 1H), 8.17 (d, J = 7.9 Hz, 1H), 7.70−7.54 (m, 4H), 7.38−7.14 (m, 5H), 4.47−4.30 (m, 1H), 3.11 (dd, J = 13.9, 4.8 Hz, 1H), 2.88 (dd, J = 13.9, 9.7 Hz, 1H). ^{13}C NMR (75 MHz, DMSO-d_6) δ 173.5, 164.5, 153.7, 145.7, 145.4, 137.7, 132.2, 132.0, 129.0, 128.2, 127.6, 126.4, 122.3, 118.5, 107.3, 54.4, 37.0.

(*S*)-3-(3”-(1-Carboxy-2-phenylethyl)ureido)-5-(4’-aminophenyl)thiophene-2-carboxylic acid (**12b**) was prepared from **12a** according to the following procedure: CuI (10 mg, 5.30 µmol), **12a** (127 mg, 0.26 mmol), Na_3PO_4·12 H_2O (100 mg, 0.26 mmol), 25−28% aqueous ammonia (0.5 mL) and PEG-400 (1 mL) were added to a sealed tube. The reaction was stirred at 100 °C for 24 h, cooled to 0 °C and cautiously acidified with 1 M HCl to pH 4−5. The resulting mixture was extracted with EtOAc (3 x 50 mL). The combined organic layers were washed with water (50 mL) and brine (50 mL), dried over $MgSO_4$ and concentrated to afford the title compound. The crude product was used in the next step without further purification.

(*S*)-3-(3”-(1-Carboxy-2-phenylethyl)ureido)-5-(4’-(2-chloroacetamido)phenyl)-thiophene-2-carboxylic acid (**12**) was prepared from **12b** according to the following procedure: A solution of **12b** (142 mg, 1.10 mmol) and triethylamine (142 mg, 1.10 mmol) in CH_2Cl_2 (6 mL) was stirred at −78 °C under stream of nitrogen. 2-Chloroacetyl chloride in CH_2Cl_2 (4 mL) was added slowly and stirring was continued for 1 h at −78 °C, 1 h at 0 °C and 1 h at room temperature. The solution was diluted with ice water (30 mL) and acidified with a saturated solution of $KHSO_4$. The resulting mixture was extracted with EtOAc (3 x 50 mL). The combined organic layers were then washed with water (50 mL) and brine (50 mL), dried over $MgSO_4$ and concentrated *in vacuo*. The crude material was purified via preparative HPLC (RP18, acetonitrile/H_2O 50% → 95%) to yield the title compound as a light green solid (Purity: 90%). ^{1}H NMR (300 MHz, DMSO-d_6) δ 12.89 (s, 2H, CCOH), 10.48 (s, 1H), 9.41 (s, 1H), 8.16 (d, J = 7.8 Hz, 1H), 8.15 (s, 1H), 7.73−7.62 (m, 4H), 7.33−7.20 (m, 5H), 4.43−4.34 (m, 1H), 4.27 (s, 2H, CH_2Cl), 3.14−3.07 (m, 1H), 2.92−2.84 (m, 1H). ^{13}C NMR (125 MHz, DMSO-d_6) δ 173.7, 164.9, 164.7, 153.8, 146.8, 145.9, 139.4, 137.8, 129.1, 128.3, 128.2, 126.5, 126.4, 119.8, 117.3, 106.3, 54.5, 43.6, 36.9.

6.3.2 SPR - studies with R223A mutant of PqsD

Preparation of PqsD mutant:

R223A PqsD mutant was generated using the QuikChange Site-Directed Mutagenesis Kit (Stratagene, La Jolla, CA) according to the manufacturer's instructions using the pET28b(+)/pqsD plasmid as a template. Briefly, pqsD gene was amplified through 16 cycles of PCR. After treatment with DpnI, the PCR product was transformed into *E. coli* strain XL1-Blue. Plasmid DNA was purified using the GenEluteTM HP Plasmid Miniprep Kit (Sigma-Aldrich, St. Louis, MO) and sequenced to confirm the site-directed mutations. The primer sequence of the mutations:

Primer-design:

Arg223Ala-Mutante:

Wild: 5‘ GCGAGTTCCTCATGCGCGGCCGGCCGATGTTCGAGC 3´

Mut: 5‘ GCGAGTTCCTCATGCGCGGCGCGCCGATGTTCGAGC 3´

Sequence of the Primer:

R223A_PqsD_Forward: 5' GCGAGTTCCTCATGCGCGGCGCGCCGATGTTCGAGC 3'

R223A_PqsD_Reverse: 5' GCTCGAACATCGGCGCGCCGCGCATGAGGAACTCGC 3'

6.3.3 Selectivity data for hit compounds: PqsD vs. RNAP inhibition

Table S1. Inhibitory activities of several virtual hit compounds against PqsD and RNAP and the derived selectivity factors.

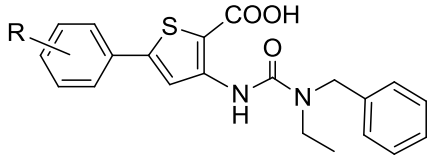

Compound	IC_{50} PqsD [µM]	IC_{50} RNAP [µM]	Selectivity factor[a]
4-OCH_3	6	241	40.2
3,4-di-Cl	4	22	5.5
3-CF_3, 4-Cl	3	21	7.0
2,5-di-Cl	9	35	4.0
4-NO_2	10	73	7.3
4-CF_3	8	51	6.4
4-OCF_3	9	45	5.0
H	50	292	6.0

[a]Selectivity factor was calculated as IC_{50}(RNAP) $IC_{50}(PqsD)^{-1}$.

6.3.4 Results of the competition experiments for identification of the binding mode

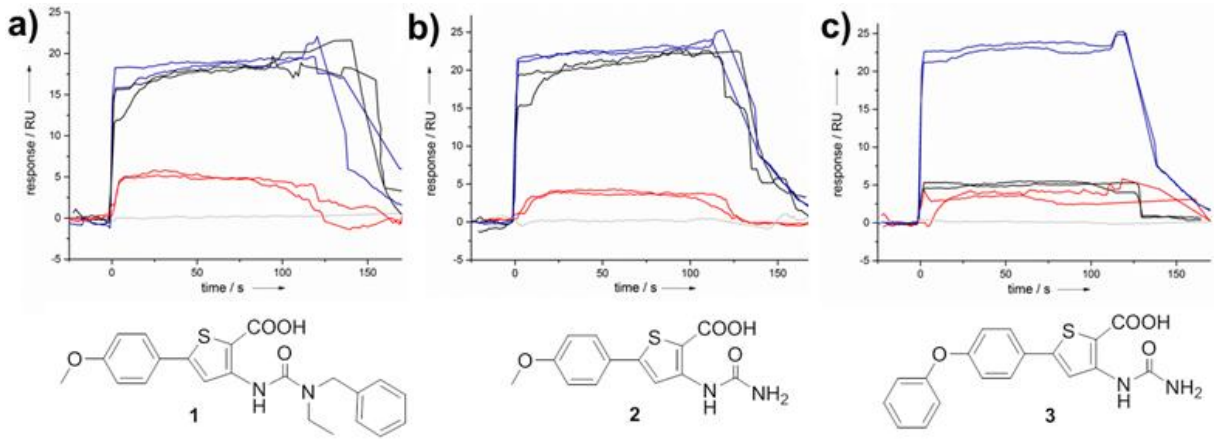

Figure S1. SPR-competition experiments with model compounds **1**–**3** and competitor compounds **A** (black) and **B** (red) from the 2-nitrophenyl methanol class. Reference without competition is shown in blue. A reduced response in competition with **A** can be observed exclusively for compound **3**. The reference signal is shown in grey.

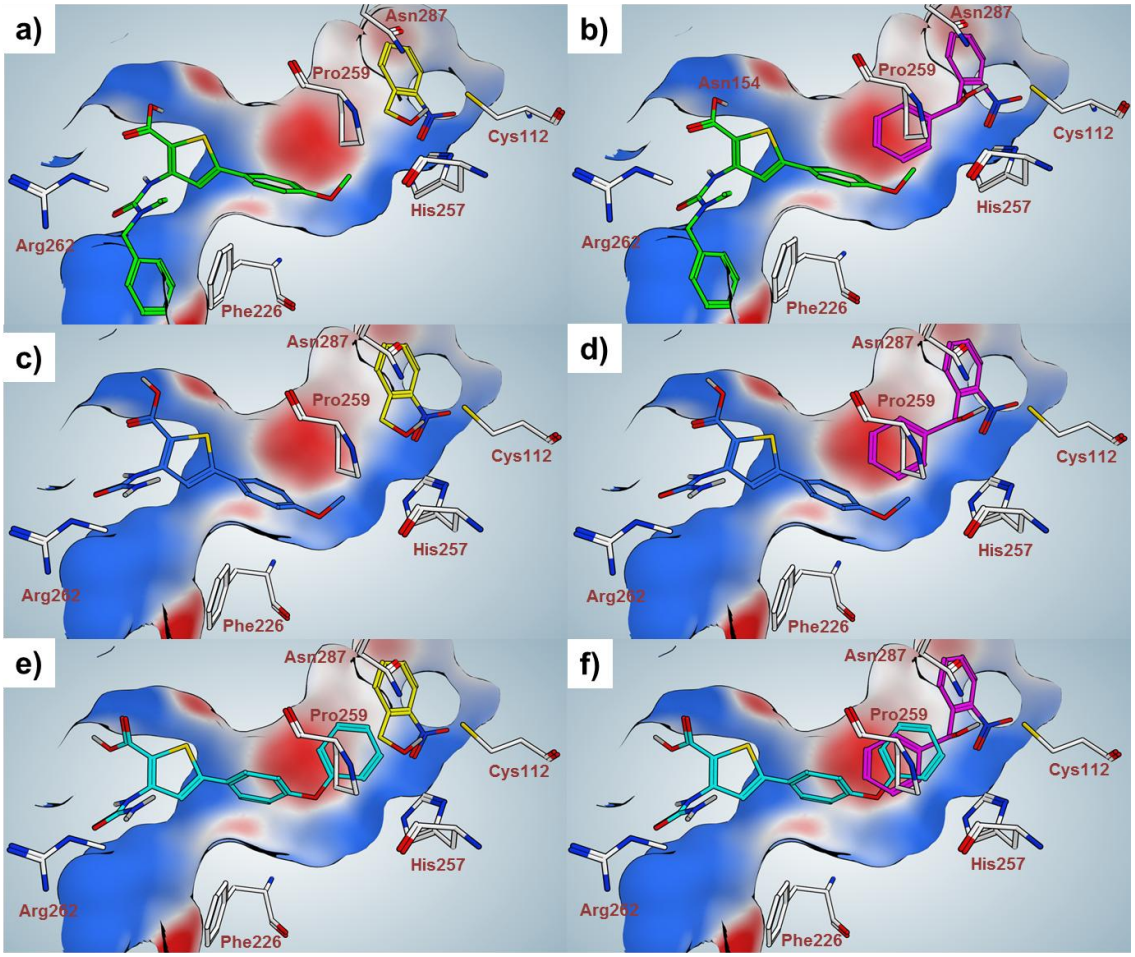

Figure S2. Visualization of the SPR-competition results shown in Figure S1. Competitor **A** (yellow), competitor **B** (magenta) a) **A** does not affect the binding of **1** (green). b) **B** leads to sterical clash with methoxy group of **1** (green). c) **A** does not affect the binding of **2** (blue). d) **B** leads to sterical clash with methoxy group of **2** (blue). e) **A** leads to sterical clash with phenoxy group of **3** (turquoise). f) **B** leads to sterical clash with phenoxy group of **3** (turquoise).

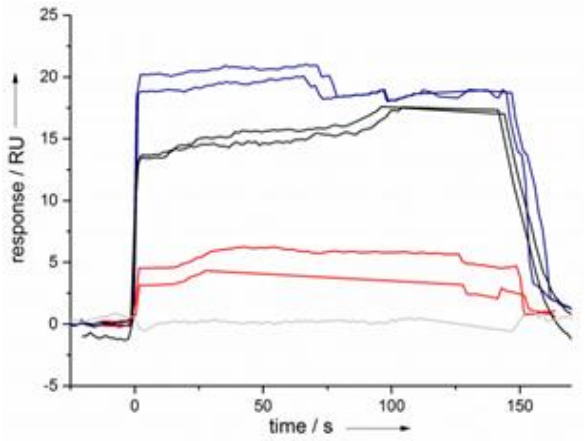

Figure S3. SPR-competition experiments with compounds **7** and competitor compounds **A** (black) and **B** (red) from the 2-nitrophenyl methanol class. Reference without competition is shown in blue. The reference signal is shown in grey.

6.3.5 Experiment with R223A mutant and compound 2

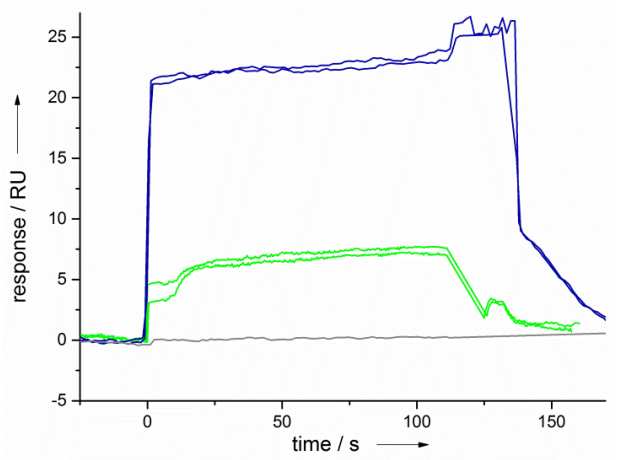

Figure S4. SPR-experiment using a R223A mutant and compound **2**. Different responses were observed when compound **2** was added to PqsD wild-type (blue) and the R223A mutant (green).

6.3.6 STD-NMR spectrum of 7

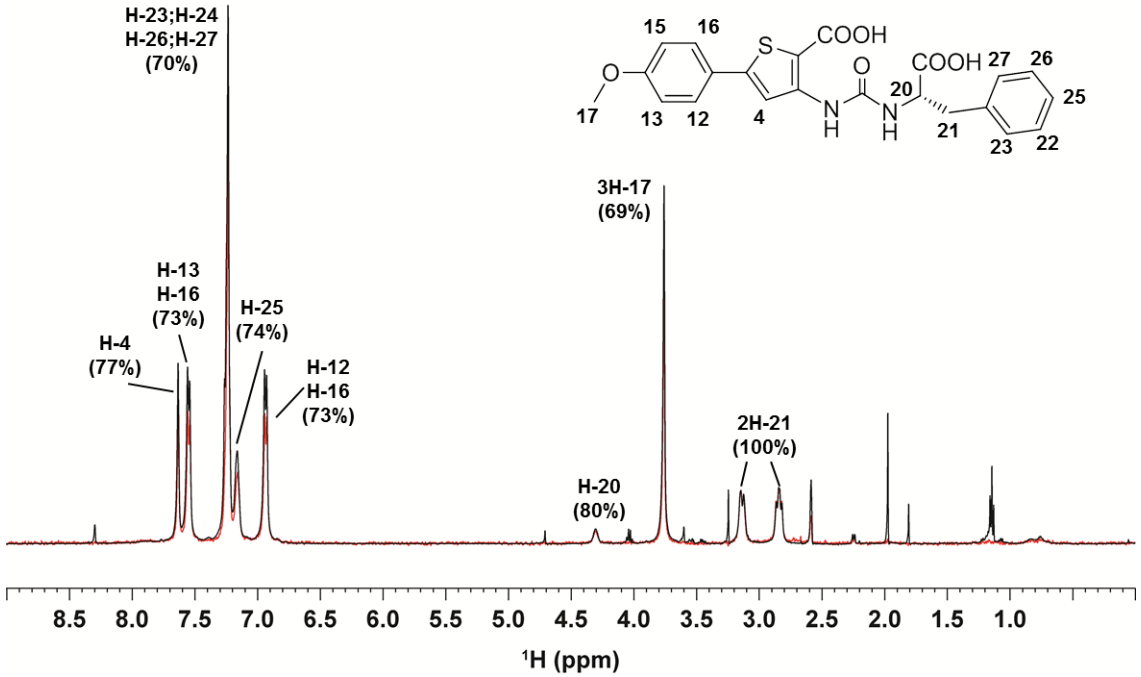

Figure S5. Reference (black) and STD NMR difference (red) spectra of compound **7** in complex with PqsD. Samples comprising 100:1 **7**/PqsD were prepared in 20 mM Na_3PO_4, 50 mM NaCl, and 5 mM $MgCl_2$, pH 7.0, and spectra were recorded at 298 K. Overlaid spectra were normalized to the signals for 2H-21, which gave the strongest enhancement.

6.3.7 MALDI-TOF MS Spectra

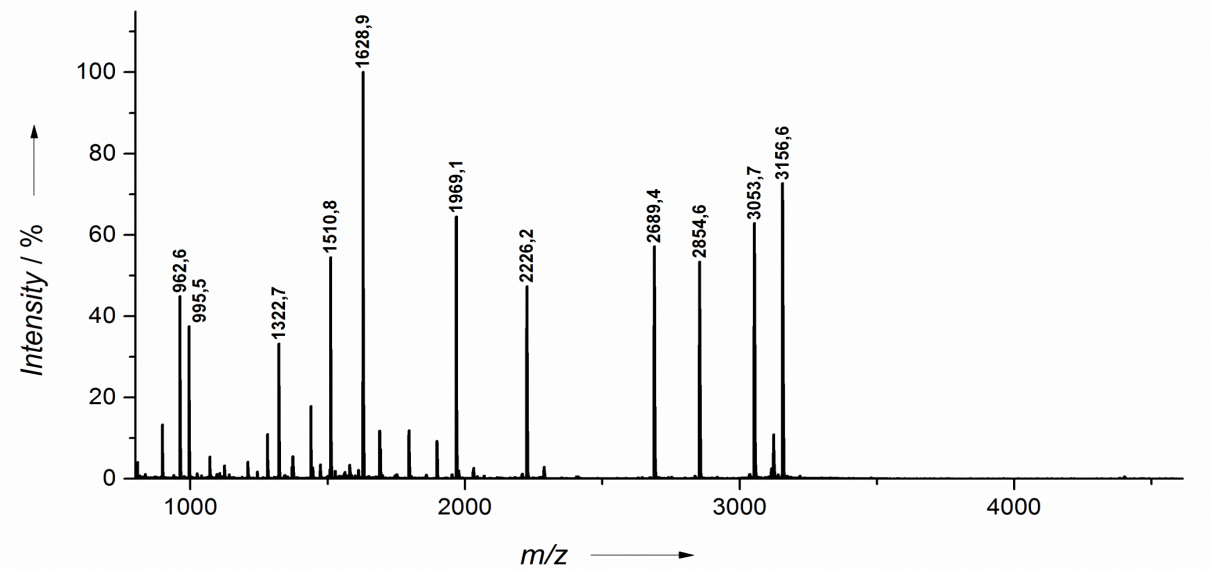

Figure S6. MALDI-TOF-MS analysis of tryptic digested PqsD. For the sake of clarity, only signals >15% intensity are labeled.

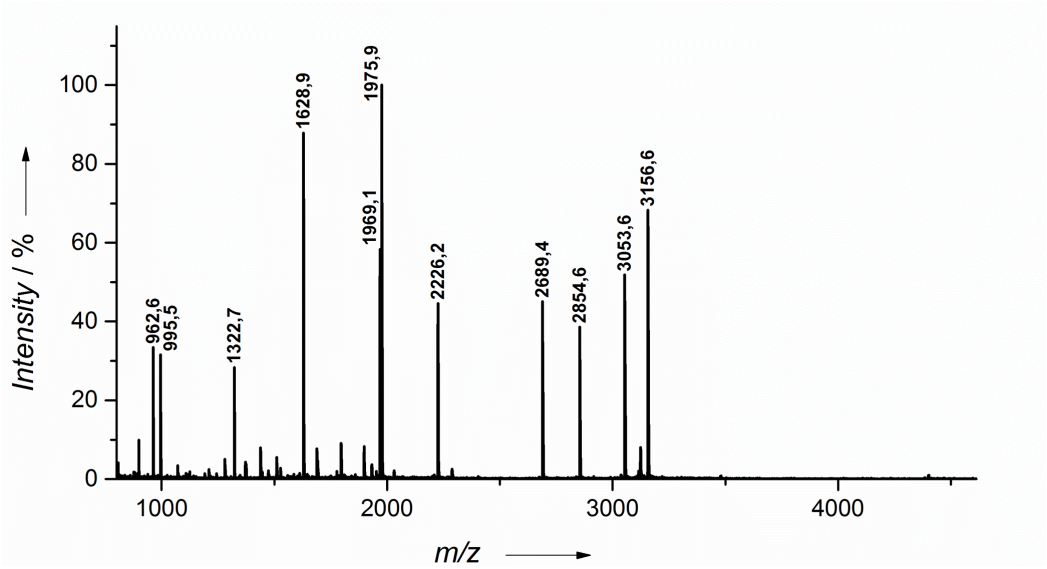

Figure S7. MALDI-ToF-MS analysis of tryptic digested PqsD after preincubation with **12**. For the sake of clarity, only signals >15% intensity are labeled.

6.3.8 LC-ESI-MS Data

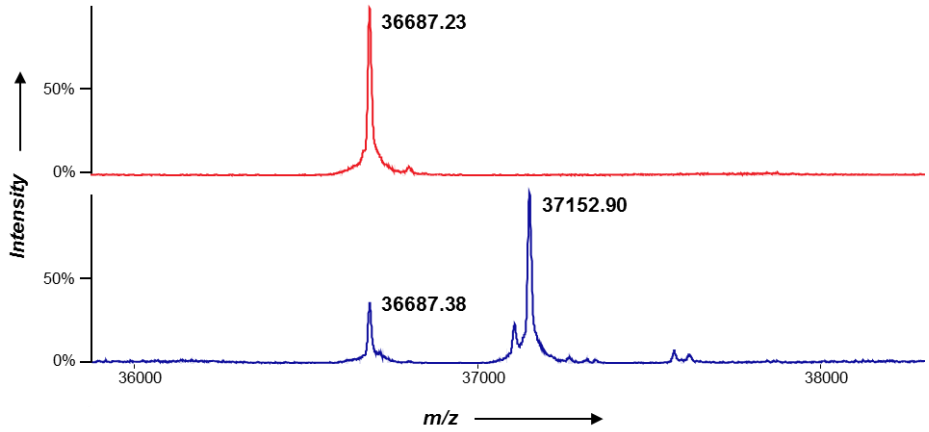

Figure S8. LC-ESI-MS data. Top panel (red): Reference sample containing only PqsD. Bottom panel (blue): PqsD after 30 minutes preincubation with compound **12**. Mass shift of 465 Da indicates covalent binding of **12**.

6.4 Supporting Information for Publication D

Full supporting information is available online:

http://www.rsc.org/suppdata/ob/c4/c4ob00707g/c4ob00707g1.pdf

6.4.1 Synthesis and analytical data of all tested compounds

(2-Nitrophenyl)(phenyl)methanol (3)[S1] The title compound was synthesized from 2-iodonitrobenzene **36** (1.00 g, 4.02 mmol) and benzaldehyde according to general method A. Purification via flash chromatography (petroleum ether/ethyl acetate 1:1) gave **3** (681 mg, 70 %) as a brown solid. ^{1}H NMR (500 MHz, $CDCl_3$) δ 6.44 (s, 1H), 7.27-7.32 (m, 1H), 7.33-7.34 (m, 4H), 7.44-7.47 (m, 1H), 7.62-7.65 (m, 1H), 7.73-7.75 (m, 1H), 7.93 (dd, J = 8.2, J = 1.3, 1H). ^{13}C NMR (125 MHz, $CDCl_3$) δ 71.7, 124.9, 127.1, 128.2, 128.7, 128.7, 129.6, 133.6, 138.6, 141.7. R_t = 9.75 min; purity $\geq$ 97 % (UV). HRMS (ESI) *m/z*: $(M\text{-}OH)^+$ calculated 212.07060, found 212.07037. Mp: 54-55°C (Lit. 59-60°C).[S2]

***tert*-Butyl phenylcarbamate (5)**[S3] To a solution of aniline (3.42 ml, 37.50 mmol) in 35 ml THF was added di-*tert*-butyl dicarbonate (9.48 ml, 41.25 mmol) and the mixture was refluxed for 3 h. The solvent was removed in vacuo and 75 ml ethyl acetate were added. The solution was washed with 1 M citric acid and brine, dried and concentrated under reduced pressure. Crystallization from hexane yielded **5** (5.013 g, 69 %) as a white solid. ^{1}H NMR (500 MHz, acetone-d_6) δ 1.48 (s, 9H), 6.98 (t, J = 7.4, 1H), 7.24-7.29 (m, 2H), 7.55 (d, J = 7.9, 2H). ^{13}C NMR (125 MHz, acetone-d_6) δ 28.5, 79.9, 119.0, 123.0, 123.0, 129.5. Mp: 135°C (Lit. 137°C).[S2]

***tert*-Butyl (2-(hydroxy(phenyl)methyl)phenyl)-carbamate (6)**[S3] A solution of *tert*-butyl phenylcarbamate **5** (1.200 g, 6.20 mmol) in 10 ml THF was cooled to -60°C and 8.76 ml of a *tert*-butyllithium solution (1.7 M in pentane, 14.89 mmol) were added slowly. The solution was stirred at -60°C for 15 min followed by 2 h at -20°C. A solution of benzaldehyde (0.63 ml, 6.20 mmol) in 5 ml THF was added and the mixture was stirred for 2 h at -20°C. The reaction was quenched with a saturated solution of NH_4Cl (10 ml) and the aqueous phase was extracted with ethyl acetate (three times). The combined organic layers were washed with brine, dried, and concentrated under reduced pressure. The residue was purified by column chromatography (petroleum ether/ethyl acetate 8:1) to yield **6** (653 mg, 35 %) as a white solid. ^{1}H NMR (500 MHz, MeOH-d_4) δ 1.41 (s, 9H), 5.88 (s, 1H), 7.07 (td, J = 7.6, J = 1.3, 1H), 7.19-7.34 (m, 7H), 7.60 (d, J = 7.6, 1H). ^{13}C NMR (125 MHz, MeOH-d_4) δ 28.6, 75.4, 81.0, 124.8, 127.3, 128.1, 129.1, 129.1, 129.4, 137.9, 144.2, 155.3. MS (ESI) *m/z*: 267.2 $(M\text{-}O^tBu)^+$. Mp: 135-137°C (Lit. 141-142°C).[S2]

4-Phenyl-1H-benzo[*d*][1,3]oxazin-2(4H)-one (7) To a solution of **6** (200 mg, 0.67 mmol) in 4 ml of dry dichloromethane at 0°C were added 0.8 ml TFA and the mixture was stirred at room temperature for 1 h. The solvent and TFA were removed in vacuo, DCM was added and the pH was adjusted to 7 using a saturated solution of sodium bicarbonate. The solution was extracted three times with ethyl acetate and the combined organic phase was dried, filtered and concentrated in vacuo. The crude product was purified by flash chromatography (petroleum ether/ethyl acetate 3:1) to give **7** (117 mg, 78 %) as a brownish solid. ^{1}H NMR (500 MHz, $CDCl_3$) δ 6.39 (s, 1H), 6.86 (d, J = 7.6, 1H), 6.92 (dd, J = 7.9, J = 0.6, 1H), 7.02 (td, J = 7.6, J = 0.9, 1H), 7.26-7.30 (m, 1H), 7.35-7.42 (m, 5H). ^{13}C

NMR (125 MHz, MeOH-d_4) δ 81.4, 114.5, 121.1, 123.5, 126.0, 127.9, 128.9, 129.3, 129.6, 135.5, 153.1. R_t = 9.46 min; purity ≥ 99 % (UV). HRMS (ESI) *m/z*: $(M+H)^+$ calculated 226.08626, found 226.08576. Mp: 57-60°C.

(2-Aminophenyl)(phenyl)methanol (8) To a solution of **7** (200 mg, 0.89 mmol) in 5 ml methanol a solution of potassium hydroxide (2.00 g) in 5 ml H_2O was added. The mixture was refluxed for 18 h, methanol was removed under reduced pressure and the phases were separated. The aqueous phase was extracted twice with ethyl acetate and the combined organic phase was dried, filtered and concentrated in vacuo. The crude product was purifed by flash chromatography (petroleum ether/ethyl acetate 4:1) to give **8** (30 mg, 17 %) as a yellowish solid. ^{1}H NMR (500 MHz, MeOH-d_4) δ 5.82 (s, 1H), 6.66 (t, *J* = 7.3, 1H), 6.72 (d, *J* = 7.9, 1H), 6.99 (d, *J* = 7.6, 1H), 7.04 (td, *J* = 7.6, *J* = 1.3, 1H), 7.25 (t, *J* = 7.3, 1H), 7.32 (t, *J* = 7.6, 2H), 7.38 (d, *J* = 7.6, 2H). ^{13}C NMR (125 MHz, MeOH-d_4) δ 74.6, 117.8, 118.9, 127.9, 128.2, 129.1, 129.2, 129.3, 129.7, 144.3, 146.6. R_t = 6.16 min; purity ≥ 97 % (UV). HRMS (ESI) *m/z*: $(M+H)^+$ calculated 200.10699, found 200.10644. Mp: 118-120°C (Lit. 115-116°C).[S4]

3-Phenylisobenzofuran-1(3H)-one (10) The title compound was prepared according to the general method B using methyl 2-iodobenzoate (2.00 g, 7.63 mmol) and purified by column chromatography (petroleum ether/ethyl acetate 6:1) to yield **10** (1.007 g, 63 %) as a white solid. ^{1}H NMR (500 MHz, DMSO-d_6) δ 6.73 (s, 1H), 7.30-7.34 (m, 2H), 7.37-7.43 (m, 3H), 7.45 (d, *J* = 7.6, 1H), 7.63 (t, *J* = 7.6, 1H), 7.76 (t, *J* = 7.6, 1H), 7.93 (d, *J* = 7.3, 1H). ^{13}C NMR (125 MHz, DMSO-d_6) δ 81.8, 123.2, 124.6, 125.0, 126.8, 128.9, 129.0, 129.5, 134.7, 136.9, 149.9, 169.9. R_t = 10.70 min; purity ≥ 95 % (UV). HRMS (ESI) *m/z*: $(M+H)^+$ calculated 226.07536, found 211.07491. Mp: 116-117°C (Lit. 115-117°C).[S5]

Sodium 2-(hydroxy(phenyl)methyl)benzoate (11) To a solution of **10** (400 mg, 1.90 mmol) in 20 ml MeOH an aqueous solution of sodium hydroxide (20 ml, 1M) was added. The mixture was stirred for 2 h at room temperature followed by 2 h at 50°C. The solvent was evaporated and **11** was isolated by preparative HPLC to afford 199 mg (39 %) as a white solid. ^{1}H NMR (500 MHz, MeOH-d_4) δ 6.10 (s, 1H), 7.16-7.21 (m, 2H), 7.23-7.30 (m, 4H), 7.36 (d, *J* = 7.9, 2H), 7.66 (d, *J* = 7.3, 1H). ^{13}C NMR (125 MHz, MeOH-d_4) δ 75.7, 127.6, 127.6 128.1, 128.8, 129.4, 129.9, 130.6. 140.8, 143.4, 145.2, 177.5. R_t = 8.80 min; purity ≥ 98 % (UV). HRMS (ESI) *m/z*: $(M-OH)^+$ calculated 211.07536, found 211.07512. IR (ATR) ν_{max} 3288, 3061, 3028, 1557 (ν_{as} COO^-) , 1385 (ν_s COO^-), 1015, 739, 699 cm^{-1}. Mp: 67-71°C.

Phenyl(2-(trifluoromethyl)phenyl)methanol (14) The title compound was prepared according to the general method B using 2-iodobenzotrifluorid (1.00 g, 3.68 mmol) and purified by column chromatography (petroleum ether/ethyl acetate 10:1) to yield **14** (665 mg, 71 %) as a colorless oil. ^{1}H NMR (500 MHz, MeOH-d_4) δ 6.21 (s, 1H), 7.22 (t, *J* = 7.6, 1H), 7.27-7.32 (m, 4H), 7.41 (t, *J* = 7.6, 1H), 7.58 (t, *J* = 7.6, 1H), 7.68 (d, *J* = 7.9, 1H), 7.70 (d, *J* = 7.9, 1H). ^{13}C NMR (125 MHz, MeOH-d_4) δ 71.5, 126.0 (q, *J* = 273), 126.3 (q, *J* = 6), 127.7, 128.3, 128.5 (q, *J* = 30), 128.7, 129.2, 130.8, 133.4, 144.4, 145.0. R_t = 11.74 min; purity ≥ 99 % (UV). HRMS (ESI) *m/z*: $(M-OH)^+$ calculated 235.07291, found 235.07263.

2-(Hydroxy(phenyl)methyl)benzonitrile (15) The title compound was prepared according to the general method B using 2-iodobenzonitril (1.00 g, 4.36 mmol) and purified by column chromatography (petroleum ether/ethyl acetate 1:1) to yield **15** (426 mg, 47 %) as a yellowish solid. ^{1}H NMR (500 MHz, MeOH-d_4) δ 6.52 (s, 1H), 7.26-7.30 (m, 3H), 7.33-7.39 (m, 3H), 7.52-7.56 (m, 1H), 7.59 (td, *J* = 7.6, *J* = 1.3, 1H), 7.95-7.97 (m, 1H). ^{13}C NMR (125 MHz, MeOH-d_4) δ 86.5, 123.9,

124.7, 126.6, 127.9, 129.4, 129.9, 130.1, 130.2, 134.0, 139.5, 149.1. R_t = 6.58 min; purity ≥ 96 % (UV). HRMS (ESI) *m/z*: $(M+H)^+$ calculated 210.09143, found 210.09094. Mp: 86-91°C.

(2-Chlorophenyl)(phenyl)methanol (21) The title compound was prepared according to the general method C using 2-chlorobenzaldehyde (0.40 ml, 3.56 mmol) and purified by column chromatography (petroleum ether/ethyl acetate 10:1) to yield **21** (450 mg, 58 %) as a grey solid. ^{1}H NMR (500 MHz, MeOH-d_4) δ 6.16 (s, 1H), 7.20-7.25 (m, 2H), 7.27-7.31 (m, 2H), 7.31-7.36 (m, 4H), 7.65-7.67 (m, 1H). ^{13}C NMR (125 MHz, MeOH-d_4) δ 73.1, 128.1, 128.2, 128.4, 129.2, 129.6, 130.3, 133.5, 143.2, 144.3. R_t = 11.07 min; purity ≥ 99 % (UV). HRMS (ESI) *m/z*: $(M-OH)^+$ calculated 201.04655, found 201.04627. Mp: 64-66°C (Lit. 64-66°C).[S6]

(2-Bromophenyl)(phenyl)methanol (22) The title compound was prepared according to the general method C using 2-bromobenzaldehyde (0.63 ml, 5.41 mmol) and purified by column chromatography (petroleum ether/ethyl acetate 10:1) to yield **22** (516 mg, 36 %) as a yellowish solid. ^{1}H NMR (500 MHz, MeOH-d_4) δ 6.12 (s, 1H), 7.17 (td, J = 7.7, J = 1.9, 1H), 7.22 (tt, J = 8.2, J = 1.4, 1H), 7.27-7.31 (m, 2H), 7.34-7.398 (m, 3H), 7.54 (dd, J = 8.2, J = 1.3, 1H), 7.64 (dd, J = 7.9, J = 1.6, 1H). ^{13}C NMR (125 MHz, MeOH-d_4) δ 75.3, 128.3, 128.4, 129.2, 129.6, 130.0, 133.7, 144.3, 144.7. R_t = 11.13 min; purity ≥ 96 % (UV). HRMS (ESI) *m/z*: $(M-OH)^+$ calculated 244.99604, found 244.99585. Mp: 56-58°C (Lit. 56°C).[S7]

Phenyl(*o*-tolyl)methanol (23) The title compound was prepared according to the general method C using 2-methylbenzaldehyde (0.42 ml, 3.67 mmol) and purified by column chromatography (petroleum ether/ethyl acetate 8:1) to yield **23** (700 mg, 92 %) as a white solid. ^{1}H NMR (500 MHz, MeOH-d_4) δ 2.22 (s, 3H), 5.96 (s, 1H), 7.10-7.25 (m, 4H), 7.27-7.31 (m, 4H), 7.47 (d, J = 7.6, 1H). ^{13}C NMR (125 MHz, MeOH-d_4) δ 19.5, 73.9, 126.8, 127.5, 128.2, 128.4, 129.2, 131.3, 136.5, 143.3, 144.8. R_t = 10.90 min; purity ≥ 95 % (UV). HRMS (ESI) *m/z*: $(M-OH)^+$ calculated 181.10118, found 181.10078. Mp: 90-91°C (Lit. 90-91°C).[S8]

2-Methoxyphenyl)(phenyl)methanol (24) To a solution of 14.20 ml 2-methoxy-magnesium bromide (1M in TFH, 14.3 mmol) in 35 ml THF at -40°C was slowly added benzaldehyde (1.73 ml, 17.03 mmol). After 3 h at -40°C the reaction was quenched with a saturated solution of NH_4Cl (10 ml) and diluted with water (10 ml). The workup was carried out as described in method A. The crude product was purified by column chromatography (petroleum ether/ethyl acetate 8:1) to give the desired product (2.098 g, 69 %). ^{1}H NMR (500 MHz, MeOH-d_4) δ 3.76 (s, 3H), 6.12 (s, 1H), 6.91-6.96 (m, 2H), 7.18 (tt, J = 7.3, J = 1.3, 1H) 7.20-7.23 (m, 1H), 7.24-7.27 (m, 2H), 7.32-7.35 (m, 2H), 7.44 (dd, J = 7,6, J = 1.9, 1H). ^{13}C NMR (125 MHz, MeOH-d_4) δ 55.8, 70.8, 111.6, 121.5, 127.8, 127.9, 129.0, 129.4, 134.0, 145.7, 157.7. R_t = 10.48 min; purity ≥ 99 % (UV). HRMS (ESI) *m/z*: $(M-OH)^+$ calculated 197.09609, found 197.09576. Mp: 37-38°C (Lit. 38-39°C).[S9]

2-(Hydroxy(phenyl)methyl)phenol (25) The title compound was prepared according to the general method C using 2-hydroxybenzaldehyde (0.87 ml, 8.19 mmol) and 2.5 eq phenylmegnesium chloride (10.23 ml, 20.47 mmol). The crude product was purified by column chromatography (petroleum ether/ethyl acetate 6:1) to yield **25** (1.160 g, 70 %) as a white solid. ^{1}H NMR (500 MHz, MeOH-d_4) δ 6.11 (s, 1H), 6.76 (dd, J = 8.2, J = 0.9, 1H), 6.80 (tt, J = 7.6, J = 1.3, 1H), 7.05-7.09 (m, 1H), 7.19 (tt, J = 6.6, J = 1.9, 1H), 7.23 (dd, J = 7.6, J = 1.8, 1H), 7.25-7.29 (m, 2H), 7.37-7.40 (m, 2H). ^{13}C NMR (125 MHz, MeOH-d_4) δ 72.3, 120.4, 127.7, 127.9, 128.4, 129.0, 129.2, 131.5, 145.6, 155.8. R_t = 9.00 min; purity ≥ 99 % (UV). HRMS (ESI) *m/z*: $(M-OH)^+$ calculated 183.08044, found 183.08003. Mp: 136-137°C (Lit. 84-86°C).[S10]

(3-Nitrophenyl)(phenyl)methanol (28) The title compound was prepared according to the general method D using *meta*-nitrobenzaldehyde **26** to yield **28** (102 mg, 7 %) as a brown oil. ^{1}H NMR (500 MHz, MeOH-d_4) δ 5.88 (s, 1H), 7.26 (tt, J = 7.3, J = 1.3, 1H), 7.32-7.35 (m, 2H), 7.37-7.40 (m, 2H), 7.54 (t, J = 7.9, 1H), 7.73-7.76 (m, 1H), 8.08-8.11 (m, 1H), 8.27-8.28 (m, 1H). ^{13}C NMR (125 MHz, MeOH-d_4) δ 75.8, 122.1, 122.9, 127.8, 128.7, 129.6, 130.5, 133.9, 148.7. R_t = 10.26 min; purity ≥ 99 % (UV). HRMS (ESI) *m/z*: $(M\text{-}OH)^+$ calculated 212.07060, found 212.07028.

(4-Nitrophenyl)(phenyl)methanol (29) The title compound was prepared according to the general method D using *para*-nitrobenzaldehyde **27** to yield **29** (176 mg, 12 %) as a green-brown solid. ^{1}H NMR (500 MHz, MeOH-d_4) δ 5.87 (s, 1H), 7.25 (t, J = 7.6, 2H), 7.36-7.39 (m, 2H), 7.62 (d, J = 8.8, 2H), 8.16-8.19 (m, 2H), 7.73-7.76 (m, 1H), 8.08-8.11 (m, 1H), 8.27-8.28 (m, 1H). ^{13}C NMR (125 MHz, MeOH-d_4) δ 76.1, 124.4, 127.8, 128.4, 128.7, 129.6, 145.0, 148.4, 153.7. R_t = 10.25 min; purity ≥ 99 % (UV). HRMS (ESI) *m/z*: $(M+H)^+$ calculated 230.08117, found 230.08099. Mp: 58-59°C (Lit. 52-53°C).[S11]

(4-Chloro-2-nitrophenyl)(phenyl)methanol (33) The title compound was prepared from phenylmagnesium chloride (0.67 ml, 2M in THF, 1.35 mmol) and 4-chloro-2-nitrobenzaldehyde (259 mg, 1.35 mmol) using the procedure described in the general method D. Pure **33** (174 mg, 49 %) was obtained as brown oil by flash chromatography (petroleum ether/ethyl acetate 8:1). ^{1}H NMR (500 MHz, MeOH-d_4) δ 6.34 (s, 1H), 7.25-7.32 (m, 5H), 7.71 (dd, J = 8.5, J = 2.2, 1H), 7.86 (d, J = 8.5, 1H), 7.92 (d, J = 2.2, 1H). ^{13}C NMR (125 MHz, MeOH-d_4) δ 71.3 125.1, 128.3, 128.8, 129.4, 131.5, 134.0, 134.7, 139.1, 143.6. R_t = 12.14 min; purity ≥ 96 % (UV). HRMS (ESI) *m/z*: $(M\text{-}OH)^+$ calculated 246.03163, found 246.03135.

(5-Chloro-2-nitrophenyl)(phenyl)methanol (34) The title compound was prepared from phenylmagnesium chloride (2.69 ml, 2M in THF, 5.39 mmol) and 5-chloro-2-nitrobenzaldehyde (1.00 g, 5.39 mmol) using the procedure described in the general method D. Pure **34** (0.792 mg, 56 %) was obtained as brown oil by flash chromatography (petroleum ether/ethyl acetate 12:1). ^{1}H NMR (500 MHz, MeOH-d_4) δ 6.40 (s, 1H), 7.23-7.27 (m, 3H), 7.29-7.32 (m, 2H), 7.50 (dd, J = 8.8, J = 2.2, 1H), 7.89-7.92 (m, 2H). ^{13}C NMR (125 MHz, MeOH-d_4) δ 71.5, 127.3, 128.4, 128.9, 129.3, 129.5, 129.7, 140.4, 142.8, 143.3. R_t = 11.29 min; purity ≥ 95 % (UV). HRMS (ESI) *m/z*: $(M\text{-}OH)^+$ calculated 246.03163, found 246.03134.

(2,4-Dinitrophenyl)(phenyl)methanol (35) The title compound was prepared from phenylmagnesium chloride (1.27 ml, 2M in THF, 2.55 mmol) and 2,4-dinitrobenzaldehyde (0.50 g, 5.39 mmol) using the procedure described in the general method D. Pure **35** (141 mg, 20 %) was obtained as brown oil by flash chromatography (petroleum ether/ethyl acetate 6:1). ^{1}H NMR (500 MHz, MeOH-d_4) δ 6.44 (s, 1H), 7.24-7.32 (m, 5H), 8.21 (dd, J = 8.8, 1H), 8.53 (dd, J = 8.8, J = 2.2, 1H), 8.69 (d, J = 2.2, 1H). ^{13}C NMR (125 MHz, MeOH-d_4) δ 71.7, 120.8, 128.1, 128.5, 129.1, 129.6, 131.4, 143.0, 147.0, 148.4, 149.5. R_t = 10.82 min; purity ≥ 95 % (UV). HRMS (ESI) *m/z*: $(M\text{-}OH)^+$ calculated 257.05568, found 257.05544.

(4-Methyl-2-nitrophenyl)(phenyl)methanol (39) The title compound was synthesized from 4-iodo-3-nitro-toluene **37** (2.00 g, 7.60 mmol) and benzaldehyde according to general method A. Purification by flash chromatography (petroleum ether/ethyl acetate 8:1) gave **39** (765 mg, 41 %) as a brown oil. ^{1}H NMR (500 MHz, MeOH-d_4) δ 2.41 (s, 3H), 6.34 (s, 1H), 7.21-7.30 (m, 5H), 7.45-7.51 (m, 1H), 7.68-7.71 (m, 2H). ^{13}C NMR (125 MHz, MeOH-d_4) δ 20.6, 71.5, 125.4, 128.3, 128.6, 129.3, 129.8, 134.7, 137.2, 140.1, 144.2, 149.7. R_t = 11.20 min; purity ≥ 95 % (UV). HRMS (ESI) *m/z*: $(M\text{-}OH)^+$ calculated 226.08626, found 226.08597.

(5-Methyl-2-nitrophenyl)(phenyl)methanol (40) The title compound was synthesized from 3-iodo-4-nitro-toluene **38** (1.00 g, 3.80 mmol) and benzaldehyde according to general method A. Purification by flash chromatography (petroleum ether/ethyl acetate 8:1) gave **40** (383 mg, 42 %) as a yellow-brown oil. ^{1}H NMR (500 MHz, MeOH-d_4) δ 2.45 (s, 3H), 6.42 (s, 1H), 7.21-7.30 (m, 6H), 7.70-7.71 (m, 1H), 7.81 (d, J = 8.2, 1H). ^{13}C NMR (125 MHz, MeOH-d_4) δ 21.6, 71.6, 125.5, 128.4, 128.6, 129.3, 129.7, 130.2, 140.4, 144.1, 145.6, 147.5. R_t = 11.09 min; purity ≥ 96 % (UV). HRMS (ESI) *m/z*: $(M\text{-}OH)^+$ calculated 226.08626, found 226.08598.

(4-Methoxy-2-nitrophenyl)(phenyl)methanol (43) A solution of 4-iodo-3-nitroanisol **41** (1.00 g, 3.59 mmol) in 25 ml THF was cooled to -40°C and a solution of 4-methoxyphenylmagnesium chloride (3.94 ml, 1M in THF, 3.94 mmol) was added drop-wise. The solution was stirred for 1 h at -20°C. Then, benzaldehyde (0.39 ml, 3.59 mmol) was added at -40°C and the mixture was stirred for further 90 min at constant temperature. The workup was carried out as described in method A. The crude product was purified by column chromatography (petroleum ether/ethyl acetate 8:1) to give the desired product (192 mg, 21 %).^{1}H NMR (500 MHz, MeOH-d_4) δ 3.86 (s, 3H), 6.30 (s, 1H), 7.21-7.31 (m, 6H), 7.40 (d, J = 2.5, 1H), 7.69 (d, J = 8.8, 1H). ^{13}C NMR (125 MHz, MeOH-d_4) δ 56.4, 71.3, 110.1, 112.0, 128.2, 128.5, 129.3, 131.1, 132.0, 144.3, 160.6. R_t = 10.57 min; purity ≥ 98 % (UV). HRMS (ESI) *m/z*: $(M\text{-}OH)^+$ calculated 226.08117, found 226.08092.

(5-Methoxy-2-nitrophenyl)(phenyl)methanol (44) A solution of 3-iodo-4-nitroanisol **42** (1.00 g, 3.59 mmol) in 25 ml THF was cooled to -40°C and a solution of 4-methoxyphenylmagnesium chloride (3.94 ml, 1M in THF, 3.94 mmol) was added drop-wise. The solution was stirred for 1 h at -20°C. Then, benzaldehyde (0.39 ml, 3.59 mmol) was added at -40°C and the mixture was stirred for further 90 min at constant temperature. The workup was carried out as described in method A. The crude product was purified by column chromatography (petroleum ether/ethyl acetate 6:1) to give the desired product (298 mg, 68 %). ^{1}H NMR (500 MHz, MeOH-d_4) δ 3.91 (s, 3H), 6.53 (s, 1H), 6.98 (dd, J = 9.1, J = 2.8, 1H), 7.21-7.30 (m, 5H), 7.48 (d, J = 2.8, 1H), 8.01 (d, J = 8.8, 1H). ^{13}C NMR (125 MHz, MeOH-d_4) δ 56.5 72.0, 113.8, 114.7, 128.5, 128.7, 129.3, 143.9, 165.0. R_t = 10.32 min; purity ≥ 95 % (UV). HRMS (ESI) *m/z*: $(M\text{-}OH)^+$ calculated 242.08117, found 226.08099.

1-(2-Nitrophenyl)ethanol (47)[S13] To a solution of 1-(2-nitrophenyl)ethanone **46** (400 mg, 2.42 mmol) in methanol (6 ml) sodium borohydride (366 mg, 9,69 mmol) was slowly added at 5°C. The reaction mixture was stirred for 16 h at room temperature, the solvent was evaporated and water was added. The solution was extracted three times with ethyl acetate and the combined organic phase was dried, filtered, and concentrated in vacuo. The crude product was purified by flash chromatography (petroleum ether/ethyl acetate 4:1) to give **47** (252 mg, 62 %) as a brownish oil. ^{1}H NMR (500 MHz, MeOH-d_4) δ 1.49 (d, J = 6.3, 3H), 5.31 (q, J = 6.3, 1H), 7.45 (td, J = 7.7, J = 1.3, 1H), 7.69 (td, J = 7.7, J = 1.3, 1H), 7.84-7.87 (m, 2H). ^{13}C NMR (125 MHz, MeOH-d_4) δ 25.1, 66.0, 124.8, 128.6, 129.0, 134.3, 142.8, 149.3. R_t = 8.21 min; purity ≥ 96 % (UV). HRMS (ESI) *m/z*: $(M\text{-}OH)^+$ calculated 168.06552, found 168.06508. Mp: 26-28°C (Lit. 40-41°C).[S12]

1-(2-Nitrophenyl)propan-1-ol (48) The title compound was synthesized from 2-iodonitrobenzene **36** (1.00 g, 4.02 mmol) and propionaldehyde according to general method A. Purification by flash chromatography (petroleum ether/ethyl acetate 6:1) gave **48** (398 mg, 55 %) as a brown oil. ^{1}H NMR (500 MHz, DMSO-d_6) δ 1.01 (t, J = 7.3, 3H), 1.62-1.71 (m, 1H), 1.76-1.84 (m, 1H), 5.07 (dd, J = 8.2, J = 3.8, 1H), 7.43-7.46 (m, 1H), 7.70 (d, J = 7.6, J = 1.3, 1H), 7.81 (dd, J = 7.9, J = 1.3, 1H), 7.85 (dd, J = 8.2, J = 1.3, 1H). ^{13}C NMR (125 MHz, DMSO-d_6) δ 10.8, 32.8, 71.0, 124.9, 129.0, 129.1, 134.1, 141.8, 149.5. R_t = 9.45 min; purity ≥ 98 % (UV). HRMS (ESI) *m/z*: $(M\text{-}OH)^+$ calculated 164.09609, found 164.07060.

1-(2-nitrophenyl)butan-1-ol (49) The title compound was synthesized from 2-iodonitrobenzene **36** (498 mg, 2.00 mmol) and butyraldehyde according to general method A. Purification by flash chromatography (petroleum ether/ethyl acetate 8:1) gave **49** (398 mg, 55 %) as a brown oil. ^{1}H NMR (500 MHz, DMSO-d_6) δ 0.97 (t, J = 7.6, 3H), 1.41-1.50 (m, 1H), 1.52-1.62 (m, 1H), 1.70-1.82 (m, 2H), 5.25 (dd, J = 7.9, J = 4.1, 1H), 7.39-7.42 (m, 1H), 7.61-7.64 (m, 1H), 7.80 (dd, J = 7.9, J = 1.3, 1H), 7.89 (dd, J = 8.2, J = 1.3, 1H). ^{13}C NMR (125 MHz, $CDCl_3$) δ 13.7, 19.3, 40.2, 69.2, 124.3, 128.0, 128.1, 133.4, 140.24, 148.0. R_t = 10.36 min; purity ≥ 98 % (UV). MS (EI) *m/z*: 152.0* $(M\text{-}C_3H_7^{\bullet})^+$, 135.0* $(M\text{-}C_3H_8O^{\bullet})^+$.

1-(2-nitrophenyl)pentan-1-ol (50) The title compound was synthesized from 2-iodonitrobenzene **36** (1.00 g, 4.02 mmol) and pentanal according to general method A. Purification by flash chromatography (petroleum ether/ethyl acetate 9:1) gave **50** (312 mg, 37 %) as a brownish solid. ^{1}H NMR (500 MHz, MeOH-d_4) δ 0.92 (t, J = 6.9, 3H), 1.33-1.45 (m, 3H), 1.45-1.56 (m, 1H), 1.61-1.68 (m, 1H), 1.71-1.78 (m, 1H), 5.14 (dd, J = 8.5, J = 3.8, 1H), 7.44 (t, J = 7.9, 1H), 7.67 (t, J = 7.6, 1H), 7.82 (d, J = 7.9, 1H), 7.85 (d, J = 8.2, 1H). ^{13}C NMR (125 MHz, MeOH-d_4) δ 14.4, 23.5, 29.4, 39.7, 69.6, 124.8, 128.9, 129.0, 134.1, 142.2, 149.4. R_t = 10.95 min; purity ≥ 99 % (UV). HRMS (ESI) *m/z*: $(M+H)^+$ calculated 210.11247, found 210.11189. Mp: 28-32°C.

1-(2-nitrophenyl)hexan-1-ol (51) The title compound was synthesized from 2-iodonitrobenzene **36** (1.00 g, 4.02 mmol) and hexanal according to general method A. Purification by flash chromatography (petroleum ether/ethyl acetate 9:1) gave **51** (349 mg, 39 %) as a brownish solid. ^{1}H NMR (500 MHz, MeOH-d_4) δ 0.91 (t, J = 6.9, 3H), 1.28-1.38 (m, 4H), 1.39-1.47 (m, 1H), 1.50-1.59 (m, 1H), 1.60-1.67 (m, 1H), 1.70-1.77 (m, 1H), 5.14 (dd, J = 8.5, J = 3.8, 1H), 7.42-7.46 (m, 1H), 7.70 (td, J = 7.3, J = 1.3, 1H), 7.81 (dd, J = 7.9, J = 1.3, 1H), 7.85 (dd, J = 8.2, J = 1.3, 1H). ^{13}C NMR (125 MHz, MeOH-d_4) δ 14.4, 23.6, 26.8, 32.7, 39.9, 69.9, 124.8, 128.9, 129.9, 134.1, 142.2, 149.4. R_t = 12.07 min; purity ≥ 99 % (UV). HRMS (ESI) *m/z*: $(M\text{-}OH)^+$ calculated 206.11756, found 206.11725. Mp: 26-29°C.

3-Methyl-1-(2-nitrophenyl)butan-1-ol (52) The title compound was synthesized from 2-iodonitrobenzene **36** (1.00 g, 4.02 mmol) and 3-methylbutanal according to general method A. Purification by flash chromatography (petroleum ether/ethyl acetate 8:1) gave **52** (417 mg, 50 %) as a brown oil. ^{1}H NMR (500 MHz, MeOH-d_4) δ 0.95 (d, J = 6.6, 3H), 1.01 (d, J = 6.6, 3H), 1.42-1.48 (m, 1H), 1.57-1.63 (m, 1H), 1.90-1.98 (m, 1H), 5.25 (dd, J = 9.8, J = 2.8, 1H), 7.43 (td, J = 7.7, J = 1.3, 1H), 7.67 (td, J = 7.6, J = 0.9, 1H), 7.84 (td, J = 8.2, J = 1.3, 1H). ^{13}C NMR (125 MHz, MeOH-d_4) δ 21.6, 24.1, 26.1, 67.8, 124.8, 128.8, 129.0, 134.2, 143.0, 149.2. R_t = 11.05 min; purity ≥ 99 % (UV). HRMS (ESI) *m/z*: $(M\text{-}OH)^+$ calculated 192.10191, found 192.10154.

3,3-Dimethyl-1-(2-nitrophenyl)butan-1-ol (53) The title compound was synthesized from 2-iodonitrobenzene **36** (1.00 g, 4.02 mmol) and 3,3-dimethylbutanal according to general method A. Purification by flash chromatography (petroleum ether/ethyl acetate 12:1) gave **53** (447 mg, 50 %) as a brown oil. ^{1}H NMR (500 MHz, MeOH-d_4) δ 1.04 (s, 9H), 1.51-1.64 (m, 2H), 5.34 (dd, J = 9.5, J = 2.2, 1H), 7.41-7.44 (m, 1H), 7.64-7.68 (m, 1H), 7.81 (dd, J = 8.2, J = 1.3, 1H), 7.83 (dd, J = 7.9, J = 1.3, 1H). ^{13}C NMR (125 MHz, MeOH-d_4) δ 30.7, 31.7, 53.1, 67.6, 124.7, 128.7, 129.3, 134.1, 143.4, 149.0. R_t = 11.91 min; purity ≥ 97 % (UV). HRMS (ESI) *m/z*: $(M\text{-}OH)^+$ calculated 206.11756, found 206.11724.

Cyclopentyl(2-nitrophenyl)methanol (54) The title compound was synthesized from 2-iodonitrobenzene **36** (1.00 g, 4.02 mmol) and cyclopentanecarbaldehyde according to general method A. Purification by flash chromatography (petroleum ether/ethyl acetate 7:1) gave **54** (574 mg, 51 %) as a brown solid. ^{1}H NMR (500 MHz, MeOH-d_4) δ 1.25-1.32 (m, 1H), 1.40-1.74 (m, 7H), 2.21-2.29

(m, 1H), 5.02 (d, *J* = 8.2, 1H), 7.41-7.45 (m, 1H), 7.63-7.66 (m, 1H), 7.77- 7.80 (m, 2H). ^{13}C NMR (125 MHz, MeOH-d_4) δ 26.4, 26.4, 29.5, 30.1, 72.3, 124.6, 129.0, 129.8, 133.7, 140.8, 150.3. R_t = 11.23 min; purity ≥ 99 % (UV). HRMS (ESI) *m/z*: $(M\text{-}OH)^+$ calculated 204.10191, found 206.10162.

Cyclohexyl(2-nitrophenyl)methanol (55) The title compound was synthesized from 2-iodonitrobenzene **36** (1.00 g, 4.02 mmol) and cyclohexanecarbaldehyde according to general method A. Purification by flash chromatography (petroleum ether/ethyl acetate 8:1) gave **55** (279 mg, 29 %) as a yellow-brown solid. ^{1}H NMR (500 MHz, MeOH-d_4) δ 1.09-1.23 (m, 5H), 1.35-1.37 (m, 1H), 1.57-1.65 (m, 1H), 1.74-1.77 (m, 1H), 1.81-1.85 (m, 1H), 4.95 (d, *J* = 6.3, 1H), 7.42-7.46 (m, 1H), 7.63-7.67 (m, 1H), 7.75 (dd, *J* = 7.9, *J* = 1.6, 1H), 7.80 (dd, *J* = 8.2, *J* = 1.3, 1H). ^{13}C NMR (125 MHz, MeOH-d_4) δ 27.2, 27.4, 27.5, 30.9, 46.2, 73.5, 124.7, 128.9, 129.9, 133.5, 140.3, 150.3. R_t = 12.10 min; purity ≥ 99 % (UV). MS (EI) *m/z*: 152.1* $(M\text{-}C_6H_{11}^{\bullet})^+$. Mp: 64-65°C.

Adamantan-1-yl(2-nitrophenyl)methanol (56) The title compound was synthesized from 2-iodonitrobenzene **36** (0.61 g, 2.44 mmol) and 1-adamantylcarboxaldehyde according to general method A. Purification by flash chromatography (petroleum ether/ethyl acetate 10:1) gave **56** (290 mg, 42 %) as a brown oil. ^{1}H NMR (500 MHz, MeOH-d_4) δ 1.42 (d, *J* = 12.0, 3H), 1.57 (t, *J* = 12.0, 6H), 1.68 (d, *J* = 12.0, 3H), 1.91 (s, 3H), 5.03 (s, 1H), 7.42-7.45 (m, 1H), 7.60-7.63 (m, 1H), 7.71-7.74 (m, 2H). ^{13}C NMR (125 MHz, MeOH-d_4) δ 29.8, 38.9, 39.3, 75.6, 124.4, 128.9, 131.4, 132.4, 136.9, 151.4. R_t = 13.74 min; purity ≥ 95 % (UV). MS HRMS (ESI) *m/z*: $(M\text{-}OH)^+$ calculated 270.14886, found 270.14863.

1-(2-Nitrophenyl)-2-phenylethanol (57) The title compound was synthesized from 2-iodonitrobenzene **36** (1.00 g, 4.02 mmol) and phenylacetaldehyde according to general method A. Purification by flash chromatography (petroleum ether/ethyl acetate 6:1) gave **57** (331 mg, 32 %) as a brown solid. ^{1}H NMR (500 MHz, MeOH-d_4) δ 2.84-2.89 (m, 1H), 3.07-3.10 (m, 1H), 5.42 (dd, *J* = 8.5, *J* = 3.8, 1H), 7.17-7.19 (m. 1H), 7.22-7.26 (m, 4H), 7.43-7.47 (m, 1H), 7.64-7.68 (m, 1H), 7.83 (dd, *J* = 7.9, *J* = 1.6, 1H), 7.87 (dd, *J* = 8.2, *J* = 1.3, 1H). ^{13}C NMR (125 MHz, MeOH-d_4) δ 46.2, 71.1, 124.9, 127.3, 129.1, 129.1, 129.4, 130.6, 134.2, 139.8, 141.6. R_t = 11.10 min; purity ≥ 97 % (UV). HRMS (ESI) *m/z*: $(M+H)^+$ calculated 244.09682, found 244.09712.

1-(2-Nitrophenyl)-3-phenylpropan-1-ol (58) The title compound was synthesized from 2-iodonitrobenzene **36** (1.00 g, 4.02 mmol) and 3-phenylpropanal according to general method A. Purification by flash chromatography (petroleum ether/ethyl acetate 6:1) gave **58** (331 mg, 32 %) as a brown solid. ^{1}H NMR (500 MHz, MeOH-d_4) δ 1.88-1.96 (m, 1H), 2.01-2.08 (m, 1H), 2.70-2.76 (m, 1H), 2.84-2.90 (m, 1H), 5.16 (dd, *J* = 8.8, *J* = 3.5, 1H), 7.12-7.16 (m, 1H), 7.18-7.20 (m, 2H), 7.22-7.26 (m, 2H), 7.42-7.46 (m, 1H), 7.66-7.69, 7.84-7.87 (m, 2H) ^{13}C NMR (125 MHz, MeOH-d_4) δ 33.6, 41.8, 69.3, 124.9, 126.8, 129.0, 129.1, 129.4, 129.4, 134.2, 141.9, 143.0. R_t = 11.55 min; purity ≥ 95 % (UV). HRMS (ESI) *m/z*: $(M\text{-}OH)^+$ calculated 240.10191, found 240.11247.

Naphthalen-1-yl(2-nitrophenyl)methanol (59) The title compound was synthesized from 2-iodonitrobenzene **36** (1.00 g, 4.02 mmol) and 1-naphthaldehyde according to general method A. Purification by flash chromatography (petroleum ether/ethyl acetate 6:1) gave **59** (302 mg, 27 %) as a brown solid. ^{1}H NMR (500 MHz, MeOH-d_4) δ 7.19 (d, *J* = 6.9, 1H), 7.23 (s, 1H), 7.35-7.38 (m, 1H), 7.47-7.53 (m, 3H), 7.62-7.65 (m, 1H), 7.69-7.71 (m, 1H), 7.81 (d, *J* = 8.2, 1H), 7.87-7.89 (m, 1H), 7.96 (dd, *J* = 8.2, *J* = 1.3, 1H). ^{13}C NMR (125 MHz, MeOH-d_4) δ 68.8, 124.8, 125.4, 125.6, 126.1, 127.3, 129.6, 129.6, 129.7, 130.5, 132.7, 134.0, 135.4, 139.4, 139.8, 150.1. R_t = 11.39 min; purity ≥ 97 % (UV). HRMS (ESI) *m/z*: $(M\text{-}OH)^+$ calculated 262.08626, found 262.08606. Mp: 74-75°C (Lit. 68-70°C).[S14]

Naphthalen-2-yl(2-nitrophenyl)methanol (60) The title compound was synthesized from 2-iodonitrobenzene **36** (1.00 g, 4.02 mmol) and 2-naphthaldehyde according to general method A. Purification by flash chromatography (petroleum ether/ethyl acetate 6:1) gave **60** (969 mg, 86 %) as a brown oil. ^{1}H NMR (500 MHz, MeOH-d_4) δ 6.56 (s, 1H), 7.42 (dd, J = 8.5, J = 1.6, 1H), 7.43-7.45 (m, 2H), 7.47-7.50 (m, 1H), 7.68-7.71 (m, 1H), 7.73-7.74 (m, 1H), 7.77-7.81 (m, 1H), 7.88 (dd, J = 8.2, J = 1.0, 1H), 7.90 (dd, J = 8.2, J = 1.6, 1H). ^{13}C NMR (125 MHz, MeOH-d_4) δ 71.7, 125.2, 126.5, 126.9, 127.1, 127.2, 128.6, 129.1, 129.1, 129.4, 130.0, 134.1, 134.3, 134.6, 140.0, 141.4, 150.0. R_t = 11.58 min; purity ≥ 95 % (UV). HRMS (ESI) *m/z*: $(M\text{-}OH)^+$ calculated 262.08626, found 262.08591.

(2-Nitrophenyl)(thiophen-2-yl)methanol (61) The title compound was synthesized from 2-iodonitrobenzene **36** (1.00 g, 4.02 mmol) and thiophen-2-carboxaldehyde according to general method A. Purification by flash chromatography (petroleum ether/ethyl acetate 5:1) gave **61** (514 mg, 54 %) as a brown oil. ^{1}H NMR (500 MHz, MeOH-d_4) δ 6.64 (s, 1H), 6.83-6.91 (m, 2H), 7.30 (d, J = 4.1, 1H), 7.50 (t, J = 7.3, 1H), 7.71 (t, J = 7.3, 1H), 7.91 (d, J = 7.9, 1H), 7.97 (d, J = 7.9, 1H). ^{13}C NMR (125 MHz, MeOH-d_4) δ 67.5, 125.2, 126.2, 126.3, 127.4, 129.4, 129.6, 134.3, 140.2, 148.2, 149.3. R_t = 9.74 min; purity ≥ 99 % (UV). HRMS (ESI) *m/z*: $(M\text{-}OH)^+$ calculated 218.02703, found 218.02672.

(2-Nitrophenyl)(thiophen-3-yl)methanol (62) The title compound was synthesized from 2-iodonitrobenzene **36** (1.00 g, 4.02 mmol) and thiophene-3-carboxaldehyde according to general method A. Purification by flash chromatography (petroleum ether/ethyl acetate 5:1) gave **62** (584 mg, 62 %) as a green-brown solid. ^{1}H NMR (500 MHz, MeOH-d_4) δ 6.45 (s, 1H), 7.01 (dd, J = 5.0, J = 1.3, 1H), 7.14-7.15 (m, 1H), 7.32 (dd, J = 5.0, J = 2.8, 1H), 7.48 (t, J = 7.8, 1H), 7.69 (t, J = 7.6, 1H), 7.87-7.90 (m, 2H). ^{13}C NMR (125 MHz, MeOH-d_4) δ 67.9, 123.2, 125.1, 126.8, 127.8, 129.4, 129.6, 134.2, 140.3, 145.4, 149.6. R_t = 9.79 min; purity ≥ 95 % (UV). HRMS (ESI) *m/z*: $(M\text{-}OH)^+$ calculated 218.02703, found 218.02670. Mp: 62-64°C.

Furan-2-yl(2-nitrophenyl)methanol (63) The title compound was synthesized from 2-iodonitrobenzene **36** (1.00 g, 4.02 mmol) and furan-2-carboxaldehyde according to general method A. Purification by flash chromatography (petroleum ether/ethyl acetate 5:1) gave **63** (391 mg, 44 %) as a red-brown solid. ^{1}H NMR (500 MHz, MeOH-d_4) δ 6.01 (dt, J = 3.2, J = 0.6, 1H), 6.31 (dd, J = 3.2, J = 1.9, 1H), 6.44 (s, 1H), 7.42 (dd, J = 1.9, J = 0.7, 1H), 7.53 (td, J = 7.7, J = 1.6, 1H), 7.73 (td, J = 7.6, J = 1.3, 1H), 7.93-7.97 (m, 2H). ^{13}C NMR (125 MHz, MeOH-d_4) δ 65.7, 108.3, 111.2, 125.3, 129.7, 129.8, 134.2, 137.9, 143.7, 149.4, 156.5. R_t = 8.97 min; purity ≥ 98 % (UV). HRMS (ESI) *m/z*: $(M\text{-}OH)^+$ calculated 202.04955, found 202.04987. Mp: 52-53°C.

Furan-3-yl(2-nitrophenyl)methanol (64) The title compound was synthesized from 2-iodonitrobenzene **36** (1.00 g, 4.02 mmol) and furan-3-carboxaldehyde according to general method A. Purification by flash chromatography (petroleum ether/ethyl acetate 7:1) gave **64** (412 mg, 47 %) as a brown solid. ^{1}H NMR (500 MHz, MeOH-d_4) δ 6.34 (s, 1H), 6.34-6.35 (m, 1H), 7.29-7.30 (m, 1H), 7.40 (t, J = 1.6, 1H), 7.47-7.05 (m, 1H), 7.70 (t, J = 7.6, 1H), 7.89 (dd, J = 8.2, J = 0.9, 1H), 7.93 (dd, J = 7.9, J = 0.9, 1H). ^{13}C NMR (125 MHz, MeOH-d_4) δ 64.8, 110.4, 125.1, 129.3, 129.4, 129.4, 134.2, 140.1, 141.2, 144.4. R_t = 8.90 min; purity ≥ 98 % (UV). HRMS (ESI) *m/z*: $(M\text{-}OH)^+$ calculated 202.04987, found 202.04947. Mp: 35-36°C.

(2-Nitrophenyl)(pyridin-2-yl)methanol (65) The title compound was synthesized from 2-iodonitrobenzene **36** (1.00 g, 4.02 mmol) and pyridine-2-carboxaldehyde according to general method A. Purification by flash chromatography (petroleum ether/ethyl acetate 3:1; TEA 0,1 %) gave **65** (410 mg, 44 %) as a brown solid. ^{1}H NMR (500 MHz, MeOH-d_4) δ 6.47 (s, 1H), 7.27-7.29 (m, 1H), 7.48-7.51 (m, 2H), 7.67 (td, J = 7.9, J = 1.3, 1H), 7.76 (dd, J = 7.9, J = 1.6, 1H), 7.80 (td, J = 7.6, J = 1.6,

1H), 7.92 (dd, *J* = 8.2, *J* = 1.3, 1H), 8.42-8.43 (m, 1H). ^{13}C NMR (125 MHz, MeOH-d_4) δ 72.5, 123.0, 124.0, 125.3, 129.6, 130.4, 134.1, 138.6, 139.0, 149.6, 150.1, 162.6. R_t = 4.92 min; purity ≥ 99 % (UV). HRMS (ESI) *m/z*: $(M+H)^+$ calculated 231.07642, found 231.07510. Mp: 71°C.

(2-Nitrophenyl)(pyridin-3-yl)methanol (66) The title compound was synthesized from 2-iodonitrobenzene **36** (1.00 g, 4.02 mmol) and pyridine-3-carboxaldehyde according to general method A. Purification by flash chromatography (petroleum ether/ethyl acetate 3:1; TEA 0.1 %) gave **66** (602 mg, 65 %) as a orange-brown solid. ^{1}H NMR (500 MHz, MeOH-d_4) δ 6.42 (s, 1H), 7.38 (dd, *J* = 7.9, *J* = 4.7, 1H), 7.52-7.56 (m, 1H), 7.73-7.78 (m, 2H), 7.94-7.98 (m, 2H), 8.42 (dd, *J* = 4.7, *J* = 1.6, 1H), 8.50 (d, *J* = 1.9, 1H). ^{13}C NMR (125 MHz, MeOH-d_4) δ 69.7, 125.1, 125.5, 129.8, 129.9, 134.6, 137.0, 139.4, 140.7, 149.0, 149.2, 149.5. R_t = 4.86 min; purity ≥ 99 % (UV).). HRMS (ESI) *m/z*: $(M+H)^+$ calculated 231.07642, found 231.07549. Mp: 78°C (Lit. 105-106).[S15]

(2-Nitrophenyl)(pyridin-4-yl)methanol (67) The title compound was synthesized from 2-iodonitrobenzene **36** (1.00 g, 4.02 mmol) and pyridine-4-carboxaldehyde according to general method A. Purification by flash chromatography (petroleum ether/ethyl acetate 1:1; TEA 0.1 %) gave **67** (553 mg, 60 %) as a brownish powder. ^{1}H NMR (500 MHz, MeOH-d_4) δ 6.37 (s, 1H), 7.40-7.41 (m, 1H), 7.41-7.42 (m, 1H), 7.52-7.56 (m, 1H), 7.71-7.74 (m, 1H), 7.81-7.83 (m, 1H), 7.95 (dd, *J* = 8.2, *J* = 1.3, 1H), 8.46-8.48 (m, 2H). ^{13}C NMR (125 MHz, MeOH-d_4) δ 70.3, 123.6, 125.4, 130.0, 130.0, 134.6, 139.0, 149.8, 150.1, 154.5. R_t = 4.79 min; purity ≥ 99 % (UV).). HRMS (ESI) *m/z*: $(M+H)^+$ calculated 231.07642, found 231.07542. Mp: 158-160°C (Lit. 169-170°C).[S15]

2-(3-Hydroxy-3-(2-nitrophenyl)propyl)isoindoline-1,3-dione (68) The title compound was synthesized from 2-iodonitrobenzene **36** (4.00 g, 16.06 mmol) and aldehyde **68i** according to general method A. Purification by flash chromatography (petroleum ether/ethyl acetate 2:1) gave **68** (2.25 g, 43 %) as a yellowish solid. ^{1}H NMR (500 MHz, DMSO-d_6) δ 1.82-1.89 (m, 1H), 1.96-2.02 (m, 1H), 3.72-3.78 (m, 1H), 3.81-3.86 (m, 1H), 5.01-5.04 (m, 1H), 5.66 (dd, *J* = 4.4, *J* = 1.1, 1H), 7.45-7.50 (m, 1H), 7.71-7.74 (m, 1H), 7.82-7.89 (m, 6H). ^{13}C NMR (125 MHz, DMSO-d_6) δ 35.0, 36.8, 65.8, 122.9, 123.9, 128.0, 128.1, 131.7, 133.5, 134.3, 140.7, 147.0, 167.9. R_t = 10.45 min; purity ≥ 98 % (UV). HRMS (ESI) *m/z*: $(M+H)^+$ calculated 327.09755, found 327.09695. Mp: 154-155°C.

2-(4-Hydroxy-4-(2-nitrophenyl)butyl)isoindoline-1,3-dione (69) The title compound was synthesized from 2-iodonitrobenzene **36** (2.49 g, 10.00 mmol) and aldehyde **69i** according to general method A. Purification by flash chromatography (petroleum ether/ethyl acetate 5:2) gave **69** (2.89 g, 85 %) as a yellowish solid. ^{1}H NMR (500 MHz, DMSO-d_6) δ 1.56-1.61 (m, 1H), 1.63-1.72 (m, 2H), 1.78-1.86 (m, 1H), 3.58-3.61 (m, 2H), 4.93-4.96 (m, 1H), 5.54 (d, *J* = 4.7, 1H), 7.46-7.49 (m, 1H), 7.70 (td, *J* = 7.3, *J* = 1.3, 1H), 7.76 (dd, *J* = 7.9, *J* = 1.3, 1H), 7.82-7.87 (m, 5H). ^{13}C NMR (125 MHz, DMSO-d_6) δ 24.0, 35.7, 37.4, 67.3, 123.0, 123.6, 128.0, 131.6, 133.2, 134.3, 140.6, 147.5, 167.9. R_t = 10.86 min; purity ≥ 99 % (UV). HRMS (ESI) *m/z*: $(M+H)^+$ calculated 341.11320, found 341.11214. Mp: 169°C.

2-(5-Hydroxy-5-(2-nitrophenyl)pentyl)isoindoline-1,3-dione (70) The title compound was synthesized from 2-iodonitrobenzene **36** (4.00 g, 16.06 mmol) and aldehyde **70i** according to general method A. Purification by flash chromatography (petroleum ether/ethyl acetate 2:1) gave **70** (2.29 g, 40 %) as a yellowish solid. ^{1}H NMR (500 MHz, DMSO-d_6) δ 1.33-1.42 (m, 1H), 1.44-1.50 (m, 1H), 1.52-1.70 (m, 4H), 3.57 (t, *J* = 7.3, 1H), 4.93 (m, 1H), 5.49 (d, *J* = 4.7, 1H), 7.50-7.48 (m, 1H), 7.68-7.71 (m, 1H), 7.77 (dd, *J* = 7.9, *J* = 1.3, 1H), 7.82-7.87 (m, 1H). ^{13}C NMR (125 MHz, DMSO-d_6) δ 23.0, 27.6, 37.4, 38.0, 67.2, 123.0, 123.6, 127.9, 128.1, 131.6, 133.2, 134.3, 141.0, 147.7, 167.9. R_t =

11.63 min; purity ≥ 99 % (UV). HRMS (ESI) *m/z*: $(M+H)^+$ calculated 355.12885, found 355.12828. Mp: 120-122°C.

1-(5-Methyl-2-nitrophenyl)propan-1-ol (71) The title compound was synthesized from 3-iodo-4-nitro-toluene **38** (500 mg, 1.90 mmol) and propionaldehyde according to general method A. Purification by column chromatography (hexane/ethyl acetate 8:1) gave **71** (244 mg, 55 %) as an orange solid. ^{1}H NMR (300 MHz, acetone-d_6) δ 1.01 (t, J = 7.3, 3H), 1.57-1.83 (m, 2H), 2.45 (s, 3H), 4.47 (d, J = 4.5, 1H), 5.16-5.22 (m, 1H), 7.29 (dd, J = 5.7, J = 1.6, 1H), 7.70 (s, 1H), 7.80 (d, J = 8.2, 1H). ^{13}C NMR (75 MHz, acetone-d_6) δ 10.9, 21.5, 32.7, 70.4, 124.9, 129.1, 129.4, 142.4, 145.0, 146.7. R_t = 11.06 min; purity ≥ 98 % (UV). HRMS (ESI) *m/z*: $(M+H)^+$ calculated 196.09646, found 196.09682. Mp: 72-74°C.

(5-Methyl-2-nitrophenyl)(thiophen-2-yl)methanol (72) The title compound was synthesized from 3-iodo-4-nitro-toluene **38** (500 mg, 1.90 mmol) and thiophen-2-carboxaldehyde according to general method A. Purification by column chromatography (hexane/ethyl acetate 8:1) gave **72** (54 mg, 11 %) as an orange solid. ^{1}H NMR (500 MHz, acetone-d_6) δ 2.47 (s, 3H), 5.45 (s, 1H), 6.72 (s, 1H), 6.85-6.87 (m, 1H), 6.91 (dd, J = 5.09, J = 3.5, 1H), 7.34 (dd, J = 5.05, J = 1.2, 1H), 7.37 (dd, J = 8.1, J = 1.6, 1H), 7.84 (m, 1H), 7.88 (d, J = 8.3, 1H). ^{13}C NMR (125 MHz, acetone-d_6) δ 21.6, 67.1, 125.3, 125.6, 126.0, 127.2, 129.6, 129.8, 140.3, 145.5, 146.6, 148.6. R_t = 11.78 min; purity ≥ 95 % (UV). HRMS (ESI) *m/z*: $(M-OH)^+$ calculated 232.04268, found 232.04251. Mp: 93-96°C.

(5-Methyl-2-nitrophenyl)(thiophen-3-yl)methanol (73) The title compound was synthesized from 3-iodo-4-nitro-toluene **38** (500 mg, 1.90 mmol) and thiophene-3-carboxaldehyde according to general method A. Purification by column chromatography (hexane/ethyl acetate 8:1) gave **73** (127 mg, 27 %) as a yellow oil. ^{1}H NMR (500 MHz, acetone-d_6) δ 2.45 (s, 3H), 5.13 (d, J = 4.7, 1H), 6.52 (d, J = 4.8, 1H), 7.06 (dd, J = 5.1, J = 1.3, 1H), 7.21-7.22 (m, 1H), 7.33 (dd, J = 7.6, J = 1.3, 1H), 7.36 (dd, J = 5, J = 3, 1H), 7.78 (m, 1H), 7.83 (d, J = 8.2, 1H). ^{13}C NMR (125 MHz, acetone-d_6) δ 21.6, 67.5, 122.6, 125.1, 126.5, 127.7, 129.5, 129.9, 142.5, 145.3, 145.8, 146.8. R_t = 12.26 min; purity ≥ 95 % (UV). HRMS (ESI) *m/z*: $(M-OH)^+$ calculated 232.04268, found 232.04242.

Furan-2-yl(5-methyl-2-nitrophenyl)methanol (74) The title compound was synthesized from 3-iodo-4-nitro-toluene **38** (500 mg, 1.90 mmol) and furan-2-carboxaldehyde according to general method A. Purification by column chromatography (hexane/ethyl acetate 8:1) gave **74** (244 mg, 44 %) as a red-brown oil. ^{1}H NMR (300 MHz, acetone-d_6) δ 2.50 (s, 3H), 5.29 (s, 1H), 6.03 (d, J = 3.3, 1H), 6.32 (dd, J = 3.3, J = 1.9, 1H), 6.53 (s, 1H), 7.39 (d, J = 8.4, 1H), 7.45 (dd, J = 1.9, J = 0.9, 1H), 7.87 (s, 1H), 7.91 (d, J = 8.3, 1H). ^{13}C NMR (75 MHz, acetone-d_6) δ 21.6, 65.3, 107.7, 111.0, 125.3, 129.8, 130.0, 138.0, 143.2, 145.4, 146.6, 156.8. R_t = 10.90 min; purity ≥ 96 % (UV). HRMS (ESI) *m/z*: $(M-OH)^+$ calculated 216.06522, found 216.06552.

2-(3-Hydroxy-3-(5-methyl-2-nitrophenyl)propyl)isoindoline-1,3-dione (75) The title compound was synthesized from 3-iodo-4-nitro-toluene **38** (500 mg, 1.90 mmol) and aldehyde **68i** according to general method A. Purification by semi-preparative HPLC gave **75** (100 mg, 15 %) as a yellow crystalline solid. ^{1}H NMR (300 MHz, $CDCl_3$) δ 1.82-1.93 (m, 1H), 2.19-2.30 (m, 1H), 2.44 (s, 3H), 3.90-3.97 (m, 1H), 4.02-4.12 (m, 1H), 5.27 (dd, J = 9.7, J = 2.8, 1H), 7.17 (dd, J = 8.7, J = 1.9, 1H), 7.67 (s, 1H), 7.73-7.77 (m, 2H), 7.85-7.89 (m, 3H). ^{13}C NMR (75 MHz, $CDCl_3$) δ 21.8, 35.0, 37.7, 66.6, 123.6, 125.0, 128.4, 128.8, 132.2, 134.3, 140.0, 144.8, 145.4, 169.2. R_t = 11.91 min; purity ≥ 98 % (UV). HRMS (ESI) *m/z*: $(M+H)^+$ calculated 341.11320, found 341.11255. Mp: 130-132°C.

2-(4-Hydroxy-4-(5-methyl-2-nitrophenyl)butyl)isoindoline-1,3-dione (76) The title compound was synthesized from 3-iodo-4-nitro-toluene **38** (500 mg, 1.90 mmol) and aldehyde **69i** according to general method A. Purification by semi-preparative HPLC gave **76** (168 mg, 25 %) as an orange oil. ^{1}H NMR (300 MHz, $CDCl_3$) δ 1.75-2.02 (m, 4H), 2.44 (s, 3H), 2.59 (s, 1H), 3.79 (t, J = 6.4, 2H), 5.32 (dd, J = 7.6, J = 3.2, 1H), 7.19 (dd, J = 8.6, J = 2.0, 1H), 7.59 (d, J = 1.6, 1H), 7.68-7.74 (m, 2H), 7.81-7.87 (m, 3H). ^{13}C NMR (75 MHz, $CDCl_3$) δ 21.8, 25.8, 35.2, 37.9, 69.4, 123.4, 125.0, 128.6, 128.9, 132.6, 134.1, 140.2, 145.1, 145.6, 168.7. R_t = 12.40 min; purity ≥ 99 % (UV). HRMS (ESI) *m/z*: $(M\text{-}OH)^+$ calculated 355.12848, found 355.12885.

3-Amino-1-(2-nitrophenyl)propan-1-ol (77) The title product was prepared according to method E to yield **77** (89 %) as a brown oil. ^{1}H NMR (500 MHz, MeOH-d_4) δ 1.77-1.84 (m, 1H), 1.91-1.97 (m, 1H), 2.81-2.91 (m, 2H), 5.26 (dd, J = 9.0, J = 3.2, 1H), 7.44-7.48 (m, 1H), 7.68-7.71 (m, 1H), 7.86-7.80 (m, 2H). ^{13}C NMR (125 MHz, MeOH-d_4) δ 40.1, 42.3, 68.6, 125.0, 129.1, 129.2, 134.3, 142.1, 149.1. R_t = 1.60 min; purity ≥ 97 % (UV).[§] HRMS (ESI) *m/z*: $(M\text{-}OH)^+$ calculated 197.09167, found 197.09207.

4-Amino-1-(2-nitrophenyl)butan-1-ol (78) The title product was prepared according to method E to yield **78** (62 %) as a brown oil. ^{1}H NMR (500 MHz, MeOH-d_4) δ 1.63-1.76 (m, 3H), 1.77-1.87 (m, 1H), 2.67-2.77 (m, 2H), 5.17 (dd, J = 7.9, J = 3.5, 1H), 7.45 (m, 1H), 7.67-7.70 (m, 1H), 7.85 (dd, J = 7.9, J = 1.6, 1H), 7.87 (dd, J = 8.2, J = 1.3, 1H). ^{13}C NMR (125 MHz, MeOH-d_4) δ 30.0, 37.3, 42.1, 69.4, 125.0, 129.0, 129.1, 134.2, 142.1, 149.3. R_t = 5.24 min; purity ≥ 98 % (UV).[§] HRMS (ESI) *m/z*: $(M+H)^+$ calculated 211.10772, found 211.10738.

5-Amino-1-(2-nitrophenyl)pentan-1-ol (79) The title product was prepared according to method E to yield **79** (86 %) as a brown oil. ^{1}H NMR (500 MHz, MeOH-d_4) δ 1.44-1.61 (m, 4H), 1.63-1.70 (m, 1H), 1.73-1.80 (m, 1H), 2.60-2.68 (m, 2H), 5.16 (dd, J = 8.5, J = 3.5, 1H), 7.43-7.47 (m, 1H), 7.66-7.70 (m, 1H), 7.83 (dd, J = 7.9, J = 1.6, 1H), 7.86 (dd, J = 8.2, J = 1.3, 1H). ^{13}C NMR (125 MHz, MeOH-d_4) δ 24.5, 33.4, 39.7, 42.4, 69.5, 124.9, 129.0, 129.1, 134.2, 142.2, 149.3. R_t = 7.04 min; purity ≥ 99 % (UV).[§] HRMS (ESI) *m/z*: $(M+H)^+$ calculated 225.12307, found 225.12337.

5-(Dimethylamino)-*N*-(3-hydroxy-3-(2-nitrophenyl)propyl)naphthalene- 1-sulfonamide (80) To a solution of the amine **77** (150 mg, 0.765 mmol) in dry DCM (40 ml) a solution of dansyl chloride (200 mg, 0.803 mmol) in dry DCM and TEA (0.158 ml, 1.137 mmol) were added. After stirring for 24 h at room temperature, the solution was washed with water and the aqueous phase was extracted twice with DCM. The combined organic layers were dried and the solvent was evaporated under reduced pressure. The crude product was purified by semi-preparative HPLC to yield **80** (147 mg, 45 %) as a yellow solid. ^{1}H NMR (500 MHz, $CDCl_3$) δ 1.69-1.74 (m, 1H), 1.92-1.98 (m, 1H), 2.60 (d, J = 3.8, 1H), 2.89 (s, 6H), 3.02-3.09 (m, 1H), 3.19-3.26 (m, 1H), 5.25-5.27 (m, 1H), 5.46 (dd, J = 7.6, J = 3.5, 1H), 7.19 (dd, J = 7.6, J = 0.6, 1H), 7.36-7.39 (m, 1H), 7.51-7.55 (m, 2H), 7.57-7.62 (m, 2H), 7.88 (dd, J = 8.2, J = 1.3, 1H), 8.26 (dd, J = 7.3, J = 1.3, 1H), 8.32-8.34 (m, 1H), 8.53-8.55 (m, 1H). ^{13}C NMR (125 MHz, $CDCl_3$) δ 36.9, 41.3, 45.6, 68.4, 115.4, 118.9, 123.4, 124.6, 128.1, 128.4, 128.6, 129.7, 130.0, 130.1, 130.6, 133.9, 134.6, 139.6, 147.3, 152.2. R_t = 8.77 min; purity ≥ 96 % (UV). HRMS (ESI) *m/z*: $(M+H)^+$ calculated 430.14312, found 430.14242. Mp: 53-56°C.

5-(Dimethylamino)-*N*-(4-hydroxy-4-(2-nitrophenyl)butyl)naphthalene-1-sulfonamide (81) Synthesis of **81** was carried out following the procedure described for **80** using **78** (85 mg, 0.404 mmol), dansyl chloride (106 mg, 0.424 mmol) and TEA (0.10 ml, 0.687 mmol). **81** (52 mg, 29 %) was obtained as a yellow solid. ^{1}H NMR (500 MHz, $CDCl_3$) δ 1.57-1.73 (m, 4H), 2.58 (s, 1H), 2.87 (s, 6H), 2.90-3.02 (m, 2H), 5.07-5.10 (m, 1H), 5.16 (t, J = 6.0, 1H), 7.15 (d, J = 7.6, 1H), 7.35-7.39 (m,

1H), 7.49-7.59 (m, 3H), 7.65 (dd, *J* = 7.9, *J* = 1.6, 1H), 7.86 (dd, *J* = 8.2, *J* = 1.3, 1H), 8.23 (dd, *J* = 7.3, *J* = 1.3, 1H), 8.27-8.30 (m, 1H), 8.50-8.53 (m, 1H). ^{13}C NMR (125 MHz, $CDCl_3$) δ 26.5, 35.1, 43.1, 45.5, 69.0, 115.3, 118.8, 123.3, 124.5, 128.0, 128.2, 128.5, 129.7, 129.8, 130.0, 130.5, 133.8, 134.8, 140.2, 147.6, 152.1. R_t = 10.18 min; purity ≥ 98 % (UV). HRMS (ESI) *m/z*: $(M+H)^+$ calculated 444.15877, found 444.15416. Mp: 47-48°C.

5-(Dimethylamino)-*N*-(5-hydroxy-5-(2-nitrophenyl)pentyl)naphthalene- 1-sulfonamide (82) Synthesis of **82** was carried out following the procedure described for **80** using **81** (150 mg, 0.669 mmol), dansyl chloride (175 mg, 0.702 mmol) and TEA (0.158 ml, 1.137 mmol). **82** (126 mg, 41 %) was obtained as a as a yellow solid. ^{1}H NMR (500 MHz, $CDCl_3$) δ 1.31-1.50 (m, 4H), 1.52-1.60 (m, 1H), 1.62-1.68 (s, 1H), 2.25 (d, *J* = 4.1, 1H), 2.88 (s, 6H), 2.90-2.94 (m, 2H), 4.70 (t, *J* = 6.3, 1H), 5.06-5.09 (m, 1H), 7.18 (dd, *J* = 7.6, *J* = 0.9, 1H), 7.38-7.41 (m, 1H), 7.51-7.56 (m, 2H), 7.59-7.63 (m, 1H), 7.72 (dd, *J* = 7.9, *J* = 1.3, 1H), 7.88 (dd, *J* = 8.2, *J* = 1.3, 1H), 8.25 (dd, *J* = 7.3, *J* = 1.3, 1H), 8.28-8.30 (m, 1H), 8.52-8.54 (m, 1H). ^{13}C NMR (125 MHz, $CDCl_3$) δ 23.1, 29.2, 37.5, 43.2, 45.5, 69.1, 115.3, 118.8, 123.4, 124.5, 128.1, 128.2, 128.6, 129.8, 129.9, 130.6, 133.7, 134.8, 140.2, 152.2. R_t = 9.51 min; purity ≥ 98 % (UV). HRMS (ESI) *m/z*: $(M+H)^+$ calculated 458.17442, found 458.17363. Mp: 50-51°C.

4-((7-Nitrobenzo[c][1,2,5]oxadiazol-4-yl)amino)-1-(2-nitrophenyl)butan-1-ol (83) At 0°C, 4-chlor-7-nitrobenzofurazan (100 mg, 0.499 mmol) and $NaHCO_3$ (126 mg, 1.497 mmol) were added to a solution of **78** (105 mg, 0.499 mmol) in 8 ml of methanol. The mixture was stirred for 30 min at 0°C, followed by 90 min at room temperature and, finally, another 90 min at 50°C. After extraction with ethyl acetate (three times) the combined organic layers were dried and concentrated under reduced pressure. The crude product was purified by flash chromatography (petroleum ether/ethyl acetate 1:2) to give **83** (74 mg, 40 %) as a brown oil. ^{1}H NMR (500 MHz, MeOH-d_4) δ 1.76-1.83 (m, 1H), 1.91-1.99 (m, 2H), 2.00-2.06 (m, 1H), 3.59 (s, 2H), 5.23 (dd, *J* = 8.5, *J* = 2.8, 1H), 6.33 (d, *J* = 8.8, 1H), 7.43-7.47 (m, 1H), 7.66-7.70 (m, 1H), 7.51-7.87 (m, 2H), 8.49 (d, *J* = 7.9, 1H). ^{13}C NMR (125 MHz, MeOH-d_4) δ 14.4, 26.0, 37.0, 61.5, 69.4, 125.0, 129.1, 129.1, 134.4, 138.5, 142.0, 149.2. R_t = 10.82 min; purity ≥ 96 % (UV). HRMS (ESI) *m/z*: $(M+H)^+$ calculated 374.10951, found 574.10908.

***N*-(4-Hydroxy-4-(2-nitrophenyl)butyl)-3-((7-nitrobenzo[c][1,2,5]oxadiazol-4-yl)amino)propanamide (84)** To a solution of **78** (200 mg, 0.951 mmol) in 12 ml of acetonitrile **84i** (240 mg, 0.951 mmol), *N*-methylmorpholine (0.52 ml, 4.755 mmol), *N*-hydroxy-benzotriazole (HOBt) hydrate (231 mg, ~1.510 mmol) and *N*-(3-dimethylaminopropyl)-*N'*-ethylcarbodiimide (EDC) hydrochloride (328 mg, 1.712 mmol) were added. After stirring for 20 h at room temperature water was added and the mixture was extracted with ethyl acetate (three times). The combined organic layers were washed with brine, dried, and concentrated in vacuo. The crude product was purified by flash chromatography (100 % ethyl acetate) to give **84** (133 mg, 32 %) as a brown oil. ^{1}H NMR (500 MHz, MeOH-d_4) δ 1.56-1.64 (m, 2H), 1.71-1.76 (m, 2H), 2.65 (t, *J* = 6.9, 2H), 3.19-3.27 (m, 2H), 3.83 (s, 2H), 5.09 (dd, *J* = 8.2, *J* = 2.7, 1H), 6.40 (d, *J* = 8.8, 1H), 6.41-6.45 (m, 1H), 7.64-7.67 (m, 1H), 7.77 (dd *J* = 7.9, *J* = 1.3, 1H), 7.82 (dd, *J* = 8.2, *J* = 1.3, 1H), 8.50 (d, *J* = 8.8, 1H). ^{13}C NMR (125 MHz, MeOH-d_4) δ 27.0, 37.0, 40.2, 69.3, 77.3, 118.0, 124.9, 129.0, 129.0, 134.3, 142.0, 149.1, 173.1. R_t = 9.22 min; purity ≥ 99 % (UV). HRMS (ESI) *m/z*: $(M+H)^+$ calculated 445.14662, found 445.14667.

***N*-(4-Hydroxy-4-(2-nitrophenyl)butyl)-6-((7-nitrobenzo[c][1,2,5]oxadiazol-4-yl)amino)hexanamide (85)** Synthesis of **85** was carried out following the procedure described for **84** using **78** (130 mg, 0.618 mmol), **85i** (182 mg, 0.618 mmol), *N*-methylmorpholine (0.340 ml, 3.092 mmol), HOBt hydrate (150 mg, ~0.980 mmol) and EDC hydrochloride (213 mg, 1.113 mmol) in 6 ml of acetonitrile. The crude product was purified by preparative HPLC to yield **85** (117 mg, 46 %) as a

brown oil. ^{1}H NMR (500 MHz, MeOH-d_4) δ 1.43-1.50 (m, 2H), 1.62-1.71 (m, 4H), 1.43-1.82 (m, 4H), 2.21 (t, J = 7.4, 2H), 3.20-3.23 (m, 2H), 3.51 (s, 2H), 5.13-5.15 (m, 1H), 6.33 (d, J = 8.8, 1H), 7.41-7.45 (m, 1H), 7.66 (td, J = 7.6, J = 1.3, 1H), 7.81-7.85 (m, 2H), 8.50 (d, J = 8.5, 1H). ^{13}C NMR (125 MHz, MeOH-d_4) δ 14.4, 26.6, 27.2, 27.5, 36.9, 37.2, 40.1, 69.4, 125.0, 129.0, 129.1, 134.3, 138.5, 142.1, 149.2, 155.3, 176.0. R_t = 13.75 min; purity ≥ 96 % (UV). HRMS (ESI) *m/z*: $(M+H)^+$ calculated 487.19357, found 487.19290.

1-(3',6'-dihydroxy-3-oxo-3H-spiro[isobenzofuran-1,9'-xanthen]-5-yl)-3-(4-hydroxy-4-(2-nitrophenyl)butyl)thiourea (86) Fluorescein isothiocyanate (111 mg, 0.285 mmol) was added to a solution of **78** (60 mg, 0.285 mmol) and DIEA (0.348 ml, 1.998 mmol) in 5 ml of DMF and the mixture was stirred for 18 h at room temperature. The solvent was evaporated under reduced pressure and the crude product was purified by preparative HPLC to give **86** (61 mg, 36 %) as an orange solid. ^{1}H NMR (500 MHz, MeOH-d_4) δ 1.71-1.96 (m, 4H), 3.49 (s, 2H), 5.21 (dd, J = 8.5, J = 2.8, 1H), 6.53 (dd, J = 8.8, J = 2.2, 2H), 6.67-6.68 (m, 4H), 7.14 (d, J = 8.2, 1H), 7.43-7.46 (m, 1H), 7.66-7.69 (m, 1H), 7.74 (dd, J = 8.2, J = 1.6, 1H), 7.85-7.89 (m, 2H), 8.19 (d, J = 1.9, 1H). ^{13}C NMR (125 MHz, MeOH-d_4) δ 26.8, 37.1, 69.5, 103.5, 111.5, 113.7, 125.0, 129.1, 129.1, 130.3, 134.3, 142.1, 149.2, 154.2, 171.2. R_t = 9.98 min; purity ≥ 97 % (UV). HRMS (ESI) *m/z*: $(M+H)^+$ calculated 600.14351, found 600.14344. Mp: 168-174°C.

6.4.2 Experiment procedure for HPLC, HRMS, and MS

The retention time R_t and purity of every compound tested in the biological assays were determined using HPLC according to the following procedure:

A SpectraSystems® LC system consisting of a pump, an autosampler, and a PDA detector was employed. The system was operated by the standard software Xcalibur®. An RP-C18 NUCLEODUR® 100-5 (125x3 mm) column (Macherey-Nagel GmbH, Düren, Germany) was used as stationary phase. All solvents were HPLC grade.
In a gradient run, the percentage of acetonitrile (containing 0.1 % trifluoroacetic acid; TFA) in an aqueous solution of 0.1 % TFA was increased from an initial concentration of 0 % at 0 min to 100 % at 15 min and kept at 100 % for 5 min. RT values determined without the use of trifluoroacetic acid are marked by a paragraph (§). The injection volume was 10 µL and flow rate was set to 800 µL/min. Chromatograms were recorded at 254 nm for the UV trace.

HRMS values were determined by the following procedure:

Measurements were performed on a Dionex Ultimate 3000 RSLC system using a Waters BEH C18, 50 x 2.1 mm, 1.7 µm dp column by injection of two µl methanolic sample. Separation was achieved by a linear gradient with (A) H2O + 0.1 % FA to (B) ACN + 0.1 % FA at a flow rate of 600 µL/min and 45 °C. The gradient was initiated by a 0.33 min isocratic step at 5 % B, followed by an increase to 95 % B in 9 min to end up with a 1 min flush step at 95 % B before reequilibration under the initial conditions. UV and MS detection were performed simultaneously. Coupling the HPLC to the MS was supported by an Advion Triversa Nanomate nano-ESI system attached to a Thermo Scientific Orbitrap. Mass spectra were acquired in centroid mode ranging from 100 – 2000 m/z at a resolution of R = 30000.

In two cases (**49** and **55**), m/z values were generated by a DSQII electron ionization analyzer (ThermoFisher, Dreieich, Germany). These values are marked by an asterisk (*).

For intermediates, m/z values were measured on an MSQ® electro spray mass spectrometer (ThermoFisher, Dreieich, Germany). A spray voltage of 3800 V, a capillary temperature of 350°C, and a source CID of 10 V was applied. MS spectra were acquired in positive mode.

6.4.3 Synthesis and analytical data of synthetic intermediates

*a) Synthesis and Analytical Data of Intermediates **68i** and **70i***[S16]

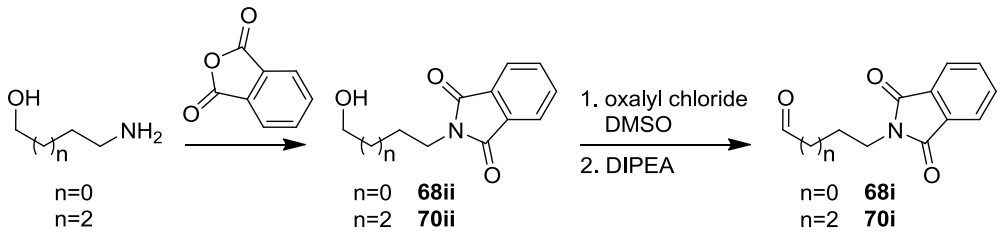

2-(3-Hydroxypropyl)isoindoline-1,3-dione (68ii) Phthalic anhydride (9.9 g, 67 mmol) was added to a solution of 3-aminopropan-1-ol (5.0 g, 67 mmol) and TEA (9.3 ml, 67 mmol) in 100 ml of toluene. The mixture was stirred for 3 h at 125°C and water was removed using a Dean-Stark apparatus. After cooling to room temperature the solvent was evaporated under reduced pressure to yield the desired product **68ii** (13.5 g, 99 %), which was used in the next step without further purification. ^{1}H NMR (500 MHz, DMSO-d_6) δ 1.71-1.76 (m, 2H), 3.43-3.46 (m, 2H), 3.63 (t, J = 7.3, 2H), 4.49 (s, 1H), 7.81-7.86 (m, 4H). ^{13}C NMR (125 MHz, DMSO-d_6) δ 31.2, 35.2, 58.5, 122.9, 131.7, 134.3, 167.9. MS (ESI) *m/z*: 206.3 $(M+H)^+$.

2-(5-Hydroxypentyl)isoindoline-1,3-dione (70ii) Following the procedure described for **68ii** using phthalic anhydride (16.1 g, 109 mmol), 5-aminopentan-1-ol (11.2 g, 109 mmol) and TEA (15.2 ml, 109 mmol) in 140 ml of toluene, the desired product **70ii** (25.1 g, 99 %) was obtained, which was used in the next step without further purification. ^{1}H NMR (500 MHz, DMSO-d_6) δ 1.25-1.32 (m, 2H), 1.40-1.46 (m, 2H), 1.56-1.62 (m, 2H), 3.34-3.38 (m, 2H), 3.56 (t, J = 7.1, 2H), 4.33 (s, 1H), 7.82-7.87 (m, 4H). ^{13}C NMR (125 MHz, DMSO-d_6) δ 22.8, 27.8, 32.0, 37.4, 60.4, 122.9, 131.6, 134.3, 167.9. MS (ESI) *m/z*: 234.2 $(M+H)^+$.

3-(1,3-Dioxoisoindolin-2-yl)propanal (68i) Oxalyl chloride (8.4 ml, 99 mmol) was added to 30 ml of dry DCM and the mixture was cooled to -78°C. Dry DMSO (21.1 ml, 297 mmol) was added drop-wise and the solution was stirred for 30 min. A solution of **68ii** (13.5 g, 66 mmol) in 25 ml of dry DCM was added drop-wise and the solution was stirred for 30 min. DIPEA (56.1 ml, 330 mmol) was added and the mixture was stirred for another 30 min at -78°C. The mixture was warmed to room temperature and a solution of NaH_2PO_4 (11.9 g, 99 mmol) in 20 ml of water was added. The aqueous layer was extracted three times with DCM and the combined organic layers were washed with 1 M HCl, saturated $NaHCO_3$ and brine. The solvent was removed under reduced pressure to yield **68i** (13.4 g, 100 %), which was sufficient pure for use in the next step. ^{1}H NMR (500 MHz, DMSO-d_6) δ 2.81 (td, J = 6.8, J = 1.6, 2H), 3.86 (t, J = 3.9, 2H), 7.82-7.87 (m, 4H), 9.67 (t, J = 1.6, 1H). ^{13}C NMR (125 MHz, DMSO-d_6) δ 31.4, 41.5, 123.0, 131.6, 134.3, 167.7.

5-(1,3-Dioxoisoindolin-2-yl)pentanal (70i) Following the procedure described for **68i** using oxalyl chloride (13.7 ml, 162 mmol) in 30 ml of DCM, DMSO (34.5 ml, 486 mmol), **70ii** (25.1 g, 108 mmol) in 20 ml of DCM, DIPEA (91.8 ml, 540 mmol) and a solution of NaH_2PO_4 (19.4 g, 162 mmol) in 30 ml of water, the desired product **70i** (20.1 g, 80 %) was obtained in sufficient purity for use in the next step without further purification. ^{1}H NMR (500 MHz, DMSO-d_6) δ 1.49-1.54 (m, 2H), 1.56-1.62 (m, 2H), 2.46 (td, J = 7.3, J = 1.6, 2H), 3.57 (t, J = 6.6, 2H), 7.78-7.87 (m, 4H), 9.64 (t, J = 1.4, 1H). ^{13}C NMR (125 MHz, DMSO-d_6) δ 18.8, 27.4, 37.1, 42.4, 122.9, 131.6, 134.3, 167.9. MS (ESI) *m/z*: 232.3 $(M+H)^+$.

*b) Synthesis and Analytical Data of Intermediate **69i***[S17]

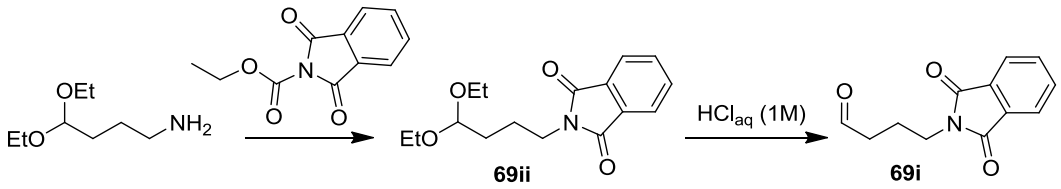

2-(4,4-Diethoxybutyl)isoindoline-1,3-dione (69ii) *N*-Carbethoxyphthalimide (13.0 g, 59 mmol) and 4-aminobutyraldehyde diethyl acetal (10.3 g, 59 mmol) were dissolved in THF (90 ml) and TEA (8.4 ml, 59 mmol) was added. After stirring for 20 h at room temperature the solvent was evaporated under reduced pressure and the remaining oil was purified by flash chromatography (*n*-hexane/ethyl acetate 8:1) to yield the title compound **69i** (15.4 g, 88 %) as a colorless oil. ^{1}H NMR (500 MHz, $CDCl_3$) δ 1.17 (t, J = 7.0, 6H), 1.62-1.67 (m, 2H), 1.72-1.78 (m, 2H), 3.44-3.50 (m, 2H), 3.58-3.64 (m, 2H), 3.70 (t, J = 7.3, 2H), 4.49 (t, J = 5.5, 1H), 7.69 (dd, J = 5.5, J = 3.0, 2H), 7.82 (dd, J = 5.5, J = 3.0, 2H). ^{13}C NMR (125 MHz, $CDCl_3$) δ 15.4, 24.1, 31.1, 37.9, 61.4, 102.5, 123.3, 132.3, 134.0, 168.5. MS (ESI) *m/z*: 246.2 $(M-OEt)^+$.

4-(1,3-Dioxoindolin-2-yl)butanal (69i) A mixture of 2-(4,4-diethoxybutyl)isoindoline-1,3-dione **69ii** (15.4 g, 53 mmol) and 1 M aqueous HCl (101 ml) in acetone (108 ml) was heated under reflux for 2 h. The solvent was removed in vacuo and the residue was extracted with ether (three times). The combined organic extracts were washed with water, dried, filtered, and concentrated in vacuo to yield the title compound **69i** (11.1 g, 97 %) as a white solid, which was used in the next step without further purification. ^{1}H NMR (500 MHz, $CDCl_3$) δ 2.02 (m, 2H), 2.53 (td, J = 7.3, J = 0.9, 2H), 3.74 (t, J = 6.7, 2H), 7.72 (dd, J = 5.5, J = 3.0, 2H), 7.84 (dd, J = 5.5, J = 3.0, 2H), 9.77 (s, 1H). ^{13}C NMR (125 MHz, $CDCl_3$) δ 21.3, 37.3, 41.2, 123.4, 132.2, 134.2, 168.5, 200.9. MS (ESI) *m/z*: 218.1 $(M+H)^+$.

*c) Synthesis and Analytical Data of Intermediate **84i***[S6]

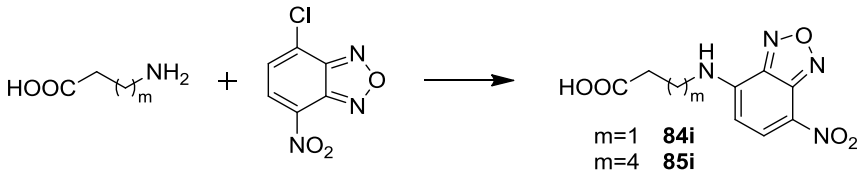

3-((7-Nitrobenzo[c][1,2,5]oxadiazol-4-yl)amino)propanoic acid (**84i**) At 0°C, 4-chlor-7-nitrobenzofurazan (300 mg, 1.503 mmol) and $NaHCO_3$ (379 mg, 4.509 mmol) were added to a solution of 3-aminopropanoic acid (134 mg, 1.503 mmol) in 30 ml of methanol. The mixture was stirred for 30 min at 0°C, followed by 90 min at room temperature and another 90 min at 50°C. The pH was adjusted to 2-3 by addition of 0.1 M aqueous HCl. After extraction with ethyl acetate (three times) the combined organic layers were dried and concentrated under reduced pressure. The crude product was purified by flash chromatography (8 % methanol/DCM) to give the title compound **84i** (211 mg). The identity of **84i** (211 mg) was proven by LC/MS (ESI) *m/z*: 253.22 $(M+H)^+$, indicating 72 % purity (UV). The product was used in the next step without further purification.

6-((7-Nitrobenzo[c][1,2,5]oxadiazol-4-yl)amino)hexanoic acid (**85i**)[S18] Following the procedure described for **84i** using 3-aminopropanoic acid (198 mg, 1.503 mmol), 4-chlor-7-nitrobenzofurazan (300 mg, 1.503 mmol) and $NaHCO_3$ (379 mg, 4.509 mmol) in 20 ml of methanol, the crude product was recrystallized from methanol to give 383 mg of the title compound **85i** (87 %). ^{1}H NMR (500 MHz, DMSO-d_6) δ 1.35-1.41 (m, 2H), 1.52-1.58 (m, 2H), 1.65-1.71 (m, 2H), 2.22 (t, J = 7.3, 2H), 3.43-3.48 (m, 2H), 6.40 (d, J = 8.8, 1H) 8.49 (d, J = 8.7, 1H), 9.52 (s, 1H), 11.98 (s, 1H). ^{13}C NMR (125 MHz, DMSO-d_6) δ 24.1, 25.9, 27.3, 43.2, 48.6, 99.1, 120.5, 137.9, 144.2, 144.4, 145.2, 174.4. MS (ESI) *m/z*: 295.01 $(M+H)^+$.

6.4.4 Synthesis of substrates used in the enzyme inhibition assay

Synthesis of anthraniloyl-S-CoA thioester[S19]

Anthraniloyl-CoA (ACoA) was synthesized from isatoic anhydride and coenzyme A (CoA) using a previously described method. ACoA was purified by HPLC (Agilent 1200 series consisting of a quaternary pump, a fraction collector and an MWD; Agilent Technologies, USA) after freeze drying of the aqueous reaction mixture (25 mL) and resuspending of the dried residue in 3 mL of a mixture of 50 % methanol and water. A 10 μm RP C18 150-30 column (30 x 100 mm, Agilent) was used along with a mobile phase consisting of water containing 1‰ TFA (A) and acetonitrile containing 1‰ TFA (B) with a flow rate of 5 mL/min. The following gradient was used: 0-35 min, linear gradient 10 % - 100 % B; 35-42 min, 100 % B; 42-43 min, 10 % B (initial conditions). ACoA containing fractions were pooled and freeze dried.

Synthesis of β-ketodecanoic acid[S20]

Ethyl 3-oxodecanoate (300 mg, 1.4 mmol, 1.0 eq) was stirred with NaOH (56 mg, 1.4 mmol, 1.0 eq) in water (2 ml) overnight. Any remaining ester was removed by washing with Et_2O (10 ml). The aqueous layer was cooled and acidified with 32 % HC1 to pH = 6. After filtration the 3-oxodecanoic acid was dried *in vacuo* and obtained as white solid (100 mg, 0.54 mmol, 38 %). ^{1}H NMR (500 MHz, $CDCl_3$) δ 0.86 (t, J = 7.0, 3H), 1.25-1.29 (m, 8H), 1.58 (quintet, J = 7.0, 2H), 2.54 (t, J = 7.5, 2H), 3.49 (s, 2H). LC/MS (ESI) no ionization, 99 % (UV).

Synthesis of ethyl 3-oxodecanoate[S21]

To a THF solution of 2M LDA (20 ml, 40 mmol 2.4 eq) was added ethyl acetoacetate (2.16 g, 16.6 mmol, 1.0 eq) at 0°C. The deep yellow clear solution was stirred at 0°C for 1 h. To this solution the 1-iodohexane was added (4.20 g, 19.81 mmol, 1.2 eq) at -78°C. The temperature was allowed to reach an ambient temperature over 14 h and the solution was stirred at room temperature for 2 h. To the solution was added 10 % HCl (200 ml) and the mixture was extracted with Et_2O (4 × 250 ml). The combined organic layers were dried over Na_2SO_4, filtered, and the filtrate was concentrated in vacuo. The residue was purified by column chromatography (*n*-hexane/ethyl acetate, 30/1) to give ethyl 3-oxodecanoate as a yellow oil (1.98 g, 9.24 mmol, 55 %). ^{1}H NMR (500 MHz, $CDCl_3$) δ 0.84 (t, J = 7.0, 3H), 1.23-1.28 (m, 11H), 1.54 (quintet, J = 7.0, 2H), 2.49 (t, J = 7.0, 2H), 3.39 (s, 2H), 4.16 (m, 2H).

6.4.5 Mutagenicity assay

The *S. typhimurium* derivatives TA100, TA1535 and TA102 were used as bacterial strains. These were provided by B. N. Ames (University of California, Berkeley, USA) or Trinova Biochem (Gießen, Germany).

The standard *S. typhimurium* plate incorporation assay was carried out.[S22] All mutagenicity assays were performed with and without S9 mix. S9, prepared from livers of male rats pre-treated with Aroclor 1254 (500 mg/kg), was provided by Trinova Biochem GmbH (Gießen, Germany). The concentrations of cofactors in the S9 mix (before adding them to the overlay) were 33 mM KCl, 8 mM $MgCl_2$, 5 mM glucose-6-phosphate, 4 mM NADP, 100 mM phosphate buffer (pH=7.4), and 5 % S9.

In absence of S9 mix sodium azide was used as positive control in TA100 (1 µg/plate) and TA1535 (2 µg/plate), whereas Mitomycin D (0.3 µg/plate) was used for TA102. When the assay was carried out with S9 mix, 2-aminoanthracen (1.5 µg/plate for TA100 and TA1535, respectively, and 8.0 µg/plate for TAS102) were added as positive control. The compound and positive controls were dissolved in DMSO was used as negative control. Doses of compound **3** for each strain with and without S9 mix were 5, 16, 50, 160, 500, 1600, and 5000 µg/plate (3 plates per dose level).

6.4.6 Effects on *P. aeruginosa* wild-type

Cultivation of *P. aeruginosa* PA14 wild-type

For determination of extracellular HHQ and PQS levels, cultivation was performed in the following way: cultures of *P. aeruginosa* PA14 wild-type cells (initial OD_{600} = 0.02) were incubated with or without inhibitor (final DMSO concentration 1 %, *v/v*) at 37°C, 200 rpm and a humidity of 75 % for 16 h in 24-well Greiner Bio-One Cellstar plates (Frickenhausen, Germany) containing 1.5 ml medium per well. Cultures were generally grown in PPGAS medium (20 mM NH_4Cl, 20 mM KCl, 120 mM Tris-HCl, 1.6 mM $MgSO_4$, 0.5 % (*w*/*v*) glucose, 1 % (*w*/*v*) $Bacto_{TM}$ Tryptone). Exceptionally, LB medium (86 mM NaCl, 0.5 % (*w*/*v*) yeast extract; 1 % (*w*/*v*) peptone from casein) was used for PQS quantification. For each sample, cultivation and sample work-up were performed in triplicates.

Determination of extracellular HHQ and PQS levels

Extracellular levels of HHQ were determined according to the method of Lépine *et al*. with the following modifications.[S23] An aliquot of 500 µl of bacterial cultures were supplemented with 50 µl of a 10 µM methanolic solution of the internal standard (IS) 5,6,7,8-tetradeutero-2-heptyl-4(1*H*)-quinolone (HHQ-d_4) and extracted with 1 ml of ethyl acetate by vigorous shaking. After centrifugation, 400 µl of the organic phase were evaporated to dryness in LC glass vials. The residue was re-dissolved in methanol. UHPLC-MS/MS analysis was performed as described in detail recently.[S24] The following ions were monitored (mother ion [m/z], product ion [m/z], scan time [s], scan width [m/z], collision energy [V], tube lens offset [V]): HHQ: 244, 159, 0.5, 0.01, 30, 106; HHQ-*d4* (IS): 248, 163, 0.1, 0.01, 32, 113. Xcalibur software was used for data acquisition and quantification with the use of a calibration curve relative to the area of the IS. Quantification of PQS produced by *P. aeruginosa* PA14 was performed as described by Maurer and colleagues.[S25]

Results: Effects on *P. aeruginosa* wild-type.

We selected three structurally divers compounds with good inhibitory potency in the *pqsH*⁻ mutant to examine their effects on *P. aeruginosa* PA14 wild-type. Since HHQ is not fully converted into PQS, both signal molecules had to be quantified to gain a full insight into inhibition of signal molecule production. All three compounds **3**, **48** and **62** were potent inhibitors of both signal molecules, whereas the most pronounced effects were exerted by **62** (Table S2). This is in accordance to the data observed in the *pqsH*⁻ mutant, which validates the latter as appropriate simplified test system to measure PqsD inhibition by quantification of only a singular reporter molecule.

Table S2. Effects of PqsD inhibitors on HHQ and PQS production in *P. aeruginosa* PA14 wild-type.

Compound	% HHQ inhibition[a]	% PQS inhibition[a]
3	38 ± 6[b]	37 ± 6[b]
48	33 ± 6	60 ± 11
62	49 ± 1	68 ± 1

[a]Planctonic *P. aeruginosa* PA14. Inhibitor concentration 250 µM. Percentage of inhibition was normalized regarding OD600.

[b]Values differ from ref. S24 due to improvements of the assay procedures.

6.4.7 References

(S1) Sapountzis, I.; Knochel, P.; General preparation of functionalized *o*-nitroarylmagnesium halides through an iodine–magnesium exchange. *Angew. Chem. Int. Ed.* 2002, **41**, 1610.

(S2) Hey, D. H.; Mulley, R. D.; Internuclear cyclization V. The cyclization of derivatives of diphenylmethane, benzophenone, and N-methyldiphenylamine. *J. Chem. Soc.* 1952, 2276.

(S3) Muchowski, J. M.; Venuti, M. C.; Ortho functionalization of N-(tert-butoxycarbonyl)aniline. *J. Org. Chem.* 1980, **45**, 4798.

(S4) Toyoda, T; Sasakura, X.; Sugasaw, T.; Aminoraloboran in organic sysnthesis. VIII. A one-step synthesis of 2-Aminobenzhydrols from anilines. *Tetrahedron Letters* 1980, **21**, 173.

(S5) Krasovskiy, A; Knochel, P.; A LiCl-mediated Br/Mg exchange reaction for the Ppreparation of functionalized aryl- and heteroarylmagnesium compounds from organic bromides. *Angew. Chem. Int. Ed.* 2004, *43*, 3333.

(S6) Winthrop, S. O.; Sybulski, S.; Gavin, G.; Gran, G. A.; New analeptics: 1-Benzhydryl-2-alkyl-2-thiopseudo-ureas. *J. Am. Chem. Soc.* 1957, **79**, 3496.

(S7) Koopal, S. A.; Molecular transposition in the α-glycols. *Recl. Trav. Chim. Pays-Bas* 1915, **34**, 115.

(S8) Kuriyama, M.; Shimazawa, R.; Enomoto, T.; Shirai, R.; Palladium-catalyzed 1,2-addition of potassium aryl- and alkenyltrifluoroborates to aldehydes using thioether-imidazolinium carbine ligands. *J. Or. Chem.* 2008, **73**, 6939.

(S9) Rybakova, M. N.; Reactions of alkoxydiarylcarbinolates with esters. *Zh. Obsh. Khim*, 1966, **2**, 470.

(S10) Fan, J.; Wang, Z.; Facile construction of functionalized 4H-chromene via tandem benzylation and cyclization. *Chem. Comm.* 2008, **42**, 5381.

(S11) Kuriyama, M.; Ishiyama, N.; Shimazawa, R.; Onomura, O.; Palladium- imidazolinium carbine-catalyzed arylation of aldehydes with arylboronic acids in water. *Tetrahedron* 2010, **66**, 6814.

(S12) Markees, D. G.; Reaction of benzyl methyl esters with bromine and N-bromosuccinimide. J. Org. Chem. 1958, **23**, 1490.

(S13) Barros-Filho, B. B.; de Oliveira, M. C. F.; Lemos, T. L. G.; de Matos, M. C.; de Gonzalo, G.; Gotor-Fernández, V.; Gotor, V.; *Lentinus strigellus*: a new versatile stereoselective biocatalyst for the bioreduction of prochiral ketones. *Tetrahedron: Asymmetry* 2009, **9**, 1057.

(S14) Qin, C.; Wu, H.; Cheng, J.; Chen, X.; Liu, M.; Zhang, W.; Su, W.; Ding, J.; The pallium-catalyzed addition of aryl- and heteroarylboronic acids to aldehydes. *J. Org. Chem.* 2007, **72**, 4102.

(S15) Carde, R. N.; Hayes P. C.; Jones, G.; Cliff, C. J.; Intramolecular nitrene insertions into aromatic and heteroaromatic systems. Part 7. Insertions into electron-deficient rings. J. Chem. Soc., Perkin Trans. 1, 1981, 1132.

(S16) Joossens, J.; Van der Veken, P.; Lambeir, A.-M.; Augustyns, K.; Haemers, A; Development of Irreversible Diphenyl Phosphonate Inhibitors for Urokinase Plasminogen Activator. *J. Med. Chem.* 2004, **47**, 2411.

(S17) Li, A.-H.; Moro, S., Forsyth, N; Melman, N.; Ji, X.-D.; Jacobson, K. A.; Synthesis, CoMFA analysis, and receptor docking of 3,5-diacyl-2,4-dialkylpyridine derivatives as selective A_3 adenosine receptor antagonists. *J. Med. Chem.* 1999, **42**, 706-721.

(S18) Novotný. J.; Pospěchová. K.; Hrabálek, A.; Čáp, R.; Vávravá, K.; Synthesis of fluorescent C_{24}-ceramide: Evidence for acyl chain length dependent differences in penetration of exogenous NBD-ceramides into human skin. *Bioorg. Med. Chem. Lett.* 2009, **19**, 6975-6977.

(S19) Simon, E. J.; Shemin, D. The preparation of S-succinyl coenzyme. A.; *J. Am. Chem. Soc.* 1953, **75**, 2520.

(S20) Cook, L.; Ternai, B.; Ghosh, P. Inhibition of human sputum elastase by substituted 2-pyrones. *J. Med. Chem.* 1987, **30**, 1017.

(S21) Synthesized according to: Nguyen, V. T. H.; Bellur, E.; Appel, B.; Langer, P.; Synthesis of 4-alkyl- and 4-(ω-chloroalkyl)-3-hydroxy-5-alkylidenebutenolides based on cyclizations of 4-alkyl- and 4-(ω-chloroalkyl)-1,3-bis(trimethylsilyloxy) buta-1,3-dienes with oxalyl chloride. *Synthesis* 2006, **17**, 2865.

(S22) Maron, D. M.; Ames, B. N.; Revised methods for the *Salmonella* mutagenicity test. *Mutat. Res.* 1983, **113**, 173.

(S23) Lépine, F.; Déziel, F. E.; Milot, S.; Rahme, L. G.; A stable isotope dilution assay for the quantification of the *Pseudomonas* Quinolone Signal in *Pseudomonas aeruginosa* cultures. *Biochim. Biophys. Acta*, 2003, **1622**, 36.

(S24) Storz, M. P.; Maurer, C. K.; Zimmer, C.; Wagner, N.; Brengel, C.; de Jong, J. C.; Lucas, S.; Müsken, M.; Häussler, S.; Steinbach, A.; Hartmann, R. W.; Validation of PqsD as an anti-biofilm target in *Pseudomonas aeruginosa* by development of small-molecule inhibitors. *J. Am. Chem. Soc.* 2012, **134**, 16143.

(S25) Maurer, C. K.; Steinbach, A.; Hartmann, R. W.; Development and validation of a UHPLC-MS/MS procedure for quantification of the *Pseudomonas* Quinolone Signal in bacterial culture after acetylation for characterization of new *quorum sensing* inhibitors. *J. Pharm. Biomed. Anal.* 2013, **86**, 127.

7 Appendix

7.1 Curriculum Vitae

PERSÖNLICHE DATEN

Name	Michael Philipp Storz
Geburtsdaten	24. März 1984 in Tübingen
Familienstand	ledig
Nationalität	deutsch

WISSENSCHAFTLICHER WERDEGANG

ab 11/2009	**Promotion** unter Anleitung von Prof. Rolf Hartmann am Helmholtz-Institut für Pharmazeutische Forschung Saarland (HIPS), Saarbrücken Titel der Dissertation: "*Development and Characterization of PqsD Inhibitors to Interrupt Cell-to-cell Communication in Pseudomonas aeruginosa"*
09/2013 – 03/2014	**Forschungsaufenthalt** bei Prof. Helen Blackwell, Department of Chemistry, University of Wisconsin-Madison
08/2007 – 12/2007	**Forschungsaufenthalt** bei Prof. Reiner Anwander, Department of Chemistry, University of Bergen
10/2003 – 08/2009	**Studium der Chemie**, Ruprecht-Karls-Universität Heidelberg Abschluss: Diplom (Note 1,3) Titel der Diplomarbeit unter der Betreuung durch Prof. Bernd Straub: "Theoretische Untersuchung zur homogen-katalytischen N_2-Aktivierung"

SCHULBILDUNG

09/1994 – 06/2003	Allgemeine Hochschulreife, Kepler-Gymnasium, Tübingen Abschluss: Abitur (Note 1,6)
09/1990 – 06/1994	Uhland-Grundschule Hirschau, Tübingen

MITGLIEDSCHAFTEN

American Chemical Society (ACS)

7.2 Publications

6.) M. P. Storz, G. Allegretta, B. Kirsch, M. Empting, R. W. Hartmann. From *in vitro* to *in cellulo*: Structure-activity relationship of (2-nitrophenyl)-methanol derivatives as inhibitors of PqsD in *Pseudomonas aeruginosa*. *Org. Biomol. Chem.* **2014**, DOI: 10.1039/c4ob00707g

5.) J. H. Sahner, C. Brengel, M. P. Storz, M. Groh, A. Plaza, R. Müller, R. W. Hartmann. Combining in Silico and Biophysical Methods for the Development of *Pseudomonas aeruginosa* Quorum Sensing Inhibitors: An Alternative Approach for Structure-Based Drug Design. *J. Med. Chem.* **2013**, *56*, 8656-8664.

4.) M. P. Storz, C. Brengel, E. Weidel, M. Hoffmann, K. Hollemeyer, A. Steinbach, R. Müller, M. Empting, R. W. Hartmann. Biochemical and Biophysical Analysis of a Chiral PqsD Inhibitor Revealing Tight-Binding Behavior and Enantiomers with Contrary Thermodynamic Signatures. *ACS Chem. Biol.* **2013**, *8*, 2794-2801.

3.) E. Weidel, J. C. de Jong, C. Brengel, M. P. Storz, M. Negri, A. Plaza, A. Steinbach, R. Müller, R. W. Hartmann. Structure Optimization of 2-Benzamidobenzoic Acids as PqsD Inhibitors for Pseudomonas aeruginosa Infections and Elucidation of Binding Mode by SPR, STD NMR, and Molecular Docking. *J. Med Chem.* **2013**, *56*, 6146-6155.

2.) M. P. Storz, C. K. Maurer, C. Zimmer, N. Wagner, C. Brengel, J. C. de Jong, S. Lucas, M. Müsken, S. Häussler, A. Steinbach, R. W. Hartmann. Validation of PqsD as an Anti-biofilm Target in *Pseudomonas aeruginosa* by Development of Small-Molecule Inhibitors. *J. Am. Chem. Soc.* **2012**, *134*, 16143-16146.

1.) E. Le Roux, Y. Lian, M. P. Storz, R. Anwander. Intramolecular hydroamination/ cyclization of aminoalkenes catalized by $Ln[N(SiMe_3)_2]_3$ grafted onto periodic mesoporous silicas. *J. Am. Chem. Soc.* **2010**, *132*, 16368-16371.

7.3 Oral Presentations

1.) M. P. Storz, C. Brengel, C. K. Maurer, M. Empting, A. Steinbach, R. W. Hartmann. Anti-infectives with novel mode of action: Development of PqsD inhibitors to interrupt *P. aeruginosa* cell-to-cell communication. *Antimicrobial Drug Discovery Conference* June **2013**, Madrid, Spain.

7.4 Poster Presentations

1.) M. P. Storz, C. K. Maurer, E. Weidel, J. C. de Jong, C. Brengel, S. Lucas, C. Zimmer, A. Steinbach, R. W. Hartmann. Anti-infectives with novel mode of action: Development of PqsD inhibitors to interrupt Pseudomonas aeruginosa cell-to-cell communication. 22nd International Symposium on Medicinal Chemistry, September **2012**, Berlin, Germany.

2.) M. P. Storz, C. K. Maurer, E. Weidel, J. C. de Jong, C. Brengel, S. Lucas, C. Zimmer, A. Steinbach, R. W. Hartmann. Anti-infectives with novel mode of action: Development of PqsD inhibitors to interrupt Pseudomonas aeruginosa cell-to-cell communication. MedChem 2012 – Annual one-day meeting on Medicinal Chemistry of SRC & KVCV, November **2012**, Liége, Belgium.

8 Acknowledgements

Mein besonderer Dank gilt Prof. Dr. Rolf W. Hartmann, der mir durch die Aufnahme in seinen Arbeitskreis und das Überlassen des interessanten und herausfordernden Themas, die Möglichkeit gab, diese Arbeit anzufertigen. Weiterhin danke ich für die stete Unterstützung und Diskussionsbereitschaft in wissenschaftlichen Belangen.

Den folgenden Personen, möchte ich meinen aufrichtigen Dank aussprechen:

Den Herren Prof. Dr. Kazmaier und Prof. Dr. Blankenfeldt für die Übernahme der Korreferate.

Dres. Simon Lucas, Christina Zimmer, Anke Steinbach und Martin Empting für die Leitung des pqs Projekts, insbesondere für eure Unterstützung, kreative Vorschläge und alle Diskussionen.

Dr. Alberto Plaza, Benjamin Kirsch, Cenbin Lu, Christian Brengel, Christian Schmitt, Christine Maurer, Jan Henning Sahner, Dr. Johannes de Jong, Lilli Weidel, Dr. Martin Empting, Simone Amann und Tobias Klein für die gute Zusammenarbeit und eure Hilfsbereitschaft.

Simone Amann und Carina Scheid für die große Hilfe durch das Ausführen vieler biologischer Tests.

Katrin Schmitt für die Organisation im Sekretariat.

Dr. Stefan Böttcher als Ansprechpartner bei allen analytischen Problemen und Dr. Josef Zapp für die Aufnahme unzähliger NMR Spektren.

Lothar Jager für alle technischen Problemlösungen.

Den aktuellen sowie ehemaligen Mitgliedern des PqsD Teams für die gute Atmosphäre und Zusammenarbeit.

Allen auch nicht namentlich genannten Mitgliedern der Arbeitskreise Hartmann (HIPS bzw. UdS) und Blackwell (University of Madison-Wisconsin) für ihre Kollegialität, Unterstützung bei technischen und experimentellen Schwierigkeiten und die nette Arbeitsatmosphäre.

Für mich noch wichtiger waren die guten Leute, welche die Promotionszeit zu einem schönen Lebensabschnitt gemacht haben. Herzlichen Dank für eure Kollegialität, die unterhaltsamen Pausen und viele unvergessliche Abende. Ohne Anspruch auf Vollständigkeit gilt besonderer Dank:

Christian Brengel, Christian Schmitt, Kristina Hüsecken, Michael Zender, Stefan Böttcher und viele Weitere.

Juliette Emmerich für die gute Zeit.

Stefan Hinsberger für seelenverwandtschaftliches Zuhören und Diskutieren.

Der Autor dankt der kleinen Autorin, dass er jeden Tag lieber am Arbeitsplatz erschienen ist.

Patrick Kotzur, der meine Freizeit durch ein institutsunabhängiges Refugium bereichert hat.

Lilli Weidel, mit der ich lange den Schreibtisch und Alltag teilen durfte, ohne dass es jemals langweilig werden oder der Gesprächsstoff ausgehen konnte.

Martina Fruth für ihre zuverlässige und allumfassende Freundschaft.

Allen meinen Freunden, die mit mir gelitten und sich mit mir gefreut haben und das auch hoffentlich weiterhin tun.

Mein besonderer Dank gilt meinen Eltern Hermine und Bernhard, die mir das Studium ermöglichten und auch während der Promotion weiterhin hinter meinem Werdegang standen. Danke für das Vertrauen und die Freiheit, die ihr mir entgegenbringt.

Sylvia Weis danke ich dafür, dass sie mir schon seit über 4 Jahren etwas geben kann, was mir noch niemand bieten konnte.